



UNIVERSITY OF
LIVERPOOL

**CHEMICAL BIOLOGY TOOLS FOR STRUCTURE-FUNCTION
STUDIES ON HEPARAN SULPHATES: DECODING SPECIFICITY
IN FGF SIGNALLING**

Thesis submitted in accordance with the requirements of the University of Liverpool
for the degree of Doctor in Philosophy

By

Emma Christelle Sery

October 2016

Abstract

Fibroblast growth factors (FGFs) regulate a broad spectrum of biological processes and aberrant FGF signalling has been linked to many disorders and diseases. Heparan sulphate (HS) is a highly sulphated glycosaminoglycan, which regulates the activity of its protein ligands, mainly through anionic interactions. The interactions between HS, FGF and FGF receptors (FGFRs) depend on the size and the spatial distribution of the anionic moieties of the saccharides. To test the effects of these on FGF signalling, the activities of well-defined HS oligosaccharides were screened in bioassays. The aim of this thesis was to study the structural determinants which underpin the specificity/selectivity in HS-FGF-FGFR interactions.

Two approaches were initially explored to generate suitable saccharides for screening. Firstly, the preparation of libraries of HS oligosaccharides was attempted by enzymatic digestion of porcine mucosal HS using heparinase III. This was followed by the sequential fractionation using size exclusion chromatography, strong anion-exchange and cetyltrimethylammonium strong anion-exchange chromatography. However, with regards to preparing saccharides of sufficient purity and amounts, this was found to be a limiting factor for bioassay screening. Secondly, the dimeric modular synthesis of HS octasaccharides was attempted by means of in-solution multi-step synthesis. The synthesis of a small oligosaccharide library was partially successful and resulted in novel synthetic routes for generation of pentasaccharide precursors, but not sulphated saccharides for screening. An alternative strategy was taken to exploit nineteen existing fully defined chemically and chemoenzymatically prepared oligosaccharides. Screening in bioassays of specific FGF ligands, using BaF3 cells expressing single receptors, showed that both general and specific structural changes, as subtle as a single additional sulphate moiety, significantly impact the ability of saccharides to support FGF signalling in a ligand-receptor complex-dependent manner. The size of the saccharides, the presence/absence of 2-*O*-, 6-*O*- and *N*-sulphate groups were shown to be crucial factors for functional activity. Most notably, the presence of a single 3-*O*-sulphate group towards the non-reducing end of the saccharides was related to high levels of activation for FGF1-FGFR1c, FGF1-FGFR2b and FGF7-FGFR2b and was demonstrated for the first time.

Overall, this thesis provides new evidence concerning structural determinants in HS that modulate FGF signalling, using fully defined saccharides for the first time. The results support the view that significant selectivity is involved, and contribute to a better fundamental understanding of how HS modulates FGF-FGFR-HS complex formation. Ultimately, this information could be relevant for the development of better targeted HS saccharide-based therapeutics.

*À ma mère,
qui m'a tout appris, sauf à vivre sans elle*

*To my mother,
who taught me everything, except how to live without her*

Remerciements

Il n'y a de tâche plus ardue que celle de résumer les quatre intenses années de thèse en quelques mots... et il n'y aura jamais assez de mots et de place pour dire à quel point je suis reconnaissante envers toutes les personnes qui m'ont aidée tout au long de ce voyage...

Je voudrais commencer par exprimer mon immense gratitude à mes directeurs de thèse, le Pr. Jerry Turnbull et le Dr. Ed Yates (University of Liverpool), ainsi que le Dr. Niels Reichardt (CIC biomaGUNE) pour m'avoir constamment soutenue, pour leur infinie patience, leur motivation et pour m'avoir partagé leur immense savoir. Ils m'ont sincèrement aidée tout au long de ce voyage, qui n'aurait pas pu être possible sans eux. Je n'oublie pas l'Institute of Integrative Biology (University of Liverpool) et le CIC biomaGUNE, qui m'ont donné l'opportunité de continuer mes études.

Je suis redevable à nombre de mes collègues. Merci au Dr. Yassir Ahmed and au Dr. Scott Guimond pour m'avoir quotidiennement aidée au labo. Merci au Dr. Rebecca Miller pour m'avoir aidée avec les techniques de chromatographie en phase liquide. Merci à Sarah, Hannah et Rachel pour toutes ces nombreuses discussions instructives et passionnantes. Un énorme « merci/muchas gracias/eskerrik asko » à Begoña, Nerea Guedes, Eli et Raquel pour leur aide dans le labo et pour leur infinie patience. Je voudrais également remercier le Dr. Javi Calvo pour toutes les analyses de spectrométrie de masse. Cette thèse n'aurait pas pu voir le jour sans vous tous. Mes plus sincères remerciements à toutes les personnes du labo B/A à Liverpool et à toutes celles de CIC biomaGUNE.

Je voudrais exprimer mon immense gratitude aux Dr. Ashley Hughes, Dr. Dada Pisconti, Dr. Tushar Chauhan, Dr. Chris Clarke, Dr. Sophie Thompson, Dr. Nerea Ruiz, Dr. Juan Echevarria, Dr. Álvaro Hernández, Dr. Carlos Lopez de Laorden, Dr. Cristina Díez, Dr. Kasia Brzezicka, Dr. Richard Murray and Dr. Maria Genua, Dr. Elizabeth Goiri, Dr. Constance Goiri, Dr Justina Aguerre ainsi qu'à Amelie, Fiona, Anna, Arturo and Ester, Silvia, et la Monofamille (spécialement Jérôme et Sarah). Merci pour votre aide et pour tous ces bons souvenirs. Un énorme merci à ma

famille, tout particulièrement à ma mère et à mes frères Karim et Maxime, à mon parrain et sa femme Rosy, ma tante Nadine et mon oncle Roland. Votre soutien et vos constants encouragements ont été énormément appréciés ces quatre dernières années.

Sans oublier ma coloc' et ma très chère amie Kate. Un énorme « merci/go raibh mile maith agat » pour son aide, son soutien sans bornes, pour m'avoir accordé autant de son temps (!) et pour m'avoir sauvé la vie de si nombreuses fois ;)

Finalement, un « merci/heel erg bedankt » tout particulier à mon très cher Andjin pour son amour, ses continuels encouragements, son infinie patience, pour m'avoir guidée et pour m'avoir partagé son amour de la recherche et ses nombreuses connaissances. Son soutien ne pourrait jamais avoir passé inaperçu ;)

Acknowledgments

There is no more arduous task than summarising the four intense years of a PhD in a few words... and there will never be enough words and space to say how grateful I am towards all the people who have helped me throughout this journey...

I would like to start by expressing my utmost gratitude to my supervisors Prof. Jerry Turnbull and Dr. Ed Yates (University of Liverpool), as well as Dr. Niels Reichardt (CIC biomaGUNE) for the continuous support, patience, motivation and immense knowledge. They truly helped me throughout the course of this journey, which would not have been possible without such invaluable guidance. Not forgetting the Institute of Integrative Biology (University of Liverpool) and CIC biomaGUNE, who afforded me the opportunity to continue my studies.

I am indebted to many of my colleagues. Thank you to Dr. Yassir Ahmed and Dr. Scott Guimond for all your guidance in the lab. Thank you to Dr. Rebecca Miller for helping me with the HPLC techniques. Thank you Sarah, Hannah and Rachel for all the insightful discussions. An enormous “thank you/muchas gracias/eskerrik asko” to Begoña, Nerea Guedes, Eli and Raquel for your help and patience in the lab. I would like to extend my gratitude to Dr. Javi Calvo for running all the mass spectrometry analyses. This thesis would not have been possible without you all. My sincerest thanks to all the people from both lab B/A in Liverpool and everyone in CIC biomaGUNE.

I owe my deepest gratitude to Dr. Ashley Hughes, Dr. Dada Pisconti, Dr. Tushar Chauhan, Dr. Chris Clarke, Dr. Sophie Thompson, Dr. Nerea Ruiz, Dr. Juan Echevarria, Dr. Álvaro Hernández, Dr. Carlos Lopez de Laorden, Dr. Cristina Díez, Dr. Kasia Brzezicka, Dr. Richard Murray and Dr. Maria Genua, Dr. Elizabeth Goiri, Dr. Constance Goiri, Dr. Justina Aguerre, Amelie, Fiona, Julie, Anna, Arturo and Ester, Silvia, and the Monofamille (especially Jérôme and Sarah). Thank you for the help and all the good memories. Also an enormous thank you to my family, especially to my mom and my brothers Karim and Maxime, my godfather and his wife Rosy, my Aunt Nadine and Uncle Roland. Your support and constant encouragement were most greatly appreciated over these last four years.

Not forgetting my roommate and dear friend Kate. A massive “thank you/go raibh mile maith agat” for her constant help, support, and time (!) and for saving my life so many times ;)

Finally, a special “thanks/heel erg bedankt” to Andjin for his loving and constant encouragement, his infinite patience, his guidance and knowledge. His endless support could never go unnoticed ;)

Table of contents

Abstract	ii
Remerciements	v
Acknowledgments	vii
Table of contents	ix
List of abbreviations	xv
List of figures	xxi
List of schemes	xxiv
List of tables	xxv
1. Chapter 1 – Background	1
1.1. Glycans and glycobiology	2
1.2. Proteoglycans	2
1.3. Glycosaminoglycans	3
1.4. Heparan sulphate proteoglycans	3
1.5. Heparin and heparan sulphate	5
1.5.1. Biosynthesis	5
1.5.1.1. <i>Initiation</i>	6
1.5.1.2. <i>Elongation</i>	6
1.5.1.3. <i>Chain modifications</i>	8
1.5.1.4. <i>Post-synthetic modifications</i>	9
1.5.2. Structural properties	10
1.5.2.1. <i>Structures</i>	10
1.5.2.2. <i>Conformations</i>	12
1.6. HS structures in biology: HS-protein interactions	13
1.6.1. HS-protein binding: basic principles and structural requirements for the HS chains and the ligands	14

1.6.2.	On the specificity/selectivity in HS-protein interactions	16
1.7.	HS-FGF-FGFR interactions.....	19
1.7.1.	Fibroblast Growth Factors	19
1.7.2.	Fibroblast Growth Factor Receptors	22
1.7.3.	Role of HS in FGF signalling	24
1.7.4.	HS specificity/selectivity in FGF-FGFR systems.....	27
1.8.	Tools for HS-FGF-FGFR interactions studies.....	30
1.8.1.	Library production methods: HS oligosaccharides from natural sources	31
1.8.1.1.	<i>Extraction of HS from natural sources</i>	31
1.8.1.2.	<i>Partial digestion of native HS polysaccharide chains</i>	32
1.8.1.3.	<i>Methods of purification of HS oligosaccharide mixtures</i>	32
1.8.2.	Library production methods: synthetic and semi-synthetic methods ...	36
1.8.3.	Tools for HS structures analysis	40
1.8.4.	Tools for HS-FGF interactions studies	42
1.9.	Aims.....	45
2.	Chapter 2 – Materials, methods, procedures and characterisation data	47
2.1.	Preparation of Hp/HS oligosaccharide libraries from natural sources .	48
2.1.1.	Materials	48
2.1.2.	Methods	48
2.1.2.1.	<i>Enzymatic partial digestion</i>	48
2.1.2.2.	<i>PAGE oligosaccharide separation</i>	49
2.1.2.3.	<i>SEC chromatography</i>	49
2.1.2.4.	<i>Desalting SEC fractions</i>	50
2.1.2.5.	<i>SAX chromatography</i>	50
2.1.2.6.	<i>CTA-SAX chromatography</i>	51

2.1.2.7.	<i>Desalting CTA-SAX fractions</i>	51
2.2.	BaF3 bioassays	52
2.2.1.	Materials	52
2.2.2.	Method	52
2.2.3.	Statistical analysis	54
2.3.	Chemical synthesis of Hp/HS oligosaccharides	54
2.3.1.	Materials	54
2.3.2.	Methods	54
2.3.2.1.	<i>Microwave-assisted synthesis</i>	54
2.3.2.2.	<i>Flash chromatography</i>	55
2.3.2.3.	<i>Mass spectrometry</i>	55
2.3.2.4.	<i>Specific rotation</i>	55
2.3.2.5.	<i>NMR</i>	55
2.3.3.	Procedures and characterisation data	56
2.3.3.1.	<i>General procedures</i>	56
2.3.3.2.	<i>Procedures and characterisation data</i>	57
3.	Chapter 3 –HS oligosaccharide library production from natural sources	87
3.1.	Introduction	88
3.1.1.	Aims	88
3.1.2.	Strategy	88
3.1.3.	Methods	88
3.2.	HS oligosaccharide library preparation: from natural sources	91
3.2.1.	Partial enzymatic digestion of PMHS	91
3.2.2.	SEC of digested PMHS	91
3.2.3.	SAX chromatography of digested PMHS: 1st run	94
3.2.4.	SAX chromatography of digested PMHS: 2nd and 3rd runs	96

3.2.5.	CTA-SAX chromatography of digested PMHS	99
3.2.5.1.	<i>Column preparation</i>	99
3.2.5.2.	<i>CTA-SAX of compounds 10-A1 and 10-A2</i>	100
3.3.	Conclusions.....	102
4.	Chapter 4 – Chemical synthesis of HS oligosaccharide structures	104
4.1.	Introduction.....	105
4.1.1.	Chemical synthesis of Hp/HS oligosaccharides	105
4.1.1.1.	<i>Protecting groups</i>	105
4.1.1.2.	<i>Glycosylation: keystone of carbohydrate synthesis</i>	106
4.1.1.3.	<i>Glycosyl donors</i>	110
4.1.2.	In solution synthesis of Hp/HS oligosaccharides: a brief historical review and remaining issues	112
4.2.	Objectives and design of general synthetic strategy	116
4.2.1.	Objectives	116
4.2.2.	General strategy	117
4.2.3.	First target structure	122
4.3.	Initial synthetic approach: synthesis of the elongation blocks	125
4.3.1.	Azidoglucose building block synthesis.....	127
4.3.1.1.	<i>Synthesis of the building block 9</i>	129
4.3.1.2.	<i>Synthesis of the building block 8</i>	131
4.3.2.	L-iduronic acid building block synthesis	131
4.3.2.1.	<i>Synthesis of the building block 10</i>	132
4.3.2.2.	<i>Synthesis of the intermediate 34</i>	134
4.3.2.3.	<i>Synthesis of the building block 11</i>	136
4.3.3.	Elongation blocks synthesis: evaluation of the azidoglucose and iduronic acid building blocks in glycosylation reactions.....	138

4.3.4.	Elongation blocks synthesis: revision of the initial strategy.....	140
4.3.5.	New azidoglucose building block synthesis	142
4.3.6.	New L-iduronic acid building block synthesis.....	143
4.3.7.	Elongation blocks synthesis: evaluation of the new azidoglucose and L-iduronic acid building blocks.....	144
4.3.8.	Conclusions.....	146
4.4.	New synthetic approach: synthesis of the new elongation blocks.....	147
4.5.	New elongation blocks synthesis	149
4.6.	Towards the synthesis of the first target	150
4.6.1.	Seeding block synthesis	150
4.6.2.	Trisaccharide precursor synthesis	151
4.6.2.1.	<i>Synthesis of the intermediate 60: preliminary results</i>	<i>152</i>
4.6.2.2.	<i>Synthesis of the intermediate 61</i>	<i>156</i>
4.6.2.3.	<i>Synthesis of the intermediate 63</i>	<i>160</i>
4.6.3.	Pentasaccharide precursor synthesis: preliminary results.....	161
4.6.4.	Synthesis of the new trisaccharide precursor 67.....	163
4.6.5.	New pentasaccharide precursor synthesis: evaluation of the new trisaccharide building block 67.....	165
4.6.6.	Conclusions.....	167
4.7.	General conclusions	168
5.	Chapter 5 – Evaluation of Hp/HS oligosaccharide specificity/selectivity in FGF signalling.....	170
5.1.	Introduction.....	171
5.1.1.	Aim	172
5.1.2.	Strategy and method	172
5.1.2.1.	<i>BaF3 bioassays.....</i>	<i>173</i>
5.2.	Libraries of well-defined Hp/HS oligosaccharides.....	174

5.2.1.	From chemical sources	175
5.2.2.	From chemoenzymatic sources.....	175
5.3.	Results.....	178
5.3.1.	Assessing the ability of Hp/HS oligosaccharides to induce FGF2 and FGF1 signalling through FGFR1c	178
5.3.2.	Assessing the ability of Hp/HS oligosaccharides to induce FGF7 and FGF1 signalling through FGFR2b	184
5.4.	Discussion.....	189
6.	Chapter 6 – General Discussion and Future Directions.....	195
7.	References.....	206

List of abbreviations

Ac	acetate
ACE	affinity co-electrophoresis
ACN	acetonitrile
AIBN	azobisisobutyronitrile
AT	anti-thrombin
BACE	beta-protease
BAIB	[bis(acetoxy)-iodo]benzene
Bn	benzyl
BP	by-product
Bz	benzoyl/benzoate
C18	octadecyl carbon chain
CAM	cell adhesion molecule
CE	capillary electrophoresis
CHD	cell adhesion molecule homology domain (CHD)
conc	concentration
CMPI	2-chloro-1-methyl-1-pyridinium iodide
COSY	correlation spectroscopy
CS	chondroitin sulphate
CSA	(1S)-(+)-10-camphorsulphonic acid
CT	C-terminal tail
CTA	cetyltrimethylammonium
Da	Dalton
DABCO	1,4-diazabicyclo[2.2.2]octane
DCM	dichloromethane
DHB	2,5-dihydroxybenzoic acid
DMAP	dimethylaminopyridine
DMSO	dimethyl sulfoxide

DNA	deoxyribonucleic acid
dp	degree of polymerisation
DQF	double quantum filtered
DS	dermatan sulphate
DSF	differential scanning fluorimetry
EC ₅₀	half maximal effective concentration
ECM	extracellular matrix
EDC	<i>N</i> -(3-dimethylaminopropyl)- <i>N'</i> -ethylcarbodiimide
Equiv	equivalent
ESI	electospray ionisation
EXT	exostosin family of genes which encodes glycosyltransferases
FBS	foetal bovine serum
FGF	fibroblast growth factor
FGFR	fibroblast growth factor receptor
FHF	fibroblast growth factor homologous factors
Fmoc	fluorenylmethyloxycarbonyl
GAG	glycosaminoglycan
Gal	D-galactose
GalNAc	<i>N</i> -acetyl-D-galactosamine
GalT	galactosyltransferase
GlcA	D-glucuronic acid
GlcA2S	<i>N</i> -sulphated-D-glucuronic acid
GlcAT	glucuronyltransferase
GlcNAc	<i>N</i> -acetyl-D-glucosamine
GlcNAc6S	<i>N</i> -acetyl-6- <i>O</i> -sulphated-D-glucosamine
GlcNAcT	<i>N</i> -acetylglucosaminyltransferase
GlcNH	D-glucosamine
GlcNS	<i>N</i> -sulphated- D-glucosamine

GlcNS6S	<i>N</i> -,6- <i>O</i> -disulphated-D-glucosamine
HA	hyaluronic acid
Hh	hedgehog
HILIC	hydrophilic interaction liquid chromatography
Hp	heparin
HPLC	high performance liquid chromatography
HS	heparan sulphate
HSPG	heparan sulphate proteoglycans
HSQC	heteronuclear single-quantum correlation spectroscopy
HSV	herpes simplex virus
IdoA	L-iduronic acid
IdoA2S	2- <i>O</i> -sulphated-L-iduronic acid
Ig	immunoglobulin-like domain
IL	interleukin
Int	intermediate
ITC	isothermal titration calorimetry
JM	juxtamembrane
k_a	association rate constant
k_d	dissociation rate constant
K_a	equilibrium association constant
K_d	equilibrium dissociation constant
kDa	kiloDalton
KI	kinase insert
KS	keratan sulphate
LC	liquid chromatography
LG	leaving group
Lev	levulinoyl
LMWHP	low molecular weight heparin

MALDI	matrix-assisted laser desorption/ionisation
mAU	milli arbitrary unit
Me	methyl
MP	methoxyphenyl
MS	mass spectrometry
MTT	3-[4,5-dimethylthiazol-2-yl]-2,5-diphenyltetrazolium bromide
mU	milliunit
NA	<i>N</i> -acetylated domain
NDST	<i>N</i> -deacetylase/ <i>N</i> -sulphotransferase
NMR	nuclear magnetic resonance
NOESY	nuclear Overhauser effect spectroscopy
NS	<i>N</i> -sulphated domain
N.S.	non significant
OST	uronosyl-2- <i>O</i> -sulphotransferase
PAGE	polyacrylamide gel electrophoresis
PAPS	3'-phosphoadenosine 5'-phosphosulphate
PBS	phosphate-buffered saline
PG	protecting group
PGC	porous graphitised carbon
Ph	phenyl
PMHS	porcine mucosa heparan sulphate
pNP	<i>para</i> -nitrophenyl
PS	polystyrene
psi	pound per square inch
<i>p</i> -TsOH	<i>p</i> -toluenesulphonic acid
rh	human recombinant
rm	mouse recombinant
RNA	ribonucleic acid

RPIP	reverse-phase ion-pairing chromatography
RPMI	Roswell Park Memorial Institute medium
S.D.	standard deviation
SAR	structure-activity relationship
SAX	strong anion-exchange
SEC	size exclusion chromatography
SM	starting material
SRCD	synchrotron radiation circular dichroism
Std	standard
Sulf	sulfatase
TBAF	tetra- <i>n</i> -butylammonium fluoride
TBAI	tetrabutylammonium iodide
TBS	<i>tert</i> -butyldimethylsilyl
TBSOTf	<i>tert</i> -butyldimethylsilyl trifluoromethanesulfonate
TCA	trichloroacetamido
TDS	dimethylhexylsilyl
Temp	temperature
TEMPO	2,2,6,6-tetramethyl-1-piperidinyloxy
Tf	trifluoromethanesulphonyl (also known as trifyl)
TFA	trifluoroacetic acid
THF	tetrahydrofuran
TK	tyrosine kinase
TLC	thin-layer chromatography
TM	transmembrane
TMSOTf	trimethylsilyl trifluoromethanesulfonate
TOCSY	total correlation spectroscopy
TOF	time of flight
ULMW	ultra low molecular weight

UPLC	ultra performance liquid chromatography
UV	ultraviolet
VEGF	vascular endothelial growth factor
Vis	visible
WT	wild type
Xyl	xylose
XylT	xylosyltransferase

List of figures

Figure 1: Schematic representation of a proteoglycan basic structure and of the disaccharide repeating units of the common GAGs.....	4
Figure 2: Schematic representation of the Hp/HS biosynthesis.....	7
Figure 3: Schematic representation of the domain structures of Hp/HS polysaccharides.	11
Figure 4: Conformational structures of the monosaccharide units found in Hp/HS.	14
Figure 5: Phylogenetic tree of human FGF family.	20
Figure 6: Schematic representation of the FGFR structure.....	22
Figure 7: Schematic representation of the formation of the two main FGF-FGFR-HS ternary complexes in competition: (a) the 2-2-1 asymmetric model and (b) the 2-2-2 symmetric model.	27
Figure 8: Cleavage specificity of heparinases and resulting products from the cleavages.	33
Figure 9: Principle of the main chromatography techniques used to purify HS oligosaccharides: (a) SEC, (b) SAX and (c) CTA-SAX chromatography.....	36
Figure 10: Monitoring the progress of the synthesis of the trisaccharide 60 by MALDI-TOF mass spectrometry.	78
Figure 11: Monitoring of the progress of the synthesis of the trisaccharide 63 by MALDI-TOF mass spectrometry.	80
Figure 12: LC-MS spectra obtained for the synthesis of pentasaccharide 64.....	81
Figure 13: LC-MS spectra obtained for the synthesis of pentasaccharide 68.....	86
Figure 14: Strategy adopted for the creation of libraries of HS oligosaccharides from natural sources and the study of HS SAR in FGF signalling.	89
Figure 15: Monitoring the evolution of PMHS partial enzymatic digestion by heparinase III using small-scale SEC.....	92
Figure 16: Estimation of the degree of polymerisation of the partially digested PMHS saccharides: comparison of the large-scale SEC profile and the PAGE analysis of the resulting SEC fractions.	93
Figure 17: Semi-prep SAX-HPLC profile for SEC fraction 10.....	95
Figure 18: SAX-HPLC profiles for fractions 10-A and 10-B.....	97
Figure 19: SAX-HPLC profiles for fractions 10-A1, 10-A2 and 10-B1.	98

Figure 20: Confirming the derivatisation of the C18 silica column by CTA: CTA-SAX profile obtained for the separation of the eight common naturally occurring disaccharides standards.....	99
Figure 21: CTA-SAX profiles for fractions 10-A1 and 10-A2.....	101
Figure 22: Some of the major protecting groups used for Hp/HS oligosaccharide synthesis.	107
Figure 23: The major types of glycosyl donors.	111
Figure 24: Structures of the disaccharide units constituting Hp/HS oligosaccharides.	118
Figure 25: Results for the desilylation of 21 using AcOH and TBAF.....	130
Figure 26: Results of the Steglich esterification of 32	133
Figure 27: Preparation of building block 10	134
Figure 28: Evaluation of the building blocks 10 and 11 as glycosyl acceptor in glycosylation reactions.....	139
Figure 29: Analysis of the evolution of the direct transformation of the azido groups of 59 into acetamido groups using thioacetic acid in pyridine.....	153
Figure 30: Analysis of the evolution of the direct transformation of the azido groups of 59 into acetamido groups using pure thioacetic acid.....	154
Figure 31: Analysis of the reduction of the azido groups using PPh ₃	157
Figure 32: LC-MS data for the microwave-assisted conversion of 59 using PS-PPh ₃	159
Figure 33: Typical LC-MS spectrum profile obtained for the assembly of 50 with 63	163
Figure 34: Analysis of the assembly of 50 with 67	167
Figure 35: Dose response curves (mean \pm S.D.) for full-length Hp activation of FGF2 (0.1 nM) and FGF1 (1 nM) signalling through FGFR1c.....	178
Figure 36: Evaluating the bioactivity of the compounds alone at 3 μ g/mL in bioassays with cells expressing FGFR1c.	179
Figure 37: Assessing the capability of fully defined Hp/HS oligosaccharides (at 3 μ g/mL) to regulate (a) FGF2 (0.1 nM) and (b) FGF1 (1 nM) signalling through FGFR1c.....	181
Figure 38: Dose response curves (mean \pm S.D.) for Dec2,6+3S and Dod2,6S activation of FGF1 signalling through FGFR1c.	183

Figure 39: Dose response curves (mean \pm S.D.) for full-length Hp activation of FGF7 (3 nM) and FGF1 (1 nM) signalling through FGFR2b.	184
Figure 40: Evaluating the bioactivity of the compounds alone at 3 μ g/mL in bioassays with cells expressing FGFR2b.	185
Figure 41: Assessing the capability of Hp/HS oligosaccharides (at 3 μ g/mL) to regulate (a) FGF7 (3 nM) and (b) FGF1 (1 nM) signalling through FGFR2b. .	187
Figure 42: Hierarchical regulatory system – Sulphation and remodelling versus diversity and functional impact.	204

List of schemes

Scheme 1: General mechanism of the chemical <i>O</i> -glycosylation.	108
Scheme 2: Synthesis of 1,2- <i>trans</i> glycoside via neighbouring group participation.	109
Scheme 3: Trichloroacetimidate glycoside rearrangement,	112
Scheme 4: General strategy for Hp/HS octasaccharide synthesis.	119
Scheme 5: Retrosynthesis of the first target – Structures of the first target and its natural analogue.	124
Scheme 6: Retrosynthesis of the first target – Building block and linker structures.	126
Scheme 7: Retrosynthesis of the elongation blocks – Monomeric building block structures.	127
Scheme 8: Synthesis of the glycosyl donors 8 and 9	128
Scheme 9: Synthesis of the intermediate 30	132
Scheme 10: Synthesis of the building block 10	133
Scheme 11: Synthesis of the building block 11	135
Scheme 12: Possible synthetic routes to prepare the building block 34	136
Scheme 13: Retrosynthesis of the new elongation blocks – Monomeric building block structures.	141
Scheme 14: Preparation of the new glycosyl donor 41	142
Scheme 15: Preparation of the new glycosyl acceptor 42	143
Scheme 16: Assembly of the disaccharides 47-49	144
Scheme 17: Retrosynthetic analysis of the new building blocks.	148
Scheme 18: Synthesis of the elongation blocks 50 and 51	149
Scheme 19: Synthesis of seeding block 58	150
Scheme 20: Synthesis of trisaccharide precursor 59	151
Scheme 21: Synthesis of trisaccharide 61	156
Scheme 22: Synthesis of the glycosyl acceptor 63	160
Scheme 23: Test synthesis of the pentasaccharide 64	161
Scheme 24: Synthesis of the glycosyl acceptor 67	165
Scheme 25: Test synthesis of the pentasaccharide 68	166

List of tables

Table 1: Major HSPG families and their tissue distribution	5
Table 2: Major differences between Hp and HS.	10
Table 3: Physiology of FGFs.	21
Table 4: Ligand specificity of the FGF receptor family.....	24
Table 5: Reaction conditions and results for the preparation of the building block 11	137
Table 6: Reaction conditions and results for the assemblies of the glycosyl donors 8 , 9 and 41 with the glycosyl donor 42	145
Table 7: Reagents, conditions and results for the direct synthesis of 60 using thioacetic acid.....	155
Table 8: Reaction conditions and results for the assemblies of the glycosyl donor 50 with the glycosyl acceptor 63	162
Table 9: Schematic representation of the structures of the HS oligosaccharides prepared by chemical synthesis.....	176
Table 10: Schematic representation of the structures of the HS oligosaccharides prepared by chemoenzymatic synthesis	177
Table 11: Results of one-sample t-tests (one-tailed, N=3) for FGF2-FGFR1c and FGF1-FGFR1c.	182
Table 12: Results of one-sample t-tests (one-tailed, N=3) for FGF7-FGFR2b and FGF1-FGFR2b.	188
Table 13: Summary of the ability of the Hp/HS oligosaccharides to activate FGF- FGFR complexes.....	190

1. Chapter 1 – Background

1.1. Glycans and glycobiology

Biomolecular interactions underlie all biological processes in living organisms, from physiological processes to responses to stimuli, including growth and development, adaptation, homeostasis, survival and reproduction. The nature and mechanisms of these interactions are diverse and driven by specific molecular recognition. Understanding these interactions is essential to comprehend the different functions of the biomolecules involved in such processes. Interacting molecules include DNA, RNA, proteins, polypeptides, polyphenols, lipids or carbohydrates. It is now understood that biomolecules are interconnected (Varki 2009) and that a given biomolecule may be involved in hundreds of interactions, concurrently with several types of other components, which makes their study a challenging task.

The science of the biosynthesis, structure and biology of glycans, also called glycobiology, is a reasonably new section of biological sciences (Rademacher *et al.* 1988). Even though glycans represent the major part of the biomolecules in cells, their biological roles have been fairly underappreciated in comparison to nucleic acids and proteins, which have monopolised attention. This is mainly explained by the complexity and heterogeneity of their chemical structures and biosynthetic origins. Although being a significant obstacle to deciphering their functions, this structural heterogeneity is also an essential factor that explains the broad range of roles played by glycans at the cellular level. In recent decades, they have been shown to play critical roles in storage and transport of energy, but also as structural molecules, signalling co-effectors, or even recognition markers. Therefore, glycans are essential actors in the transmission of important biological signals at the cellular level.

1.2. Proteoglycans

Proteoglycans are found in all multicellular organisms and are major constituents of the extracellular matrix (ECM), the cell surface and also in secretory granules (Kjellen and Lindahl 1991). These macromolecules are involved in a multitude of processes, ranging from the basic structural organisation and mechanical support of tissues to highly specialised biological processes such as cellular growth,

specialisation and maturation through their interactions with a broad variety of proteins, including cytokines and growth factors (Lennarz 2012). Proteoglycans are comprised of a core protein to which polyanionic glycosaminoglycan (GAG) chains are covalently attached (Figure 1).

1.3. Glycosaminoglycans

GAGs are linear heteropolysaccharides whose repeating disaccharide units are made of hexosamine (either *N*-acetyl-D-galactosamine/D-galactosamine or *N*-acetyl-D-glucosamine/D-glucosamine-*N*-sulphated) and hexuronic acid (either D-glucuronic acid or L-iduronic acid) residues, except for keratan sulphate, whose repeating disaccharide unit is made of a D-galactosamine and a *N*-acetyl-D-glucosamine residues (Hook *et al.* 1984). These polyanionic structures have been classified into different species mainly based on their disaccharide repeating unit structure: hyaluronic acid (HA), chondroitin sulphate (CS), dermatan sulphate (DS), keratan sulphate (KS), heparan sulphate (HS) and heparin (Hp) (Figure 1). These polysaccharides are sulphated at different positions of the chains, except for the non-sulphated HA. The diversity of roles played by the proteoglycans, to which they are associated (except for HA, which is the only GAG that is not attached to a core protein), is mainly explained by the heterogeneity of their structures and their ability to bind many types of ligands (mainly proteins and protein conjugates) (Lindahl and Hook 1978).

1.4. Heparan sulphate proteoglycans

Heparan sulphate proteoglycans (HSPGs), which consist - as suggested by their name - of HS polysaccharide chains attached to a core protein, are an important class of proteoglycans (Varki 2009). Their classification is based on the type of core protein and their number of HS chains (Table 1). As for the other proteoglycans, HSPGs are implicated in a broad variety of biological phenomena, ranging from angiogenesis and organogenesis to cell adhesion and migration, wound healing, blood coagulation regulation and lipid metabolism (Bishop *et al.* 2007, Sarrazin *et al.* 2011). They are also involved extensively in signalling pathway mechanisms, for

example for fibroblast growth factors (FGFs), vascular endothelial growth factors (VEGFs), Wnt and Hedgehog (Hh) (Forsberg and Kjellén 2001).

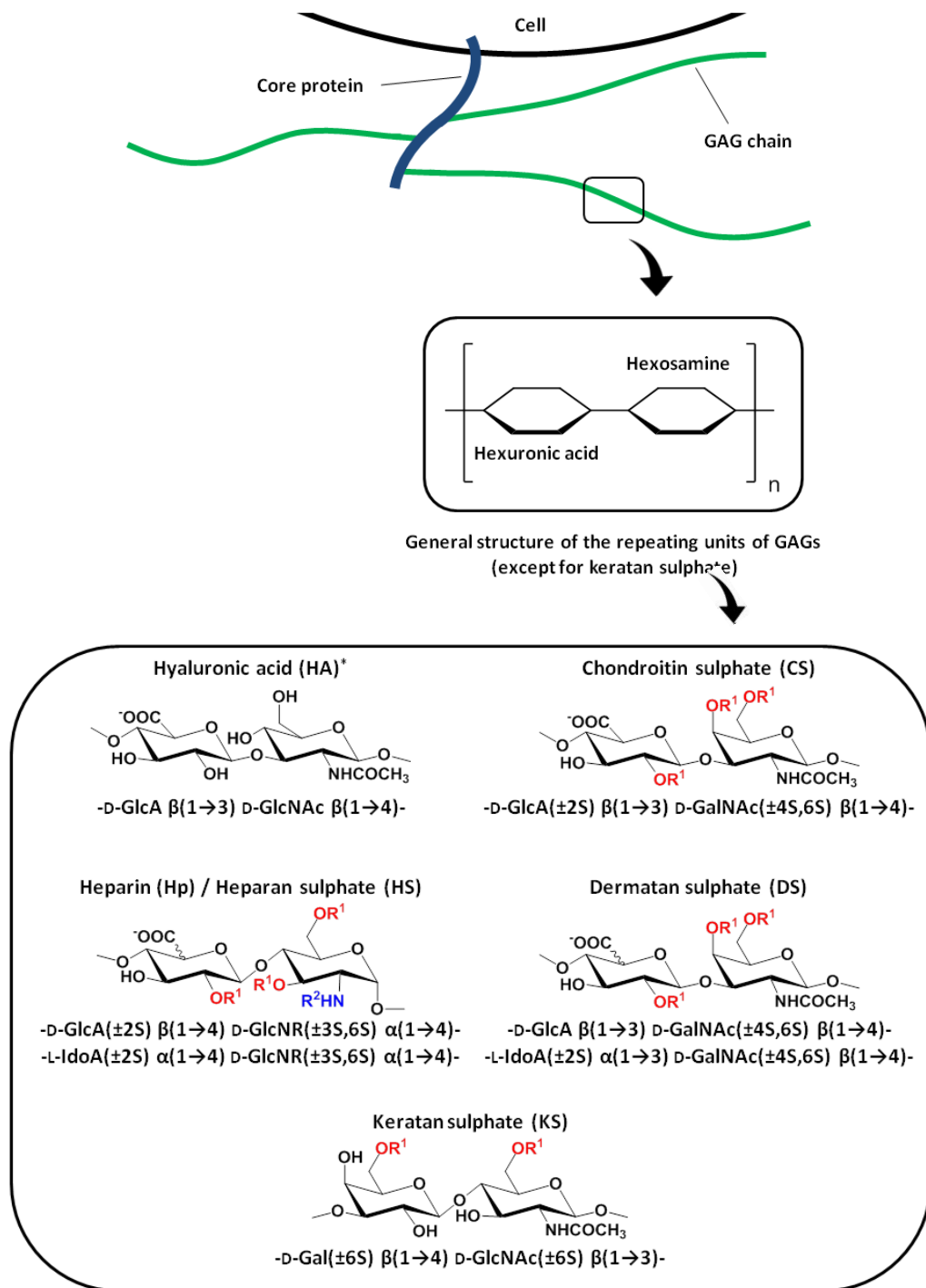


Figure 1: Schematic representation of a proteoglycan basic structure and of the disaccharide repeating units of the common GAGs. 2S: 2-*O*-sulphate; 3S: 3-*O*-sulphate; 4S: 4-*O*-sulphate; 6S: 6-*O*-sulphate; Gal: D-galactosamine; GalNAc: *N*-acetyl-D-galactosamine; GlcA: D-glucuronic acid; GlcNAc: *N*-acetyl-D-glucosamine; IdoA: L-iduronic acid. R = *N*-acetyl or *N*-sulphate; $\text{R}^1 = \text{H}$ or SO_3^- ; $\text{R}^2 = \text{Ac}$ or SO_3^- . *HA is the only GAG which is not bound to a core protein.

Class	Proteoglycan	Core protein (kDa)	Number of GAG chains
Extracellular matrix	Agrin	~200	HS (2-3)
	Collagen XVIII	~180	HS (1-3)
	Perlecan	~400	HS (1-4)
Membrane-bound	Glypicans 1-6	~60	HS (1-3)
	Syndecans 1-4	~35	HS (1-2) CS (1-3)

Table 1: Major HSPG families and their tissue distribution (Iozzo 1998, 2001, Bandtlow and Zimmermann 2000).

1.5. Heparin and heparan sulphate

1.5.1. Biosynthesis

Unlike HS, which is synthesised by almost all types of cells, Hp is made exclusively in mast cells (Rabenstein 2002). Amongst GAGs, Hp and HS display the highest variability in sequence. The latter can be regrouped into a vast repertoire called the “heparanome” (Turnbull *et al.* 2001). This observed heterogeneity results from the complex biosynthetic processes involved in their generation. Currently, the exact biosynthesis mechanism still remains unknown. The sequential pathway described by Lindahl *et al.* (1989) is commonly agreed, even though it does not explain some structures such as GlcNAc6S (Rudd and Yates 2012). Both Hp/HS biosynthetic pathways are similar, template-free driven, mainly take place in the Golgi apparatus and are regulated by more than 20 enzymes and their isoforms (Liu and Pedersen 2007). The enzymes operate in a stepwise manner in four main stages (Figure 2), which are described in more detail in the following sections: the initiation, the chain elongation, the enzymatic structural modifications and finally the post-synthetic modifications.

1.5.1.1. Initiation

Prior to the synthesis of the Hp/HS polysaccharide backbone, the tetrasaccharide linkage D-GlcA $\beta(1\rightarrow3)$ D-Gal $\beta(1\rightarrow3)$ D-Gal $\beta(1\rightarrow4)$ D-Xyl $\beta(1\rightarrow O)$ [Serine] is produced (Sugahara and Kitagawa 2000). The first step of the synthesis of the linkage region consists of the attachment of a xylose (Xyl) residue to a serine residue of the core protein, performed by the enzyme xylosyltransferase (XylT), which exists as two isomers XylT-1 and XylT-2 in mammals (Götting *et al.* 2000). The next step is the successive transfer of two galactose (Gal) residues by the enzymes galactosyltransferases 1 and 2 (GalT-1 and GalT-2) respectively at the non-reducing end of the nascent polysaccharide chain. The final addition of a glucuronic acid (GlcA) residue by glucuronyltransferase 1 (GlcAT-1) completes the synthesis of the linkage region, which has been found to be common to Hp, HS, CS and DS. Several structural modifications may occur, such as the 2-*O*-phosphorylation of the xylose residue (Fransson *et al.* 1985) or the 2-*O*-sulphation/6-*O*-sulphation of the Gal residues in the case of CS/DS (Sugahara and Kitagawa 2000). The nature of the fifth residue attached to the non-reducing end of the linkage domain GlcA residue then determines the type of polysaccharide chain: the addition of *N*-acetyl-D-glucosamine ($\alpha(1\rightarrow4)$ D-GlcNAc) will lead to Hp/HS chains whereas the introduction of *N*-acetyl-D-galactosamine ($\beta(1\rightarrow4)$ D-GalNAc) will lead to the formation of CS/DS chains (Sugahara and Kitagawa 2000).

1.5.1.2. Elongation

The addition of the fifth sugar motif $\alpha(1\rightarrow4)$ D-GlcNAc by the enzyme *N*-acetylglucosaminyltransferase 1 (α -GlcNAcT-1) triggers the elongation process (Fritz *et al.* 1994). The stepwise and alternating addition of $\beta(1\rightarrow4)$ D-GlcA and $\alpha(1\rightarrow4)$ D-GlcNAc residues is achieved by the action of two glycosyltransferase enzymes encoded by the genes EXT-1 and EXT-2 and which work as a complex (McCormick *et al.* 1998, 2000, Stickens *et al.* 2005). As the Hp/HS chain is extended (the chains are generally 50-200 disaccharides long, 25-100 kDa), it undergoes several enzymatic modifications, in a sequential manner. In this way, the product of an enzymatic reaction serves as the substrate for the next reaction.

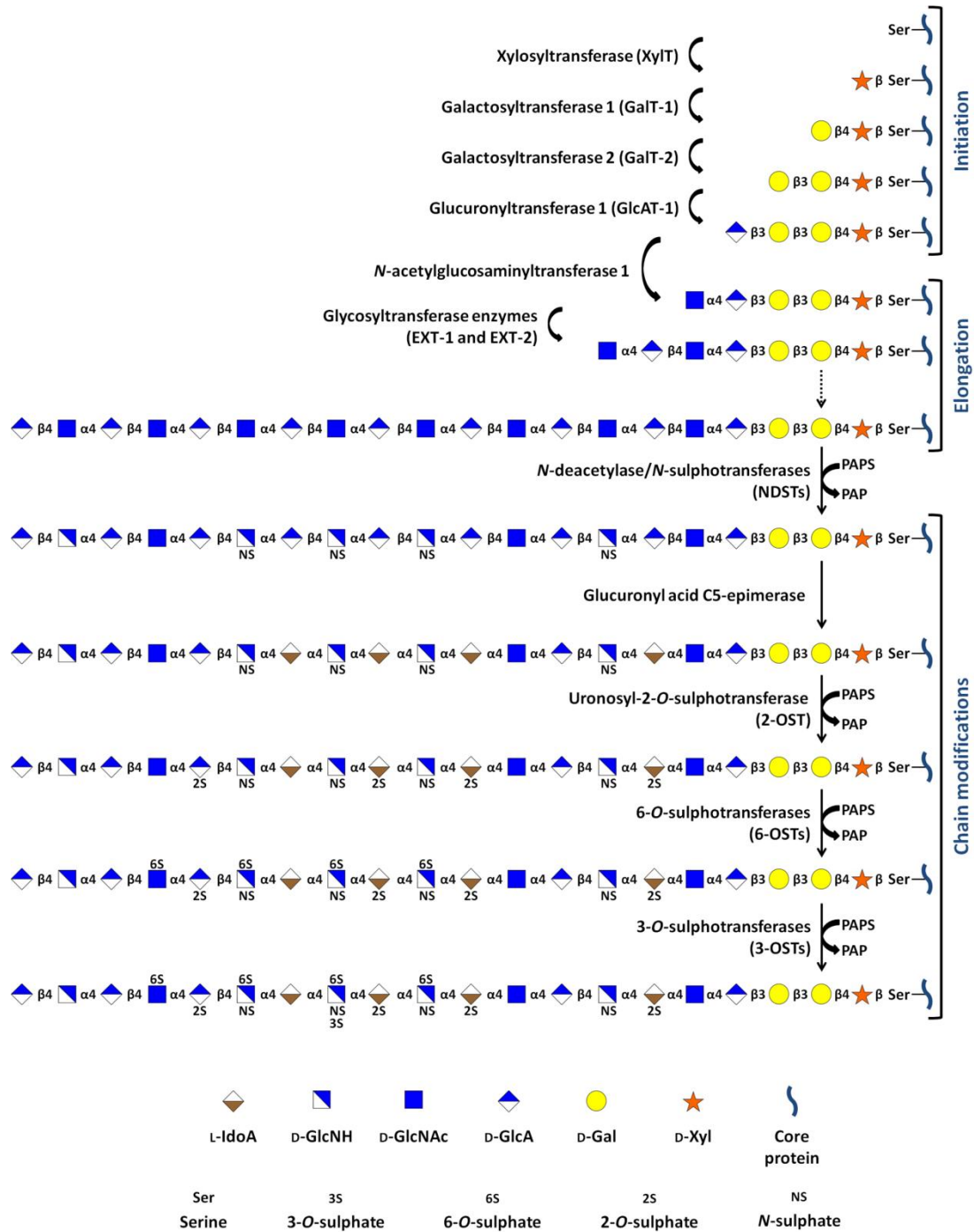


Figure 2: Schematic representation of the Hp/HS biosynthesis, as proposed by Lindahl *et al.* (1989). The synthesis starts with the tetrasaccharide linkage preparation (Xyl-Gal-Gal-GlcA), attached to a serine residue of the core protein. The sequential addition of the GlcA and GlcNAc residues is followed by several steps of chain modifications, including: N-deacetylation, N-sulphation, GlcA C5 epimerisation and 2-O-, 6-O- and 3-O-sulphations. PAPS is used as a sulphate donor. D-Gal: D-galactosamine; D-GlcA: D-glucuronic acid; D-GlcNAc: N-acetyl-D-glucosamine; D-GlcNH: D-glucosamine, L-IdoA: L-iduronic acid; D-Xyl: D-xylose.

1.5.1.3. Chain modifications

Unlike the polymerisation process, enzymatic modifications of the HS backbone may occur in a concomitant manner, even though a relatively well-established order can be drawn from researchers' observations. The GlcNAc residues of the unmodified polysaccharide HS chain first undergo *N*-deacetylation followed by *N*-sulphation, both catalysed by Hp/HS GlcNAc *N*-deacetylase/*N*-sulphotransferases (NDSTs). Four different isomers are found in vertebrates and display sequential different catalytic activities (Orellana *et al.* 1994, Aikawa *et al.* 2001). The *N*-deacetylation step is generally immediately followed by the transfer of a sulphate group (provided by the sulphate donor 3'-phosphoadenosine 5'-phosphosulphate (PAPS) (Liu and Pedersen 2007)). However, this reaction is not always completed and so can lead to the formation of rare unsubstituted D-glucosamine residues. This first step is of utmost importance as *N*-sulphated glucosamine (GlcNS) is needed for some of the subsequent modifications. More specifically, the presence of GlcNS at the non-reducing end of D-GlcA is required for the epimerisation of this latter into L-IdoA (Jacobsson *et al.* 1984). Studies have shown that HS C5-epimerase is selective towards non-sulphated uronic acids or the ones that are not adjacent to *O*-sulphated glucosamine units (Bäckström *et al.* 1979, Jacobsson *et al.* 1984, Hagner-McWhirter *et al.* 2000, Qin *et al.* 2015). In another study, the epimerisation step has been shown to be crucial for the sulphation of the Hp/HS chain (Feyerabend *et al.* 2006). These findings strongly suggest that the epimerisation of the uronic acids most likely occurs before the sulphation of both uronic and glucosamine residues.

Besides the epimerisation reaction, uronic acid units may also undergo 2-*O*-sulphation by the action of the enzyme uronosyl-2-*O*-sulphotransferase (2-OST) (Habuchi *et al.* 1998). Despite its ability to catalyse the sulphation of both types of uronic acids, 2-OST shows a net preference towards IdoA over GlcA, resulting in the rarity of GlcA2S (Rong *et al.* 2001). Remarkably, other studies have shown that 2-*O*-sulphation of uronic acids may have an impact on *N*-deacetylation/*N*-sulphation of glucosamine units as a lack of 2-*O*-sulphated iduronic acids resulted in the increase of *N*-sulphated-glucosamines (Bai and Esko 1996, Merry *et al.* 2001). These findings suggest that these steps may concomitantly occur, that the order may be more flexible than expected or that the process can go backwards and be repeated. The

next enzymes to go into action are the three isoforms of 6-*O*-sulphotransferase (6-OST-1, 6-OST-2 and 6-OST-3) which transfer a sulphate group to the C6 position of the D-glucosamine units. The majority of the 6-*O*-sulphation reactions in most of tissues is through the action of 6-OST-1 (Habuchi *et al.* 2007). As for the other enzymes, 6-OST-1-3 display different substrate preferences, even though, ultimately, GlcNS are generally sulphated more than GlcNAc (Habuchi *et al.* 2000, Smeds *et al.* 2003).

The final but rarest step of Hp/HS chain modification consists of 3-*O*-sulphation of the D-glucosamine residues, performed by 3-*O*-sulphotransferases (3-OSTs), remarkably found as seven different isomers in vertebrates (Liu *et al.* 1999, Shworak *et al.* 1999). Each isoenzyme displays different substrate preferences, which impacts the synthesis of specific sequences necessary for some vital interactions of Hp/HS with proteins (Xia *et al.* 2002, Ding *et al.* 2005). The abundance of isoforms, their substrate specificities and the importance of such a transformation (e.g., for the interactions between Hp/HS with anti-thrombin III and herpes simplex virus) clearly indicate the importance of 3-*O*-sulphation pattern in the regulation of biological functions.

1.5.1.4. Post-synthetic modifications

Until recently, the enzymatic modifications described above were believed to be the only ones to occur and to shape Hp and HS polysaccharide chains. However, a study led by Dhoot *et al.* (2001) highlighted the role of a class of cell-surface enzymes in the biosynthetic pathway of Hp/HS. Two endosulphatases (Sulf-1 and Sulf-2) (Morimoto-Tomita *et al.* 2002) selectively remove 6-*O*-sulphate groups from *N*-sulphated glucosamine residues (Ai *et al.* 2006, Lamanna *et al.* 2006). The importance of these enzymes has been re-evaluated, as new studies showed both the impact they have on the structure of the polysaccharides and their interactions with proteins (Lamanna *et al.* 2007). They have also been directly linked to cancers (Solari *et al.* 2014, Vicente *et al.* 2015). The enzymatic activity of Sulf-1 has been shown to decrease FGF binding (Wang *et al.* 2004), but to promote Wnt1 signalling (Dhoot *et al.* 2001).

1.5.2. Structural properties

1.5.2.1. Structures

Despite sharing the same biosynthetic pathway, Hp and HS are relatively distinct products (Table 2). Unlike the fairly homogeneous Hp chains (high level of sulphation: 2.0-3.0 sulphate groups/disaccharide unit) which mainly consists of repeats of the trisulphated disaccharide IdoA2S-GlcNS6S (Gallagher and Walker 1985), HS chains display a higher degree of structural diversity (with a relatively low level of sulphation: 0.5-2.0 sulphate groups/disaccharide unit). These diverse structural compositions are explained by the incomplete synthetic activities of the enzymes, which are template-free driven. However, fairly recent studies have helped understand the underlying mechanisms regulating the whole process.

Characteristics	Heparan Sulphate (HS)	Heparin (Hp)
Site of synthesis	Virtually all cells	Mast cells
Core protein	Many	Serglycin
Cell membrane attached?	Yes	No
Size	20-100 kDa	7-20 kDa
Alternate NS/NA domains	Yes	Minimal
Average sulphate/disaccharide	0.5-2.0	2.0-3.0
IdoA	20-50%	≥80%
N-sulphate	30-60%	≥80%
2-O-sulphate	10-40%	≥80%
6-O-sulphate	10-40%	≥80%
Binding to antithrombin	0-0.3%	~30%

Table 2: Major differences between Hp and HS. Adapted from Xu and Esko (2014).

Theoretically, no less than 48 different disaccharides can be found in native Hp/HS. However, only 23 different disaccharides have yet been found to occur in nature (Esko and Selleck 2002). *In vivo* and *in vitro* studies have also shown that important structural changes can be observed depending on the nature, the maturity and the health state (healthy/disease) of the tissues (Maccarana *et al.* 1996, Cheng *et al.* 2001, Netelenbos *et al.* 2001, Allen and Rapraeger 2003, Ledin *et al.* 2004). However, the structures of the HS extracted from the same tissues are consistent amongst individuals (Ledin *et al.* 2004). This suggests that the physical and chemical state of the Golgi and cellular environments have a direct impact on the biosynthetic outcome. Therefore, some kind of regulation must be ordering the whole process. Substrate specificities and incomplete activities of the enzymes are directly responsible for the formation of heterogeneous structures and the creation of domain structure. The selective and incomplete action of NDST in particular, which has been shown to act on the chain in both random and ordered fashions (Sheng *et al.* 2011), is mainly responsible for the presence of three types of domains found along the sugar chains (Figure 3).

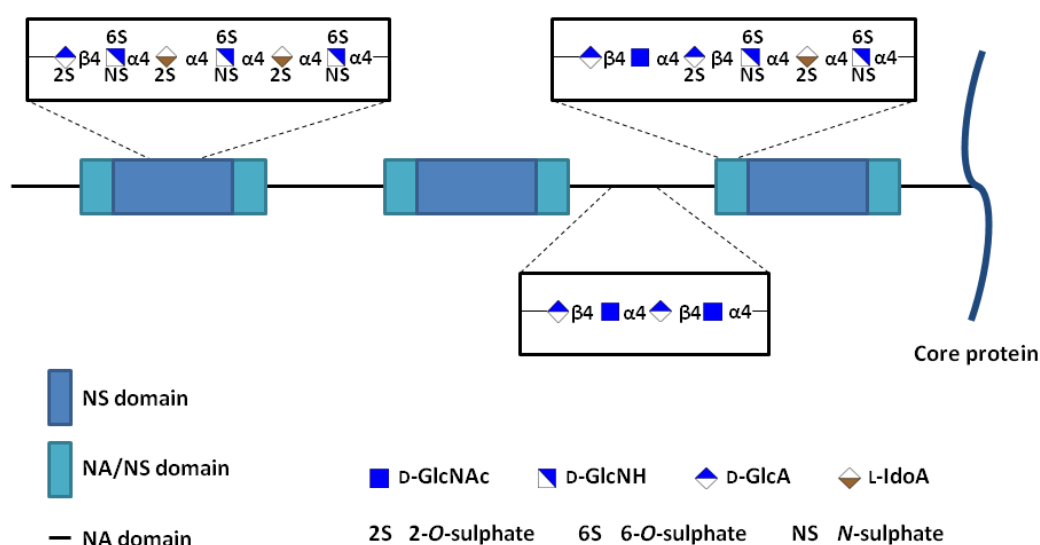


Figure 3: Schematic representation of the domain structures of Hp/HS polysaccharides. The three types of domains that are found all along the polysaccharide chains are represented: the highly sulphated NS domains, the unmodified NA domains and the mixed NA/NS domains. D-GlcA: D-glucuronic acid; D-GlcNAc: N-acetyl-D-glucosamine; D-GlcNH: D-glucosamine; L-IdoA: L-iduronic acid.

The NS domains consist of repeating disaccharide units displaying *N*-sulphated units, whereas NA domains essentially contain unmodified *N*-acetylated disaccharide units, both delimited by transition structures containing alternating *N*-acetylated/*N*-sulphated units (NA/NS domains) (Turnbull and Gallagher 1990, Maccarana *et al.* 1996, Murphy *et al.* 2004). The layout and formation of those domains are still under investigation, even though noticeable advances have been made in this area (Murphy *et al.* 2004, Rudd and Yates 2012). The structure of the repeating disaccharide unit differs, depending on the domain type. NA domains are constituted of unsulphated disaccharide units and of GlcA residues only. On the contrary, NS domains are constituted of heavily sulphated disaccharide units. Therefore, the disaccharide unit IdoA2S-GlcNS represents the major repeating unit throughout the NS region (Merry *et al.* 1999). 2-*O*-sulphation is generally restricted to the IdoA units of the NS domains (Merry *et al.* 1999). 6-*O*-sulphation does not display such restrictions and may occur on both NS and NA/NS domains, even though it may not be automatically found in those regions. Finally, NS and NA/NS regions also contain the rare 3-*O*-sulphated residues as well as the unsubstituted glucosamine residues at a very low rate (Van Den Born *et al.* 1995, Liu *et al.* 1999). These different domains, which are specific to HS, confer on these polysaccharides several structural (chemical and physical) properties, such as specific conformations or the presence of unusual sequences, and to a much higher extent than for Hp polysaccharides.

1.5.2.2. Conformations

Owing to their compositional differences, each domain found along the HS chains possesses its own structural characteristics. The three-dimensional properties of these GAGs are dictated by several parameters such as the nature of the saccharides, the presence and nature of functional groups as well as the glycosidic bonds. Based on the results obtained from solid experimental data (Nieduszynski *et al.* 1977, Gatti *et al.* 1979, Mulloy *et al.* 1993), the proposed helix conformation adopted by both Hp and HS polysaccharide chains, similar to the one adopted by nucleic acids, was initially thought to be rather rigid. However, Hp and HS are soluble polysaccharides, which indicates some flexibility. This flexibility can be explained by the interactions between the polysaccharides and molecular water (Almond and Sheehan 2003). Work published later showed that modified Hp polysaccharides actually display

some flexibility (Hricovini *et al.* 1995). Additional work identified that this flexibility is actually due to the highly sulphated NS regions, as the NA domains (which are mainly composed of GlcA-GlcNAc disaccharide units) have been shown to be relatively rigid (Hricovini *et al.* 1997). D-glucosamine residues and D-glucuronic acid units indeed adopt a rather rigid 4C_1 ring conformation for steric hindrance reasons (Figure 4). Nuclear magnetic resonance (NMR) studies demonstrated that the flexibility of the NS domains is mainly caused by the IdoA2S units which display quite a high level of conformational plasticity as they oscillate between 4C_1 , 1C_4 and 2S_0 forms - the two latter forms being generally preferred in polysaccharides (Sanderson *et al.* 1987, Ferro *et al.* 1990). The sulphation state of both IdoA units and the one of their adjacent monosaccharides has a direct impact on their conformational equilibrium (Ferro *et al.* 1990, Mulloy and Forster 2000). More specifically, all 2-*O*-, 3-*O*- and 6-*O*-sulphate groups have been shown to have an influence, up to a certain extent, on the ring conformation of the L-iduronic acid residues (Muñoz-García *et al.* 2012, 2013, Hsieh *et al.* 2016). These conclusions have yet been drawn from the study of isolated structures and more systematic studies are required. The sulphation of the D-glucosamine (GlcNS) and L-iduronic acid (IdoA2S) residues have been shown to be linked to the observed variations of the glycosidic linkages, unlike the 6-*O*-sulphate groups, which seemed to have much less impact (Rudd and Yates 2010). Moreover, it has been shown that the glycosidic bonds of the NS domains are less flexible than the ones of the NA domains. This relative rigidity is explained by the presence of the *N*-sulphate groups which tend to lock the GlcNS-IdoA(\pm 2S) disaccharide units by forming a hydrogen bond with the hydroxyl group of the uronic acid moiety (Yates *et al.* 1996). Finally, the nature of the counter/coordinate ions can also alter the conformations of the polysaccharide chains and therefore their activity (Ayotte and Perlin 1986, Rabenstein *et al.* 1995, Rudd *et al.* 2007).

1.6. HS structures in biology: HS-protein interactions

Owing to their intrinsic properties (wealth of structures, polyionic properties, chain flexibility, structural conformations, etc.), HS possesses the ability to interact with a vast interactome, comprising hundreds of protein ligands. These interactions are of utmost importance and regulate a broad variety of biological functions (Ori *et al.*

2008). Many of these interactions remain a mystery regarding their biological importance. This is mainly due to the difficulties encountered by researchers aiming to decipher the interactions of such complex polysaccharides with their ligands, even though many advances have been made (Xu and Esko 2014).

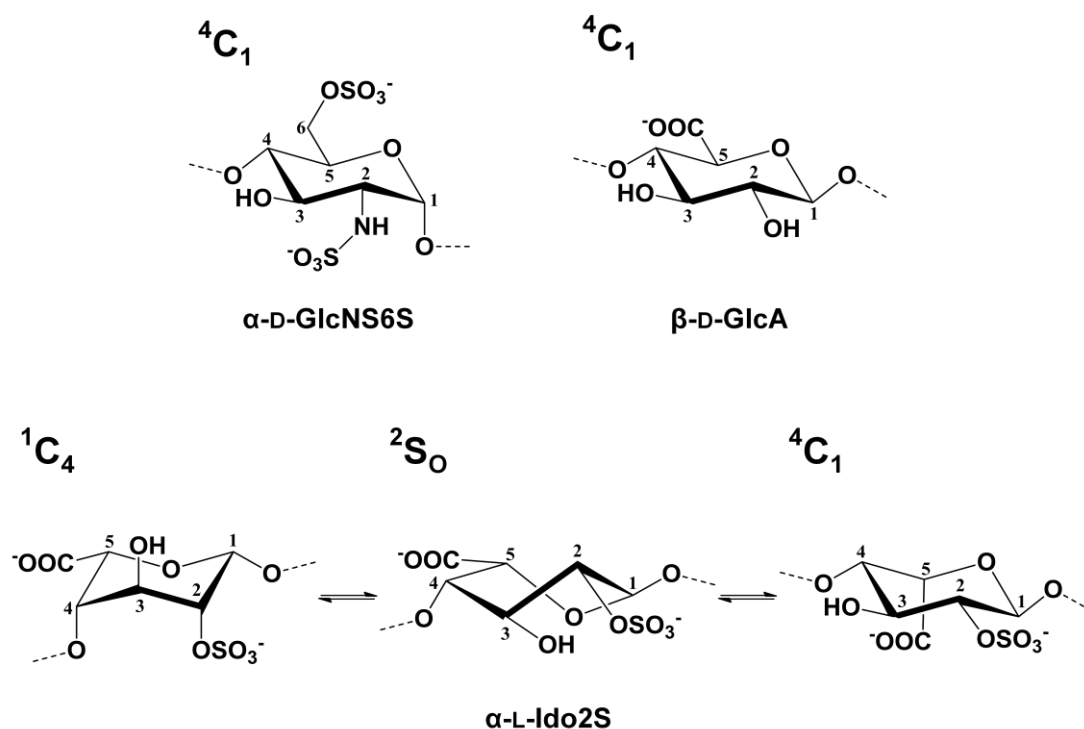


Figure 4: Conformational structures of the monosaccharide units found in Hp/HS. Unlike both D-glucuronic acid and D-glucosamine residues, which are locked in 4C_1 conformation, L-iduronic acid residues oscillate between 4C_1 , 1C_4 and 2S_0 forms. D-GlcNS6S: N-,6-O-disulphated-D-glucosamine; D-GlcA: D-glucuronic acid; L-IdoA2S: 2-O-sulphated-L-iduronic acid.

1.6.1. HS-protein binding: basic principles and structural requirements for the HS chains and the ligands

Prior to triggering any biological activity, the HS chain must be put in contact with its ligands. This first binding step is thought to be mainly driven by electrostatic forces between the anionic groups at the surface of the carbohydrate chains (sulphate and carboxylate groups) and the amino acids of the proteins bearing cationic charges (arginine and lysine) (Rabenstein 2002). Proteins interacting with HS often bear a charged sequence called HS-binding domains (HSBD), which has been the subject of

many studies. Cardin and Weintraub (1989) were first to investigate the structural features required for GAG-protein interactions. The comparison of a set of heparin-binding sequences from several proteins led to the first identification of two consensus sequences XBBXBX and XBBBXXBX where B represents a basic amino acid and X represents a hydrophobic residue (neutral or hydrophobic). Further studies, conducted by Sobel *et al.* (1992) and Hileman *et al.* (1998), led to the identification of two other consensus sequences: XBBBXXBBBXXBBX and TXXBXXTBXXXTBB, for the von Willebrand factor and for growth factors respectively (T represents a turn). However, these rigid linear models do not universally fit all HS-protein interactions, suggesting that other HSBD architectures are possible, such as the spatial distribution of basic amino acids along longer linear sequences that, when the protein is folded, provide residues close in the tertiary protein structure, as suggested by Spillmann and Lindahl (1994). The proposed helical nature of HS chains leads to the projection of its negatively charged moieties out of the backbone towards the protein residues (Casu 1979). These anionic moieties could hence interact with amino acids from juxtapositioned loops.

At the saccharide level, the protein-binding domain sizes often vary from a few disaccharides (such as the prototypic antithrombin-binding pentasaccharide) up to dodecasaccharides. Sometimes, even longer domains are needed (Spillmann *et al.* 1998, Gallagher 2001), as first indicated for binding of HS to interferon- γ (Lortat-Jacob *et al.* 1995).

Importantly, once the HS chain and the protein interact, conformational changes may be observed on both polysaccharide and protein levels (Faller *et al.* 1992, Skinner *et al.* 1997, Guimond *et al.* 2009, Li, Sun, *et al.* 2016). Earlier work claimed that the changes induced were actually negligible on the protein scale, but these results were based on X-ray experiments (Faham *et al.* 1996). The free energy released by these conformational changes is part of the total energy involved in the binding mechanism. Along with the electrostatic forces, other forces are believed to modulate the interactions. Thompson *et al.* (1994) showed that solely 30% of the binding free energy derives from electrostatic forces in the case of Hp polysaccharides interacting with FGF2. Other factors such as van der Waals' forces and hydrogen bonding (Hileman, Jennings, *et al.* 1998) or even the interactions with the hydrophobic amino

acids adjacent to the HSBD (Jairajpuri *et al.* 2003) are believed to take part in the binding process.

1.6.2. On the specificity/selectivity in HS-protein interactions

Owing to the apparently controlled biosynthesis of HS polysaccharides and its resulting consequences (presence of structural domains, tissue specificity of the polysaccharide chain compositions - see Section 1.5.2.1), a high degree of specificity/selectivity could, on the face of it, be expected for the interactions of these polysaccharides with proteins. The partial and specificity-based activities of the enzymes suggest that some sequences could be preferentially synthesised, implying that HS-protein interactions could be sequence-specificity driven. HS-anti-thrombin III (AT-III) interaction is often referred as the example which endorses this hypothesis as it has been shown, originally in the 1900's, to require the well-defined DEFGH pentasaccharide sequence to take place (reviewed in Petitou *et al.* (2003)). Any alteration to this pentasaccharide sequence results in significant binding and functional defects (Desai *et al.* 1998, McKeehan *et al.* 1999, Petitou *et al.* 2003). By way of example, Petitou *et al.* (1988) claimed that the rare 3-*O*-sulphate group borne by the F residue is of critical importance. However, these types of studies, meant for finding binding sequences, are often restricted in terms of sequences that are actually screened in the salt-based screens generally used. They also tend to find the most avid binders, which are usually the most highly charged saccharides. However, low sulphated structures have also been shown to fairly strongly interact with proteins (Yates *et al.* 2004, Duckworth *et al.* 2015). Other AT-binding sequences have also since been identified (Guerrini, Guglieri, *et al.* 2008, Guerrini *et al.* 2013). Another interesting example is the case of HS interacting with herpes simplex virus 1 (HSV 1). Studies conducted to determine the minimal HS-binding sequence provided evidences suggesting that an octasaccharide sequence is needed to induce the infection of the target cell (Copeland *et al.* 2008). A high-specificity interaction has not yet been fully established for HSV 1 (Liu *et al.* 2002, Copeland *et al.* 2008).

At the very opposite of its high-specificity interaction with AT-III, HS interacts with the counterpart thrombin in a more non-specific manner, requiring simply a highly sulphated saccharide sequence (Olson *et al.* 1991). Other studies showed that

distinct HS sequences may interact with a protein with comparable affinities, showing that unique sequences are not always needed for protein-binding and biological activity (Ashikari-Hada *et al.* 2004, Zhang, Zhang, *et al.* 2009, Rudd *et al.* 2010). These findings indicate a broad range of relative selectivities. Salmivirta *et al.* (1996) however proposed that a few common residues arranged in a specific order may provide specificity/selectivity to HS-protein interactions as well. These epitopes would however be masked in the whole HS or Hp chain, thus explaining why some proteins might appear to interact with HS in a “non-specific” manner. Thus, Hp may bind to many ligands, yet the minimum binding sites are cryptic within its highly sulphated sequences. This could at least apply in cases where excess sulphation does not inhibit binding.

Owing to the lack of template-regulated biosynthesis, the synthesis of long very specific sequences appears unlikely. Instead, more discrete sequences and specific structural features could be more easily produced compared to whole sequences. The presence of such unusual residues may be the key aspect of specificity/selectivity in HS-protein interactions. This view is supported by the presence of very specific and rare structural modifications, such as 3-*O*-sulphations or unsubstituted glucosamines. As mentioned above, the 3-*O*-sulphate group is a vital feature for interaction with both AT-III and HSV 1. In the case of HSV 1, evidence suggest that an octasaccharide sequence bearing a 3-*O*-sulphate (Shukla *et al.* 1999, Tiwari *et al.* 2005, O'Donnell *et al.* 2006) as well as an *N*-unsubstituted D-glucosamine residue (Liu *et al.* 2002), is required to induce the infection of the target cell. The interactions of HS with L-selectin and Cyclophilin B, as other examples, have also been linked to the presence of these unusual residues (Norgard-Sumnicht and Varki 1995, Vanpouille *et al.* 2007).

According to the accumulation of data obtained in recent decades (as illustrated by the examples given above), there is little evidence that HS recognise their targets with high specificity through entire long sequences. The view that HS-protein interactions are regulated by the specific spatial distribution of the sulphate groups only, as assumed by some groups (Kreuger *et al.* (2001), Nakato and Kimata (2002), Gama *et al.* (2006) and Lamanna *et al.* (2007) to name a few), is also compromised. An appreciation of the HS polysaccharide structures should not be confined to their

primary and linear structural layout and substitution patterns only. Instead, the three-dimensional aspect should be appraised, as well as the impact of the saccharides' direct environment on their architecture and behaviours. The role of many factors such as the chain flexibility and plasticity (Casu *et al.* 1988, Mulloy and Forster 2000, Solari *et al.* 2015), the domain organisation of the HS chains (Kreuger *et al.* 2002), the counter/coordinated ions (Hileman, Fromm, *et al.* 1998, Guimond *et al.* 2009), the solvent (Hricovíni 2011, Li *et al.* 2014) or even the specificities of the HSBDs of the ligands (Mosier *et al.* 2012) should hence be taken into account. As an example, the different conformations adopted by the L-iduronic acid residues, which are found in all characterised HS binding sites, allow the sulphate and carboxylate groups as well as the hydroxyl hydrogens to be presented to the amino acids in different ways in order to favour stronger electrostatic interactions (Das *et al.* 2001, Raman *et al.* 2003). However, these factors should not be considered separately, as they may depend on factors such as the L-iduronic acids' plasticity and the sulphation pattern (Hsieh *et al.* 2016). The investigation of the physico-chemical attributes of these GAGs may also offer a subtler view. Seyrek and Dubin (2010) recently suggested that glycosaminoglycans should be considered as polyelectrolytes, owing to their polyanionic nature. By doing so, many aspects, such as the role of non-specific electrostatic forces (Raman *et al.* 2003, Seyrek *et al.* 2007), the charge density of the GAGs (Meneghetti *et al.* 2015) and the nature and concentration of the ionic environment (Seyrek *et al.* 2003) for example, should be considered in the recognition process. All the factors cited above are believed to have an impact on both binding and biological activation pathways, as they also do for the coordinated ions which have been shown to alter both the structural properties of the ligands and the biological function (Rudd *et al.* 2007, Guimond *et al.* 2009). However, it should be noted that high affinity binding does not always imply high functional activity even though both phenomena appear to be regulated by similar rules (some binding sequences may be inhibitory, for example, as shown by Ashikari-Hada *et al.* (2009)).

In light of what is discussed above, it clearly appears that the notion of specificity/selectivity is still being debated and finding a definitive answer to this question necessitates further investigation. As an example, understanding the exact biosynthesis pathway of Hp/HS could be a first step to decipher the nature of natural variation in HS that underpins its interactions with ligands. Alternatively, the study

of HS Structure Activity Relationship (SAR), with well-defined HS saccharides, would clearly be expected to lead to new insights.

1.7. HS-FGF-FGFR interactions

1.7.1. Fibroblast Growth Factors

The fibroblast growth factor (FGF) family is a family of small extracellular signalling peptides (~150-300 amino acids in total, between 17 and 34 kDa) which all share a core domain of ~120-130 amino acids, with 28 and 6 highly conserved ones and invariant amino acids respectively (Ornitz 2000, Itoh and Ornitz 2004). FGFs are found in both vertebrates and invertebrates and a total of twenty-two members (FGF1-FGF23) have been identified in humans and mice - considering that FGF19 is the human homolog to the rodent FGF15 (Ornitz and Itoh 2001). The human proteins are classified into seven subfamilies according to their structural homologies, as well as their biochemical and developmental properties (Figure 5) (Oulion *et al.* 2012). In addition, they can also be divided into two major groups, according to their mode of action/secretion: the secreted signalling group and the intracellular non-signalling group (Ornitz and Itoh 2015). The secreted signalling group comprises both paracrine (FGF1-FGF10, FGF16-18, FGF20 and FGF22) and endocrine factors (FGF19, FGF21 and FGF23). The intracellular non-signalling group comprises of the rest of the factors (FGF11-14, also called fibroblast growth factor homologous factors (FHF)). FHF's members do not signal through a tyrosine kinase receptor unlike the secreted FGFs (Olsen *et al.* 2003). Instead, they target and regulate the intracellular voltage-gated channels (Goetz *et al.* 2009).

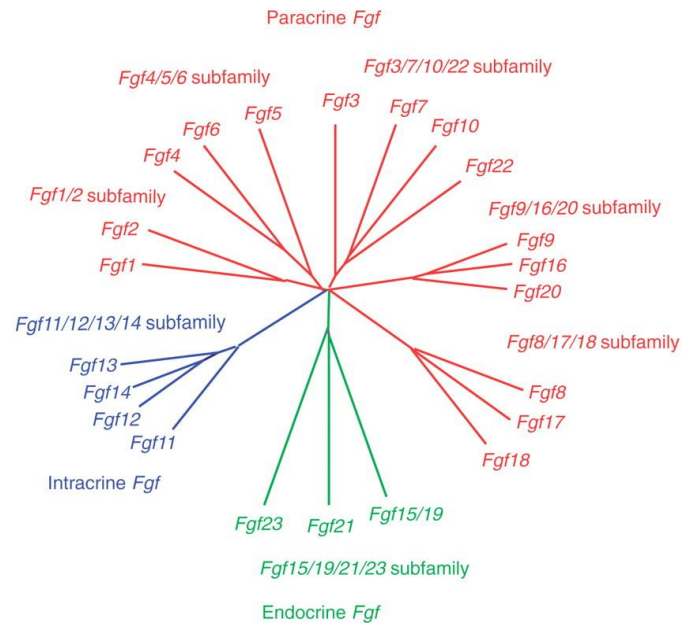


Figure 5: Phylogenetic tree of human FGF family. FGFs are divided into three main groups: the **paracrine**, **endocrine** and **intracrine** FGFs which interact with Hp/HS with high, moderate or no affinity, respectively. Adapted from Itoh and Ornitz (2011) with permission of Oxford University Press.

FGFs have been shown to be involved in and to regulate a broad spectrum of biological processes, including developmental and physiological processes, such as cellular proliferation and migration (Wesley *et al.* 2005), survival (Bouleau *et al.* 2005), differentiation (Spivak-Kroizman, Mohammadi, *et al.* 1994), morphogenesis (Qiao *et al.* 1999) as well as tissue homeostasis (Yamashita *et al.* 2002), wound healing (Mellin *et al.* 1995), and angiogenesis (Ornitz and Itoh 2001). The development of many organs also strongly relies on the signalling of FGFs (Park *et al.* 1998, Robinson 2006, Bates 2007). The importance of FGFs for the integrity of the organisms has been shown by many genetic studies (Itoh and Ornitz 2011). The phenotypes displayed by the knockout mice range from lethality to changes of the physiology of the adult individuals for the majority of the factors (Table 3) (Powers *et al.* 2000). Under normal laboratory conditions, FGF1 knockout mice do not display any significant phenotype as they are viable and look normal (Miller *et al.* 2000). Jonker *et al.* (2012) recently showed that FGF1 is intimately induced in adipose tissues. Moreover, diverse studies have shown that an aberrant signalling of FGFs also leads to diverse human pathologies (Beenken and Mohammadi 2009) such as cancer (Jorgen *et al.* 2011), but also Michel aplasia hereditary disease (Tekin *et al.* 2007) or even phosphate wasting disorders (White *et al.* 2000), to name a few.

FGF	Phenotype of knockout mouse	Physiological role
FGF1*	Diabetes; aberrant adipose expansion (high-fat diet conditions)	Adipose remodelling; metabolic homeostasis
FGF2	Loss of vascular tone; slight loss of cortex neurons	Not established
FGF3	Inner ear agenesis in humans	Inner ear development
FGF4	Embryonic lethal	Cardiac valve leaflet formation; limb development
FGF5	Abnormally long hair	Hair growth cycle regulation
FGF6	Defective muscle regeneration	Myogenesis
FGF7	Matted hair; reduced nephron branching in kidney	Branching morphogenesis
FGF8	Embryonic lethal	Brain, eye, ear and limb development
FGF9	Postnatal death; gender reversal; lung hypoplasia	Gonadal development; organogenesis
FGF10	Failed limb and lung development	Branching morphogenesis
FGF16	Embryonic lethal	Heart development
FGF17	Abnormal brain development	Cerebral and cerebellar development
FGF18	Delayed long-bone ossification	Bone development
FGF19	Increased bile acid pool	Bile acid homeostasis; lipolysis; gallbladder filling
FGF20	No knockout model	Neurotrophic factor
FGF21	No knockout model	Fasting response; glucose homeostasis; lipolysis and lipogenesis
FGF22	No knockout model	Presynaptic neural organiser
FGF23	Hyperphosphataemia; Hypoglycaemia; immature sexual organs	Phosphate homeostasis; vitamin D homeostasis

Table 3: Physiology of FGFs. Adapted from Beenken and Mohammadi (2009), with permission of Oxford University Press. *: see (Jonker *et al.* 2012)

1.7.2. Fibroblast Growth Factor Receptors

The FGF receptors (FGFRs) are essential for the secreted FGFs to signal (Coughlin *et al.* 1988, Lee *et al.* 1989). A total of five genes encoding for the FGFRs have been identified in mammals (Ornitz and Itoh 2015): four which encode for the tyrosine kinase receptors (FGFR1-4, ~800 amino acids) and one which encodes for the non-tyrosine kinase receptor (FGFR5, ~500 amino acids) (Wiedemann and Trueb 2000). The tyrosine kinase receptors consist of two distinct parts, separated by a transmembrane domain (TM). The extracellular part is composed of a cleavable signal peptide (S), followed by three immunoglobulin (Ig)-like domains (IgI-III) with an acid box situated between Ig-I and Ig-II, a Hp-binding site and a cell adhesion molecule (CAM) homology domain (CHD). The intracellular part comprises of a juxtamembrane region (JM), a split tyrosine kinase (TK) domain separated by a kinase insert domain (KI) and a C-terminal tail (CT) (Figure 6) (Mohammadi *et al.* 2005).

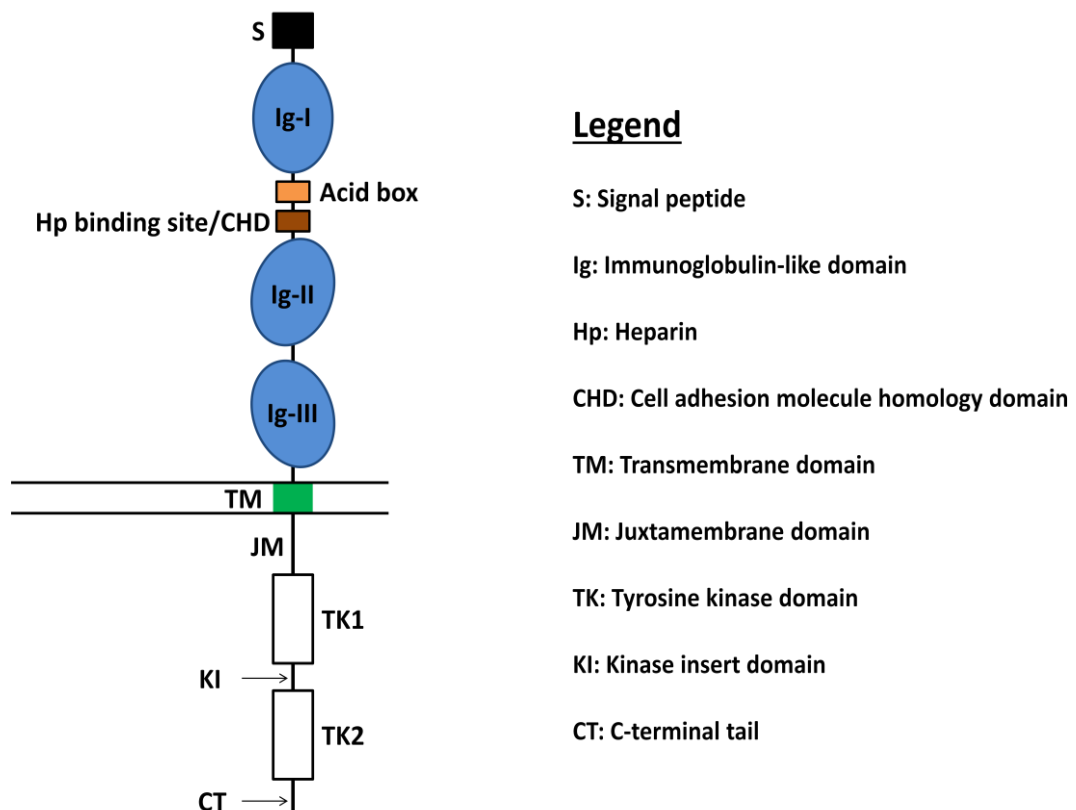


Figure 6: Schematic representation of the FGFR structure.

Several splice variants naturally occur for each variant, except for FGFR4 (Ornitz and Itoh 2015), and their tissue-specific expression has been demonstrated (Fernig and Gallagher 1994). The splicing isoforms differ in their extracellular part, and thus display relatively specific ligand interaction properties (Table 4) (Ornitz *et al.* 1996, Eswarakumar *et al.* 2005, Zhang *et al.* 2006). One main splicing event leads to receptors lacking the Ig-I domain (Johnson *et al.* 1991). However, the major splicing event occurs at the Ig-III domain level and leads to the formation of three types of isoforms. The first of those variants, called Ig-IIIa, codes for a secreted FGF-binding protein which terminates in the Ig-III domain (Duan *et al.* 1992). The two other splice variants, namely Ig-IIIb and Ig-IIIc, are of utmost importance as they determine the ligand-binding properties of the receptors (Ornitz and Itoh 2015). FGF-FGFR specificity has been investigated, mainly with the help of BaF3- and L6 myoblast-based bioassays. FGF1 was found to signal through all receptors whereas some FGFs signal solely through a specific receptor (Table 4). The HS-mediated signalling process is carried out in a cascade manner and starts with the recruitment of the secreted signalling protein which next binds and induces the receptor dimerisation, causing the autophosphorylation of the TKs domain. These first steps trigger successive phosphorylation steps of intracellular substrates, constituting the intracellular transduction signal (Ornitz and Itoh 2015).

As for their counterparts the FGFs, FGFRs have been thoroughly investigated in genetic studies (Eswarakumar *et al.* 2005). As for FGFs, the targeted disruption of specific receptor splice variants causes several phenotypes, ranging from lethality (Yamaguchi *et al.* 1994, Xu *et al.* 1998) to viable and normal individuals (Partanen *et al.* 1998). Mutations have also been shown to be involved in several human diseases (Ornitz and Itoh 2015), notably in Pfeiffer, Crouzon (Rutland *et al.* 1995) and Apert syndroms (Wilkie *et al.* 1995), but also dwarfism (Eswarakumar *et al.* 2002) and cancer (Jorgen *et al.* 2011).

		FGFR						
		1b	1c	2b	2c	3b	3c	4
Paracrine	FGF1	•	•	•	•	•	•	•
	FGF2	•	•		•		•	•
	FGF3	•		•				
	FGF4		•		•		•	•
	FGF5		•		•			
	FGF6		•		•			•
	FGF7			•				
	FGF8				•		•	•
	FGF9		•		•	•	•	•
	FGF10	•		•				
	FGF16				•	•	•	•
	FGF17		•		•		•	•
	FGF18				•		•	•
	FGF20		•	•	•	•	•	•
	FGF22	•		•				•
Endocrine	FGF19		•		•		•	•
	FGF21		•		•		•	•
	FGF23		•		•		•	•

Table 4: Ligand specificity of the FGF receptor family (Ornitz *et al.* 1996, Eswarakumar *et al.* 2005, Zhang *et al.* 2006).

1.7.3. Role of HS in FGF signalling

FGF signalling requires the involvement of many regulating cofactors. Paracrine FGFs display a relatively strong affinity towards Hp and HS, unlike endocrine FGFs and FGFs which display very low or no affinity (Asada *et al.* 2009). Endocrine FGFs require the action of protein cofactors to signal, all members of the Klotho protein

family (Kuro-o 2012) whereas FGFs do not interact with HS. Since the pioneering work of Klagsbrun and Baird (1991), Rapraeger *et al.* (1991) and Yayon *et al.* (1991) who established the role of HS as a cofactor, the complexes FGF1-FGFR2 and FGF2-FGFR1 have served as archetypes to determine the features inherent to the interactions between the signalling protein and its receptor. Despite two decades of investigation using biochemical and crystallographic studies, the exact mechanism is still debated (Pomin 2016).

In the early nineties, Yayon *et al.* (1991) suggested that HS binding to FGF2 was leading to conformational changes of FGF2 into a receptor-compatible - therefore a biologically active - conformation of FGF2. Many studies conducted the following years did not yet corroborate this model (Roghani *et al.* 1994, Springer *et al.* 1994, Faham *et al.* 1996). Even though conformational changes occur upon interaction between the saccharides and FGF (as previously described in Section 1.6.1), other studies showed that HS must bind both FGF and FGFR (Guimond *et al.* 1993) to lead to their dimerisation/oligomerisation - the dimerisation of the receptor then triggering the signal transduction (Kan *et al.* 1993, Spivak-Kroizman, Lemmon, *et al.* 1994, DiGabriele *et al.* 1998). These assumptions were later verified with the help of co-crystallography studies of the ternary complexes (Pellegrini *et al.* 2000, Schlessinger *et al.* 2000). These two studies concurrently led to two conflicting models to explain the molecular interactions between the three entities, even though other models have been proposed as well (Mohammadi *et al.* 2005).

These models mainly differ in their architectures, the molecular assembly mechanism, the stoichiometry of the entities, the attributes of the molecular interactions and the role of the Hp/HS oligosaccharide. Schlessinger *et al.* (2000) described and studied the crystal structure resulting from the manual combination of the crystallographic data of the FGF2-FGFR1 complex with the ones of Hp oligosaccharides. Based on data previously collected (Plotnikov *et al.* 1999), they reasoned that Hp/HS oligosaccharides interact with FGF2 and FGFR1 through the positively charged canyon formed during the assembly of the signalling protein and its receptor. The authors therefore suggested that a stable but biologically inactive 1-1-1 FGF2-FGFR1-Hp/HS ternary complex is first assembled. The recruitment of a second 1-1-1 complex follows this first step and results in the critical dimerisation of

the receptor, thus allowing the formation of the symmetric and biologically active 2-2 entity (Figure 7). This symmetric model is characterised by the critical role played by the non-reducing ends of the oligosaccharides which tightly hold each FGF2-FGFR1 monomer together, as well as the physical contact between the two receptor Ig-II domains, unlike in the asymmetric model proposed by Pellegrini *et al.* (2000). Pellegrini *et al.* (2000) studied the crystal structures they obtained after co-crystallisation of a 2-2-1 stoichiometric ratio mixture of FGF1-FGFR2c-Hp decasaccharide. The authors suggested in this case that, after encounter and assembly of the three entities, Hp induces the dimerisation of FGF1, thus leading to the formation of the biologically inactive 2-1-1 FGF1-FGFR2c-Hp complex. This complex next recruits a second FGFR2c, necessary for receptor dimerisation, to ultimately form the asymmetric 2-2-1 ternary complex (Figure 7). In this model and in the absence of any protein-protein interaction, the two monomeric halves of the complex are held together by the Hp/HS oligosaccharide only. Hp/HS thus plays the role of a “molecular bridge” between the two halves of the ternary complex and displays strong interactions with only the first monomer of the complex but none with the second receptor. The main architecture differences observed between these two models are due to the *cis*- or *trans*-conformation of the invariant proline of the Ig-II/Ig-III linker region of the receptors (Mohammadi *et al.* 2005). The orientation of the Ig-III domains - and thus their interactions with FGFs and Hp/HS - indeed depends on the conformation adopted by this proline residue. It should however be noted that these works were conducted using highly sulphated Hp oligosaccharides, and not with lower sulphated HS saccharides.

Since the publication of these studies, many works have been carried out to identify which architecture is preferred *in vivo*. Each work, based on the combination of several experimental procedures (including analytical ultracentrifugation, bioassays, isothermal titration calorimetry, mass spectrometry, mutational studies, nuclear magnetic resonance, size-exclusion chromatography, three-dimensional cell microarray to name a few) has provided conflicting experimental evidence but most support the symmetric model (Harmer *et al.* 2004, Ibrahimi *et al.* 2005, Brown *et al.* 2013, Nieto *et al.* 2013, Sterner *et al.* 2014). Harmer *et al.* (2004) and Goodger *et al.* (2008), however, suggested the existence of both models in solution. They suggested

that these findings might be relevant *in vivo* as well, and thus constitute proof of the existence of several FGF signalling states.

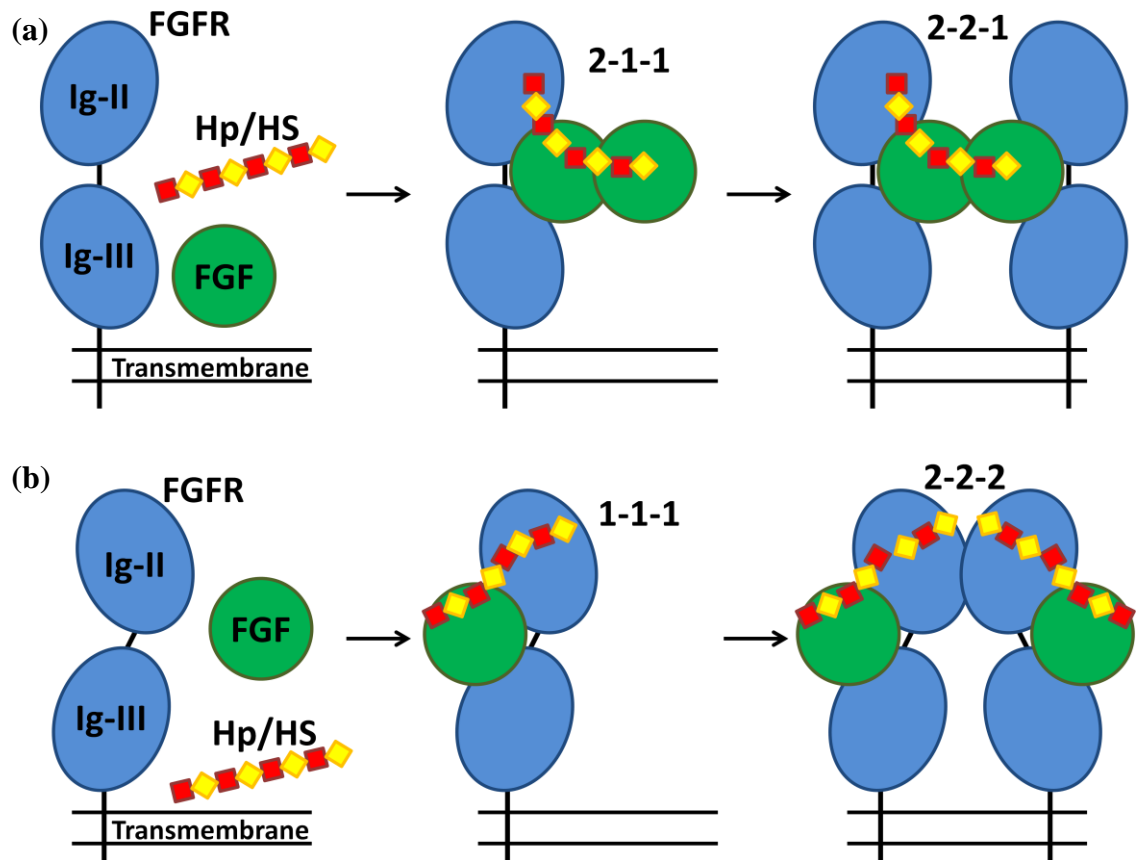


Figure 7: Schematic representation of the formation of the two main FGF-FGFR-HS ternary complexes in competition: (a) the 2-2-1 asymmetric model and (b) the 2-2-2 symmetric model.

(a) The dimerisation of FGF occurs first and results in the formation of the 2-1-1 complex. The receptor dimerisation occurs next and results in the formation of the biologically complex 2-2-1.

(b) The stable 1-1-1 complex is formed first. Both FGF and FGFR dimerisations result from the recruitment of another 1-1-1 complex and lead to the formation of the biologically active 2-2-2 complex.

FGF: fibroblast growth factor; FGFR: fibroblast growth factor receptor; Hp: heparin; HS: heparan sulphate; Ig: immunoglobulin-like domain.

1.7.4. HS specificity/selectivity in FGF-FGFR systems

Owing to the architecture adopted by the protein complexes, FGF signalling requires oligosaccharides long and flexible enough to connect both the signalling proteins and the receptors. Ornitz *et al.* (1992) first showed that octasaccharides were the minimum size required to induce significant biological activity. These findings were

supported by studies carried out later (Mach *et al.* 1993, Fromm *et al.* 1997). However, other groups later showed that even shorter Hp oligosaccharides (down to disaccharides) may be able to induce FGF signalling, even though their mitogenic activities were relatively weak (Tyrrell *et al.* 1993, Ornitz *et al.* 1995, Delehedde *et al.* 2002, Ostrovsky *et al.* 2002, Guglieri *et al.* 2008, Zhang, Zhang, *et al.* 2009). Furthermore, they also showed that the results obtained were dependent on the FGF-FGFR complex studied (Gambarini *et al.* 1993, Ornitz *et al.* 1995, Pye *et al.* 2000, Ye *et al.* 2001, Delehedde *et al.* 2002, Ostrovsky *et al.* 2002). Therefore, no consensus has yet been reached about the minimal size for FGF signalling.

The structural characteristics of the saccharides that are required for optimal binding and biological activity also remain rather unclear. As for the majority of the proteins interacting with HS, the notion of specificity/selectivity in HS-FGF-FGFR interactions is a matter of extensive debate. Over the years, two major concepts have been developed to address the notion of specificity/selectivity in HS-FGF-FGFR interactions. The first concept suggests that there is indeed a link between the discrete and subtle structural properties of the HS polysaccharides and their ability to activate the protein complexes (Guimond and Turnbull 1999, Pye *et al.* 2000, Nakato and Kimata 2002). On the other hand, other groups have suggested that the interactions largely depend on the general structural layout of the glycans and not on their subtle structural differences (Kreuger *et al.* 2005, Jastrebova *et al.* 2006).

Conflicting paradigms and views can be illustrated with the research surrounding the minimal FGF binding motif. Similarly to AT-III, the existence of binding domain, criterion of high-specificity interactions, was first being postulated. Turnbull *et al.* (1992) first reported the characterisation of the binding domain for FGF2 in the literature. The authors determined that the binding sequence was comprised of seven disaccharides and was enriched of the minimal Ido2S-GlcNS disaccharide unit – results supported by other studies (Maccarana *et al.* 1993, Ishihara 1994, Walker *et al.* 1994, Kreuger *et al.* 1999). They next exposed the dependence of FGF1 towards 6-*O*-sulphate groups and the dependence of FGF2 towards 2-*O*-sulphate groups for binding. The latter results were also observed by other groups (Turnbull *et al.* 1992, Maccarana *et al.* 1993, Ashikari-Hada *et al.* 2004, Yuguchi *et al.* 2005). As for AT-III and HSV 1 (see Section 1.6.2), 3-*O*-sulphate groups have been suggested to be of

critical importance for HS oligosaccharides to bind FGF7 and induce its signalling (Capila and Linhardt 2002, Luo *et al.* 2006a, 2006b). Ye *et al.* (2001) also showed that this type of sulphate groups is able to protect FGF7 from proteolysis as well, thus illustrating the importance of this unusual residue.

All these studies helped reveal that specific structural determinants are required for each FGF-FGFR system, on both protein binding and FGF signalling levels (Guimond *et al.* 1993, Ishihara 1994, Pye *et al.* 2000, Ye *et al.* 2001, Allen and Rapraeger 2003, Ashikari-Hada *et al.* 2004, Luo *et al.* 2006a). The existence of this minimal FGF binding site is still discussed in light of other results reported in the literature. Other research groups indeed showed that distinct HS sequences may interact with a protein with comparable affinities, demonstrating that unique sequences are not always needed for protein-binding and biological activity (Ashikari-Hada *et al.* 2004, Zhang, Zhang, *et al.* 2009, Yu *et al.* 2014). Other groups also attempted the re-investigation of this binding domain and its structural characteristics. They came to the conclusion that other sequences may bind FGF with high-affinity and that FGF proteins share binding sites in HS oligosaccharides (Kreuger *et al.* 2001, 2005, Ye *et al.* 2001, Guerrini *et al.* 2002, Guglieri *et al.* 2008). These findings therefore challenge the notion of exquisite specificity of HS-FGF-FGFR interactions.

The two concepts described above mainly rely on the notion of spatial distribution of the ionic charges (sulphate and carboxylate groups) alongside the saccharide chain. However, despite the important role played by the sulphate groups in HS-FGF-FGFR interactions, low sulphated oligosaccharides have also been shown to be good activators (Guimond and Turnbull 1999, Powell *et al.* 2004, Ahmed 2010). Other parameters are now believed to be implicated in the process as well, such as the plasticity of both oligosaccharide chains and specific monosaccharide residues (particularly the L-iduronic residues) (Raman *et al.* 2003, Solari *et al.* 2015) or the nature of the coordinated ions (Rudd *et al.* 2007, Guimond *et al.* 2009). Unsurprisingly, the exclusive presence of flexible L-iduronic acid residues in Hp/HS oligosaccharides has then been shown to be important for high-affinity interactions between the oligosaccharides and FGF2 (Kovensky *et al.* 1996, 1999). Guglieri *et al.* (2008) suggested that the plasticity displayed by the L-iduronic acid residues may be

able to compensate the micro-changes induced by subtle modifications of the sulphation pattern. Later, Rudd and Yates (2010) showed that not all sulphate groups are equivalent in terms of effects on the linkage variations, so affect local chain conformation differently. Finally, it has been found that HS can play the role of both positive and negative regulators, with some saccharides identified in a screen either activating or inhibiting FGF2 signalling or showing neutral activity (Guimond and Turnbull 1999).

1.8. Tools for HS-FGF-FGFR interactions studies

In light of the importance of Hp and HS in biological events (Capila and Linhardt 2002), it then quickly appeared necessary to develop biochemical and biophysical tools to study both these GAGs and their interactions with their ligands. Every tool can help to answer a specific biological question and presents its benefits and limitations (such as the cost, the rapidity to run experiments or the time needed to analyse the results, the biological relevance of the results, etc.). Each of these aspects must be taken into account in the process of selection. The combination of several methods offers a better overview of the biological problem. It must however be noted that the results obtained with *in vitro* and *in vivo* measurements may greatly differ. Reproducing the conditions found *in vivo* (which are often known in vague terms) is nearly impossible due to the complexity of the biological systems that are usually studied. In the case of the study of HS-FGF-FGFR interactions, the density, concentration and distribution of all interacting elements (the signalling proteins, the receptors and all other elements such as ions) found at the *in vivo* level can hardly be reproduced *in vitro*. Different techniques used to study the interactions between HS, FGF and FGFR are briefly discussed in the following sections. The tools used for the preparation of libraries of HS oligosaccharides are discussed first, followed by those used for the structural analysis and the characterisation of the oligosaccharides. The final section will consider the tools applied to the study of the interactions of the saccharides with their protein ligands at a biological level.

1.8.1. Library production methods: HS oligosaccharides from natural sources

1.8.1.1. Extraction of HS from natural sources

The relatively cheap and commercially available Hp has often been preferred over HS as a model for studying Hp/HS-protein interactions. The results obtained are then usually extrapolated to the case of HS. However, due to the structural differences between Hp and HS, the results may be biased. Access to HS oligosaccharide libraries thus appears to be of crucial importance. This has been made possible by the development of techniques of extraction of HS polysaccharide chains from natural sources, mainly from mammals (porcine or bovine origins) (Oduah *et al.* 2016). The extracted polysaccharide chains then usually undergo partial digestion - either by chemical (Shively and Conrad 1976) or enzymatic methods (Linhardt *et al.* 1990) - followed by purification steps and even chemical modifications in some cases (Kariya *et al.* 2000).

Over the years, Hp and HS structures extracted from natural sources have been of great help in answering a multitude of important biological questions, notably the underlying characteristics regulating HS-protein interactions (Pellegrini *et al.* 2000, Petitou *et al.* 2003, Robinson *et al.* 2006) and the natural distribution of the saccharides in tissues (Maccarana *et al.* 1996, Cheng *et al.* 2001, Netelenbos *et al.* 2001, Ledin *et al.* 2004). Extraction from natural sources ideally offers the possibility of accessing a large variety of structures from a single starting batch. However, the amounts of structures that are generally obtained are rather low (usually at the µg scale). The depolymerisation of the chains results in highly structurally heterogeneous mixtures, which then require intensive use of purification methods to obtain pure single structures. The purification steps also cause a significant loss of material. Besides, the full structural characterisation of isolated carbohydrates is only possible during the very last steps of the whole purification process, which makes the isolation of structures of interest, displaying specific sulphation patterns, virtually impossible. In addition, the purity of the material extracted from natural sources may be compromised and go unnoticed. For example, the “2008 Chinese heparin crisis”, which consisted of severe contamination of the Hp supplies by chemically-modified CS polysaccharides, resulted in acute allergic reactions of patients and ultimately led

to more than 200 deaths (Guerrini, Beccati, *et al.* 2008). The contamination went unnoticed because of the limitations of the screening tests that were being used at the time. The extraction from other sources such as invertebrates has since been suggested, even though these GAGs may differ from the mammalian ones on the structural level (Pomin 2015).

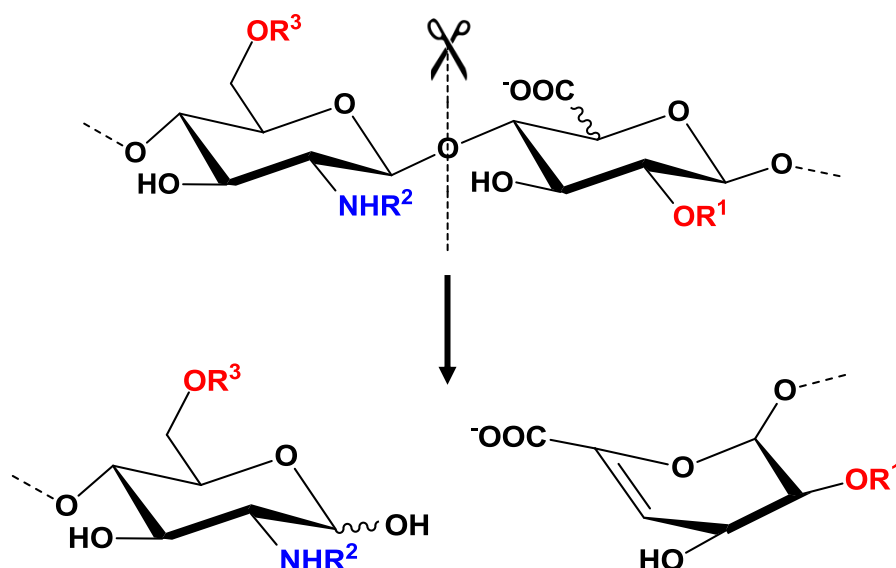
1.8.1.2. Partial digestion of native HS polysaccharide chains

The first step of the preparation of libraries of HS oligosaccharides consists of the degradation of native HS polysaccharide chains into fragments of smaller sizes. This step can be performed by enzymatic digestion, as described below. Other methods such as chemical digestion (Shively and Conrad 1976) or even radical degradation fragmentation are also possible (Kennett and Davies 2009, Higashi *et al.* 2012).

Three different enzymes, expressed from *Flavobacterium heparinum* and named heparinase I-III (also known as heparin lyase I-III or even heparitinase III-I, respectively), are commonly used to enzymatically digest native Hp and HS chains. These enzymes cleave the glycosidic bond between uronic acid and glucosamine residues, as illustrated in Figure 8. The combination of the three enzymes can lead to the near-complete degradation of the chains into disaccharide residues. The enzymatic elimination reactions result in the formation of an intact D-glucosamine residue at the reducing end of the chain and an unsaturated uronic acid residue at the non-reducing end. This double bond which absorbs at $\lambda_{\text{ABS}} = 232$ nm makes the detection of the oligosaccharides by chromatography relatively easy to perform. Each enzyme possesses its own substrate specificities, as described in Figure 8 (Linhardt *et al.* 1990). The partial digestion hence affords heterogeneous mixtures of oligosaccharides of different even-numbered length.

1.8.1.3. Methods of purification of HS oligosaccharide mixtures

Pure single Hp/HS structures are often considered the ultimate tools with which to study details of the biological processes. Nowadays, the access to these structures still remains hampered by diverse technical difficulties, such as the lack of selective and sensitive methods of purification for both isolation and analytical analyses.



Heparinase I ^a	Heparinase II ^b	Heparinase III ^c
$R^1 = \text{SO}_3^-$	$R^1 = \text{H or SO}_3^-$	$R^1 = \text{H}$
$R^2 = \text{SO}_3^-$	$R^2 = \text{Ac or SO}_3^-$	$R^2 = \text{Ac or SO}_3^-$
$R^3 = \text{H or SO}_3^-$	$R^3 = \text{H or SO}_3^-$	$R^3 = \text{H or SO}_3^-$
^a L-IdoA ; ^b D-GlcA or L-IdoA; ^c D-GlcA		

Figure 8: Cleavage specificity of heparinases and resulting products from the cleavages. Enzymatic digestion of HS saccharides results in the formation of an unsaturated uronic acid residue and an intact glucosamine residue at the non-reducing and the reducing end, respectively. The cleavage specificities are described in the table.

However, many have been developed over the years, mainly liquid chromatography-based methods (Korir and Larive 2009). These methods are broadly categorised into two groups, according to the types of separation they allow to perform: either based on the size of the saccharides or on their charges.

Size exclusion chromatography (SEC) - also called gel permeation chromatography or gel filtration - separates heterogeneous mixtures according to their size - or more specifically according to the hydrodynamic volume - of the compounds (Ziegler and Zaia 2006). The compounds are generally eluted with a volatile ammonium salt (isocratic elution), on a stationary phase, which is composed of a matrix beads of

varying pore sizes. The architecture of the matrix creates channels in which the analytes will be diffused. Molecules with a large hydrodynamic radius have limited access to the pores, unlike those with a small hydrodynamic radius, that have an unlimited access to the same pores. Therefore, large molecules have a shorter pathway through the column and are eluted first (Figure 9 (a)). In the case of HS oligosaccharide purification, it should be noted that size-uniform, but structurally heterogeneous mixtures of oligosaccharides are obtained. Same length oligosaccharides may indeed bear the same number of sulphate groups, but at different positions, resulting in equivalent hydrodynamic volumes and elution times. Furthermore, the rigorous separation of the analytes according to their length is unlikely to occur. Following the same reasoning, a low sulphated oligosaccharide may follow a similar path as a highly sulphated but smaller saccharide, resulting in the same elution time for both. Therefore, pure single fractions are unlikely to be obtained with this method of purification alone.

Strong anion-exchange (SAX) chromatography is another commonly used technique in the field, usually to further purify the SEC fractions (Rice *et al.* 1985). SAX has historically been used for the quantification of the disaccharide composition of Hp and HS polysaccharides. This technique separates compounds according to their net charges. The saccharides are retained on a stationary phase composed of a matrix displaying many positively charged functional groups through ionic interactions (the matrix is usually derivatised with quaternary ammonium moieties). The strength of the interactions, therefore, depends of the content of sulphate and carboxylate groups of the analyte. Once the saccharides are bound to the matrix, the ionic strength of the mobile phase (generally a sodium chloride solution) is increased over a gradient in order to detach the analytes from the matrix (Figure 9 (b)). Therefore, low charged analytes will elute first, as they will require a low concentration of counter ion. However, as for SEC chromatography, the use of SAX alone, as a method of purification according to the charge of the saccharide, is usually insufficient. Structurally disparate oligosaccharides, but displaying the same number of sulphate and carboxylate groups, will be eluted with the same or very similar elution times. The use of concentrated solutions of sodium chloride also represents an obstacle to subsequent direct analysis by mass spectrometry (MS), so samples must be desalted prior to any analysis. Since its first use to purify Hp and HS oligosaccharides, SAX

chromatography, as well as other methods, has evolved and been refined. High resolution SAX chromatography on Propac PA1 columns has been described for HS library preparation (Guimond and Turnbull 1999, Powell *et al.* 2010). CTA-SAX chromatography – which has been developed on the model of reverse-phase ion-pairing chromatography (RPIP) - can also be used in combination with SAX chromatography to give another degree of resolution to the separation techniques (Mourier and Viskov 2004). With CTA-SAX, the silica-based and largely hydrophobic matrix of the C18 column is derivatised with cetyltrimethylammonium (CTA) (Figure 9 (c)). The principle of elution is the same as for SAX chromatography (a gradient of salt buffer is used to detach the analytes from the matrix). Recently, a volatile salt-based CTA-SAX method has been described which simplifies oligosaccharide desalting and permits subsequent MS studies of samples (Miller *et al.* 2016). Comparatively, CTA-SAX offers a better resolution than SAX. Yet, the C18 column is less stable and needs to be re-derivatised every 3-4 months.

Other methods such as porous graphitised carbon (PGC) chromatography (Karlsson *et al.* 2005), hydrophilic interaction liquid chromatography (HILIC) (Naimy *et al.* 2008), capillary electrophoresis (CE) (Karamanos *et al.* 1996) and polyacrylamide gel electrophoresis (PAGE) (Turnbull and Gallagher 1990) are also used to perform the composition analysis/achieve the separation of HS oligosaccharides.

The numerous methods of purification that have been developed the past decades and which are cited above make the isolation of single structures from natural sources possible. However, many difficulties still remain (i.e., the low quantity of compound that can be isolated and the lack of control over the structures which can be isolated), which encouraged the development of other methods of production.

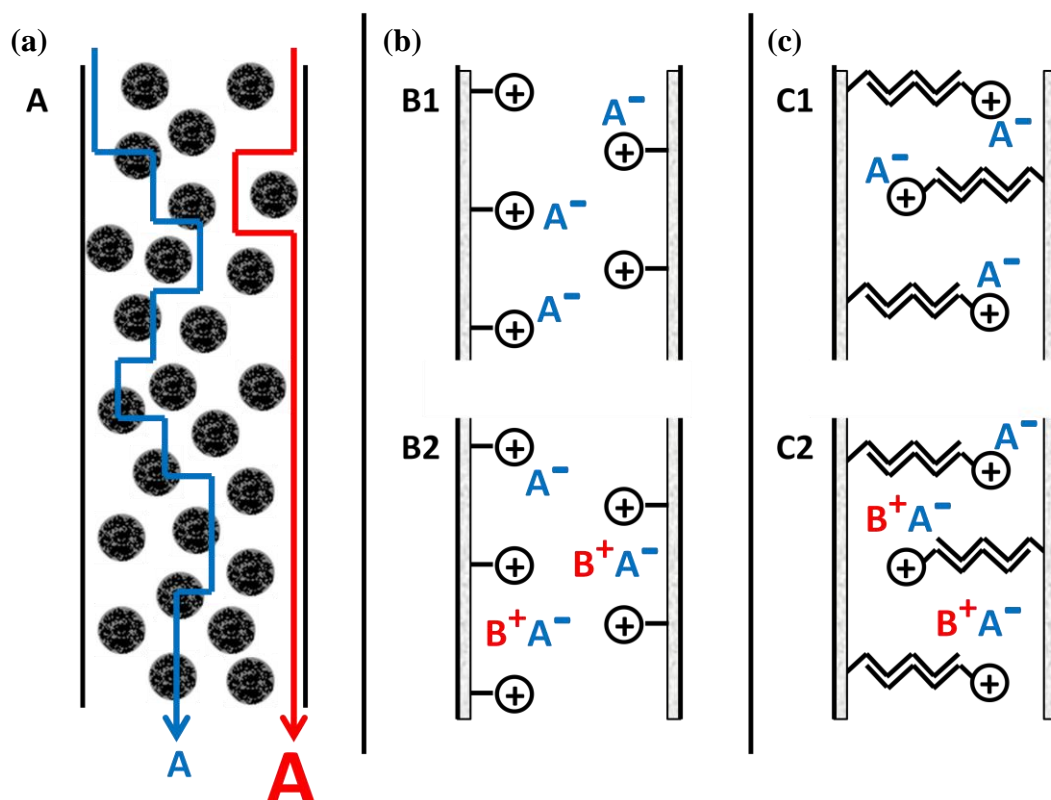


Figure 9: Principle of the main chromatography techniques used to purify HS oligosaccharides: (a) SEC, (b) SAX and (c) CTA-SAX chromatography
 (a) For SEC, the compounds are eluted on stationary phase composed of porous beads and are separated according to their hydrodynamic volumes: the large analytes (**A**) are eluted first and the smaller analytes (**A**) are eluted last.
 (b) For SAX, the negatively charged analytes (A^-) are first retained on the positively charged matrix (**B1**) and are next eluted with a gradient of a positively charged buffer (B^+) (**B2**).
 (c) For CTA-SAX, the negatively charged analytes (A^-) are first retained on a CTA-derivatised C18 column (**C1**) and are next eluted with a gradient of a positively charged buffer (B^+) (**C2**).

1.8.2. Library production methods: synthetic and semi-synthetic methods

Over recent decades, the possibility of preparing relatively complex carbohydrate oligosaccharides from simple and commercially available monosaccharide material has become a reality (Poletti and Lay 2003, Codée *et al.* 2004, Petitou and van Boeckel 2004, Dulaney and Huang 2012, Driguez *et al.* 2014). The relatively fast and recent developments of both organic carbohydrate and enzymatic synthesis methods are intimately linked to the growing demand for pure and well-characterised Hp/HS structures in large quantities. This appraisal can be explained for two

essential reasons. First of all, unlike the preparation of Hp/HS oligosaccharides from biological sources, these methods allow the preparation of structures with specific structural and conformational properties (the structures are followed up at each synthetic step), which ultimately makes the meticulous investigation of the structure activity relationships (SAR) of these GAGs more accessible (Duchaussoy *et al.* 1991, Kovensky *et al.* 1996, De Paz and Martín-Lomas 2005). Secondly, obtaining large quantities of homogeneous batches of glycan oligosaccharides is possible with synthetic and semi-synthetic methods. However, carbohydrate synthesis remains challenging, as a few limitations remain to be overcome. First of all, the synthesis of a single Hp/HS oligosaccharide may be lengthy. A famous example, the chemical synthesis of Fondaparinux (Arixtra), requires more than 50 steps to be achieved (Petitou *et al.* 1989). In most cases, this kind of synthesis indeed requires the manipulation of specific hydroxyl groups in the presence of many others, as well as the manipulation of chemical moieties that must remain unaffected until they need to be modified in their turn. Secondly, the poor reliability of the glycosylation reactions also remains problematic. Another major issue is related to the intrinsic nature of the glycans themselves. Owing to the structural heterogeneity of Hp/HS saccharides, it is extremely complicated to set up a general method to prepare distinct structures. Every structure is hence often considered as the target of a whole project that may take months or even years to be carried out. Moreover, even the slightest modification of a glycan structure might require redesigning the whole synthetic route.

Since the pioneering work by Sinaÿ, Petitou and others in the eighties who first synthesised the DEFGH pentasaccharide sequence that binds AT-III with high affinity (Sinaÿ *et al.* 1984), several approaches have been developed in order to synthetically prepare saccharides of various lengths. These approaches can be divided into three main categories. The first approach is the classical multi-step solution-phase synthesis, which is the most common way of synthesising saccharides and laid the foundations for most of the other approaches. In this case, orthogonally protected synthons are prepared in solution and then assembled in order to form oligosaccharides/polysaccharides of the desired length through chemical glycosylation reactions. This step is followed by further modifications of the glycan backbones (modification of the protecting groups (PGs), deprotection) and finally by

the functionalisation of the compounds (sulphation, acetylation). The strength of in-solution synthesis lies in the fact that it has been extensively developed and a consequent number of synthons and PGs have already been described in the literature (Wuts and Greene 2006, Dulaney and Huang 2012, Mende *et al.* 2016). Nevertheless, this approach is material and time-consuming, as it requires a consequent number of manipulations and purifications at each stage of the synthesis. It also does not offer the possibility to develop an automated and high-throughput synthesis of oligosaccharides. This last point is a considerable disadvantage compared to the other methods that have been developed and which, therefore, offer the possibility of creating libraries of glycans presenting a broad range of structural differences in a relatively short period of time.

The second category, the automated synthetic approach, includes both the one-pot multi-step synthesis and the solid-phase synthesis (also called polymer-supported synthesis). One-pot multi-step synthesis has known major advances (Polat and Wong 2007, Wang *et al.* 2010, Wu and Wong 2015). In the late nineties, Zhang *et al.* (1999) even paved the way for programmable one-pot synthesis. On the other hand, solid-phase synthesis still remains a great challenge for chemists (Sears and Wong 2001). Interest in solid-phase glycan synthesis has emerged after the success encountered by polymer-supported peptide synthesis. However, many issues arose while trying to adapt this strategy, mainly due to the lack of adapted materials (resins, linkers, PGs) and the absence of efficient glycosylation methods. Nevertheless, recent advances in chemistry have helped address some of those issues and the possibility of finding a solution for a routine and automated synthesis of oligosaccharides is getting closer (Sears and Wong 2001, De Paz *et al.* 2006, Lepenies *et al.* 2010, Czechura *et al.* 2011, Guedes *et al.* 2015). For both cases, selectively protected glycosyl donors and acceptors are prepared in advance in solution. Then, in the case of one-pot multi-step synthesis, the synthons are sequentially assembled in the same flask and then modified before functionalisation of the oligosaccharides. In the case of polymer-supported synthesis, a first synthon is attached to a resin which has been previously derivatised with a linker, followed by the elongation of the glycan through successive glycosylation reactions. Once the right size is obtained, the glycan is cleaved from the resin and then deprotected before its sulphation. Cleaving the glycan from the resin is carried out before the

deprotection step in order to facilitate the purification of the glycan at two levels. Firstly, the absorbance of the benzyl ether and benzoyl ester protecting groups greatly helps monitoring. Secondly, purifying the fully protected glycan from unwanted side-products, like glycans with a lower degree of polymerisation, is significantly easier than carrying out the purification at the stage of unprotected carbohydrates.

As its name suggests, the automated approach would allow the rapid and high-throughput production of glycan libraries for a relatively low number of manipulations, even though much remains to be done. One-pot multi-step synthesis still indeed requires researchers to progress in the elaboration of suitable building blocks, with the appropriate reactivity properties, as well as some progress in synthetic strategies. Regarding solid-phase synthesis, research is still focused on finding the appropriate conditions for each step that will be easily applicable to an automated version of this kind of synthesis. Other issues still need to be addressed such as the fact that a substantial amount of glycosyl donor is required to complete a single step of chemical glycosylation, or even the last steps for the linker functionalisation and PG modifications.

The last category includes both the enzymatic and the chemoenzymatic approaches, which - as their name suggest - involves enzymes in order to introduce, modify or remove chemical functions or even sugar moieties to or from a maturing oligosaccharide chain (Wong 1995, Blixt and Razi 2006). Two main methods have been investigated, involving glycosyltransferases and reverse-activity glycosyl hydrolases, even though glycosynthases have also been introduced as new efficient tools (Mackenzie *et al.* 1998, Cobucci-Ponzano and Moracci 2012). Enzymatic and chemoenzymatic approaches are both powerful tools that can help shorten the synthetic routes, and, therefore, help save a considerable amount of time when preparing libraries of glycan oligosaccharides (Kuberan *et al.* 2003, Chappell and Liu 2013, DeAngelis *et al.* 2013, Liu and Linhardt 2014). Unlike the first two approaches, this one does not rely on the use of PGs at all and the reactions are carried out in aqueous solutions at room temperature. Many sequences of interest have been synthesised, proving the efficacy/efficiency of these methods. Amongst those sequences, the well-known AT-III binding domain has been produced

(Kuberan *et al.* 2003). Examples of other works of interest are: 1) the syntheses of oligosaccharides concurrently displaying anti-factor Xa and IIa activities (Xu, Pempe, *et al.* 2012); 2) the syntheses of ultra low molecular weight heparins (ULMW) (Xu *et al.* 2011, Masuko and Linhardt 2012) and 3) the synthesis of HS oligosaccharides displaying a range of affinity towards FGF2 and which, therefore, allow the SAR of these GAGs (Xu, Wang, *et al.* 2012). Yet, many issues still need to be addressed, such as the substrate selectivity of the enzymes, which are not yet well characterised, the expense which also limits the number of usable building blocks, or even the lack of readily available glycotransferases and glucuronyl C-5 epimerase (converting glucuronyl residues into iduronyl residues), as well as the limited life-time of those enzymes. Ultimately, both enzymatic and chemoenzymatic approaches will help develop another type of automated glycan synthesis.

1.8.3. Tools for HS structures analysis

Deciphering the SAR of HS with its ligands is intrinsically linked to the structural analysis of the saccharides. This latter is hampered by the lack of a unique, cheap, fast and consistent method to analyse any type of oligosaccharide. Many techniques have been developed, each allowing the study of specific structural characteristics of HS saccharides, such as their sequences, the exact nature and anomeric state of their monosaccharide components or their conformations. The combination of several methods is hence generally required to gather sufficient data to precisely sequence the saccharides. However, HS sequencing is hampered by a number of factors. First of all, the oligosaccharides must be sufficiently pure and clear of any contaminants such as salts. A rigorous and lengthy purification process of the glycans (as described in Section 1.8.1.3) is required, even though this involves significant losses of material. This, therefore, aggravates the fact that the access to consequent amounts of material is limited, mostly due to the intrinsic heterogeneity of HS. Some techniques, such as nuclear magnetic resonance (NMR), require large amounts of material (generally a few mg). Finally, HS is very sensitive to high and low pH conditions, its sulphate groups are prone to migration during ionisation processes (mass spectrometry (MS)), and it is insoluble in the common organic solvents (Drummond *et al.* 2001, Powell *et al.* 2004), which complicates its manipulation. It hence appears that developing fast, cheap, sensitive, consistent and reliable methods/methodologies

are required. All the problems mentioned above are not encountered during the production of HS oligosaccharides by both synthetic and semi-synthetic methods, as their structural properties are monitored throughout the synthesis.

Two main approaches have been developed to determine the structures of the HS oligosaccharides. The first approach consists of enzymatic or chemical degradation of the HS oligosaccharides (labelled or not), the separation of the fragments (CE, PAGE or SAX), followed by their analysis by chromatography or MS (disaccharide composition quantification) (Turnbull *et al.* 1999, Vivès *et al.* 1999, Mourier and Viskov 2004, Skidmore *et al.* 2010, Leary *et al.* 2015). The second approach relies on the direct structural characterisation of the whole sequences by NMR (Yates *et al.* 1996, Mulloy and Forster 2000) or MS (Miller 2011).

NMR spectroscopy is based on the study of the behaviour of the atoms nuclei (mainly ^1H , ^{13}C , but also ^{15}N , ^{31}P isotopes) in a magnetic field and subjected to an electromagnetic pulse (Gerothanassis *et al.* 2002). Their behavioural variations are directly linked to their direct environment (neighbouring atoms). The energy accumulated (field on), then released during the relaxation by the nuclei (field off) is recorded as spectra for interpretation. Two types of spectra can be recorded: the one-dimensional (1D) or two-dimensional (2D) spectra, which both give different insights at the structural organisation of the saccharides (Bubb 2003). ^1H and ^{13}C NMR spectra (both 1D NMR experiments) are used to have an overview of the structure of the saccharide, determine the number of residues, as well as the anomeric state of each one of them. However, 1D NMR techniques appear limited when it comes to the full characterisation of long saccharides, largely because of signal overlap. In this case, the combination of 2D NMR techniques allows the full assignment of the ^1H and ^{13}C NMR spectra (common 2D NMR techniques include COSY, TOCSY, HSQC, and NOESY) (Bubb 2003). Despite the advantages offered by this technique (fast, cheap, precise characterisation of the residues), NMR requires a relatively large amount of pure material (though reduced with recent cryo probes) and is not suitable for the study of structurally redundant oligosaccharides, even though it has been shown to be possible (Shriver *et al.* 2000).

MS is an analytical method which involves the ionisation of molecules and which affords charged molecules or molecular fragments. The mass-to-charge ratios (m/z) of the fragments are measured and recorded for interpretation. To sequence HS oligosaccharides, two main techniques are commonly used: electrospray ionisation (ESI) (Zhang and Linhardt 2009) and matrix-assisted laser desorption/ionisation (MALDI) which is often used in tandem with time of flight detection (TOF) (MALDI-TOF) (Tissot *et al.* 2007). Therefore, despite the challenging task that represents HS sequencing for MS, mainly due to the heterogeneity of the glycans, the presence of isomers, the loss of sulphate groups during ionisation (Strecker *et al.* 1987) and the difficulty for HS oligosaccharides to fly (due to their highly charged properties), this technique has been intensively used in the field. MS has been mainly used for disaccharide composition quantification, either on its own (offline mode) or in tandem with CE or HPLC (online mode) (Linhardt *et al.* 1989, Chi *et al.* 2005, Doneanu *et al.* 2009, Zaia 2009). Many advances have been made, including the use of better and more appropriate matrixes or complexing cations (Tissot *et al.* 2007). Another breakthrough in the domain is the use of tandem MS (also called MS/MS or MS²) for HS sequencing (Saad and Leary 2003, Naggar *et al.* 2004, Zhang and Linhardt 2009, Miller 2011). Even more recently, Ion Mobility MS (IMMS) has also been shown to offer the possibility of distinguishing the uronic acid isomers (Leary *et al.* 2015). These recent advances make routine sequencing of HS by MS a possibility in the future.

1.8.4. Tools for HS-FGF interactions studies

Aberrant FGF signalling has been linked to many diseases (Belov and Mohammadi 2013). Understanding the interactions between the saccharides and their protein ligands - in other words, identifying the structural determinants of HS-FGF-FGFR interactions – therefore, appears to be necessary to fully decipher these disease pathways and potentially develop HS saccharides-based therapeutics (Coombe and Kett 2005). Both aspects of these interactions - the binding and the functional activity interactions – have been thoroughly investigated over the last decades, as described in the following sections. The combination of both types of analyses is vital to understand the SAR of HS with FGF, as subtle structural changes may greatly affect the biological activity of the proteins (Rahmoune *et al.* 1998).

Numerous techniques and methods have been developed to have a better insight into the structural determinants of HS-FGF interactions. Depending on the method/technique used, the type of information obtained will vary, ranging from data about binding kinetics/thermodynamics to binding affinities and structural information.

Surface plasmon resonance (SPR) is a powerful technique that allows binding events to be measured in real time and, therefore, makes the study of the kinetics of heparin-protein interactions possible (Capila *et al.* 1999). Here, one of the interacting species (usually FGF) is flowed over the surface of a chip, onto which the other interacting species (usually the saccharides) has been immobilized. Upon interactions, the refractive index of the chip changes. This change is directly proportional to the amount of the species being bound, which gives a real-time measurement of the association and dissociation rate constants (k_a and k_d , respectively). The SPR technique can also be used to study the binding affinities between HS and its ligands (Cochran *et al.* 2009).

Other methods to study binding affinities exist. Most of the techniques requires the immobilisation of one of the interacting elements (either the saccharide or the protein) onto a surface and allow the direct measure of binding parameters such as the equilibrium binding and dissociation constants (K_a and K_d respectively). Notably the binding affinities of HS for FGF and FGFR have mainly been studied with the help of affinity chromatography (Rapraeger *et al.* 1991, Jemth *et al.* 2002). This technique helps measuring the contribution of the ionic forces in the binding affinities. Other techniques such as affinity co-electrophoresis (ACE) (San Antonio *et al.* 1993) and ultracentrifugation (Harmer *et al.* 2004, Nieto *et al.* 2013) as well as optical/competition biosensors (Mach *et al.* 1993, Powell *et al.* 2002, Cochran *et al.* 2009, Xu, Ori, *et al.* 2012) have also been intensively employed. Lately, Uniewicz *et al.* (2010) developed a method based on the principle of the differential scanning fluorimetry (DSF) technique to study binding affinities and which later helped unravel secondary binding sites in FGFs (Xu, Ori, *et al.* 2012). DSF is a powerful technique which is routinely used to evaluate the conformational changes that occur at the protein level, when the latter is put in the presence of a binding partner.

The thermodynamic parameters of HS-protein interactions can also be evaluated with the help of isothermal titration calorimetry (ITC), a technique which gives a better overview of the contribution of the non-ionic forces to the binding interactions (Pantoliano *et al.* 1994, Fromm *et al.* 1997, Leavitt and Freire 2001). This last technique, however, requires large amounts of material for both the saccharide and the binding protein (on the order of mgs).

All the techniques that are cited above allow the direct measurements of the interactions. Performing such measurements requires the constant development of more robust, reliable platforms. Lately, the recent advances made in carbohydrate chemistry have provided the possibility of developing microarrays (Noti *et al.* 2006, Takada *et al.* 2013, Sterner *et al.* 2014) which could be used to carry out the quantitative and qualitative analyses of binding interactions in a high-throughput manner. Obtaining structural information, such as the contact points, is another vital element to better understand HS-protein interactions. Such information can routinely be obtained with the study of crystallographic structures of HS-FGF-FGFR complexes (Ye *et al.* 2001), the study of HS-FGF complexes by NMR (Nieto *et al.* 2013) or the use of molecular modelling/molecular dynamics techniques to identify the residues involved in both the binding and functional interactions. Despite being very promising, these methodologies are not always well-suited because they require large amounts of material. Moreover, other types of limitations, such as having access to powerful computer clusters, or the time needed to run a simulation, often limit the use of these techniques. On the other hand, investigations into the structural changes that occur at both the protein and saccharide levels are of utmost importance, as saccharide-protein interactions are believed to induce conformational changes (Guimond *et al.* 2009). DSF and synchrotron radiation circular dichroism (SRCD) (Wallace and Janes 2010, Xu, Ori, *et al.* 2012), crystallographic studies (DiGabriele *et al.* 1998, Pellegrini 2001, Xu, Ori, *et al.* 2012), and others provide the possibility of carrying out such studies.

As seen above, there is an extensive (but not exhaustive) list of techniques that can be used to study the binding interactions. Each has allowed the structural determinants of HS-FGF-FGFR interactions, as seen in Section 1.7.4, to be determined. In contrast, functional activity analysis of HS requires the use of cell-

based assays. As most of the cells express endogenous HS, it is extremely difficult to work with any type of cells. Therefore, cell lines have been derived which lack endogenous HS (e.g. BaF3 cells (Ornitz *et al.* 1992, Zhang *et al.* 2006)). This can also be achieved by treating the cells with sodium chlorate for example. This leads to the inhibition of the enzyme synthesising the sulphate donor PAPS (Rapraeger *et al.* 1994). PAPS is required for the biosynthesis of HS chains as described in Section 1.5.1.3. Treating the cells in such a way hence leads to the synthesis of unsulphated (and therefore inactive) HS chains (e.g. the Swiss 3T3 fibroblasts (Rapraeger *et al.* 1991) and Rama 27 (Rahmoune *et al.* 1998) cell lines).

1.9. Aims

The role played by HS in the regulation of FGF signalling has been well established throughout the years, as reviewed in this chapter. Despite the considerable effort put into the study of the SAR of HS, little is known about the determinants of the interactions between the saccharides and FGF and FGFR. This can be mainly explained by the limitations that are inherent to the methodologies and techniques that are commonly used in such studies. Access to both large amounts of material and broad libraries of saccharides are indeed impeded by the methods of production and extraction of the HS saccharides. In addition, only a few papers in the literature report the study of the saccharides SAR with the help of relatively similar structures. The majority of the HS oligosaccharide libraries used in most works published in the literature are structurally heterogeneous. This negates the possibility of studying the impact of subtle structural changes on the functional activity of the saccharides. The development of fast and robust synthetic routes should be able to overcome this problem.

The aims of this thesis were therefore the following:

- The preparation of a library of HS structures from porcine mucosal HS (PMHS) and their screening in BaF3-bioassays.
- The development of a new synthetic strategy to aid the fast and efficient preparation of HS oligosaccharides and therefore the chemical synthesis of defined structures.

- The screening in BaF3-based bioassays of chemically and enzymatically prepared oligosaccharides displaying relatively similar structures (in collaboration with Prof. J. Liu (The University of North Carolina, Chapel Hill, NC, USA) and Prof. P. Tyler (Victoria University, Wellington, New Zealand)).
- The evaluation of the impact of structural changes on FGF signalling.

2. Chapter 2 – Materials, methods, procedures and characterisation data

2.1. Preparation of Hp/HS oligosaccharide libraries from natural sources

2.1.1. Materials

Porcine Mucosal HS (PMHS) was purchased from Celsus Laboratories (Cincinnati, Ohio, USA) and stored at -20 °C, until use. Recombinant heparinase III from *Flavobacterium heparinum* was purchased from IBEX (Montreal, Quebec, Canada) and stored at -80 °C, until use. Disaccharide standards were purchased from Dextra Laboratories (Reading, UK) and stored at -20 °C. All chemical and biochemical reagents were of analytical grade, used as received unless otherwise stated and were purchased from Sigma and VWR (UK). Milli-Q water was obtained from a ELGA purelab flex system (ELGA, Veolia Water, Marlow, UK). All reagents were stored as instructed by suppliers. Unless otherwise indicated, all experiments were performed in sterile and dry laboratory glassware/plasticware.

2.1.2. Methods

2.1.2.1. Enzymatic partial digestion

Before performing the large-scale enzymatic partial digestion, a small-scale enzymatic digestion was carried out on a 1 mg trial batch, in order to determine the right conditions needed for successful partial digestion. Once the appropriate amount of enzyme and the reaction time were established, the partial digestion of 400 mg PMHS was carried out. Both small and large-scale experiments were performed in 1x lyase buffer (100 mM sodium acetate, 10 mM calcium acetate, (pH 7.0) at 37 °C (Powell *et al.* 2010)) and were monitored at several time points by small scale Size Exclusion Chromatography (SEC). For small-scale SEC, the isocratic elution of 100 µg material was carried out using a Superdex™ peptide 7.5/300 small scale SEC column, at 0.2 mL/min (buffer: 0.5 M ammonium bicarbonate) and was monitored by absorbance at $\lambda_{\text{ABS}} = 232$ nm. The digestion processes were stopped by boiling at 100 °C for 2 minutes. The 400 mg PMHS were first digested with heparinase III at a concentration of 2 mU/mg PMHS (80 mU/mL) for 1 hour. At the end of the first hour of digestion, more heparinase III was added (at the rate of another 2 mU

enzyme/mg of PMHS) and the digestion was performed for 9 hours. All enzymatic partial digested saccharides were lyophilised and stored at -20 °C, until further use.

2.1.2.2. PAGE oligosaccharide separation

Polyacrylamide gel electrophoresis (PAGE) was used to analyse size fractionated digested PMHS oligosaccharides (Turnbull and Gallagher 1988). The running buffer used was 30 mM Tris, 20 mM MES (pH 8.0). The samples were first diluted with sample buffer (70% glycerol/30% running buffer, v/v), to which 10% phenol red (w/v) was added. The samples were next loaded into the wells of the loading gel (7.5% acrylamide, w/v). The electrophoresis was achieved at a constant voltage of 200V for 4 hours, until the phenol red marker migrated to about 2/3 of the way down of the resolving gel (33% acrylamide, w/v). Oligosaccharides were stained with 0.08% Azure A solution (w/v) for 1 hour. Excess dye was then removed by washing the gels several times (and overnight) with deionised water. Images of the gels were taken using a digital camera.

2.1.2.3. SEC chromatography

The partially digested samples were re-suspended in Milli Q water to obtain solutions at a concentration of 50 mg/mL. With the help of a Hamilton syringe, 1 mL of sample was loaded into the 5 mL loop of the AKTA purifier 10 (GE Healthcare), after verifying that the sample was free of air bubbles. The fractions were eluted through two Superdex™ 30 XK 16 columns connected in series, with 0.5 M ammonium bicarbonate NH_4CO_3 (isocratic buffer) at a constant flow rate of 0.5 mL/min (Feyzi *et al.* 1997). The elution of the samples was monitored at $\lambda_{\text{ABS}} = 232$ nm (wavelength of absorption of the unsaturated double bond at the non-reducing end of the saccharides generated during the lyase enzymatic digestion). One mL fractions were collected between 130 and 330 mL of elution volume. Selected peak fractions were pooled, prior to desalting.

2.1.2.4. Desalting SEC fractions

Pooled SEC fractions underwent several cycles of lyophilisation in order to remove volatile ammonium bicarbonate salt (Goodger *et al.* 2008). Samples were first diluted with Milli-Q water (up to a total volume of 5 mL), frozen at -80 °C for 30 minutes and then freeze-dried until complete evaporation of the solvent. The dilution/freezing/freeze-drying cycle was repeated until complete removal of ammonium bicarbonate salt (generally, 5 cycles were sufficient).

2.1.2.5. SAX chromatography

Further fractionation and purification of the partially digested PMHS oligosaccharides was performed based on their charges, applying strong anion-exchange (SAX) chromatography (Turnbull *et al.* 1999), using Shimadzu LC-20AD HPLC equipped with a semi-preparative Propac-PA1 column (9 x 250 mm, Dionex). Prior to any run, the whole system was washed sequentially, at a flow rate of 1 mL/min, with Milli-Q water (10 min), 2 M sodium chloride (10 min) and finally with Milli-Q water (10 min). The sample was re-suspended in Milli-Q water (maximum 5 mg/0.5 mL), loaded onto the 1 mL injection loop and applied to the Propac PA1 column at a constant temperature of 40 °C with Milli-Q water (1 mL/min). The flow rate was maintained at 1 mL/min, and the sample was eluted with a linear gradient of 0-80% solvent B over 120 minutes (solvent A: Milli-Q water; solvent B: 2 M NaCl (HPLC grade), (Powell *et al.* 2010)). The elution was monitored by absorbance at $\lambda_{\text{ABS}} = 232$ nm. The fractions were manually collected, after considering the short delay time between the UV/Vis detector unit (SPD-20A, Shimadzu) and the collector. Fractions corresponding to the same elution times were pooled and stored for further use.

Further separations of selected fractions were performed on the same HPLC system, using a Propac PA1 analytical column (4 x 250 mm, Dionex). Prior to any run, the whole system was washed sequentially, at a flow rate of 1 mL/min, with Milli-Q water (10 min), 2 M NaCl (10 min) and finally with Milli-Q water (10 min). Each fraction was diluted with Milli-Q water (1/10 to 1/20, v/v) and individually loaded onto the column at a constant temperature of 40 °C with Milli-Q water (1 mL/min). Each sample was eluted with a suitable gradient of NaCl buffer (HPLC grade,

gradient details are given for each individual chromatogram, see Sections 3.2.3 and 3.2.4). The elution was monitored by absorbance at 232 nm. Fractions were manually collected and stored for further use. The column was reconditioned in Milli-Q water prior to purification of the next sample.

2.1.2.6. CTA-SAX chromatography

Final fractionation and purification of the PMHS oligosaccharides was performed applying CTA-SAX chromatography (Mourier and Viskov 2004) and using a Shimadzu LC-20AD HPLC equipped with a C18 column (4.6 x 250 mm, 5 μ m bead size, Supelco) derivatised with cetyltrimethylammonium (CTA). The derivatisation of the C18 column was performed in three stages. First, the column was pre-conditioned by washing with pure methanol (MeOH) overnight. Secondly, the column was equilibrated overnight with a 1 mM CTA hydrogen sulphate in MeOH/water (50/50, v/v) solution. Finally, the whole system was washed sequentially, at 1 mL/min, with buffer A over 10 minutes (buffer A: Milli-Q water), buffer B over 10 minutes (buffer B: 2 M ammonium bicarbonate, HPLC grade) and finally with buffer A over 60 minutes. Each SAX sample was individually diluted with Milli-Q water (1/15, v/v), loaded onto the 1 mL injection loop and applied to the column with Milli-Q water (1 mL/min). The flow rate was maintained at 1 mL/min, and each sample was eluted with a 25-70% gradient over 60 min using 2 M NH_4CO_3 (HPLC grade) as the elution buffer. The elution was monitored by absorbance at $\lambda_{\text{ABS}} = 232$ nm. The fractions were manually collected, after considering the short delay time between the UV/Vis detector unit (SPD-20A, Shimadzu) and the collector. Fractions corresponding to the same elution times were pooled prior to desalting. The column was reconditioned in Milli-Q water prior to the separation of the next sample.

2.1.2.7. Desalting CTA-SAX fractions

CTA-SAX fractions underwent several cycles of desalting to remove the volatile ammonium bicarbonate salt using a Univapo 150 ECH vacuum concentrator (UniEquip) connected to a cold trap. Between each cycle, the samples were diluted with Milli-Q water (up to 800 μ L maximum) and a total of 5 cycles were performed for complete desalting.

2.2. BaF3 bioassays

2.2.1. Materials

Chemoenzymatically prepared octasaccharides [Oct2S, Oct2,6S and Oct2,6+3S], decasaccharides [Dec2S, Dec2,6S and Dec2,6+3S], and dodecasaccharides [Dod2S, Dod2,6S and Dod2,6+3S] were a gift from Prof. J. Liu (The University of North Carolina, Chapel Hill, NC, USA). Chemically prepared octasaccharides [Oct6SIdo, Oct6SIdo2S, Oct6SGlc and Oct6SGlc2S], decasaccharides [Dec6SIdo, Dec6SIdo2S, Dec6SGlc and Dec6SGlc2S], and dodecasaccharides [Dod6SIdo and Dod6SIdo2S] were a gift from Prof. P. Tyler (Victoria University of Wellington, New Zealand). All oligosaccharides were diluted in Milli-Q water and stored at -20 °C until use. Human recombinant (rh) Fibroblast Growth Factors (FGF) rhFGF1, rhFGF2, rhFGF7 were purchased from R&D systems and stored as instructed by the supplier. All chemical and biochemical products were of analytical grade, purchased from Sigma, VWR, R&D, Invitrogen/Gibco (Spain) and used as supplied, unless otherwise stated. Milli-Q water was obtained from a water purifier. Unless otherwise indicated, all experiments were performed in sterile and dry laboratory glassware or plasticware.

2.2.2. Method

BaF3, a murine Interleukin-3 (IL-3) dependent pro-B cell line that does not express either endogenous HS or FGFR, was used in bioassays to investigate FGF signalling. These cells, which are transfected with cDNAs encoding specific FGF isomers, can be used as an HS-dependent assay for FGF signalling responses (Ornitz *et al.* 1992). The BaF3 cells used for this project have previously been transfected with specific FGFRs (FGFR1c and FGFR2b) (Ornitz *et al.* 1996), and were maintained in BaF3 growth medium (RPMI 1640 medium, 10% (v/v) Foetal Bovine Serum (FBS), 1 mM L-glutamine, 1 mM penicillin G, 1 mM streptomycin), in the presence of mouse recombinant (rm) rmIL-3 (1 ng/mL) and G418 (600 µg/mL). Cells were routinely maintained at a density of 500,000 – 1,000,000 cells/mL, in the incubator at 37 °C, in 5% CO₂ (v/v).

For testing signalling responses of different FGF-FGFR combinations to the presence of HS oligosaccharides, all solutions were prepared with BaF3 growth medium. The

combinations tested were: FGF1-FGFR1c, FGF1-FGFR2b, FGF2-FGFR1c and FGF7-FGFR2b. Prior to any bioassay, the cells were washed 3 times with BaF3 growth medium. FGF (concentrations: 0.1 nM for FGF2, 1 nM for FGF1 and 3 nM for FGF7) was spotted on a 96 well plate, in the presence of selected HS oligosaccharides (concentration of 3 µg/mL for primary assays and concentrations ranging from 3 ng/mL to 10 µg/mL for titration assays, for a volume of 50 µL). Cells in culture medium were next added to the wells (10,000 cells per well, 50 µL per well). The plate was then incubated at 37 °C, in 5% CO₂ (v/v) for 72 hours. Several controls were carried out. As positive controls, cells were incubated in BaF3 growth medium with 1 ng/mL IL-3 or in BaF3 growth medium with FGFs and heparin (concentrations ranging from 3 ng/mL to 10 µg/mL). As negative controls, cells were incubated in BaF3 growth medium only, in BaF3 growth medium and in the presence of FGF or in BaF3 growth medium and in the presence of the saccharides. Typical A₅₇₀ values for controls in the MTT assays were: IL-3 controls (1.144±0.035, 1.173±0.041, 1.076±0.003, 1.279±0.021), FGF plus heparin controls (0.546±0.011, 0.515±0.008, 0.421±0.016, 0.459±0.026), background level controls with no added FGF, FGF alone or saccharides alone (0.156±0.003, 0.114±0.001, 0.098±0.001, 0.124±0.002) for FGF2-FGFR1c, FGF1-FGFR1c, FGF1-FGFR2b and FGF7-FGFR2b respectively. Each condition was tested as triplicate on the bioassay plate (for both primary bioassay and titration assay). In the case of primary assays, for each oligosaccharide-FGF-FGFR combination, the assays were carried out three times (for a total of 3 plates, 9 absorbance values for each oligosaccharide-FGF-FGFR condition). In the case of dose response curve experiments, bioassays were carried out only once.

After 72 hours, 10 µL 3-[4,5-dimethylthiazol-2-yl]-2,5-diphenyltetrazolium bromide (MTT) (5 mg/mL in sterile PBS) was added to each well and the plate was incubated for 4 hours at 37 °C, in 5% CO₂ (v/v). MTT is reduced by the mitochondrial reductase enzymes of viable cells to afford insoluble purple formazan. After 4 hours of incubation, 100 µL 10% (w/v) SDS/0.01 M HCl was added to each well (to dissolve formazan) and incubated overnight. Cell growth was determined by measuring the absorbance at λ_{abs} = 570 nm using a plate reader (the absorbance is proportional to the cell number).

2.2.3. Statistical analysis

For primary bioassays, the average of activity was calculated for each plate and used for statistical evaluations. The compounds were tested using a one-sample t-test (one tailed) to determine whether their relative activities were significantly higher than the different reference values or not (reference values: 5%, 50% and 100% activity, relative to full-length Hp). 5% was designated as the value for minimal activity (comparatively to Hp). Selected compounds were also tested using a two-sided t-test. Statistical significance was reported if $p < 0.05^*$, $p < 0.01^{**}$ and $p < 0.001^{***}$. Data analyses were performed with R statistical software v.3.3.0.

2.3. Chemical synthesis of Hp/HS oligosaccharides

2.3.1. Materials

All chemicals were reagent grade, used as they were supplied unless described otherwise and purchased from Sigma, Acros and Biotage (Spain). All reagents were stored as instructed by suppliers. All solvents used for air and moisture-sensitive reactions were dried and stored over 4 Å molecular sieves under argon prior to use. Water was simply distilled prior to use. All anhydrous reactions were carried out in oven-dried glassware and under argon. All air and moisture-sensitive chemicals and anhydrous solvents were manipulated and transferred with oven-dried syringes or cannulae.

2.3.2. Methods

2.3.2.1. Microwave-assisted synthesis

Microwave-assisted synthesis was performed using a Biotage Initiator Classic microwave monomode oven, equipped with a Robot Eight/Robot Sixty (Biotage). Samples were diluted with the appropriate solvent in a microwave vial (Biotage) equipped with a magnetic stir bar and placed onto the sample bed. The reaction conditions (irradiation time, stirring time, vial type, temperature) were set up on the fully integrated computer.

2.3.2.2. *Flash chromatography*

Conventional flash chromatography was performed using silica gel 60 (63-200 μm). Automated flash chromatography was performed using Biotage SP, equipped with Biotage SNAP KP-Sil cartridges (50 μm silica particles with a surface area of 500 $\text{m}^2\cdot\text{g}^{-1}$). For both techniques, the sample was diluted in a minimum solvent (usually dichloromethane (DCM)) and loaded onto the column which had been preconditioned in the appropriate solvent mixture.

2.3.2.3. *Mass spectrometry*

Reaction monitoring and exact mass measurements were performed using either an Acquity UPLC (5 $\mu\text{L}/\text{min}$, MeOH) coupled to a LCT XE time-of-flight mass spectrometry detector with electrospray ionisation source (LC-ESI-TOF) or a Bruker UltrafleXtreme III MALDI tandem mass spectrometer (MALDI-TOF/TOF). Analyses were made in positive mode for both methods. 2,5-Dihydroxybenzoic acid (DHB) in MeOH was used as MALDI matrix.

2.3.2.4. *Specific rotation*

Specific rotation values α_D^{20} were measured with a PerkinElmer 341 polarimeter equipped with sodium lamp and wavelength filter (589 nm) and at a constant temperature of 20 $^{\circ}\text{C}$. Prior to any measurement, pure chloroform was used for calibration. Samples were diluted in chloroform for measurements.

2.3.2.5. *NMR*

^1H , ^{13}C , DQF-COSY and HSQC spectra were obtained at room temperature using a 500 MHz NMR spectrometer equipped with a $^1\text{H}/^{19}\text{F}$ BBI 5 mm probe and a HRMAS (High Resolution Magic Angle Spinning) 4 mm probe. Samples were diluted with deuterated chloroform (CDCl_3), methanol (CD_3OD) or water (D_2O) for recording of the NMR spectra, unless otherwise stated.

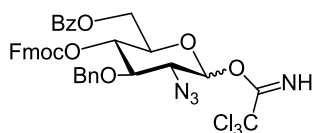
2.3.3. Procedures and characterisation data

Copies of all NMR spectra can be accessed at: <http://datacat.liverpool.ac.uk/>

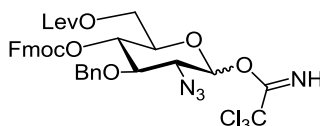
2.3.3.1. General procedures

Procedure A: Prior to the reaction, the solvent was dried over freshly activated 4 Å molecular sieve beads for a minimum of 12 hours. Syringes and needles were dried under high vacuum for a minimum of 12 hours as well. The glycosyl acceptor and donor were dissolved together in dry solvent at the desired concentration under argon, in a flask containing freshly activated 4 Å molecular sieves powder. The mixture was cooled to the desired temperature and the activator was added. The reaction mixture was stirred at the desired temperature for a minimum of 15 min and a maximum of 2 hours. The reaction was quenched by addition of water (in the case of compounds bearing a Fmoc group) or Et₃N. The reaction mixture was diluted with the corresponding solvent and filtered through a pad of celite. The concentrated crude reaction was then purified by silica gel chromatography.

Procedure B: Prior to the reaction, the solvent was dried over freshly activated 4 Å molecular sieve beads for a minimum of 12 hours. Syringes, needles and canulae were dried under high vacuum for a minimum of 12 hours as well. The glycosyl acceptor and donor were separately dissolved in dry solvent at the desired concentrations, under argon, and in flasks containing freshly activated 4 Å molecular sieves powder. The activator was added to the glycosyl acceptor solution and the mixture was then cooled to the desired temperature. The donor solution was added dropwise via a canula to the acceptor solution. The reaction mixture was stirred at the desired temperature for a minimum of 15 min and a maximum of 2 hours. The reaction was quenched by addition of water (in the case of compounds bearing a Fmoc group) or Et₃N. The reaction mixture was diluted with the corresponding solvent and filtered through a pad of celite. The concentrated crude reaction was then purified by silica gel chromatography.

2.3.3.2. *Procedures and characterisation data***2-Azido-6-*O*-benzoyl-3-*O*-benzyl-2-deoxy-4-*O*-(9-fluorenylmethoxycarbonyl)- α/β -D-glucopyranosyl trichloroacetimidate (8)**

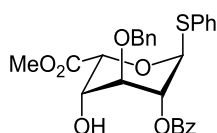
The hemiacetal **22** (1 g, 1.61 mmol) was dissolved in trichloroacetonitrile (30 mL) and sodium hydride (0.01 g, 0.161 mmol) was added. After stirring at room temperature for 15 min, the mixture was concentrated, and the residue was loaded onto a short pad of silica for flash chromatography purification (hexane/ethyl acetate 7:3, 1% Et₃N). The imidate **8** (1.17 g, 95%) was obtained as a mixture of anomers (α/β 1/2). R_f = 0.66 (hexane/ethyl acetate 7:3); ¹H NMR (500 MHz, CDCl₃) δ = 8.76 (s, 0.35H, NHCCCl₃), 8.74 (s, 0.65H, NHCCCl₃), 8.09 – 7.15 (m, 18H, aromatic), 6.45 (d, J = 3.5 Hz, 0.35H, H-1 α), 5.68 (d, J = 8.5 Hz, 0.65H, H-1 β), 5.16 – 5.02 (m, 1H, H-4 α , H-4 β), 4.83 – 4.79 (m, 1H, CH₂Ph), 4.75 – 4.68 (m, 1H, CH₂Ph), 4.57 – 4.29 (m, 4.35H, H-5 α , H-6, CH₂Fmoc), 4.17 – 4.12 (m, 1.35H, CH_{Fmoc}, H-3 α), 3.93 (dd, J = 8.3, 5.0 Hz, 0.65H, H-5 β), 3.81 – 3.76 (m, 1H, H-2 α , H-2 β), 3.64 (t, J = 9.5 Hz, 0.65H, H-3 β). ¹³C NMR (126 MHz, CDCl₃) δ = 166.14 - 166.11 (Cq_{Bz}), 160.99 - 160.59 (Cq_{C=NH}), 154.28 (Cq_{Fmoc}), 143.31 - 143.08 (Cq_{Fmoc}), 143.05 (Cq_{Fmoc}), 141.44 - 141.40 (Cq_{Fmoc}), 137.19 - 137.03 (Cq_{aromatic}), 133.33 - 119.88 (CH_{aromatic}), 96.63 (C-1 β), 94.28 (C-1 α), 80.24 (C-3 β), 77.75 (C-3 α), 75.58 (CH₂Bn), 74.56 - 74.45 (C-4 α , C-4 β), 72.65 (C-5 β), 70.55 - 70.43 (C-5 α , CH₂Fmoc), 65.37 (C-2 β), 62.71 - 62.33 (C-6, C-2 α), 46.84 - 46.28 (CH_{Fmoc}); LRMS (ESI MS) m/z calcd for C₃₇H₃₁Cl₃N₄O₈ [M + H]⁺ 765.1, found 765.2.

2-Azido-3-*O*-benzyl-2-deoxy-4-*O*-(9-fluorenylmethoxycarbonyl)-6-*O*-levulinoyl- α/β -D-glucopyranosyl trichloroacetimidate (9)

The hemiacetal **23** (2.4 g, 3.9 mmol) was dissolved in trichloroacetonitrile (73 mL) under argon. Sodium hydride (0.16 g, 0.39 mmol) was added to the solution and complete consumption of the starting material was revealed by TLC analysis after 10

minutes. The solvent was evaporated and the crude was loaded on a short pad of silica for purification (hexane/ethyl acetate 7:3, 1% Et₃N). The desired product **9** (2.49 g, 85%) was obtained as a mixture of anomers (α/β 1/4). R_f = 0.66 (hexane/ethyl acetate 1:1); ¹H NMR (500 MHz, CDCl₃) δ = 8.79 (s, 0.2H, NHCCCl₃), 8.78 (s, 0.8H, NHCCCl₃), 7.81 – 7.21 (m, 13H, aromatic), 6.42 (d, J = 3.4 Hz, 0.2H, H-1 α), 5.62 (d, J = 8.5 Hz, 0.8H, H-1 β), 5.03 (t, J = 9.7 Hz, 0.2H, H-4 α), 4.96 (t, J = 9.7 Hz, 0.8H, H-4 β), 4.83 – 4.75 (m, 1H, CH₂Ph), 4.73 – 4.64 (m, J = 10.9 Hz, 1H, CH₂Ph), 4.52 (m, 1H, CH₂Fmoc), 4.39 – 4.14 (m, 4.2H, CH₂Fmoc, H-6, CH_{Fmoc}, H-5 α), 4.08 (t, J = 9.7 Hz, 0.2H, H-3 α), 3.81 – 3.72 (m, 1.8H, H-5 β , H-2 β , H-2 α), 3.58 (t, J = 9.5 Hz, 0.8H, H-3 β), 2.81 – 2.52 (m, 4H, CH₂Lev), 2.16 (s, 3H, CH₃Lev). ¹³C NMR (126 MHz, CDCl₃) δ = 206.76 – 206.66 (C_qLev), 172.38 (C_qLev), 160.87 – 160.46 (C_qC=NH), 154.20 (C_qFmoc), 143.29 – 142.92 (C_qFmoc), 141.36 – 141.30 (C_qFmoc), 137.07 – 136.91 (C_qaromatic), 128.82 – 119.84 (CH_{aromatic}), 96.45 (C-1 β), 94.12 (C-1 α), 90.66 – 90.27 (CCl₃), 79.94 (C-3 β), 77.51 (C-3 α), 75.40 (CH₂Bn), 73.94 – 73.64 (C-4 α , C-4 β), 72.47 (C-5 β), 70.48 – 70.32 (CH₂Fmoc, C-5 α), 65.20 (C-2 β), 62.40 (C-2 α), 61.87 – 61.73 (C-6), 46.66 (CH_{Fmoc}), 38.02 – 37.84 (CH₂Lev), 30.00 – 29.80 (CH₃Lev), 27.86 – 27.80 (CH₂Lev); LRMS (ESI MS) m/z calcd for C₃₅H₃₃Cl₃N₄O₉ [M + H]⁺ 759.1, found 759.2.

Methyl (Phenyl 2-*O*-benzoyl-3-*O*-benzyl-1-thio- α -L-idopyranoside) uronate (**10**)

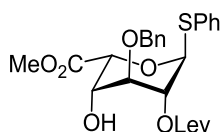


Compound **32** was first treated with a combination of 2,2,6,6-tetramethyl-1-piperidinyloxy (TEMPO) and a catalytic amount of [bis(acetoxy)-iodo]benzene (BAIB) to obtain the iduronic acid intermediate as described by Codée and colleagues. The spectral data was in good agreement with published values. (Codée *et al.* 2005).

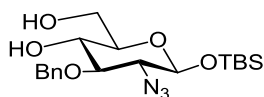
The L-iduronic acid intermediate (1 g, 2.08 mmol) was then dried in high vacuum. The crude was placed in a microwave vial equipped with a stirring bar and containing freshly activated molecular sieve beads. Dry MeOH (15 mL) and Amberlite IR-120 (H⁺) (0.5 g) were added. The solution was irradiated in a

microwave oven at 100 °C for 1h30 with pre-stirring for 30 s. The vial was cooled to room temperature and the solution filtered. The solvent was evaporated, the residual crude was purified by flash chromatography (hexane/ethyl acetate 7:3) to afford the desired product **10** (0.84 g, 82%). The structural data were in agreement with published values (Codée *et al.* 2005).

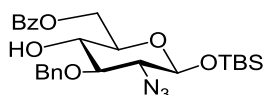
Methyl (Phenyl 3-*O*-benzyl-2-*O*-levulinoyl-1-thio- α -L-idopyranoside) uronate (11)



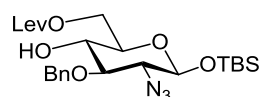
To a vigorously stirred solution of the diol **37** (100 mg, 0.22 mmol) in a mixture of DCM/H₂O (0.3 M, 2:1), TEMPO (7 mg, 0.044 mmol) and BAIB (177 mg, 0.55 mmol) were added. After 1 hour, analysis by TLC indicated complete conversion of the starting material. The mixture was co-evaporated with toluene, dried under high vacuum (minimum 3 hours) and used in the next reaction without further purification. Freshly activated 4 Å molecular sieve beads and dry Amberlite IR-120 (H⁺) (50 mg) were added to a solution of the iduronic acid in dry MeOH (5 mL) in a microwave vial equipped with a magnetic stirring bar. The mixture was irradiated in the microwave oven for 1.5 hours at 95°C. The mixture was filtrated, concentrated and purified by column chromatography to yield **11** (82 mg, 76% in two steps). *R*_f = 0.3 (hexane/ethyl acetate 3:7); α_D^{20} = -56.1 (*c* = 0.65, CHCl₃); ¹H NMR (500 MHz, CDCl₃) δ = 7.55 – 7.22 (m, 10H, aromatic), 5.57 (s, 1H, H-1), 5.32 (d, *J* = 1.5 Hz, 1H, H-5), 5.29 – 5.26 (m, 1H, H-2), 4.85 (d, *J* = 11.8 Hz, 1H, CH₂Ph), 4.64 (d, *J* = 11.8 Hz, 1H, CH₂Ph), 4.10 (bs, 1H, H-4), 3.83 (s, 3H, CH₃COOMe), 3.79 (t, *J* = 2.3 Hz, 1H, H-3), 2.88 – 2.68 (m, 3H, 4-OH, CH₂Lev), 2.64 – 2.53 (m, 2H, CH₂Lev), 2.17 (s, 3H, CH₃Lev). ¹³C NMR (126 MHz, CDCl₃) δ = 206.33 (Cq_{Lev}), 171.21 (Cq_{Lev}), 169.68 (Cq_{COOMe}), 137.10 (Cq_{aromatic}), 135.71 (Cq_{aromatic}), 131.57 – 127.35 (CH_{aromatic}), 86.64 (C-1), 73.39 (C-3), 72.50 (CH₂Bn), 69.42 (C-2), 69.08 (C-5), 68.28 (C-4), 52.52 (CH₃COOMe), 37.88 (CH₂Lev), 29.83 (CH₃Lev), 28.06 (CH₂Lev); HRMS (ESI-TOF MS) *m/z* calcd for C₂₅H₂₈O₈S [M + Na]⁺ 511.1397, found 511.1371.

***tert*-Butyldimethylsilyl 2-Azido-3-*O*-benzyl-2-deoxy- β -D-glucopyranoside (17)**

To a solution of compound **16** (10.3 g, 20.7 mmol) in dry DCM (207 mL), EtSH (8 mL, 103.52 mmol) and a catalytic amount of $\text{BF}_3 \cdot \text{O}(\text{Et})_2$ (255 μL , 2.07 mmol) were added sequentially. The solution was stirred for 3 hours under argon, and the solvent was next evaporated. The resulting crude was subsequently loaded onto a silica gel based column for purification (hexane/ethyl acetate 7:3) yielding of **17** (7.25g, 89%). The physical data was in good agreement with published values (Guedes *et al.* 2013).

***tert*-Butyldimethylsilyl 2-Azido-6-*O*-benzoyl-3-*O*-benzyl-2-deoxy- β -D-glucopyranoside (18)**

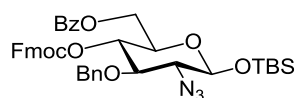
Compound **18** was prepared from compound **17** following the procedures described by Guedes and colleagues and the physical data was in good agreement with published values (Guedes *et al.* 2013).

***tert*-Butyldimethylsilyl 2-Azido-3-*O*-benzyl-2-deoxy-6-*O*-levulinoyl- β -D-glucopyranoside (19)**

Compound **17** (6 g, 14.71 mmol) was dissolved in dry DCM (221 mL) and LevOH (2.2 mL, 22.07 mmol) and CMPI (10.52 g, 41.19 mmol) were added subsequently. The reaction mixture was firstly stirred for 15 min then cooled to $-20\text{ }^{\circ}\text{C}$. DABCO (6.6 g, 58.84 mmol) was added to the mixture and the reaction was slowly warmed to room temperature over 3 hours. The reaction mixture was diluted with DCM and washed with 1 M HCl, water, 1 M NaOH, water and brine. The organic layer was dried over MgSO_4 , filtered and concentrated. The crude product was purified by flash chromatography on silica gel (toluene/ethyl acetate 7:3) and the desired product **19** was obtained (7.03 g, 94%). $R_f = 0.37$ (toluene/ethyl acetate 7:3); $\alpha_D^{20} = -31.4$ ($c = 0.5$, CHCl_3); $^1\text{H NMR}$ (500 MHz, CDCl_3) $\delta = 7.41 - 7.28$ (m, 5H, aromatic), 4.93 (d,

$J = 11.4$ Hz, 1H, CH₂Ph), 4.74 (d, $J = 11.4$ Hz, 1H, CH₂Ph), 4.53 (d, $J = 7.6$ Hz, 1H, H-1), 4.35 (dd, $J = 12.0, 5.4$ Hz, 1H, H-6a), 4.28 (dd, $J = 12.0, 2.3$ Hz, 1H, H-6b), 3.52 – 3.44 (m, 1H, H-4), 3.43 – 3.37 (m, 1H, H-5), 3.31 (dd, $J = 9.9, 7.7$ Hz, 1H, H-2), 3.20 (dd, $J = 9.9, 8.7$ Hz, 1H, H-3), 2.80 – 2.70 (m, 2H, CH_{2Lev}), 2.64 (d, $J = 3.3$ Hz, 1H, 4-OH), 2.61 – 2.56 (m, 2H, CH_{2Lev}), 2.18 (s, 3H, CH_{3Lev}), 0.93 (s, 9H, CH_{3TBS}), 0.16 (d, $J = 2.6$ Hz, 6H, CH_{3TBS}) ; ¹³C NMR (126 MHz, CDCl₃) δ = 206.81 (Cq_{Lev}), 173.17 (Cq_{Lev}), 138.21 (Cq_{aromatic}), 130.10 – 126.78 (CH_{aromatic}), 97.42 (C-1), 82.16 (C-3), 75.20 (CH_{2Bn}), 73.83 (C-5), 70.25 (C-4), 68.29 (C-2), 63.61 (C-6), 38.07 (CH_{2Lev}), 29.98 (CH_{3Lev}), 27.97 (CH_{2Lev}), 25.73 (CH_{3TBS}), 18.13 (Cq_{TBS}), -4.20 (CH_{3TBS}), -5.07 (CH_{3TBS}); HRMS (ESI-TOF MS) m/z calcd for C₂₄H₃₇N₃O₇Si [M + Na]⁺ 530.2293, found 530.2294.

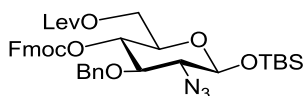
***tert*-Butyldimethylsilyl 2-Azido-6-*O*-benzoyl-3-*O*-benzyl-2-deoxy-4-*O*-(9-fluorenyl-methoxycarbonyl)- β -D-glucopyranoside (**20**)**



To a solution of **18** (1.9 g, 3.7 mmol) in DCM (75 mL) at 0 °C, pyridine (7.5 mL), FmocCl (2.4 g, 9.25 mmol) and a catalytic amount of DMAP (0.45 mg, 0.37 mmol) were added. The reaction was slowly warmed to room temperature and was stirred for 2h until completion was detected by TLC analysis. The mixture was diluted with DCM, washed consecutively with water, saturated CuSO₄ aq. solution, water, and brine. The organic layer was dried over MgSO₄ and concentrated. Flash column chromatography on silica gel (hexane/ethyl acetate 3:2) afforded the desired product **20** (2.58 g, 96%). $R_f = 0.50$ (hexane/ethyl acetate 4:1); $\alpha_D^{20} = -12$ (c = 0.5, CHCl₃); ¹H NMR (500 MHz, CDCl₃) δ = 8.08 – 7.18 (m, 18H, aromatic), 4.91 (dd, $J = 10.0, 8.9$ Hz, 1H, H-4), 4.80 (d, $J = 11.2$ Hz, 1H, CH₂Ph), 4.66 (d, $J = 11.2$ Hz, 1H, CH₂Ph), 4.59 (d, $J = 7.3$ Hz, 1H, H-1), 4.52 (dd, $J = 12.0, 2.8$ Hz, 1H, H-6a), 4.42 (dd, $J = 10.5, 7.0$ Hz, 1H, CH_{2Fmoc}), 4.37 – 4.30 (m, 2H, CH_{2Fmoc}, H-6b), 4.15 (t, $J = 7.1$ Hz, 1H, CH_{Fmoc}), 3.82 – 3.74 (m, 1H, H-5), 3.50 – 3.40 (m, 2H, H-3, H-2), 0.90 (s, 9H, CH_{3TBS}), 0.13 (d, $J = 3.3$ Hz, 6H, CH_{3TBS}) ; ¹³C NMR (126 MHz, CDCl₃) δ = 166.14 (Cq_{Bz}), 154.45 (Cq_{Fmoc}), 143.30 - 143.19 (Cq_{Fmoc}), 141.43 - 141.41 (Cq_{Fmoc}), 137.59 (Cq_{aromatic}), 133.30 - 120.19 (CH_{aromatic}), 97.36 (C-1), 79.95 (C-3), 75.28 (CH_{2Bn}), 75.08 (C-4), 71.93 (C-5), 70.34 (CH_{2Fmoc}), 68.30 (C-2), 63.32 (C-6),

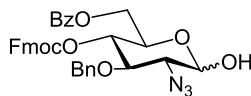
46.82 (CH_{Fmoc}), 25.66 (CH_{3TBS}), 18.06 (Cq_{TBS}), -4.20 (CH_{3TBS}), -5.11 (CH_{3TBS}); HRMS (ESI-TOF MS) m/z calcd for C₄₁H₄₅N₃O₈Si [M + Na]⁺ 758.2868, found 758.2798.

***tert*-Butyldimethylsilyl 2-Azido-3-*O*-benzyl-2-deoxy-4-*O*-(9-fluorenylmethoxy-carbonyl)-6-*O*-levulinoyl- β -D-glucopyranoside (**21**)**

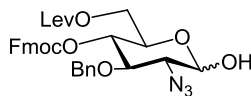


To a solution of **19** (7.03 g, 13.85 mmol) in dry DCM (280 mL) at 0 °C, FmocCl (9 g, 34.63 mmol) was added, along with DMAP (0.17 g, 1.39 mmol) and pyridine (28 mL). The reaction mixture was slowly warmed to room temperature over 1 hour. The mixture was diluted with DCM and the organic phase was washed with water, saturated CuSO₄ aq. solution, water and brine. The organic phase was dried over MgSO₄, filtered and concentrated. Flash chromatography on silica column gel (toluene/ethyl acetate 9:1) afforded **21** (9.60 g, 95%). R_f = 0.36 (toluene/ethyl acetate 9:1); α_D^{20} = -13.7 (c = 0.65, CHCl₃); ¹H NMR (500 MHz, CDCl₃) δ = 7.80 – 7.20 (m, 13H, aromatic), 4.85 – 4.75 (m, 2H, H-4, CH₂Ph), 4.64 (d, J = 11.2 Hz, 1H, CH₂Ph), 4.55 (d, J = 7.3 Hz, 1H, H-1), 4.47 (dd, J = 10.5, 7.0 Hz, 1H, CH₂Fmoc), 4.35 (dd, J = 10.5, 7.3 Hz, 1H, CH₂Fmoc), 4.24 – 4.15 (m, 3H, H-6a, H-6b, CH_{Fmoc}), 3.62 (dt, J = 9.9, 4.4 Hz, 1H, H-5), 3.45 – 3.36 (m, 2H, H-3, H-2), 2.81 – 2.50 (m, 4H, CH₂Lev), 2.17 (s, 3H, CH₃Lev), 0.94 (s, 9H, CH₃TBS), 0.17 (d, J = 2.9 Hz, 6H, CH₃TBS); ¹³C NMR (126 MHz, CDCl₃) δ = 206.35 (Cq_{Lev}), 172.33 (Cq_{Lev}), 154.35 (Cq_{Fmoc}), 143.30 (Cq_{Fmoc}), 143.17 (s), 141.37 (Cq_{Fmoc}), 141.35 (Cq_{Fmoc}), 137.57 (Cq_{aromatic}), 128.71 – 119.53 (CH_{aromatic}), 97.23 (C-1), 79.82 (C-3), 75.10 (CH₂Bn), 74.66 (C-4), 71.74 (C-5), 70.31 (CH₂Fmoc), 68.18 (C-2), 62.79 (C-6), 46.77 (CH_{Fmoc}), 37.86 (CH₂Lev), 29.88 (CH₃Lev), 27.83 (CH₂Lev), 25.65 (CH₃TBS), 18.03 (Cq_{TBS}), -4.26 (CH₃TBS), -5.14 (CH₃TBS); HRMS (ESI-TOF MS) m/z calcd for C₃₉H₄₇N₃O₉Si [M + Na]⁺ 752.2974, found 752.2921.

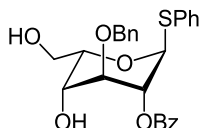
2-Azido-6-*O*-benzoyl-3-*O*-benzyl-2-deoxy-4-*O*-(9-fluorenylmethoxycarbonyl)- α/β -D-glucopyranose (22**)**



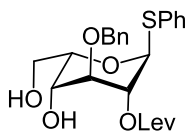
To a solution of **20** (2 g, 2.72 mmol) in dry THF (32 mL) at 0 °C, HF.pyridine (70% solution, 7.2 mL) was added. The reaction was stirred at room temperature over night and quenched with a saturated NaHCO₃ aq. solution. The mixture was diluted with ethyl acetate and consequently washed with water, saturated CuSO₄ aq. solution, water and brine. After being dried over MgSO₄ and filtered, the organic layer was concentrated. The resulting residue was then loaded onto a silica gel based column for purification (hexane/ethyl acetate 3:7). The desired hemiacetal **22** was obtained (1.37 g, 81%) as a mixture of anomers (α/β 2/1). R_f = 0.20 (hexane/ethyl acetate 1:4); ¹H NMR (500 MHz, CDCl₃) δ = 8.11 – 7.19 (m, 18H, aromatic), 5.34 (t, J = 3.2 Hz, 0.65H, H-1 α), 5.10 – 5.03 (m, 0.65H, H-4 α), 5.03 – 4.97 (m, 0.35H, H-4 β), 4.85 – 4.76 (m, J = 10.0 Hz, 1H, CH₂Ph), 4.73 – 4.63 (m, 1.35H, CH₂Ph, H-1 β), 4.58 (ddd, J = 11.1, 8.3, 2.7 Hz, 1H, H-6), 4.45 (dt, J = 10.5, 7.2 Hz, 1H, CH₂Fmoc), 4.39 – 4.26 (m, 3H, H-5 α , CH₂Fmoc, H-6), 4.20 – 4.06 (m, 1.65H, CH_{Fmoc}, H-3 α), 3.79 (ddd, J = 10.0, 4.7, 2.9 Hz, 0.35H, H-5 β), 3.63 (bs, 0.35H, 1-OH β), 3.57 – 3.43 (m, 1.35H, H-3 β , H-2 α , H-2 β), 3.12 (d, J = 2.7 Hz, 0.65H, 1-OH α). ¹³C NMR (126 MHz, CDCl₃) δ = 166.49 - 166.41 (Cq_{Bz}), 154.45 - 154.41 (Cq_{Fmoc}), 143.32 - 143.28 (Cq_{Fmoc}), 143.16 - 143.10 (Cq_{Fmoc}), 141.44 - 141.40 (Cq_{Fmoc}), 137.32 - 137.23 (Cq_{aromatic}), 133.44 - 120.19 (CH_{aromatic}), 96.51 (C-1 β), 92.04 (C-1 α), 80.29 (C-3 β), 77.70 (C-3 α), 75.54 (CH₂Bn), 75.20 (C-4 α), 74.59 (C-4 β), 71.98 (C-5 β), 70.38 - 70.33 (CH₂Fmoc), 67.94 (C-5 α), 67.08 (C-2 β), 63.58 (C-2 α), 62.81 - 62.66 (C-6), 46.83 (CH_{Fmoc}); LRMS (ESI MS) m/z calcd for C₃₅H₃₁N₃O₈ [M + H]⁺ 622.2, found 622.3.

2-Azido-3-*O*-benzyl-2-deoxy-4-*O*-(9-fluorenylmethoxycarbonyl)-6-*O*-levulinoyl- α/β -D-glucopyranose (23)

To a solution of compound **21** (3 g, 4.11 mmol) in dry THF (41 mL) at 0 °C, HF.pyridine (70% solution, 2.7 mL) was added. The reaction was stirred at room temperature overnight and was quenched with a saturated NaHCO₃ aq. solution. The mixture was diluted in ethyl acetate and washed with water, saturated CuSO₄ aq. solution, water and brine. The organic phase was dried over MgSO₄, filtered and concentrated. The residue was purified by flash chromatography on silica gel (toluene/ethyl acetate, 7:3) and delivered 1.97 g (78%) of **23** as a mixture of anomers (α/β 2/1). R_f = 0.3 (toluene/ethyl acetate 7:3); ¹H NMR (500 MHz, CDCl₃) δ = 7.82 – 7.15 (m, 13H, aromatic), 5.34 (t, J = 2.9 Hz, 0.65H, H-1 α), 4.89 – 4.76 (m, 2H, H-4 α , H-4 β , CH₂Ph), 4.72 – 4.60 (m, 1.35H, CH₂Ph, H-1 β), 4.53 – 4.45 (m, 1H, CH₂Fmoc), 4.39 – 4.14 (m, 5H, CH₂Fmoc, H-5 α , H-6 α , CH_{Fmoc}, 1-OH β), 4.11 – 4.05 (m, 0.65H, H-3 α), 3.86 (d, J = 1.7 Hz, 0.65H, 1-OH α), 3.66 (ddd, J = 10.1, 4.9, 3.2 Hz, 0.35H, H-5 β), 3.53 – 3.42 (m, 1.35H, H-3 β , H-2 α , H-2 β), 2.84 – 2.69 (m, 2H, CH₂Lev), 2.66 – 2.51 (m, 2H, CH₂Lev), 2.18 (s, 3H, CH₃Lev); ¹³C NMR (126 MHz, CDCl₃) δ = 207.78 - 207.38 (Cq_{Lev}), 172.51 - 172.47 (Cq_{Lev}), 154.54 - 154.40 (Cq_{Fmoc}), 143.35 - 143.21 (Cq_{Fmoc}), 141.44 - 141.40 (Cq_{Fmoc}), 137.43 - 137.37 (Cq_{aromatic}), 128.50 - 120.23 (CH_{aromatic}), 96.39 (C-1 β), 92.01 (C-1 α), 80.24 (C-3 β), 77.73 (C-3 α), 75.43 - 74.51 (CH₂Bn, C-4 β , C-4 α), 71.86 (C-5 β), 70.45 (CH₂Fmoc), 67.58 (C-5 α), 67.08 (C-2 β), 63.61 (C-2 α), 62.61 - 62.43 (C-6), 46.80 (CH_{Fmoc}), 38.29 - 38.03 (CH₂Lev), 30.00 - 29.97 (CH₃Lev), 28.15 - 28.02 (CH₂Lev); HRMS (ESI-TOF MS) m/z calcd for C₃₃H₃₃N₃O₉ [M + Na]⁺ 638.2109, found 638.2089.

Phenyl 2-*O*-benzoyl-3-*O*-benzyl-1-thio- α -L-idopyranoside (32)

Compound **32** was prepared from compound **30** following the procedures described by Guedes and colleagues and the physical data was in good agreement with published values (Guedes *et al.* 2013).

Phenyl 3-*O*-benzyl-2-*O*-levulinoyl-1-thio- α -L-idopyranoside (37)

To a solution of **30** (2 g, 7.93 mmol) in dry DCM (31 mL), trimethyl(phenylthio)silane (4.6 mL, 24 mmol) and zinc iodide ZnI_2 (5.77 g, 16 mmol, protected from light and dried under high vacuum) were added. The mixture was stirred at room temperature for 4 hours and filtered through a pad of Celite. The filtrate was diluted with DCM, after a solution of 4 M HCl in dioxane (20 mL, 1 equivalent) and 20 mL water were added. The mixture was stirred at room temperature for 15 min until complete conversion was detected by TLC analysis. The mixture was washed with 1 M HCl aq. solution, saturated NaHCO_3 aq. solution, water and brine, filtered, concentrated and dried under high vacuum. The resulting triol was dissolved in dry pyridine (10 mL) and acetic anhydride (5 mL) was added at 0 °C. The mixture was stirred at room temperature overnight, and the reaction was hence quenched with ethanol. The mixture was diluted with DCM, washed with saturated NaHCO_3 aq. solution, water, saturated CuSO_4 aq. solution, water and brine. The aqueous phase was extracted with DCM. The organic layers were dried over MgSO_4 and concentrated. The residue was purified by column chromatography (hexane/ethyl acetate 8:1) to afford the peracetylated intermediate (3.25 g, 85% over two steps). The structural data were in good agreement with published data (Tatai *et al.* 2008).

To a solution of the peracetylated intermediate (293 mg, 0.60 mmol) in dry MeOH (4 mL), a catalytic amount of NaOMe (200 μL of a 0.5 M solution) was added. The mixture was stirred for 3 hours at room temperature, neutralized with Amberlite IR 120 (H+) resin, filtered, and concentrated to give the corresponding triol **34** (202 mg, 93%). The structural data was in good agreement with published data (Tatai *et al.* 2008).

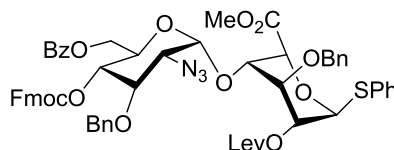
The intermediate triol (150 mg, 0.42 mmol) was dissolved in dry acetonitrile (1.5 mL), and benzaldehyde dimethyl acetal (120 μL , 0.84 mmol) and a catalytic amount of CSA (~3 mg) were added (until an acid pH was obtained). After 1.5 hours of stirring, the mixture was neutralized with Et_3N and concentrated. The residue was

purified by silica gel column chromatography (hexane/ethyl acetate 4:1) and afforded the desired compound **35** (140 mg, 75%) as a mixture of anomers (α/β 3/1). The anomers were separated by flash chromatography. The structural data was in agreement with published data (Tatai *et al.* 2008).

A suspension of EDC.HCl (127 mg, 0.66 mmol) and DMAP (36 mg, 0.30 mmol) in DCM (10 mL) was added to a solution of the 4,6-*O*-benzylidene protected intermediate **a-35** (0.20 g, 0.44 mmol) and levulinic acid (77 mg, 0.66 mmol) in DCM (4 mL). After stirring for 2 hours at ambient temperature, two more equivalents of EDC.HCl and of levulinic acid were added. The reaction was stirred overnight. The reaction mixture was diluted with DCM, washed with 1 M HCl aq. solution, saturated NaHCO₃ aq. solution, water and brine. The organic layer was dried and concentrated. The product was purified by column chromatography to afford the fully protected intermediate **36** (0.222 g, 92%). Structural data was in agreement with published data (Dhamale *et al.* 2014).

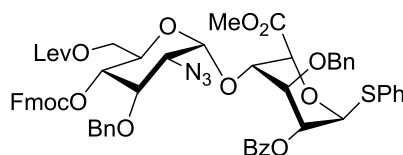
A solution of the fully protected intermediate (200 mg, 0.365 mmol) in a mixture of DCM/TFA/H₂O (0.06M, 10:1:0.1, v/v/v) was stirred at 0°C for 3 hours. The reaction mixture was quenched with solid NaHCO₃, washed with 1 M HCl aq. solution, saturated NaHCO₃ aq. solution and water. The residue was purified by flash column chromatography (DCM/MeOH 99:1) to give pure product **37** (126 mg, 75%). R_f = 0.3 (hexane/ethyl acetate 7:3); α_D^{20} = -59.5 (c = 0.5, CHCl₃); ¹H NMR (500 MHz, CDCl₃) δ = 7.56 – 7.24 (m, 10H, aromatic), 5.49 (s, 1H, H-1), 5.31 – 5.26 (m, 1H, H-2), 4.85 (d, J = 11.8 Hz, 1H, CH₂Ph), 4.70 (t, J = 4.7 Hz, 1H, H-5), 4.60 (d, J = 11.8 Hz, 1H, CH₂Ph), 4.00 – 3.77 (m, J = 25.7, 21.6, 11.8, 6.3 Hz, 3H, H-6a, H-6b, H-4), 3.74 – 3.69 (m, J = 2.9, 1.2 Hz, 1H, H-3), 2.85 (d, J = 9.6 Hz, 1H, 4-OH), 2.82 – 2.71 (m, 2H, CH₂Lev), 2.62 – 2.56 (m, 2H, CH₂Lev), 2.19 (s, 3H, CH₃Lev), 2.11 (dd, J = 8.3, 4.2 Hz, 1H, 6-OH). ¹³C NMR (126 MHz, CDCl₃) δ = 206.72 (Cq_{Lev}), 171.35 (Cq_{Lev}), 137.36 (Cq_{aromatic}), 135.83 (Cq_{aromatic}), 132.41 – 126.73 (CH_{aromatic}), 86.49 (C-1), 73.80 (C-3), 72.41 (CH₂Bn), 69.71 (C-2), 68.33 (C-4), 68.27 (C-5), 63.36 (C-6), 38.04 (CH₂Lev), 29.84 (CH₃Lev), 28.16 (CH₂Lev); HRMS (ESI-TOF MS) m/z calcd for C₂₄H₂₈O₇S [M+Na]⁺ 483.1448, found 483.1411.

Methyl (Phenyl [2-azido-6-*O*-benzoyl-3-*O*-benzyl-2-deoxy-4-*O*-(9-fluorenyl-methoxycarbonyl)- α -D-glucopyranosyl]-3-*O*-benzyl-2-*O*-levulinoyl-1-thio- α -L-idopyranoside) uronate (38**)**



The reaction was carried out following procedure A using glycosyl acceptor **11** (50 mg, 0.102 mmol) and glycosyl donor **8** (117 mg, 0.153 mmol). TMSOTf (0.1 equivalents, 2 μ L, 0.01 mmol) was added at -30 °C. The reaction was quenched by the addition of water (10 μ L), and the mixture was filtered and concentrated. The flash chromatography purification of the crude (hexane/ethyl acetate 4:1) gave the desired disaccharide **38** (36 mg, 32%). R_f = 0.40 (hexane/ethyl acetate 3:1); α_D^{20} = +4.4 (c = 0.85, CHCl_3); ^1H NMR (500 MHz, CDCl_3) δ = 8.09 – 7.17 (m, 28H, aromatic), 5.65 (s, 1H, H-1), 5.34 (d, J = 2.2 Hz, 1H, H-5), 5.20 (t, 1H, H-2), 5.09 – 4.98 (m, 2H, H-4', H-1'), 4.85 (d, J = 11.6 Hz, 1H, CH_2Ph), 4.76 (d, J = 10.8 Hz, 1H, CH_2Ph), 4.64 (dd, J = 11.3, 2.8 Hz, 2H, CH_2Ph), 4.57 (dd, J = 12.4, 2.5 Hz, 1H, H-6'), 4.42 (dd, J = 10.5, 6.9 Hz, 1H, CH_2Fmoc), 4.31 – 4.24 (m, 2H, CH_2Fmoc , H-6'), 4.20 – 4.11 (m, 3H, H-4, H-5', CH_{Fmoc}), 4.01 (t, J = 2.7 Hz, 1H, H-3), 3.98 – 3.92 (m, 1H, H-3'), 3.81 (s, 3H, CH_3COOMe), 3.45 (dd, J = 10.2, 3.5 Hz, 1H, H-2'), 2.82 – 2.53 (m, 4H, CH_2Lev), 2.13 (s, 3H, CH_3Lev). ^{13}C NMR (126 MHz, CDCl_3) δ = 206.24 (C_{qLev}), 172.23 (C_{qLev}), 169.43 (C_{qCOOMe}), 166.19 (C_{qBz}), 154.30 (C_{qFmoc}), 143.28 (C_{qFmoc}), 143.17 (C_{qFmoc}), 141.38 (C_{qFmoc}), 137.30 – 136.99 ($\text{C}_{\text{qaromatic}}$), 135.34 ($\text{C}_{\text{qaromatic}}$), 133.25 – 120.18 ($\text{CH}_{\text{aromatic}}$), 96.88 (C-1'), 86.33 (C-1), 77.92 (C-3'), 75.32 (CH_2Bn), 74.80 (C-4'), 72.95 (C-4, CH_2Bn), 71.30 (C-3), 70.25 (CH_2Fmoc), 68.97 (C-2), 68.65 (C-5'), 68.52 (C-5), 63.14 (C-2'), 62.43 (C-6'), 52.52 (CH_3COOMe), 46.79 (CH_{Fmoc}), 37.88 (CH_2Lev), 29.85 (CH_3Lev), 27.92 (CH_2Lev); HRMS (MALDI-TOF MS) m/z calcd for $\text{C}_{60}\text{H}_{57}\text{N}_3\text{O}_{15}\text{S}$ [$\text{M} + \text{Na}$] $^+$ 1114.3403, found 1114.3444.

Methyl (Phenyl [2-azido-3-*O*-benzyl-2-deoxy-4-*O*-(9-fluorenylmethoxy-carbonyl)-6-*O*-levulinoyl- α -D-glucopyranosyl]-2-*O*-benzoyl-3-*O*-benzyl-1-thio- α -L-idopyranoside) uronate (39**)**



The reaction was carried out following procedure A or procedure B using glycosyl acceptor **10** and glycosyl donor **9**.

Procedure A: To a solution of **10** (50 mg, 0.101 mmol) and **9** (115 mg, 0.152 mmol) in DCM (2 mL), TMSOTf (0.1 equivalents, 2 μ L, 0.01 mmol) was added at -20 $^{\circ}$ C. The reaction was quenched by the addition of water (30 μ L), and the mixture was filtered and concentrated. The flash chromatography purification of the crude (hexane/ethyl acetate 3:2) gave the desired disaccharide **39** (56 mg, 51%).

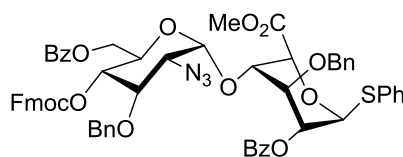
Procedure B: To a solution of **10** (100 mg, 0.202 mmol) and TMSOTf (0.1 equivalents, 4 μ L, 0.02 mmol) in DCM (1 mL), a solution of **9** (230 mg, 0.304 mmol) in DCM (0.5 mL) at -30 $^{\circ}$ C was slowly added. The reaction was quenched by the addition of water (20 μ L), and the mixture was filtered and concentrated. The flash chromatography purification of the crude (hexane/ethyl acetate 3:2) gave the desired disaccharide **39** (42 mg, 19%).

Procedure B: To a solution of **10** (100 mg, 0.202 mmol) and TBSOTf (0.1 equivalents, 5 μ L, 0.02 mmol) in DCM (1 mL), a solution of **9** (230 mg, 0.304 mmol) in DCM (0.5 mL) at -30 $^{\circ}$ C was slowly added. The reaction was quenched by the addition of water (20 μ L), and the mixture was filtered and concentrated. The flash chromatography purification of the crude (hexane/ethyl acetate 3:2) gave the desired disaccharide **39** (55 mg, 25%).

Structural data: R_f = 0.40 (hexane/ethyl acetate 3:1); α_D^{20} = -21.7 (c = 0.5, CHCl_3); ^1H NMR (500 MHz, CDCl_3) δ = 8.14 - 6.95 (m, 28H, aromatic), 5.78 (s, 1H, H-1), 5.44 (s, 1H, H-2), 5.40 (d, J = 1.7 Hz, 1H, H-5), 5.01 (d, J = 11.7 Hz, 1H, CH_2Ph), 4.82 - 4.74 (m, 3H, H-4', CH_2Ph , H-1'), 4.55 (dd, J = 10.5, 6.4 Hz, 1H, CH_2Fmoc), 4.32 (dd,

$J = 10.5, 6.9$ Hz, 1H, CH_2Fmoc), 4.26 – 4.16 (m, $J = 12.7, 2.6$ Hz, 4H, H-3, H-6', CH_{Fmoc}), 4.14 – 4.07 (m, 2H, H-5', H-4), 3.82 (s, 3H, CH_3COOMe), 3.77 (d, $J = 10.8$ Hz, 1H, CH_2Ph), 3.70 (d, $J = 10.8$ Hz, 1H, CH_2Ph), 3.45 (t, $J = 9.7$ Hz, 1H, H-3'), 3.26 (dd, $J = 10.2, 3.5$ Hz, 1H, H-2'), 2.78 – 2.52 (m, 4H, CH_2Lev), 2.14 (s, 3H, CH_3Lev). ^{13}C NMR (126 MHz, CDCl_3) $\delta = 206.57$ (C_{qLev}), 172.44 (C_{qLev}), 169.27 (C_{qCOOMe}), 165.47 (C_{qBz}), 154.32 (C_{qFmoc}), 143.40 – 143.28 (C_{qFmoc}), 141.52 (C_{qFmoc}), 141.40 ($\text{C}_{\text{qaromatic}}$), 137.32 – 137.13 ($\text{C}_{\text{qaromatic}}$), 135.46 ($\text{C}_{\text{qaromatic}}$), 133.68 – 120.23 ($\text{CH}_{\text{aromatic}}$), 100.38 (C-1'), 87.31 (C-1), 78.01 (C-3'), 77.52 (C-4), 74.66 (CH_2Bn), 74.11 (C-4'), 72.86 (CH_2Bn), 72.37 (C-3), 70.06 (CH_2Fmoc), 69.26 (C-2), 68.85 (C-5'), 68.16 (C-5), 63.38 (C-2'), 61.53 (C-6'), 52.62 (CH_3COOMe), 46.89 (CH_{Fmoc}), 37.97 (CH_2Lev), 29.92 (CH_3Lev), 27.97 (CH_2Lev); HRMS (MALDI-TOF MS) m/z calcd for $\text{C}_{60}\text{H}_{57}\text{N}_3\text{O}_{15}\text{S}$ $[\text{M} + \text{Na}]^+$ 1114.3403, found 1114.3455.

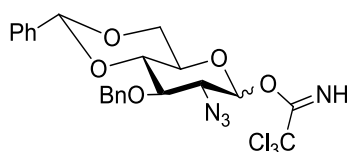
Methyl (Phenyl [2-azido-6-*O*-benzoyl-3-*O*-benzyl-2-deoxy-4-*O*-(9-fluorenyl-methoxycarbonyl)- α -D-glucopyranosyl]-2-*O*-benzoyl-3-*O*-benzyl-1-thio- α -L-idopyranoside) uronate (40)



The reaction was carried out following procedure A using glycosyl acceptor **10** and glycosyl donor **8**. To a solution of **10** (90 mg, 0.174 mmol) and **8** (200 mg, 0.261 mmol) in DCM (3.5 mL), TMSOTf (0.1 equivalents, 3 μL , 0.017 mmol) was added at -20 $^{\circ}\text{C}$. The reaction was quenched by the addition of water (30 μL), and the mixture was filtered and concentrated. The flash chromatography purification of the crude (hexane/ethyl acetate 6:1) gave the desired disaccharide **40** (56 mg, 40%). $R_f = 0.61$ (hexane/ethyl acetate 3:1). $\alpha_D^{20} = -14.6$ ($c = 0.5$, CHCl_3); ^1H NMR (500 MHz, CDCl_3) $\delta = 8.10 - 6.96$ (m, 33H, aromatic), 5.80 (s, 1H, H-1), 5.44 (s, 1H, H-2), 5.41 (s, 1H, H-5), 5.03 – 4.94 (m, $J = 20.5, 10.7$ Hz, 2H, CH_2Ph , H-4'), 4.80 – 4.73 (m, 2H, CH_2Ph , H-1'), 4.68 (d, $J = 10.8$ Hz, 1H, H-6'), 4.50 (dd, $J = 10.5, 6.4$ Hz, 1H, CH_2Fmoc), 4.32 (dd, $J = 10.5, 6.8$ Hz, 1H, CH_2Fmoc), 4.25 – 4.08 (m, 5H, H-3, H-5', H-6', CH_{Fmoc} , H-4), 3.82 (s, 3H, CH_3COOMe), 3.78 (d, $J = 10.6$ Hz, 1H, CH_2Ph), 3.72 (d, $J = 10.6$ Hz, 1H, CH_2Ph), 3.49 (t, $J = 9.7$ Hz, 1H, H-3'), 3.27 (dd, $J = 10.2, 3.3$ Hz, 1H, H-2'). ^{13}C NMR (126 MHz, CDCl_3) $\delta = 169.33$ (C_{qCOOMe}), 166.15 (C_{qBz}),

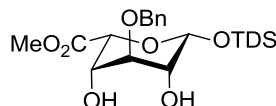
165.49 (C_{qBz}), 154.30 (C_{qFmoc}), 143.28 (C_{qFmoc}), 141.51 (C_{qFmoc}), 141.42 (C_{qFmoc}), 137.22 (C_{qaromatic}), 137.11 (C_{qaromatic}), 135.49 (C_{qaromatic}), 133.70 - 120.21 (CH_{aromatic}), 100.39 (C-1'), 87.30 (C-1), 78.14 (C-3'), 77.55 (C-4), 74.83 (CH_{2Bn}), 74.46 (C-4'), 72.86 (CH_{2Bn}), 72.31 (C-3), 69.94 (CH_{2Fmoc}), 69.29 (C-2), 68.87 (C-5'), 68.21 (C-5), 63.45 (C-2'), 61.85 (C-6'), 52.68 (CH_{3COOMe}), 46.92 (CH_{Fmoc}); HRMS (MALDI-TOF MS) m/z calcd for C₆₂H₅₅N₃O₁₄S [M + Na]⁺ 1120.3297, found 1120.3262.

2-Azido-3-*O*-benzyl-4,6-*O*-benzylidene-2-deoxy- α / β -D-glucopyranosyl trichloroacetimidate (41)



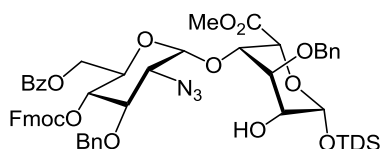
Compound **33** was prepared from compound **12** following the procedures described by de Paz and colleagues (De Paz *et al.* 2003) and the physical data was in good agreement with published values (La Ferla *et al.* 1999).

Methyl (Dimethylthexylsilyl 3-*O*-benzyl- β -L-idopyranoside) uronate (42)



Compound **42** was prepared from compound **24** following the described procedures (Ojeda *et al.* 1999, Lohman *et al.* 2003) and the physical data was in good agreement with published values (Ojeda *et al.* 1999).

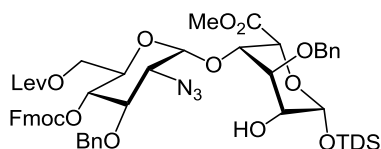
Methyl (Dimethylthexylsilyl 4-*O*-[2-Azido-6-*O*-benzoyl-3-*O*-benzyl-2-deoxy-4-*O*-(9-fluorenylmethoxycarbonyl)- α -D-glucopyranosyl]-3-*O*-benzyl- β -L-idopyranoside) uronate (47)



The reaction was carried out following procedure B. To a solution of glycosyl acceptor **42** (114 mg, 0.26 mmol) and the Lewis acid TBSOTf, (0.2 equivalents, 125 μ L of a 0.26 M solution, 0.032 mmol) in dry DCM (4 mL) at 0 °C, a solution of

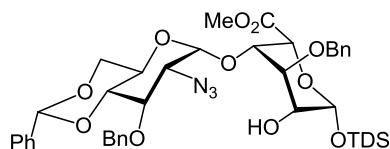
glycosyl donor **8** (122 mg, 0.16 mmol) in dry DCM (1.5 mL) was slowly added. The reaction was quenched by the addition of water (30 μ L). A small aliquot of the reaction was dried with an air stream and analysed by LC-MS.

Methyl (Dimethylthexylsilyl 4-*O*-[2-Azido-3-*O*-benzyl-2-deoxy-4-*O*-(9-fluorenyl-methoxycarbonyl)-6-*O*-levulinoyl- α -D-glucopyranosyl]-3-*O*-benzyl- β -L-ido-pyranoside) uronate (48**)**



The reaction was carried out following the procedure B. To a solution of glycosyl acceptor **42** (100 mg, 0.231 mmol) and TMSOTf (0.2 equivalents, 5 μ L, 0.028 mmol) in dry DCM (3.5 mL) at 0 °C, a solution of glycosyl donor **9** (0.106 mg, 0.14 mmol) in dry DCM (1.5 mL) was slowly added. The reaction was quenched by the addition of Et₃N, and the mixture was filtered and concentrated. Flash chromatography (hexane/ethyl acetate 4:1) gave **48** (65 mg, 45%). R_f = 0.38 (hexane/ethyl acetate 7:3); ¹H NMR (500 MHz, CDCl₃) δ = 7.76 – 7.16 (m, 18H, aromatic), 5.06 (s, 1H, H-1), 5.03 (d, J = 3.5 Hz, 1H, H-1'), 4.88 (t, J = 9.8 Hz, 1H, H-4'), 4.79 (d, J = 10.8 Hz, 1H, CH₂Ph), 4.69 – 4.61 (m, 3H, CH₂Ph), 4.58 (d, J = 1.2 Hz, 1H, H-5), 4.45 (dd, J = 10.0, 6.6 Hz, 1H, CH₂Fmoc), 4.28 – 4.16 (m, 4H, CH₂Fmoc, H-6', CH_{Fmoc}), 4.10 (s, 1H, H-4), 4.08 – 4.03 (m, 1H, H-3), 3.94 – 3.86 (m, 2H, H-3', H-5'), 3.80 (s, 3H, CH₃COOMe), 3.67 (d, J = 8.8 Hz, 1H, H-2), 3.55 (dd, J = 10.1, 3.5 Hz, 1H, H-2'), 2.91 (d, J = 9.2 Hz, 1H, 2-OH), 2.79 – 2.53 (m, 4H, CH₂Lev), 2.14 (s, 3H, CH₃Lev), 1.72 – 1.67 (m, 1H, CH(CH₃)₂), 0.97 – 0.87 (m, 12H, C(CH₃)₂ and CH(CH₃)₂), 0.25 (d, J = 27.5 Hz, 6H, Si(CH₃)₂). ¹³C NMR (from HSQC) (500 MHz, CDCl₃) δ = 129.1– 120.1 (C_{aromatic}), 95.4 (C-1'), 94.9 (C-1), 78.1 (C-3'), 75.5 (CH₂Bn), 74.2 (C-4'), 73.7 (C-5), 73.6 (C-3), 72.8 (CH₂Bn), 71.7 (C-4), 70.4 (CH₂Fmoc), 68.6 (C-5'), 68.5 (C-2), 63.2 (C-2'), 61.8 (C-6'), 52.3 (CH₃COOMe), 46.8 (CH_{Fmoc}), 37.8 (CH₂Lev), 34.1 (CH(CH₃)₂), 29.9 (CH₃Lev), 28.1 (CH₂Lev), 19.5 (C(CH₃)₂ and CH(CH₃)₂), -2.9 (Si(CH₃)₂); LRMS (ESI MS) m/z calcd for C₅₅H₆₇N₃O₁₅Si [M + H]⁺ 1038.4, found 1038.6.

Methyl (Dimethylthexylsilyl 4-*O*-[2-Azido-3-*O*-benzyl-4,6-*O*-benzylidene-2-deoxy-4-*O*-(9-fluorenyl-methoxycarbonyl)- α -D-glucopyranosyl]-3-*O*-benzyl- β -L-idopyranoside) uronate (49)



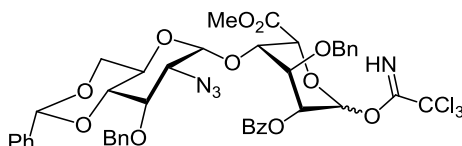
The reaction was carried out following procedure A and procedure B.

Procedure A: To a solution of glycosyl acceptor **42** (55 mg, 0.125 mmol) and glycosyl donor **41** (40 mg, 0.076 mmol) in dry DCM (2.2 mL), TMSOTf (0.2 equivalents, 3 μ L, 0.0152 mmol) at -10 °C was added. The reaction was quenched by the addition of Et₃N, and the mixture was filtered and concentrated. Flash chromatography (toluene/ethyl acetate 15:1) afforded the desired disaccharide **49** (19 mg, 32%).

Procedure B: To a solution of glycosyl acceptor **42** (1.5 g, 3.4 mmol) and TMSOTf (0.2 equivalents, 72 μ L, 0.4 mmol) in dry DCM (26 mL) at 0 °C, a solution of glycosyl donor **41** (1.06 g, 2 mmol) in dry DCM (9 mL) was slowly added. The reaction was quenched by the addition of Et₃N, and the mixture was filtered and concentrated. Flash chromatography (toluene/ethyl acetate 15:1) afforded the desired disaccharide **49** (0.95 g, 59%).

Physical data was in good agreement with published values (De Paz *et al.* 2003).

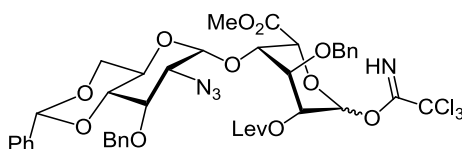
Methyl (4-*O*-[2-Azido-3-*O*-benzyl-4,6-*O*-benzylidene-2-deoxy- α -D-glucopyranosyl]-2-*O*-benzoyl-3-*O*-benzyl- α/β -L-idopyranosyluronate) trichloroacetimidate (50)



Compound **50** was prepared from the disaccharide **49** following the procedures described by Lucas and colleagues. The physical data of the intermediates **52** and **54**

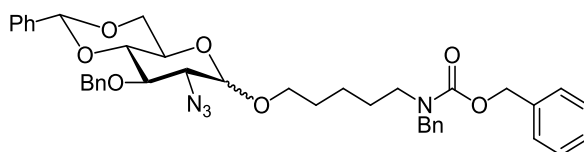
and of the final product **50** were in good agreement with published values (Lucas *et al.* 2003).

Methyl (4-*O*-[2-Azido-3-*O*-benzyl-4,6-*O*-benzylidene-2-deoxy- α -D-glucopyranosyl]-3-*O*-benzyl-2-*O*-levulinoyl- α/β -L-idopyranosyluronate) trichloroacetimidate (51**)**

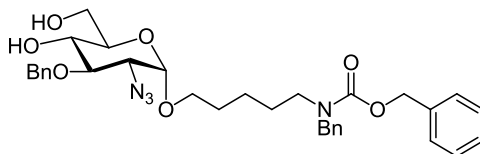


Compound **51** was prepared from the disaccharide **49** following the procedures described by De Paz and colleagues. The physical data of the intermediates **53** and **55**, and the final product **51**, were in good agreement with published values (De Paz and Martín-Lomas 2005).

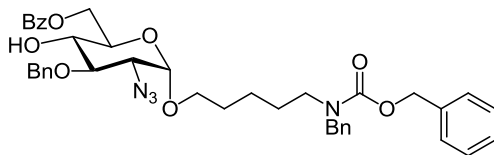
***N*-(Benzyl)-benzyloxycarbonyl-5-aminopentyl 2-Azido-3-*O*-benzyl-4,6-*O*-benzylidene-2-deoxy- α/β -D-glucopyranoside (**56**)**



The reaction was carried out according to procedure A. To a solution of glycosyl acceptor **6** (0.5 g, 1.52 mmol) and glycosyl donor **41** (1.21 g, 2.29 mmol) in dry Et₂O (15 mL), TMSOTf (0.1 equivalents, 30 μ L, 0.15 mmol) was added at 0 °C. The reaction was quenched by the addition of Et₃N, and the mixture was filtered and concentrated. The flash chromatography purification of the crude (hexane/ethyl acetate 4:1) gave the desired product **56** (0.75 g, 72%) as a mixture of anomers (α/β 2/1). The structural data was in good agreement with published data (Arungundram *et al.* 2009).

***N*-(Benzyl)-benzyloxycarbonyl-5-aminopentyl 2-Azido-3-*O*-benzyl-2-deoxy- α -D-glucopyranoside (**57**)**

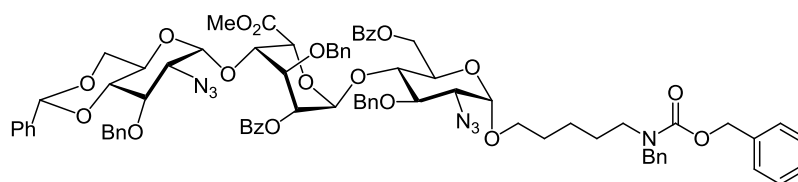
Compound **56** (0.693 g, 1 mmol) was diluted with dry DCM (10 mL) and EtSH (360 μ L, 5 mmol) and a catalytic amount of $\text{BF}_3 \cdot \text{O}(\text{Et})_2$ (12 μ L, 0.5 mmol) were added. The reaction was stirred at room temperature for 1 hour and quenched by the addition of Et_3N . The crude was concentrated and loaded onto a silica gel-based column for purification. Flash chromatography (hexane/ethyl acetate 1:1) afforded the desired product **57** (0.554 g, 92%). The structural data was in good agreement with published data (Arungundram *et al.* 2009).

***N*-(Benzyl)-benzyloxycarbonyl-5-aminopentyl 2-Azido-6-*O*-benzoyl-3-*O*-benzyl-2-deoxy- α -D-glucopyranoside (**58**)**

To a solution of compound **57** (0.78 g, 1.29 mmol) in dry acetonitrile (28 mL), Et_3N (36 μ L, 0.258 mmol) was added. The solution was cooled to -30°C and a 0.9 M benzoyl cyanide BzCN solution in dry acetonitrile (1 equivalent, 1.43 mL, 1.29 mmol) was added dropwise over 1 hour at -30°C . The reaction was monitored by TLC analysis (hexane/ethyl acetate 1:1) to avoid the formation of the di-benzoylated by-product. At the end of the addition of the BzCN solution, the reaction was quenched by the addition of methanol. The reaction crude was concentrated and purified by flash column chromatography (hexane/ethyl acetate 4:1) to afford the desired mono-benzoylated product **58** (0.809 g, 89%). $R_f = 0.31$ (hexane/ethyl acetate 4:1); $\alpha_D^{20} = +25.5$ ($c = 0.5$, CHCl_3); ^1H NMR (500 MHz, CDCl_3) $\delta = 8.04 - 7.06$ (m, 18H, aromatic), 5.19 (d, $J = 20.2$ Hz, 2H, $\text{OCH}_2\text{Ph}_{\text{Cbz}}$), 4.98 – 4.79 (m, 3H, CH_2Ph , H-1), 4.72 (d, $J = 11.9$ Hz, 1H, H-6), 4.60 – 4.39 (m, 3H, H-6, NCH_2Ph), 3.99 – 3.80 (m, 2H, H-5, H-3), 3.78 – 3.55 (m, 2H, $\text{OCH}_{2\text{linker}}$, H-4), 3.52 – 3.36 (m, 1H, $\text{OCH}_{2\text{linker}}$), 3.34 – 3.14 (m, 3H, $\text{NCH}_{2\text{linker}}$, H-2), 2.95 (bs, 1H, 4-OH), 1.74–

1.24 (m, 6H, CH_{2linker}); ¹³C NMR (126 MHz, CDCl₃) δ = 167.10 (Cq_{Bz}), 156.40 (Cq_{Cbz}), 138.12 - 137.95 (Cq_{aromatic}), 133.45 - 127.34 (CH_{aromatic}), 98.02 (C-1), 79.75 (C-3), 75.41 (CH_{2Bn}), 71.28 (C-4), 70.41 (C-5), 68.26 (OCH_{2linker}), 67.38 (OCH_{2PhCbz}), 63.66 (C-6), 63.01 (C-2), 50.50 (NCH_{2Ph}), 47.46 - 46.19 (NCH_{2linker}), 29.14 - 23.42 (CH_{2linker}); HRMS (ESI-TOF MS) m/z calcd for C₄₀H₄₄N₄O₈ [M + Na]⁺ 731.3051, found 731.2989.

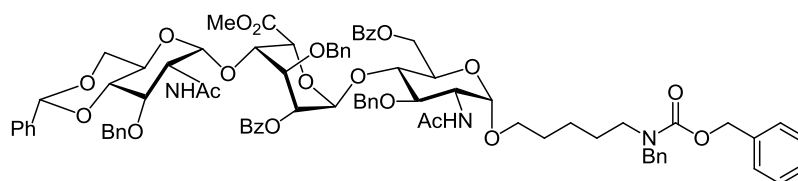
***N*-(Benzyl)-benzyloxycarbonyl-5-aminopentyl (2-azido-3-*O*-benzyl-4,6-*O*-benzylidene-2-deoxy- α -D-glucopyranosyl)-(1 \rightarrow 4)-(methyl 2-*O*-benzoyl-3-*O*-benzyl- α -L-idopyranosyluronate)-(1 \rightarrow 4)-2-azido-3-*O*-benzyl-6-*O*-benzoyl-2-deoxy- α -D-glucopyranoside (**59**)**



The reaction was carried out according to procedure A. To a solution of glycosyl acceptor **58** (230 mg, 0.325 mmol) and glycosyl donor **50** (444 mg, 0.487 mmol) in dry DCM (3.3 mL), TMSOTf (0.1 equivalents, 6 μ L, 0.032 mmol) was added at -20 °C. The reaction was quenched by the addition of Et₃N, and the mixture was filtered and concentrated. The flash chromatography purification of the crude (toluene/ethyl acetate 7:1) gave the desired product **59** (452 mg, 95%). R_f = 0.43 (toluene/ethyl acetate 6:1); α_D^{20} = +1.3 (c = 0.5, CHCl₃); ¹H NMR (500 MHz, CDCl₃) δ = 8.09 – 7.15 (m, 40H, aromatic), 5.58 (d, J = 3.0 Hz, 1H, H-1'), 5.53 (s, 1H, Ph-CH), 5.23 – 5.12 (m, 3H, H-2', OCH_{2PhCbz}), 4.95 (d, J = 10.3 Hz, 1H, CH_{2Ph}), 4.87 – 4.71 (m, 6H, CH_{2Ph}, H-1, H-5', H-1''), 4.66 (dd, J = 12.0, 1.9 Hz, 1H, H-6), 4.58 – 4.41 (m, 4H, CH_{2Ph}, NCH_{2Ph}, H-6), 4.28 (dd, J = 10.2, 4.9 Hz, 1H, H-6''), 4.21 – 4.10 (m, 2H, H-3', CH_{2Ph}), 4.08 – 3.99 (m, 2H, H-4', H-4), 3.98 – 3.88 (m, 3H, H-5'', H-3, H-5), 3.69 – 3.54 (m, 4H, H-6'', OCH_{2linker}, H-3'', H-4''), 3.46 (s, 3H, CH_{3COOMe}), 3.43 – 3.15 (m, 5H, OCH_{2linker}, H-2, NCH_{2linker}, H-2''), 1.69 – 1.20 (m, 6H, CH_{2linker}); ¹³C NMR (126 MHz, CDCl₃) δ = 169.25 (Cq_{COOMe}), 166.15 (Cq_{Bz}), 165.47 (Cq_{Bz}), 163.53 (Cq_{Cbz}), 137.99 - 137.35 (Cq_{aromatic}), 133.44 - 126.20 (CH_{aromatic}), 101.46 (Ph-CH), 99.72 (C-1''), 98.70 (C1'), 97.59 (C-1), 82.48 (C-4''), 78.70 (C-3), 76.32 (C-3''), 75.97 (C-4), 75.32 (C-4'), 75.09 (CH_{2Bn}), 74.80 (C-3'), 73.60

(CH₂Bn), 69.33 (C-2', C-5', C-5), 68.59 (C-6''), 68.30 (OCH₂linker), 67.29 (OCH₂Ph_{Cbz}), 63.51 (C-5'', C-2), 63.11 (C-2''), 62.82 (C-6), 52.00 (CH₃COOMe), 50.67 – 50.34 (NCH₂Ph), 46.28 (NCH₂linker), 29.09 – 23.34 (CH₂linker); HRMS (MALDI-TOF MS) m/z calcd for C₈₁H₈₃N₇O₁₉ [M + Na]⁺ 1480.5636, found 1480.5663.

***N*-(Benzyl)-benzyloxycarbonyl-5-aminopentyl (2-acetamido-3-*O*-benzyl-4,6-*O*-benzylidene-2-deoxy- α -D-glucopyranosyl)-(1→4)-(methyl 2-*O*-benzoyl-3-*O*-benzyl- α -L-idopyranosyluronate)-(1→4)-2-acetamido-3-*O*-benzyl-6-*O*-benzoyl-2-deoxy- α -D-glucopyranoside (**60**)**



To a solution of **59** (150 mg, 0.103 mmol) in THF/H₂O (10.1 mL, 8 mL:2.1 mL), a 1 M PMe₃ solution in THF (10 equivalents per azido group, 2.1 mL, 2.06 mmol) was added, followed by the addition of a 1 M sodium hydroxide NaOH solution (1 equivalent per azido group, 206 μ L, 0.206 mmol). The solution was vigorously stirred at room temperature for 3 hours and another amount of PMe₃ solution (1 mL, 1.03 mmol) and 1 M NaOH solution (103 μ L, 0.103 mmol) were added to the reaction mixture. After another 2 hours of vigorous stirring at room temperature, MALDI-TOF analysis of a small aliquot revealed the completion of the reaction (detection of the mass of the intermediate **61** only was detected). The reaction was quenched by the addition of 1 M HCl solution (309 μ L, 0.309 mmol). The solution was evaporated and the resulting crude was dried overnight under high vacuum to obtain the crude diamino residue **61**.

The crude of the diamino intermediate **61** was dissolved in dry Et₃N (2.8 mL, 8 mL/0.3 mmol) and dry acetic anhydride Ac₂O (1.4 mL, 4 mL/0.3 mmol) was added to the solution under argon at 0 °C. The progress of the reaction was monitored by MALDI-TOF analysis. After 1 hour of stirring at room temperature, ethanol EtOH was added to quench the reaction. The solvent was evaporated and dried under high vacuum. The resulting crude was dissolved in a minimum volume of methanol MeOH and loaded onto a Sephadex LH-20 for purification (MeOH). The desired

bisacetamide product **60** was obtained (106 mg, 69% over two steps). $R_f = 0.29$ (hexane/ethyl acetate 2:3); $\alpha_D^{20} = +13.0$ ($c = 0.56$, CHCl_3); ^1H NMR (500 MHz, CDCl_3) $\delta = 8.04 - 7.10$ (m, 40H, aromatic), 5.77 (d, $J = 9.0$ Hz, 1H, NHAc), 5.53 (s, 1H, Ph-CH), 5.47 – 5.39 (m, 2H, NHAc'', H-1'), 5.23 – 5.08 (m, 3H, H-2', OCH_2PhCbz), 4.93 – 4.83 (m, 3H, H-1'', CH_2Ph , H-5'), 4.76 – 4.68 (m, 3H, CH_2Ph , H-1), 4.65 – 4.47 (m, 6H, CH_2Ph , NCH_2Ph , H-6), 4.32 – 4.17 (m, 4H, CH_2Ph , H-2, H-6'', H-2''), 4.07 – 3.96 (m, 3H, H-3', H-4, H-4'), 3.88 – 3.80 (m, 1H, H-5), 3.78 – 3.54 (m, 5H, H-5'', H-6'', H-3, H-4'', $\text{OCH}_{2\text{linker}}$), 3.53 – 3.37 (m, 4H, H-3'', CH_3COOMe), 3.31 – 3.13 (m, 3H, $\text{OCH}_{2\text{linker}}$, $\text{NCH}_{2\text{linker}}$), 1.80 (s, 3H, CH_3Ac), 1.60 – 1.44 (m, 4H, $\text{CH}_{2\text{linker}}$), 1.41 (s, 3H, CH_3Ac), 1.26 (s, 2H, $\text{CH}_{2\text{linker}}$); ^{13}C NMR (126 MHz, CDCl_3) $\delta = 170.19$, 169.00, 166.24, 165.55, 138.48 - 136.96 ($\text{C}_{\text{qaromatic}}$), 133.80 - 126.17 ($\text{CH}_{\text{aromatic}}$), 101.43 (Ph-CH), 99.23 (C-1''), 98.61 (C-1'), 97.44 (C-1), 82.38 (C-4''), 78.74 (C-3), 76.54 (C-3''), 76.08 (C-4), 74.44 (C-4', $\text{CH}_{2\text{Bn}}$), 74.08 (C-3', $\text{CH}_{2\text{Bn}}$), 73.56 ($\text{CH}_{2\text{Bn}}$), 70.38 (C-2'), 69.38 (C-5', C-5), 68.71 (C-6''), 68.24 ($\text{OCH}_{2\text{linker}}$), 67.31 (OCH_2PhCbz), 63.83 (C-5''), 62.85 (C-6), 52.59 (C-2, C-2''), 52.05 (CH_3COOMe), 50.38 (NCH_2Ph), 47.20 ($\text{NCH}_{2\text{linker}}$), 30.42 - 23.88 ($\text{CH}_{2\text{linker}}$), 23.34 - 22.82 (CH_3Ac); HRMS (MALDI-TOF MS) m/z calcd for $\text{C}_{85}\text{H}_{91}\text{N}_3\text{O}_{21}$ [$\text{M} + \text{Na}$] $^+$ 1512.6037, found 1512.6014.

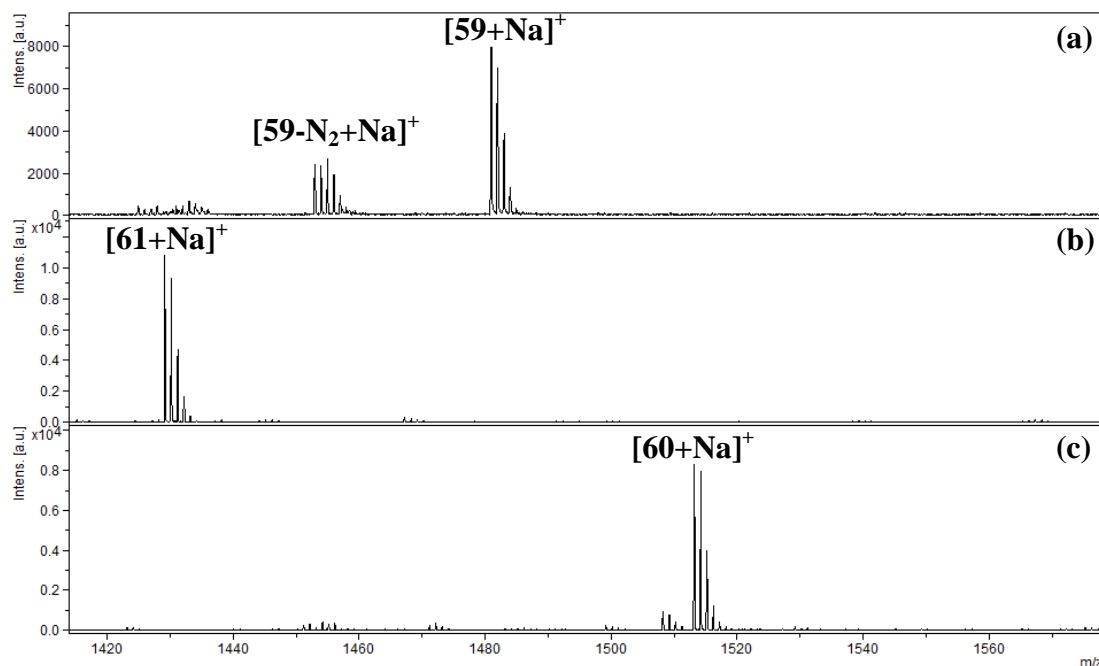


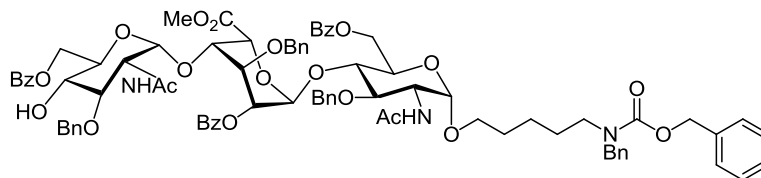
Figure 10: Monitoring the progress of the synthesis of the trisaccharide 60 by MALDI-TOF mass spectrometry.

(a) MALDI-TOF mass spectrum of the starting material **59**. Calcd for $C_{81}H_{83}N_7O_{19}$: 1458.6 [M], found m/z 1481.0 [M+Na]⁺, 1453.0 [M-N₂+Na]⁺;

(b) MALDI-TOF mass spectrum of the reaction crude after 5 hours stirring at R.T. Calcd for $C_{81}H_{87}N_3O_{19}$: 1405.6 [M], found m/z 1429.2 [M+Na]⁺: trisaccharide intermediate **61**;

(c) MALDI-TOF mass spectrum of the reaction crude after 1 hour stirring at R.T. Calcd for $C_{85}H_{91}N_3O_{21}$: 1489.6 [M], found 1513.2 [M+Na]⁺: trisaccharide **60**.

***N*-(Benzyl)-benzyloxycarbonyl-5-aminopentyl (2-acetamido-6-*O*-benzoyl-3-*O*-benzyl-2-deoxy- α -D-glucopyranosyl)-(1 \rightarrow 4)-(methyl 2-*O*-benzoyl-3-*O*-benzyl- α -L-idopyranosyluronate)-(1 \rightarrow 4)-2-acetamido-3-*O*-benzyl-6-*O*-benzoyl-2-deoxy- α -D-glucopyranoside (**63**)**



Compound **60** (90 mg, 0.06 mmol) was diluted with dry DCM (600 μ L) and EtSH (222 μ L, 3 mmol) was added, followed by the addition of a catalytic amount of TMSOTf (0.2 equivalents, 2 μ L, 0.012 mmol). After 12 hour stirring at room temperature, TLC analysis (R_f = 0.12, hexane/ethyl acetate 3:7) and MALDI-TOF analysis showed a complete conversion of the starting material. The reaction was

quenched by the addition of Et₃N. The solvent was evaporated and the crude eluted on a Sephadex column to remove salts and excess of reagents. The resulting residue was then dried under high vacuum overnight to afford the crude intermediate **62**.

The diol intermediate was dissolved in dry acetonitrile ACN (1.2 mL) and a catalytic amount of Et₃N was added. The solution was cooled to -30 °C and a 0.9 M benzoyl cyanide BzCN solution in dry acetonitrile (1 equivalent, 67 µL, 0.06 mmol) was added dropwise at -30 °C. The reaction was monitored by TLC analysis (toluene/ethyl acetate 7:3) and MALDI-TOF analysis to avoid the formation of the di-benzoylated by-product. At the end of the addition of the BzCN solution, the reaction was quenched by addition of methanol. The solvent was evaporated and the crude was eluted from a Sephadex LH-20 for purification (MeOH). The desired monobenzoylated compound **63** was obtained (63 mg, 70% over two steps). R_f = 0.65 (toluene/ethyl acetate 7:3); α_D^{20} = +21.4 (c = 0.5, CHCl₃); ¹H NMR (500 MHz, CDCl₃) δ = 8.05 – 7.13 (m, 40H, aromatic), 5.76 (d, J = 9.4 Hz, 1H, NHAc), 5.57 (d, J = 9.4 Hz, 1H, NHAc''), 5.42 (s, 1H, H-1'), 5.23 – 5.09 (m, 3H, H-2', OCH₂Ph_{Cbz}), 4.96 (s, 1H, H-1''), 4.91 (s, 1H, H-5'), 4.84 (d, J = 11.5 Hz, 1H, CH₂Ph), 4.78 – 4.69 (m, 3H, CH₂Ph, H-1, H-6''), 4.67 – 4.54 (m, 5H, CH₂Ph, H-6), 4.50 (s, 2H, NCH₂Ph), 4.40 (d, J = 12.2 Hz, 2H, CH₂Ph, H-6''), 4.36 – 4.24 (m, 1H, H-2), 4.19 (td, J = 10.1, 3.5 Hz, 1H, H-2''), 4.10 – 4.03 (m, 3H, H-3', H-4, H-4'), 3.92 – 3.82 (m, 1H, H-5), 3.79 (d, J = 9.3 Hz, 1H, H-5''), 3.75 – 3.55 (m, 3H, H-3, H-4'', OCH₂linker), 3.48 – 3.40 (m, 3H, CH₃COOMe), 3.36 – 3.15 (m, 4H, H-3'', OCH₂linker, NCH₂linker), 2.96 (bs, 1H, 4-OH''), 1.78 (d, J = 16.5 Hz, 3H, CH₃Ac), 1.61 – 1.45 (m, 4H, CH₂linker), 1.40 (s, 3H, CH₃Ac), 1.34 – 1.26 (m, 2H, CH₂linker); ¹³C NMR (126 MHz, CDCl₃) δ = 170.17, 169.13, 167.29, 166.31, 165.71, 138.31 - 136.96 (C_qaromatic), 133.85 - 127.31 (CH_{aromatic}), 98.46 (C-1'), 98.14 (C-1''), 97.50 (C-1), 79.77 (C-3''), 78.65 (C-3), 75.90 (C-4), 74.31 (CH₂Bn), 73.33 (C-4', C-3', CH₂Bn), 71.52 (C-5''), 70.49 (C-2'), 69.86 (C-4''), 69.43 (C-5, C-5'), 68.25 (OCH₂linker), 67.32 (OCH₂Ph_{Cbz}), 63.05 - 62.93 (C-6, C-6''), 52.49 (C-2), 52.13 (C-2'', CH₃COOMe), 50.38 (NCH₂Ph), 47.22 - 46.10 (NCH₂linker), 29.80 - 27.32 (CH₂linker), 23.87 (CH₂linker), 23.36 - 22.93 (CH₃Ac); HRMS (MALDI-TOF MS) m/z calcd for C₈₅H₉₁N₃O₂₂ [M + Na]⁺ 1528.5986, found 1528.5992.

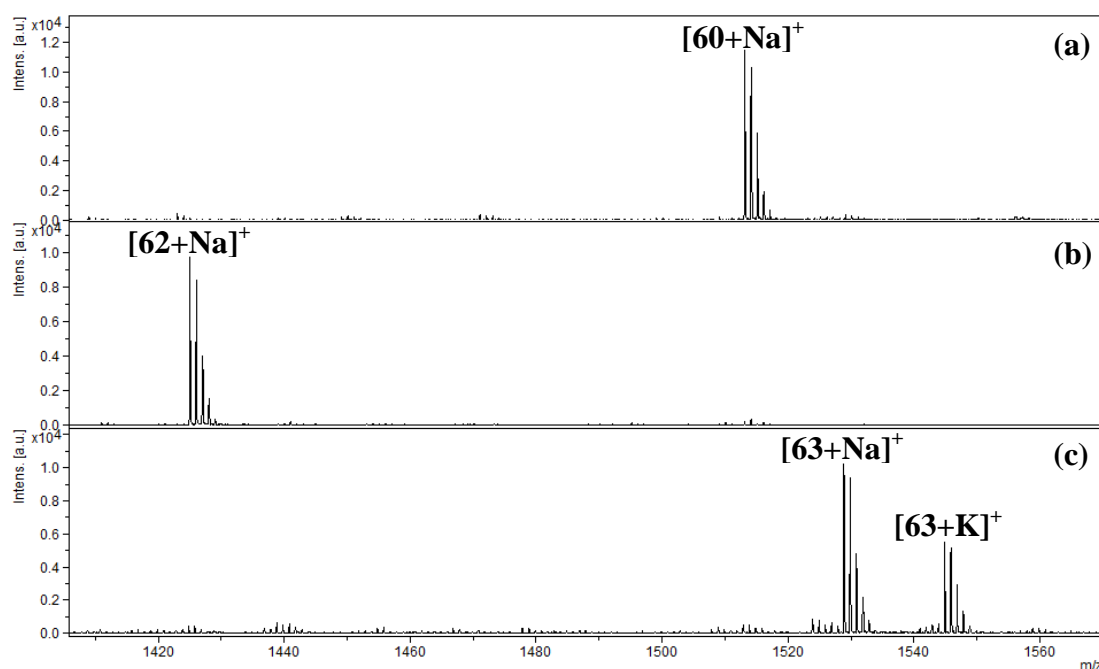


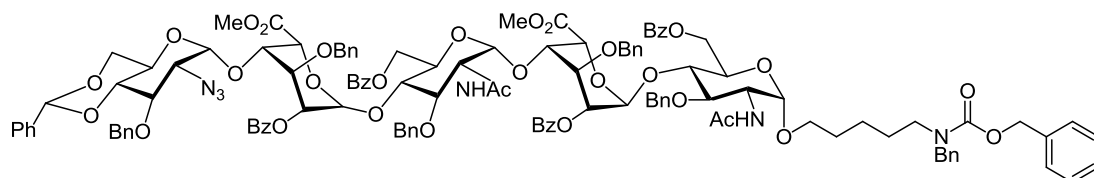
Figure 11: Monitoring of the progress of the synthesis of the trisaccharide 63 by MALDI-TOF mass spectrometry.

(a) MALDI-TOF mass spectrum of the starting material **60**. Calcd for $C_{85}H_{91}N_3O_{21}$: 1489.6 [M], found 1513.2 [M+Na]⁺;

(b) MALDI-TOF mass spectrum of the reaction crude after 12 hours stirring at R.T. Calcd for $C_{78}H_{87}N_3O_{21}$: 1401.6 [M], found m/z 1425.1 [M+Na]⁺: trisaccharide intermediate **62**;

(c) MALDI-TOF mass spectrum of the reaction crude after 1 hour stirring at -30°C. Calcd for $C_{85}H_{91}N_3O_{22}$: 1505.6 [M], found 1528.9 [M+Na]⁺, 1544.9 [M+K]⁺: trisaccharide **63**.

***N*-(Benzyl)-benzyloxycarbonyl-5-aminopentyl (2-azido-3-*O*-benzyl-4,6-*O*-benzylidene-2-deoxy- α -D-glucopyranosyl)-(1 \rightarrow 4)-(methyl 2-*O*-benzoyl-3-*O*-benzyl- α -L-idopyranosyluronate)-(1 \rightarrow 4)-(2-acetamido-6-*O*-benzoyl-3-*O*-benzyl-2-deoxy- α -D-glucopyranosyl)-(1 \rightarrow 4)-(methyl 2-*O*-benzoyl-3-*O*-benzyl- α -L-idopyranosyluronate)-(1 \rightarrow 4)-2-acetamido-3-*O*-benzyl-6-*O*-benzoyl-2-deoxy- α -D-glucopyranoside (**64**)**



The reaction was carried out according to procedure A. To a solution of glycosyl acceptor **63** (5 mg, 0.0033 mmol) and glycosyl donor **50** (0.015 mg, 0.016 mmol) in dry DCM (50 μ L), TMSOTf (0.2 equivalents, 0.0007 mmol) was added at -20 °C.

The reaction was quenched by the addition of Et₃N, and the mixture was filtered and concentrated. A small aliquot of the reaction was dried with an air stream and analysed by LC-MS.

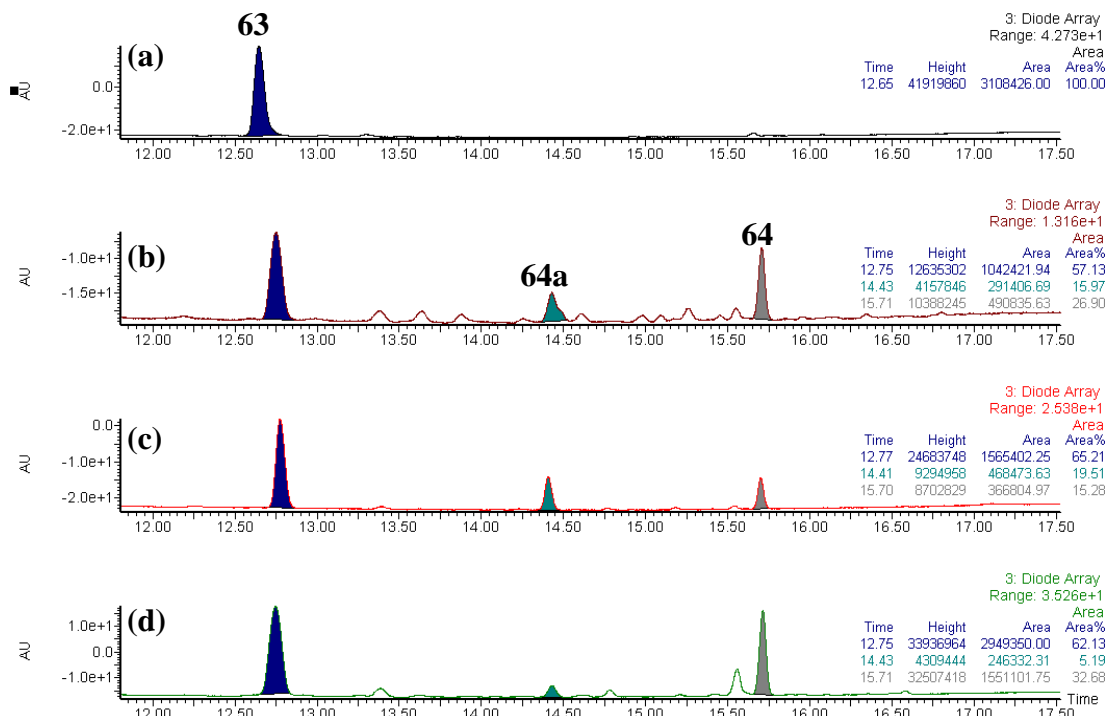


Figure 12: LC-MS spectra obtained for the synthesis of pentasaccharide **64.**

Retention times: 12.75 min (calcd for C₈₅H₉₁N₃O₂₂: 1505.6 [M], found m/z 1506.8 [M+NH₄]⁺, 1528.9 [M+Na]⁺): acceptor **63**; retention time: 14.43 min (calcd for C₈₈H₉₉N₃O₂₂Si: 1578.8 [M], found m/z 1601.8 [M+Na]⁺): silylated acceptor **64a**; retention time: 15.71 min (calcd for C₁₂₆H₁₃₀N₆O₃₃: 2254.9, found m/z 1128.7 [M+2H]²⁺, 1140.2 [M+H+Na]²⁺): product **64**.

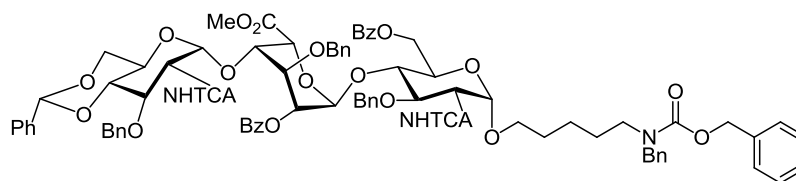
(a) Conditions: 1.5 equiv. of donor, 0.2 equiv. of activator (TfOH), -20°C, 0.01 M; peak areas: **63** (100%);

(b) Conditions: 1.5 equiv. of donor, 0.2 equiv. of activator (TMSOTf), 0°C, 0.5 M; peak areas: **63** (57.13%), **64a** (15.97%), **64** (26.90%);

(c) Conditions: 1.5 equiv. of donor, 0.2 equiv. of activator (TMSOTf), -80°C, 0.01 M; **63** (65.21%), **64a** (19.51%), **64** (15.28%);

(d) Conditions: 1.5 equiv. of donor, 0.2 equiv. of activator (TMSOTf), -20°C, 0.01 M; **63** (62.13%), **64a** (5.19%), **64** (32.68%)

***N*-(Benzyl)-benzyloxycarbonyl-5-aminopentyl (3-*O*-benzyl-4,6-*O*-benzylidene-2-deoxy-2-trichloroacetamido- α -D-glucopyranosyl)-(1 \rightarrow 4)-(methyl 2-*O*-benzoyl-3-*O*-benzyl- α -L-idopyranosyluronate)-(1 \rightarrow 4)-6-*O*-benzoyl-3-*O*-benzyl-2-deoxy-2-trichloroacetamido- α -D-glucopyranoside (**65**)**

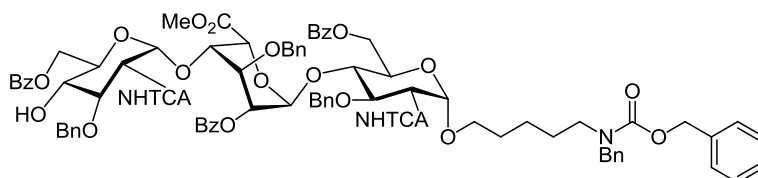


To a solution of **59** (102 mg, 0.07 mmol) in THF/H₂O (6.72 mL, 5.5 mL:1.22 mL), a 1 M solution of trimethylphosphine PMe₃ in THF (10 equivalents per azido group, 1.4 mL, 1.4 mmol) was added, followed by the addition of a 1 M NaOH solution (1 equivalent per azido group, 140 μ L, 0.14 mmol). The solution was stirred at room temperature for 3 hours and another aliquot of PMe₃ solution (0.7 mL, 0.7 mmol) and 1 M NaOH solution (70 μ L, 0.070 mmol) were added to the reaction mixture. After another 2 hours of stirring at room temperature, MALDI-TOF analysis of a reaction sample revealed the completion of the reaction (detection of the mass of the intermediate **61** only). The reaction was quenched by the addition of 1 M HCl solution (210 μ L, 0.21 mmol). The solution was evaporated and dried overnight under high vacuum to afford the crude diamino intermediate **61**.

The crude intermediate **61** was dissolved in dry Et₃N (700 μ L) and the solution was cooled to 0 °C. Trichloroacetyl chloride CCl₃COCl (1.5 equivalents per amino group, 24 μ L, 0.21 mmol) was added to the solution under argon. The reaction was monitored by TLC analysis (toluene/acetone 9:1) and stopped when the starting material was all consumed. The reaction solution was diluted with DCM and washed with water. The organic phase was dried over MgSO₄, filtered and concentrated. The resulting crude was dissolved in a minimum volume of methanol MeOH and loaded onto a Sephadex LH-20 for purification (MeOH). The desired ditrichloroacetamido product **65** was obtained (65 mg, 55% over two steps). R_f = 0.50 (toluene/acetone 9:1); α_D^{20} = +5.6 (c = 0.5, CHCl₃); ¹H NMR (500 MHz, CDCl₃) δ = 8.00 – 6.97 (m, 40H, aromatic), 6.92 – 6.80 (dd, J = 8.6 Hz, 1H, NHCCl₃), 6.48 (d, J = 8.3 Hz, 1H, NHCCl₃'), 5.56 (s, 1H, Ph-CH), 5.49 (d, J = 1.9 Hz, 1H, H-1'), 5.20 – 5.13 (m, 3H, H-2', OCH₂Ph_{Cbz}), 5.05 (s, 1H, H-1''), 4.93 – 4.82 (m, 2H, H-5', CH₂Ph), 4.82 –

4.72 (m, $J = 11.7$ Hz, 2H, CH_2Ph , H-1), 4.71 – 4.57 (m, 3H, CH_2Ph , H-6), 4.54 – 4.39 (m, 5H, CH_2Ph , NCH_2Ph , H-6, H-6''), 4.30 – 4.23 (m, 1H, H-2), 4.18 – 3.85 (m, 7H, CH_2Ph , H-4', H-3', H-4, H-2'', H-5'', H-5), 3.82 – 3.75 (m, 1H, H-3), 3.72 – 3.60 (m, 3H, H-4'', H-6'', $\text{OCH}_2\text{linker}$), 3.45 – 3.32 (m, 4H, CH_3COOMe , H-3''), 3.21 (d, $J = 39.8$ Hz, 2H, $\text{NCH}_2\text{linker}$), 1.57 – 1.41 (m, 4H, CH_2linker), 1.38 – 1.27 (m, $J = 47.4$ Hz, 2H, CH_2linker); ^{13}C NMR (126 MHz, CDCl_3) $\delta = 168.70, 166.19, 165.29, 161.69, 148.38, 138.88 - 137.06$ ($\text{C}_{\text{aromatic}}$), $133.78 - 126.24$ ($\text{CH}_{\text{aromatic}}$), 101.33 (Ph-CH), 99.25 (C-1''), 98.79 (C-1'), 96.78 (C-1), 82.22 (C-4''), 79.33 (C-3), 76.57 (C-3''), 75.97 - 75.16 (C-4, C-4', C-3', CH_2Bn), 74.56 (CH_2Bn), 73.40 (CH_2Bn), 69.45 (C-5), 68.50 (C-2', C-6'', $\text{OCH}_2\text{linker}$, C-5'), 67.38 (OCH_2PhCbz), 63.77 (C-5''), 62.83 (C-6), 54.93 (C-2, C-2''), 52.00 (CH_3COOMe), 50.43 (NCH_2Ph), 47.11 - 46.20 ($\text{NCH}_2\text{linker}$), 29.02 - 23.58 (CH_2linker); HRMS (MALDI-TOF MS) m/z calcd for $\text{C}_{85}\text{H}_{85}\text{Cl}_6\text{N}_3\text{O}_{21}$ $[\text{M} + \text{Na}]^+$ 1716.3699, found 1716.3761.

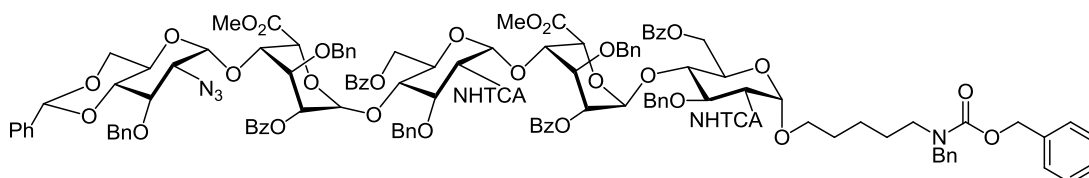
***N*-(Benzyl)-benzyloxycarbonyl-5-aminopentyl (6-*O*-benzoyl-3-*O*-benzyl-2-deoxy-2-trichloroacetamido- α -D-glucopyranosyl)-(1 \rightarrow 4)-(methyl 2-*O*-benzoyl-3-*O*-benzyl- α -L-idopyranosyluronate)]-(1 \rightarrow 4)-6-*O*-benzoyl-3-*O*-benzyl-2-deoxy-2-trichloroacetamido- α -D-glucopyranoside (67)**



Compound **65** (50 mg, 0.03 mmol) was diluted with dry DCM (500 μL) and EtSH (111 μL , 1.5 mmol) was added, followed by the addition of a catalytic amount of TMSOTf (0.2 equivalents, 1 μL , 0.006 mmol). After 1 hour stirring, TLC analysis ($R_f = 0.41$, toluene/ethyl acetate 3:2) and MALDI-TOF analysis showed a complete conversion of the SM. The reaction was then quenched by addition of Et_3N . The solvent was evaporated and the residue was loaded onto a Sephadex LH-20 column to remove the majority of the salts and the excess of the reagent. The resulting residue was hence dried under high vacuum overnight to afford the crude intermediate **66**.

The diol intermediate **66** was dissolved in dry acetonitrile ACN (600 μ L) and a catalytic amount of Et₃N was added. The solution was cooled to -30 °C and a 0.9 M benzoyl cyanide BzCN solution in dry acetonitrile (1 equivalent, 33 μ L, 0.03 mmol) was added dropwise at -30 °C. The reaction was monitored by TLC analysis (toluene/ethyl acetate 7:3) and MALDI-TOF analysis to avoid the formation of the di-benzoylated by-product. At the end of the addition of the BzCN solution, the reaction was quenched by addition of methanol. The solvent was evaporated and the crude was eluted from a Sephadex LH-20 for purification (MeOH). The desired monobenzoylated compound **67** was obtained (26 mg, 51%). R_f = 0.65 (toluene/ethyl acetate 7:3); ¹H NMR (500 MHz, CDCl₃) δ = 8.00 – 7.03 (m, 40H, aromatic), 6.92 (d, J = 8.2 Hz, 1H, NHCCl₃), 6.80 (bs, 1H, NHCCl₃), 6.53 (d, J = 8.2 Hz, 1H, NHCCl₃'), 5.45 (s, 1H, H-1'), 5.20 – 5.14 (m, J = 2.9 Hz, 3H, H-2', OCH₂Ph_{Cbz}), 5.06 (s, 1H, H-1''), 4.92 – 4.85 (m, 2H, CH₂Ph, H-5'), 4.84 – 4.76 (m, 3H, H-6'', CH₂Ph, H-1), 4.69 – 4.61 (m, J = 18.8 Hz, 3H, CH₂Ph, H-6), 4.49 (bs, 3H, NCH₂Ph, H-6), 4.43 – 4.36 (m, J = 10.7 Hz, 2H, H-6'', NCH₂Ph), 4.29 (bs, 1H, H-2), 4.12 – 3.98 (m, 4H, H-4', H-3', H-4, CH₂Ph), 3.97 – 3.87 (m, J = 10.6 Hz, 3H, H-5, H-5'', H-2''), 3.79 (bs, 1H, H-3), 3.60 (s, 1H, OCH₂linker), 3.55 – 3.46 (m, 4H, CH₃COOMe, H-4''), 3.34 – 3.13 (m, 4H, OCH₂linker, H-3'', NCH₂linker), 1.60 – 1.18 (m, 6H, CH₂linker); ¹³C NMR (from HSQC) (500 MHz, CDCl₃) δ = 133.3 – 126.5 (C_{aromatic}), 98.7 (C-1'), 98.6 (C-1''), 96.6 (C-1), 79.2 (C-3''), 78.9 (C-3), 75.4 (C-4'), 74.9 (CH₂Bn), 74.8 (C-4, C-3', CH₂Bn), 73.1 (CH₂Bn), 71.7 (C-5''), 70.0 (C-4''), 69.4 (C-5), 68.9 (C-2'), 68.2 (C-5'), 68.0 (OCH₂linker), 67.2 (OCH₂Ph_{Cbz}), 62.9 (C-6), 62.6 (C-6''), 54.9 (C-2), 54.6 (C-2''), 52.1 (CH₃COOMe), 50.4 (NCH₂Ph), 46.9 – 46.3 (NCH₂linker), 30.2 – 23.3 (CH₂linker); LRMS (ESI MS) m/z calcd for C₈₅H₈₅Cl₆N₃O₂₂ [M + H]⁺ 1710.4, found 1710.6.

***N*-(Benzyl)-benzyloxycarbonyl-5-aminopentyl (2-azido-3-*O*-benzyl-4,6-*O*-benzylidene-2-deoxy- α -D-glucopyranosyl)-(1 \rightarrow 4)-(methyl 2-*O*-benzoyl-3-*O*-benzyl- α -L-idopyranosyluronate)-(1 \rightarrow 4)-(6-*O*-benzoyl-3-*O*-benzyl-2-deoxy-2-trichloroacetamido- α -D-glucopyranosyl)-(1 \rightarrow 4)-(methyl 2-*O*-benzoyl-3-*O*-benzyl- α -L-idopyranosyluronate)]-(1 \rightarrow 4)-6-*O*-benzoyl-3-*O*-benzyl-2-deoxy-2-trichloroacetamido- α -D-glucopyranoside (68)**



The reaction was carried out according to procedure A. To a solution of glycosyl acceptor **67** (13 mg, 0.008 mmol) and glycosyl donor **50** (11 mg, 0.012 mmol) in dry DCM (160 μ L), TMSOTf (0.2 equivalents, 0.016 mmol) was added at -20 $^{\circ}$ C. The reaction was quenched by the addition of Et₃N, and the mixture was filtered and concentrated. A small aliquot of the reaction was dried with an air stream and analysed by LC-MS.

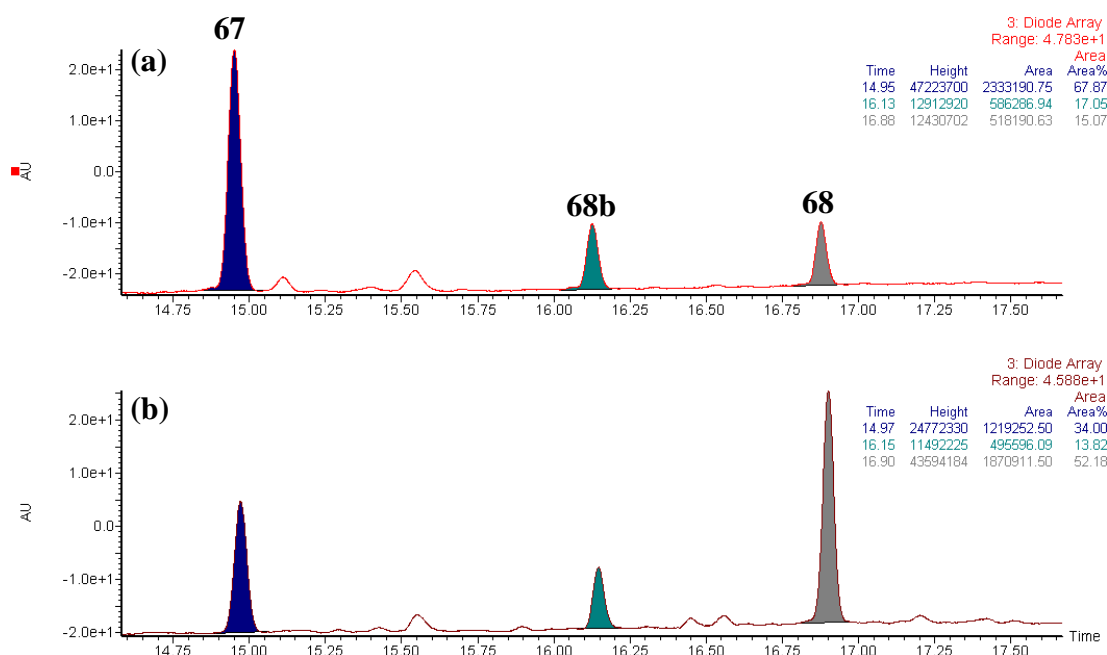


Figure 13: LC-MS spectra obtained for the synthesis of pentasaccharide 68.

Retention time: 14.97 min (calcd for $C_{85}H_{85}Cl_6N_3O_{22}$: 1713.3 [M], found m/z 1714.4 $[M+H]^+$, 1731.4 $[M+NH_4]^+$, 1736.3 $[M+Na]^+$): acceptor **67**; retention time: 16.15 min (calcd for $C_{88}H_{93}Cl_6N_3O_{22}Si$: 1785.5 [M], found m/z 1786.5 $[M+NH_4]^+$, 1803.5 $[M+H]^+$, 1809.5 $[M+Na]^+$): silylated acceptor **68a** (by-product); retention time: 16.90 min (calcd for $C_{126}H_{124}Cl_6N_6O_{33}$: 2463.1, found m/z 1254.4 $[M+2Na]^{2+}$): product **68**.

(a) Conditions: 1.5 equiv. of donor, 0.2 equiv. of activator (TMSOTf), -20°C , 0.05 M; peak areas: **67** (67.87%), **68a** (17.05%), **68** (15.07%);

(b) Conditions: 1.5 equiv. of donor, 0.2 equiv. of activator (TMSOTf), -20°C , 0.05 M; peak areas: **67** (34.00%), **68a** (13.82%), **68** (52.18%).

3. Chapter 3 –HS oligosaccharide library production from natural sources

3.1. Introduction

3.1.1. Aims

Libraries of HS oligosaccharides from different sources (notably from natural sources) have been used to assess a number of biological problems, such as the minimum size for functional activity (Ornitz *et al.* 1992, Gambarini *et al.* 1993, Ostrovsky *et al.* 2002), the existence of specific protein-binding sequences (Cardin and Weintraub 1989, Sobel *et al.* 1992, Hileman, Fromm, *et al.* 1998) and the specificity of the saccharides in their interactions with proteins (Xu and Esko 2014). Using such short saccharides decreases the complexity of studies as it greatly reduces the number of possible epitopes in a single structure. Therefore, in order to investigate the specificity of HS in FGF signalling, the preparation of a library of HS oligosaccharides from natural sources was attempted in this chapter.

3.1.2. Strategy

The strategy adopted for this chapter relied on the preparation/isolation of HS oligosaccharides from natural sources. The enzymatic digestion of porcine mucosal HS (PMHS) was carried out, followed by the purification of the resulting saccharide mixtures by different chromatographic techniques to isolate pure HS hexa-, octa- and deca-saccharides. Pure compounds are required to perform the sequencing of HS saccharides by MS and MS/MS and, therefore, requires the use of several techniques of purification. The general strategy adopted for the study of SAR of HS in FGF signalling is described in Figure 14.

3.1.3. Methods

This section describes briefly the techniques and methods used for the isolation of PMHS oligosaccharides (for further detail about the principles of the different methods, see Section 1.8.1).

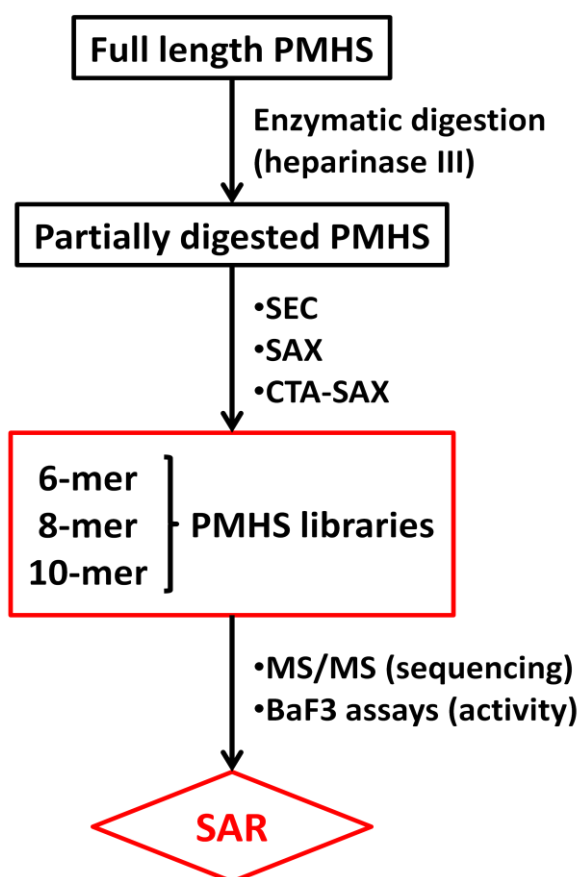


Figure 14: Strategy adopted for the creation of libraries of HS oligosaccharides from natural sources and the study of HS SAR in FGF signalling.

The preparation of the first set of HS oligosaccharides was performed following the protocol described by Powell *et al.* (2010). Native PMHS was first enzymatically digested with heparinase III which selectively cleaves the glycosidic bond D-GlcNR(\pm 6S) α (1 \rightarrow 4) D-GlcA (with R = *N*-acetyl or *N*-sulphate). The two other glycosidic bonds are D-GlcNS(\pm 6S) α (1 \rightarrow 4) L-IdoA(2S) and D-GlcNR(\pm 6S) α (1 \rightarrow 4) D-GlcA/L-IdoA(\pm 2S), which are cleaved by heparinase I and heparinase II, respectively (Linhardt *et al.* 1990). The enzymatic elimination reactions resulted in the formation of an intact D-glucosamine residue at the reducing end of the chain and an unsaturated uronic acid residue at the non-reducing end. This double bond absorbs at 232 nm which makes the detection of the oligosaccharides by UV relatively easy to perform. The resulting saccharide mixtures were next partitioned first according to their sizes and second according to their charges.

SEC helps separating heterogeneous mixtures according to the hydrodynamic volume of the compounds (Ziegler and Zaia 2006). The saccharides were eluted through two Superdex™ 30 XK 16 columns connected in series, with 0.5 M ammonium bicarbonate NH_4CO_3 (isocratic buffer), and the elution was monitored at $\lambda_{\text{ABS}} = 232$ nm. SAX chromatography is a common technique used to further purify the SEC fractions (Rice *et al.* 1985, Powell *et al.* 2010). This technique separated the compounds according to their net charges and often requires several runs to afford pure fractions (here, two runs were necessary). The saccharides were first eluted through a Propac PA1 column (semi-preparative column: 9 x 250 mm) with a linear gradient of 0-50% 2 M NaCl over 120 minutes. An additional run was carried out using a Propac PA1 analytical column (analytical column: 4 x 250 mm) with a gradient of NaCl solution suited to every individual sample. As for SEC, the saccharides were monitored by detection at 232 nm.

In order to ensure the effective isolation of pure single structures, CTA-SAX chromatography was used to complement the SAX-Propac chromatography. The development of the CTA-SAX chromatography technique by Mourier and Viskov (2004) was inspired by the reverse-phase ion pairing (RPIP) chromatography, a robust technique, which efficiently separates highly sulphated oligosaccharides such as HS and Hp (Zhang, Xie, *et al.* 2009, Yang *et al.* 2011, Du *et al.* 2016). However, until the work published by Mourier and Viskov (2004), many problems were encountered with this technique. The ion pairing agents (mainly quaternary amines) were often not adapted to mass spectrometry, as they caused a severe loss of sensitivity and a reduced signal-to-noise ratio (Doneanu *et al.* 2009). Therefore, Mourier and Viskov (2004) coated a C18 column with cetyltrimethylammonium (CTA) instead of using the ion-pairing agent in the mobile phase. This technique permitted the separation of saccharides displaying up to 20 sulphate groups, which perfectly suited this project. The buffer used here was ammonium bicarbonate NH_4CO_3 , which is volatile and is not corrosive, thus granting a longer life-time to the column (Miller *et al.* 2016).

To broadly determine the size of the oligosaccharides, PAGE was used to complement the small-scale SEC technique. PAGE is a routine technique that separates molecules based on their sizes, charges and conformations. The electric field applied across the gel will cause the migration of the compounds from the negative electrode (cathode) to the positive electrode (anode) through a gel (30% polyacrylamide gels (w/v) are generally used for separation of HS saccharides). The gels were stained with a 0.08% Azure A solution (w/v), which interacts with the negatively charged groups of the saccharides.

3.2. HS oligosaccharide library preparation: from natural sources

3.2.1. Partial enzymatic digestion of PMHS

A small-scale enzymatic digestion was first carried out to determine the appropriate ratio of enzyme/PMHS. From this trial digestion, it was determined that the most suitable ratio to use was 2 mU/mg PMHS for the first hour of the digestion, followed by the addition of another 2 mU/mg PMHS of heparinase III at the end of the first hour. A total of 400 mg of PMHS was digested for a total digestion time of 9 hours. The evolution of the digestion was monitored by small-scale SEC (Figure 15).

The enzymatic digestion of the native PMHS led to the consequent formation of saccharides of small sizes (represented by the peaks at 25-35 mins) in comparison to the formation of longer saccharides (represented by the peaks at 15-25 mins).

3.2.2. SEC of digested PMHS

The oligosaccharide mixtures resulting from the enzymatic digestion were separated according to their hydrodynamic volumes using large-scale SEC chromatography (buffer: 0.5 M NH_4HCO_3). Batches of 50 mg were fractionated separately to optimise the separation and avoid overloading the column. Similar chromatograms were obtained for each batch, therefore demonstrating that the technique is consistent between each run (data not shown). In all cases, there was no base line resolution, therefore confirming the incomplete fractionation of the saccharides. The sizes of the

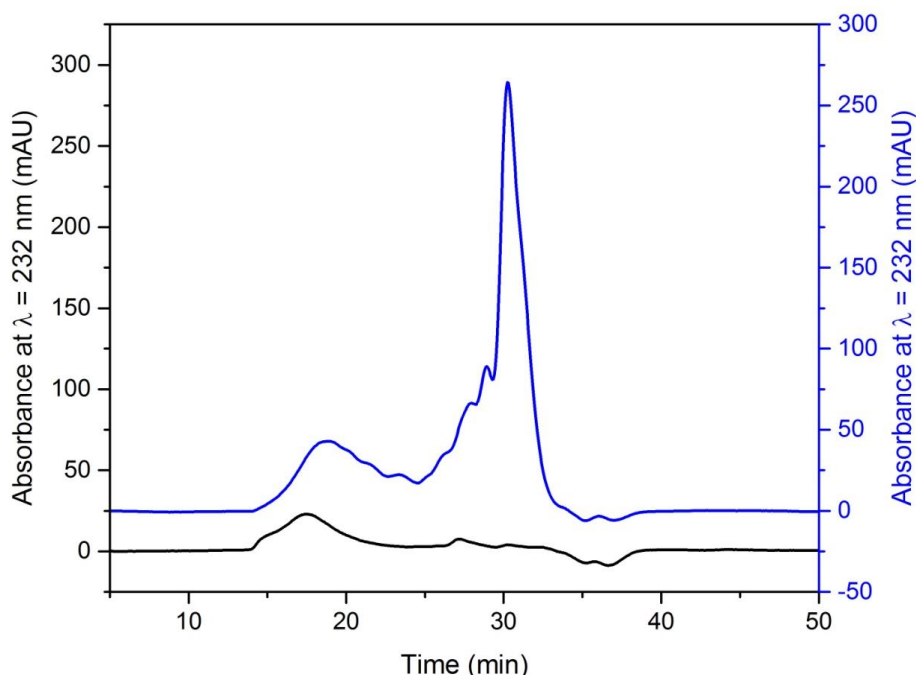


Figure 15: Monitoring the evolution of PMHS partial enzymatic digestion by heparinase III using small-scale SEC. In black is represented the profile obtained for the starting material (digestion time point t_{0h}). In blue is represented the profile obtained for the partially digested PMHS (digestion time point t_{9h}). For small-scale SEC, the isocratic elution of 100 μ g material was carried out using a Superdex™ peptide 7.5/300 small scale SEC column, at 0.2 mL/min (buffer: 0.5 M ammonium bicarbonate) and was monitored by absorbance at $\lambda_{ABS} = 232$ nm.

saccharides were assigned by reference to standard Hp saccharides of known size with the help of the results obtained from the PAGE analysis of the pooled fractions from SEC chromatography (Figure 16). However, owing to the lack of sensitivity of Azure A for low sulphated oligosaccharides, the sizes could only be estimated approximately. Moreover, even though the degree of polymerisation (dp) of the oligosaccharide chain could be expected to increase by two units (peak(n): dp(2n)) between each peak, this was not apparent for the complex mixture shown in Figure 16. This was due to the mode of separation of SEC chromatography, as the saccharides were fractionated according to their hydrodynamic volumes and not according to their number of disaccharide units only. This mode of separation led to pooled fractions that contained heterogeneous mixtures of saccharides of varying sizes and sulphation, which explains why the bands did not appear to be sharp on the PAGE gel. However, for this project, oligosaccharides ranging from hexa- to deca-saccharides were desired. Therefore, such mixtures of saccharides of different sizes

were not considered to be a major drawback. The SEC fraction corresponding to the SEC chromatography profile peak n° 10 (Figure 16) was selected for further work. Prior to further purification, fraction 10 was desalted by means of several cycles of lyophilisation (ammonium bicarbonate is a volatile salt, easily removable by lyophilisation) and stored for further use. In total, five cycles were necessary to achieve complete desalting.

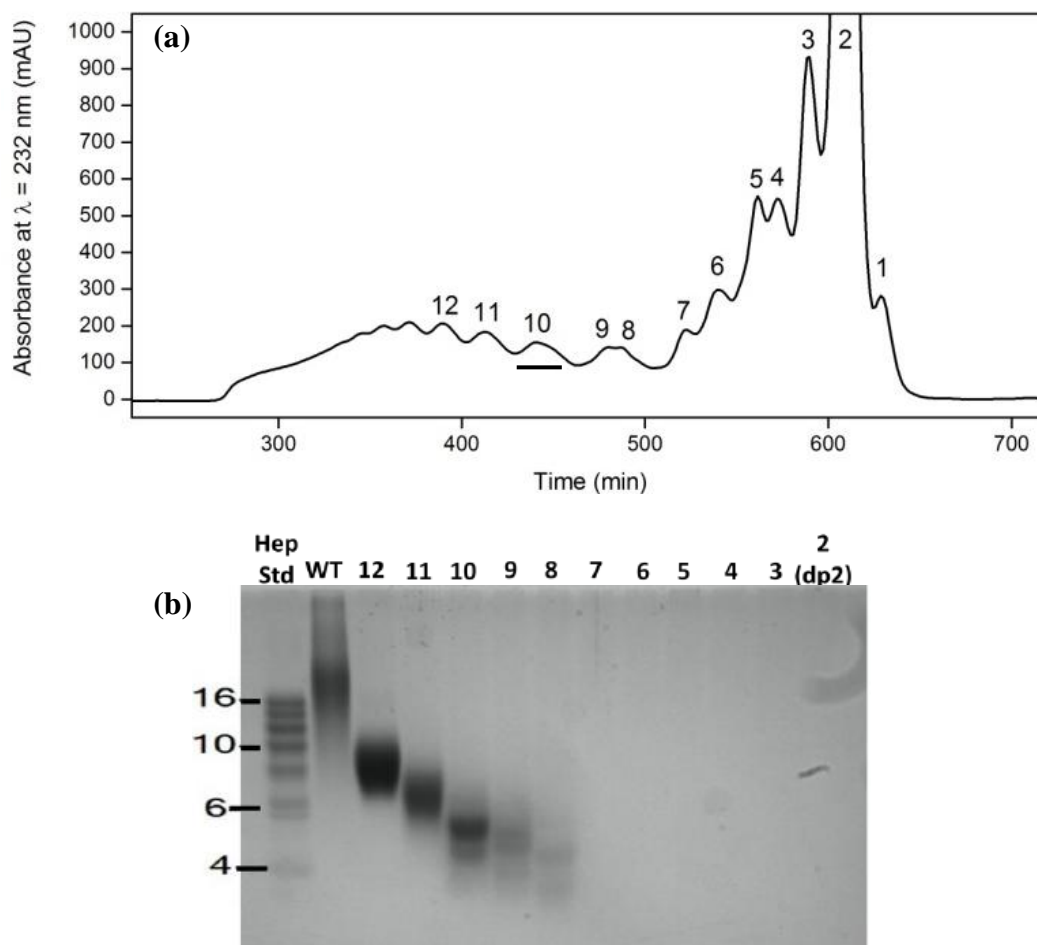


Figure 16: Estimation of the degree of polymerisation of the partially digested PMHS saccharides: comparison of the large-scale SEC profile and the PAGE analysis of the resulting SEC fractions.

(a) Typical SEC profile of PMHS partially digested by heparinase III. The isocratic elution was made using a solution of 0.5 M NH_4HCO_3 over 900 min at a flow rate of 0.5 mL/min. The peaks (and thus pooled fractions) were numbered 1 - 12, starting from the right hand side of the profile (for details about large-scale SEC run conditions, see Section 2.1.2.3).

(b) PAGE analysis of the pooled SEC fractions. The numbers 2 - 12 correspond to the SEC fraction numbers. Fraction number 10 (underlined) was selected for further work.

3.2.3. SAX chromatography of digested PMHS: 1st run

SEC fraction 10 was next purified using SAX chromatography with a semi-preparative ProPac PA1 column (9 x 250 mm), which allows the purification of a maximum of 5 mg material per run. The saccharides were eluted with a gradient of 0-80% 2 M NaCl over 120 min and the resulting SAX profile is shown in Figure 17. The chromatogram showed a spread of peaks across the gradient, confirming the structural heterogeneity of the compounds of the SEC fraction. There was no baseline resolution, suggesting that the multiple peaks in the complex mixture were overlapping and that no complete separation of the saccharides was accomplished. This was also confirmed by the different shapes of the peaks (sharp or broad, single or double peaks). However, it must be noted that SAX chromatography can provide separation of anomers of a single structure (Skidmore *et al.* 2010). Therefore, the apparent structural heterogeneity suggested by such type of profile may not be as high as predicted. The two sets of peaks 10-A (59-63 min) and 10-B (68-73 min) were selected for an additional step of SAX-HPLC, as they were assumed to grant a high diversity of structures.

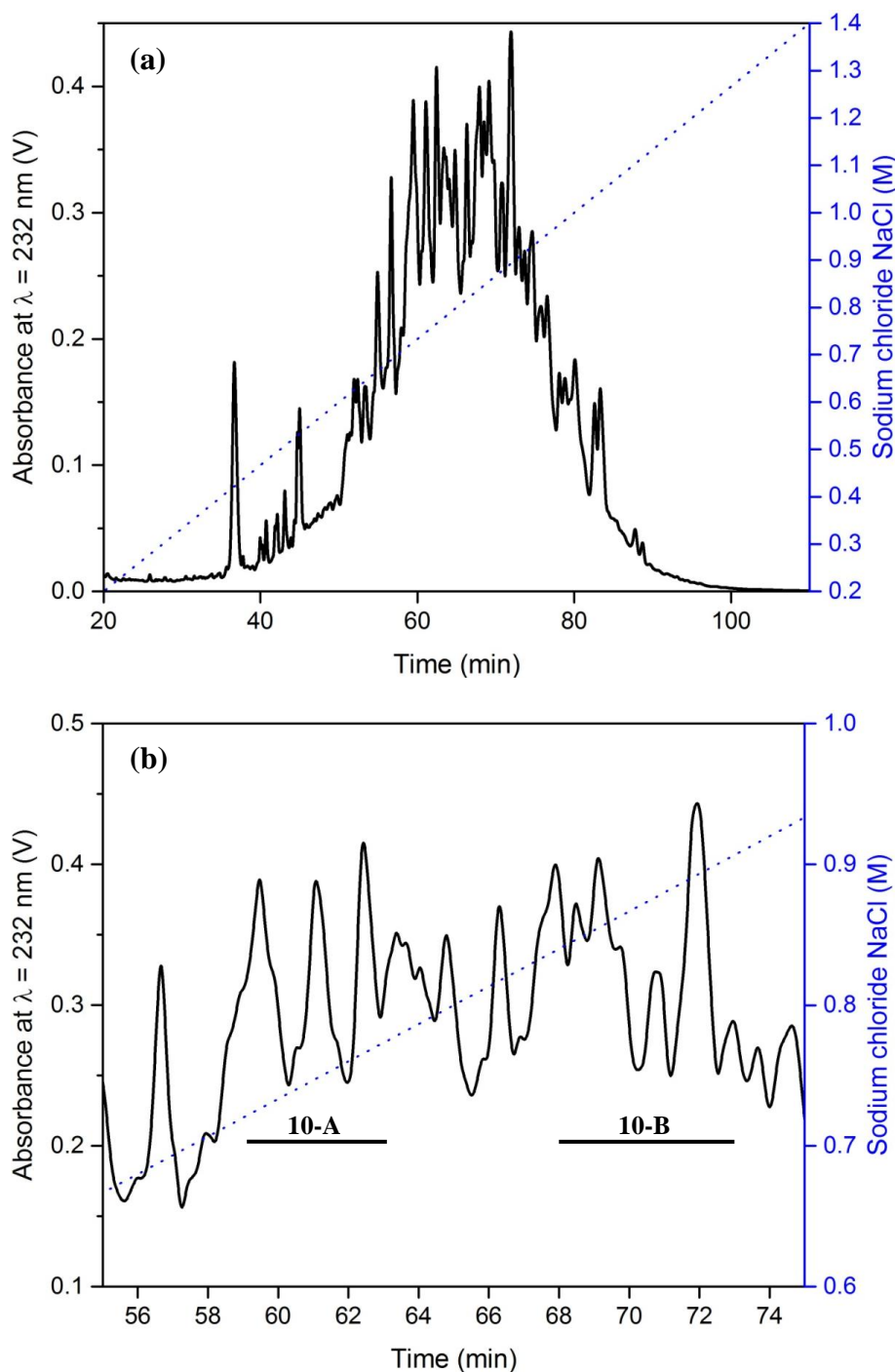


Figure 17: Semi-prep SAX-HPLC profile for SEC fraction 10. The saccharides were eluted with a 0-80% gradient over 120 min (buffer: 2 M NaCl) at a flow rate of 1 mL/min. The conditions for SAX-HPLC purification of SEC fractions are described in more detail in Section 2.1.2.5.

(a) Shows the complete SAX-HPLC profile.

(b) Shows a region of the SAX-HPLC profile (56-74 min). Peaks representing the fractions that have been selected for further work have been assigned the labels 10-A (59-63 min) and 10-B (68-73 min).

3.2.4. SAX chromatography of digested PMHS: 2nd and 3rd runs

Further separation of the fractions 10-A and 10-B was performed using an analytical Propac PA1 column (4 x 250 mm). Fractions were not desalted and were simply diluted with water (1/15 dilution) prior to loading and absorption onto the column. Each sample was eluted with an appropriate gradient of NaCl solution (gradient details are given for each individual chromatogram in Figure 18). As expected, the chromatograms showed a spread of peaks across the gradient. No base line resolution was detected, again suggesting that the multiple peaks in the complex mixture were overlapping, despite very shallow gradients being used for this second step. This, therefore, demonstrated the limitation of SAX chromatography for the separation of oligosaccharides bearing similar levels of anionic moieties. However, it should be noted that using less steep gradients resulted in a better separation of the peaks. Three sets of peaks (10-A1, 10-A2 and 10-B1, Figure 18) were selected for further work. Prior to the last step of purification by CTA-SAX chromatography (see Section 3.2.5 below), selected peaks were purified for a third and last time with SAX-HPLC on Propac PA1 column, with an even shallower gradient. However, no improved purification was observed (see Figure 19). Even though complete separation of the peaks was not achieved using standard SAX chromatography, it assisted in the further purification of the saccharides according to their charge.

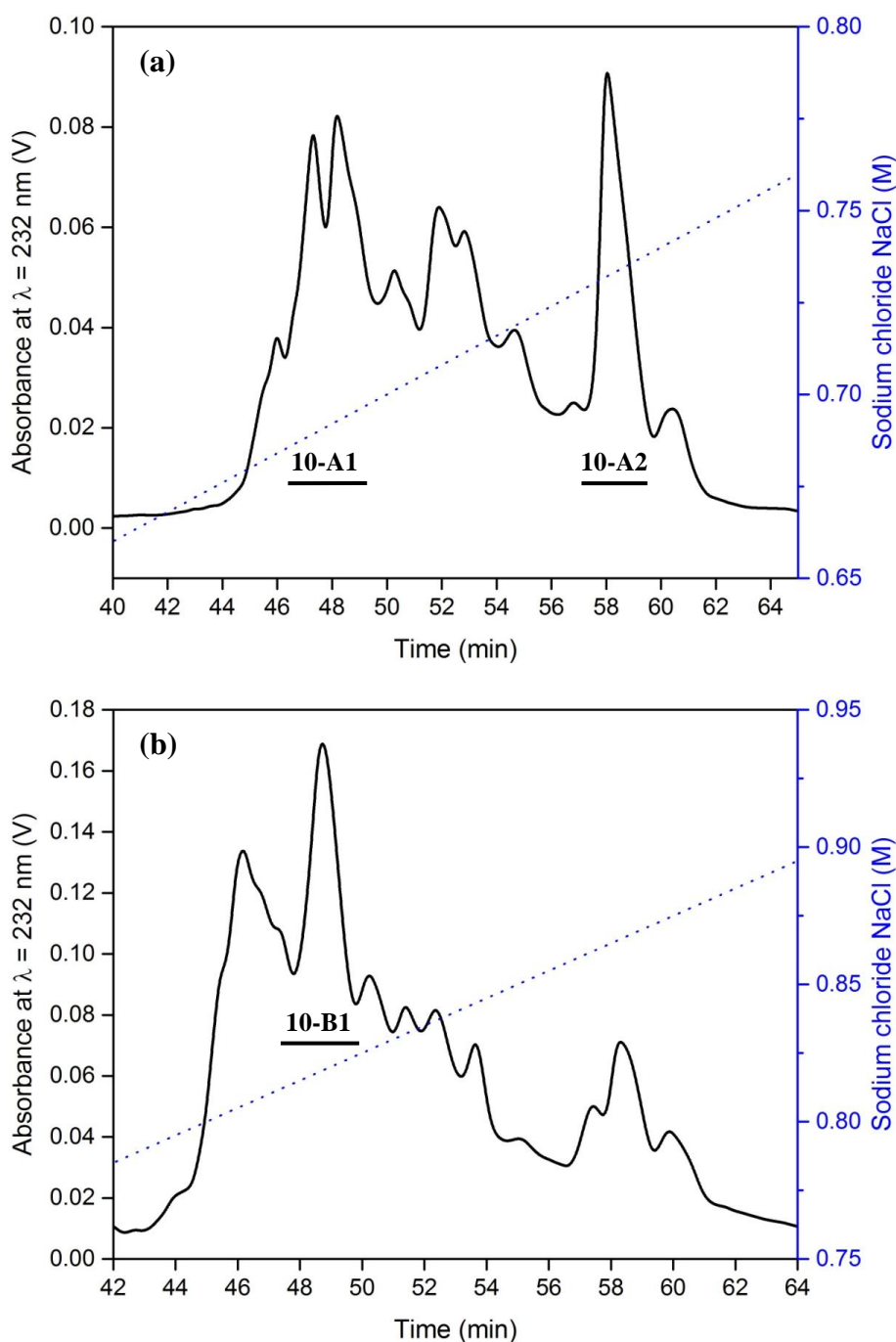


Figure 18: SAX-HPLC profiles for fractions 10-A and 10-B. The conditions for the improved separation of the SAX-HPLC fractions are described in more detail in Section 2.1.2.5.

(a) Shows the SAX-HPLC profile obtained for the purification of fraction 10-A. The saccharides were eluted with a 30-38% gradient over 40 min (buffer: 2 M NaCl) at a flow rate of 1 mL/min. The peaks representing the fractions that were selected for further work were assigned the labels 10-A1 (46-49 min) and 10-A2 (57-60 min).

(b) Shows the SAX-HPLC profile obtained for the purification of fraction 10-B. The saccharides were eluted with a 35-45% gradient over 40 min (buffer: 2 M NaCl) at a flow rate of 1 mL/min. The peak representing the fraction that was selected for further work was assigned the label 10-B1 (47-50 min).

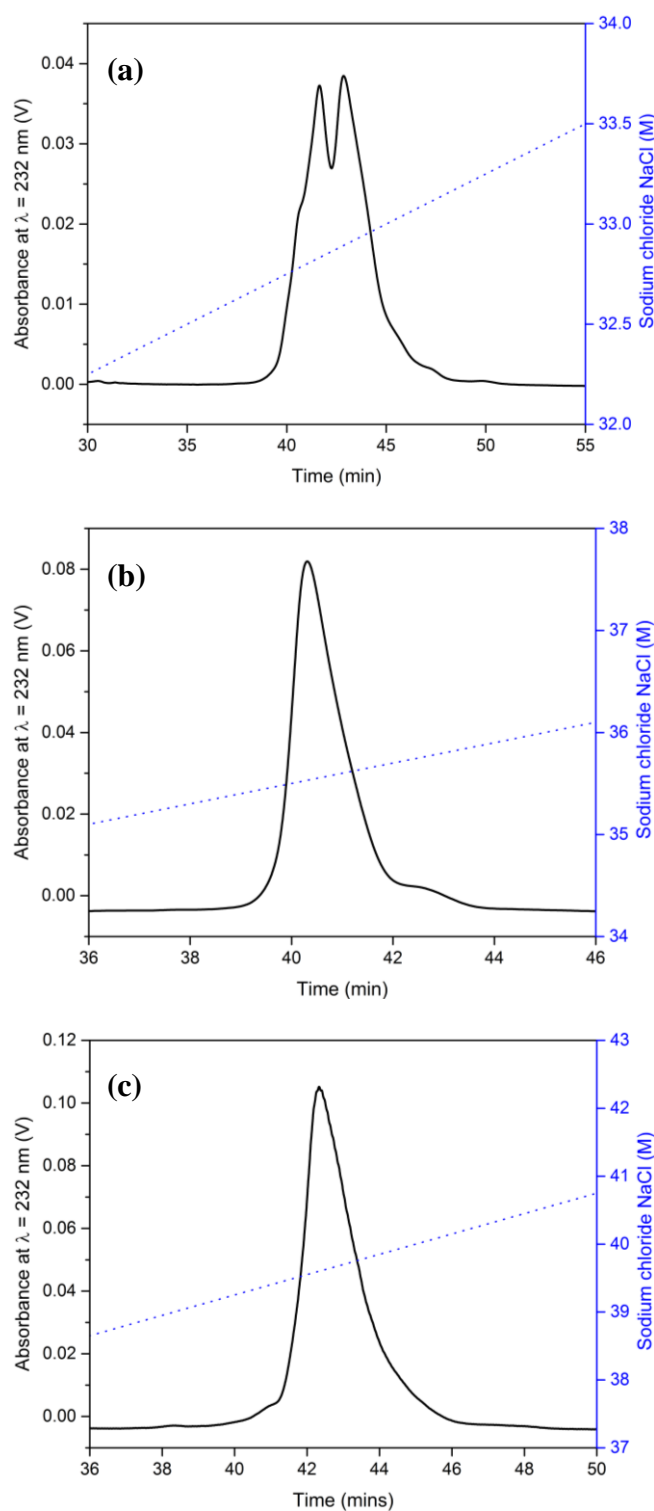


Figure 19: SAX-HPLC profiles for fractions 10-A1, 10-A2 and 10-B1. The fractions were eluted at a flow rate of 1 mL/min (buffer: 2 M NaCl).
 (a) Shows the SAX-HPLC profile obtained for the purification of fraction 10-A1. The saccharides were eluted with a 32-34% gradient over 40 min.
 (b) Shows the SAX-HPLC profile obtained for the purification of fraction 10-A2. The saccharides were eluted with a 35-45% gradient over 40 min.
 (c) Shows the SAX-HPLC profile obtained for the purification of fraction 10-B1. The saccharides were eluted with a 32-34% gradient over 40 min.

3.2.5. CTA-SAX chromatography of digested PMHS

3.2.5.1. Column preparation

CTA-SAX chromatography was next used to further purify structures, as originally described by Mourier and Viskov (2004). Prior to any purification of the SAX fractions, the derivatisation of the C18 column with CTA was performed. This was done by eluting a 1 nM CTA solution in methanol/water (MeOH/H₂O). The appropriate coating of the column was assessed by fractionating a mixture of the eight common naturally occurring disaccharide standards with the freshly derivatised column. The ratio (MeOH/H₂O 50/50, v/v) offered both ideal resolution and retention times for the disaccharide standards, as seen in Figure 20 (Std 6 (Δ UA2S-GlcNS,6S) should not be eluted at more than 0.6 - 0.8 M NH₄CO₃). Ammonium bicarbonate was chosen as solvent for the elution (2 M solution) in order to simplify/reduce the loss of material during the desalting process (Miller *et al.* 2016).

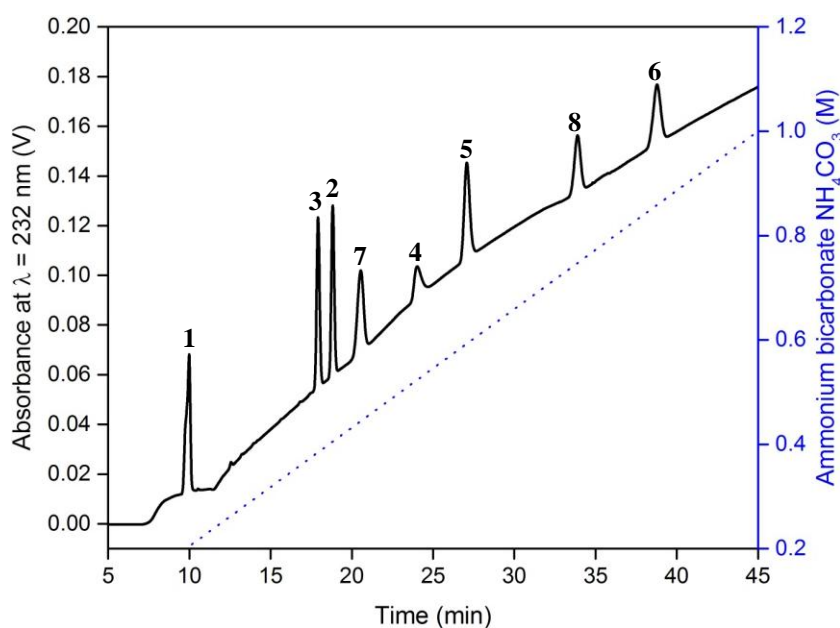


Figure 20: Confirming the derivatisation of the C18 silica column by CTA: CTA-SAX profile obtained for the separation of the eight common naturally occurring disaccharides standards. Profile obtained for derivatisation with a 1 nM CTA solution of MeOH/H₂O (50/50, v/v). The conditions for the column coating are described in detail in Section 2.1.2.6. The disaccharide standards were eluted with a 0-50% gradient over 45 min (buffer: 2 M NH₄CO₃) at a flow rate of 1 mL/min. The peak labels refer to the reference numbers assigned to the disaccharide standards: 1. Δ UA-GlcNAc; 2. Δ UA-GlcNAc(6S); 3. Δ UA-GlcNS; 4. Δ UA-GlcNS(6S); 5. Δ UA(2S)-GlcNS; 6. Δ UA(2S)-GlcNS(6S); 7. Δ UA(2S)-GlcNAc; 8. Δ UA (2S)-GlcNAc(6S).

3.2.5.2. CTA-SAX of compounds 10-A1 and 10-A2

SAX fractions 10-A1 and 10-A2 were not desalted and were simply diluted with water (1/15 dilution) prior to absorption onto a freshly derivatised C18 column. Each sample was eluted with a 25-70% gradient over 60 min (elution buffer: 2 M NH_4CO_3). As shown by the chromatogram in Figure 21 (a), CTA-SAX allowed the separation of the double peak for the fraction 10-A1 - separation which could not be achieved by standard SAX chromatography (Figure 19). For fraction 10-A2, the separation of the minor and major peaks was also achieved. Therefore, the CTA-SAX technique appeared to offer a better resolution than regular SAX. However, it should be noted that CTA-SAX has also been shown to allow the separation of the anomers of a same structure (Mourier and Viskov 2004). In order to verify the purity of the structures and to sequence them by MS/MS, the collected fractions were desalted and dried using a vacuum concentrator for a total of 5 cycles (the material loss is generally limited with a vacuum concentrator compared to a freeze-dryer). However, at the end of the drying process, a fine white powder - soluble in DMSO but not in water - was observed in the Eppendorf tubes. It was concluded that this powder was organic material and was neither a saccharide nor a salt (the latter are both soluble in water). In order to determine the nature of the contaminant, the pH of the buffer used for both runs was measured (expected value: 7.6, read value: 9.25). According to the supplier (Supelco HPLC Column - Selection Guide, Sigma Aldrich), the C18 column used is stable for pH ranging between 2 and 8. The white powder was therefore thought to be some CTA-derivatised silica that became detached from the column and was eluted along with the compounds. The high pH obtained for the buffer may be explained by the decomposition of the hydrogen bicarbonate in water to form both volatile carbon dioxide and soluble ammonia. A high concentration of ammonia would have, therefore, led to a higher pH. This assumption was confirmed by the fact that the column could not be used at all after running the fractions 10-A1 and 10-A2 as the pressure of the system was above the threshold value (4000 psi), advised by the manufacturer for normal elution conditions (1 mL/min, water). No further purification was conducted as it would have resulted in yields of the compounds (approximately a few μg) that were too low to allow further work (bioassays and structural analysis).

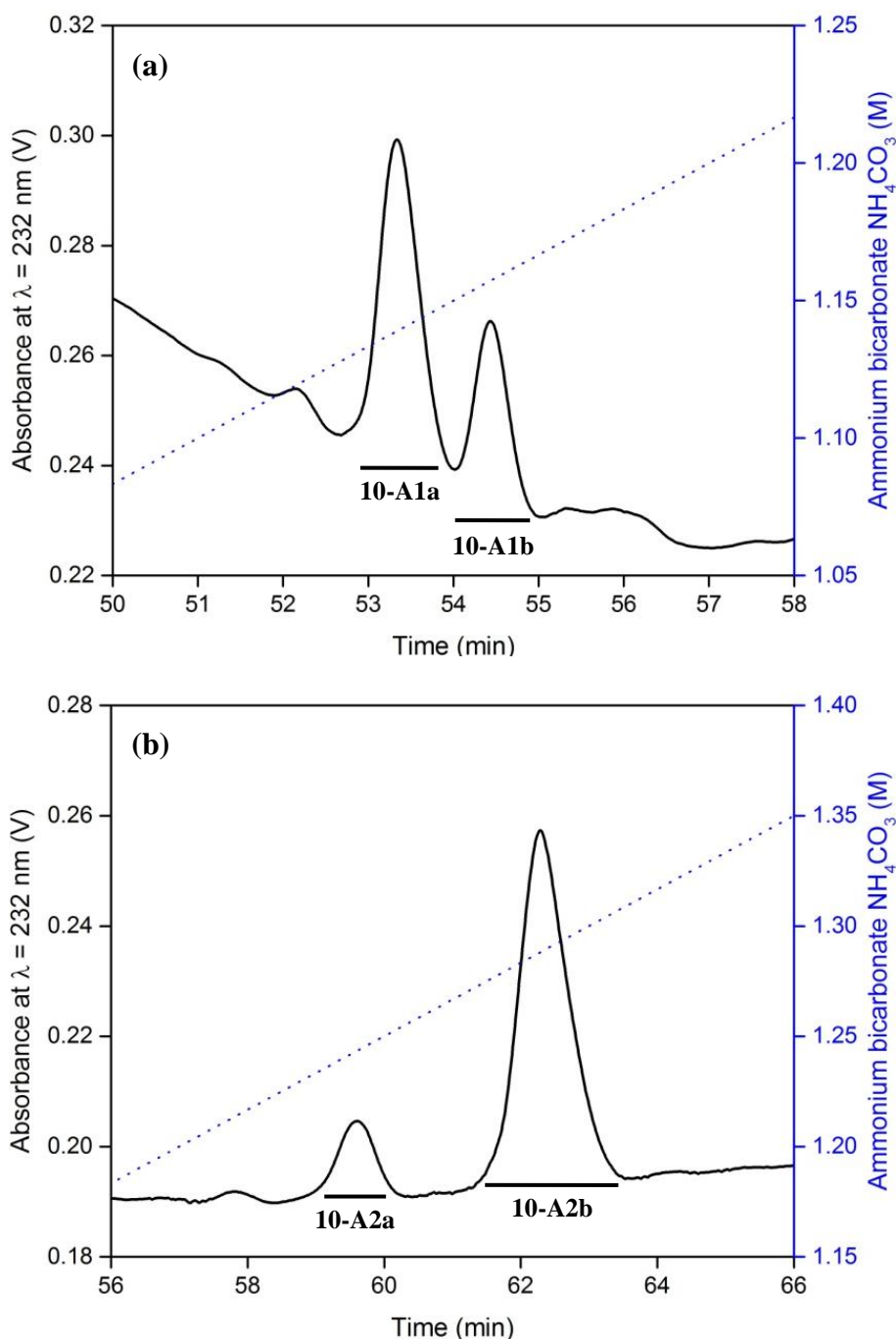


Figure 21: CTA-SAX profiles for fractions 10-A1 and 10-A2. Each sample was eluted with a 25-70% gradient over 60 min (elution buffer: 2 M NH_4CO_3) at a flow rate of 1 mL/min. The conditions for CTA-SAX purification are described in detail in Section 2.1.2.6.

(a) SAX-HPLC profile obtained for the purification of fraction 10-A1. Peaks representing the fractions that were selected for further work were assigned the labels 10-A1a (52.6-54 min) and 10-A1b (54-55 min).

(b) SAX-HPLC profile obtained for the purification of fraction 10-A2. Peaks representing the fractions that were selected for further work were assigned the labels 10-A2a (59-60 min) and 10-A2b (61.5-63.5 min).

3.3. Conclusions

Establishing the structural determinants underpinning the interactions of HS with FGF and FGFR requires the preparation of oligosaccharide libraries. For this project, one approach attempted was the preparation of a library of HS oligosaccharides, ranging from octa- to dodeca-saccharides, by partial enzymatic digestion of native PMHS. The preparation of the oligosaccharide was initially carried out following the protocol developed by Powell *et al.* (2010). The first step of the process consisted of the degradation of native PMHS polysaccharide chains by heparinase III to afford resistant sulphated saccharides. The PMHS digests were sequentially purified by chromatographic fractionation. Several fractions (10-A1, 10-A2 and 10-B1) were successfully isolated according to their sizes and partially according to their charges, by SEC and subsequent SAX-HPLC. The last purification step (by means of CTA-SAX chromatography) was, however, unsuccessful and resulted in low amounts of contaminated compounds. The degradation of the column - and therefore the elution of CTA-coated silica along with the analytes – was observed during the last step of purification of the digested PMHS samples, caused by the decomposition of the salt into soluble ammonia. The high pH of the buffer may have also altered the structures of the saccharides, as HS and Hp are known to be sensitive to extreme pH (Skidmore *et al.* 2009). Developing more appropriate buffers is clearly required to overcome this problem (such as non-volatile ammonium methane sulphonate, sodium methane sulphonate, or even the volatile ammonium acetate). Alternatively, other methods of purification including reverse-phase ion-pairing chromatography (Ponnusamy 2013), porous graphitised carbon chromatography (Karlsson *et al.* 2005) and hydrophilic interaction liquid chromatography (Naimy *et al.* 2008) could also be used instead of CTA-SAX.

The partially successful purification exposed some of the limitations of the preparation of HS oligosaccharides from natural sources. Firstly, even though it has been shown to afford access to a certain number of structures in a relatively short amount of time, working with tissue-derived HS structures rarely allows the isolation of highly pure saccharides. Moreover, their structures are unknown and require difficult analytical procedures to be determined, therefore limiting the rigorous study of the SAR of HS. Secondly, the isolation of PMHS oligosaccharides greatly relies

on an extensive range of orthogonal purification methods. This leads to a substantial loss of material, meaning that preparation of HS oligosaccharides derived from tissues generally results in access to very restricted amounts of final material (of the order of low μg amounts). Such low amounts seriously hamper the further analysis and SAR studies. For example, BaF3 bioassays, as used in Chapter 5 to study the SAR of HS in FGF signalling, require a minimum of a few μg of compound (Guimond *et al.* 2009). Similar amounts are likely to be needed to permit sequencing using recently developed MS methods (Jones *et al.* 2011, Yang *et al.* 2011, Du *et al.* 2016). Thus, the amounts of material are just on the limit of the minimum needed to tackle such studies. In contrast, chemical and enzymatic/chemoenzymatic syntheses could be seen as potential alternative to the extraction of the saccharides from tissues for the study of the SAR of HS as these methods permit the preparation of relatively large amounts of well-defined structures. It was thus decided to continue work using compounds derived by these approaches as a more productive line of research.

4. Chapter 4 – Chemical synthesis of HS oligosaccharide structures

4.1. Introduction

Several approaches - namely the multi-step and one-pot solution-phase syntheses, the solid-phase synthesis, and finally the enzymatic/chemoenzymatic syntheses - have been developed for the preparation of HS oligosaccharide libraries, as mentioned in Section 1.8.2. However, given the difficulties still encountered with the high-throughput methods, the traditional multi-step solution-phase synthesis generally seems like the most convenient alternative for the preparation of such compounds. The wealth of glycosylating agents, synthetic routes and the fairly good understanding of its mechanisms indeed make it appear the most reliable and efficient approach. Thus, to meet the requirements and expectations of this project - the production of several octasaccharide targets in a relatively short period of time - it was decided to resort to the development of a multi-step solution-phase method. In the following sections, a general overview of the chemical synthesis of carbohydrates (and more specifically of Hp/HS), but also an overview of the advances that have been made in the field of Hp/HS oligosaccharide synthesis and the challenges that remain will be addressed.

4.1.1. Chemical synthesis of Hp/HS oligosaccharides

4.1.1.1. *Protecting groups*

Owing to the intrinsic polyfunctional nature of the Hp/HS carbohydrates, their synthesis requires the extensive use of protecting groups (PGs) to appropriately and temporarily mask the different hydroxyl, carboxyl and amino groups. A broad variety of PGs is available (Wuts and Greene 2006), which therefore permits the precise control of the availability of each functional moiety at each step of the synthetic process. To be considered suitable for such lengthy and complex syntheses, the PGs must fulfil a certain number of conditions. First of all, ideally, the environment and user friendly reagents used to install and remove a PG must be relatively easy to access. Secondly, the installation and cleavage reactions themselves must preferably be carried out in mild conditions and not affect any other PG (the ability to add/remove PGs in the presence of others is termed orthogonality). Thirdly, the groups must also remain stable throughout the synthesis, as well as during the work-

up and purification steps. Ideally, the installation of a PG will afford a final product that will be more hydrophobic than the starting material. Hydrophobic compounds are indeed easier to handle during work-up steps and may also be crystallised for more convenient purification. Finally, the starting material, the final product and the reagents must be easily separated from one another during the work-up and purification steps. The timing of the introduction of the different PGs is determined by the relative reactivity of the hydroxyl groups. Primary hydroxyl groups are known to be more reactive than secondary ones. In addition, the anomeric hydroxyl group is the most reactive of the secondary hydroxyl groups. Finally, to a first approximation, the reactivity of the hydroxyl groups generally decreases as they get further away from the anomeric position. It is however to be noted that this rule of thumb is not valid in the presence of both axial/equatorial hydroxyl groups (axial hydroxyl groups are far less reactive than equatorial ones (Orgueira *et al.* 2002, Pedersen *et al.* 2011)).

PGs can be classified into two distinct categories. Permanent groups will be used to mask the hydroxyl groups that will ultimately be exposed at the very last step of the synthesis. Benzyl, benzyl-derivative and benzoate ester groups are widely used as permanent groups. Unlike permanent groups, temporary groups will be subjected to manipulations, thus selectively installed and removed according as required. Various acetyl-derivative, silyl, ester, ether, carbonate and acetal groups are often used as temporary groups. In the case of Hp/HS carbohydrates, chemists need to resort to numerous orthogonal permanent/temporary groups that can be selectively installed and removed to obtain compounds that display discrete sulphation and acetylation patterns (Figure 22).

4.1.1.2. Glycosylation: keystone of carbohydrate synthesis

Chemical synthesis of carbohydrate oligo- and poly-saccharides mainly relies on the formation of a covalent bond - glycosidic linkage - between two sugar units or between a sugar unit and an aglycon in a reaction termed chemical glycosylation. Although several types of glycosidic linkages can be formed, such a linkage generally consists of an acetal connecting two sugar residues and has been formed between the hemiacetal of one of the residues and a hydroxyl group of the other.

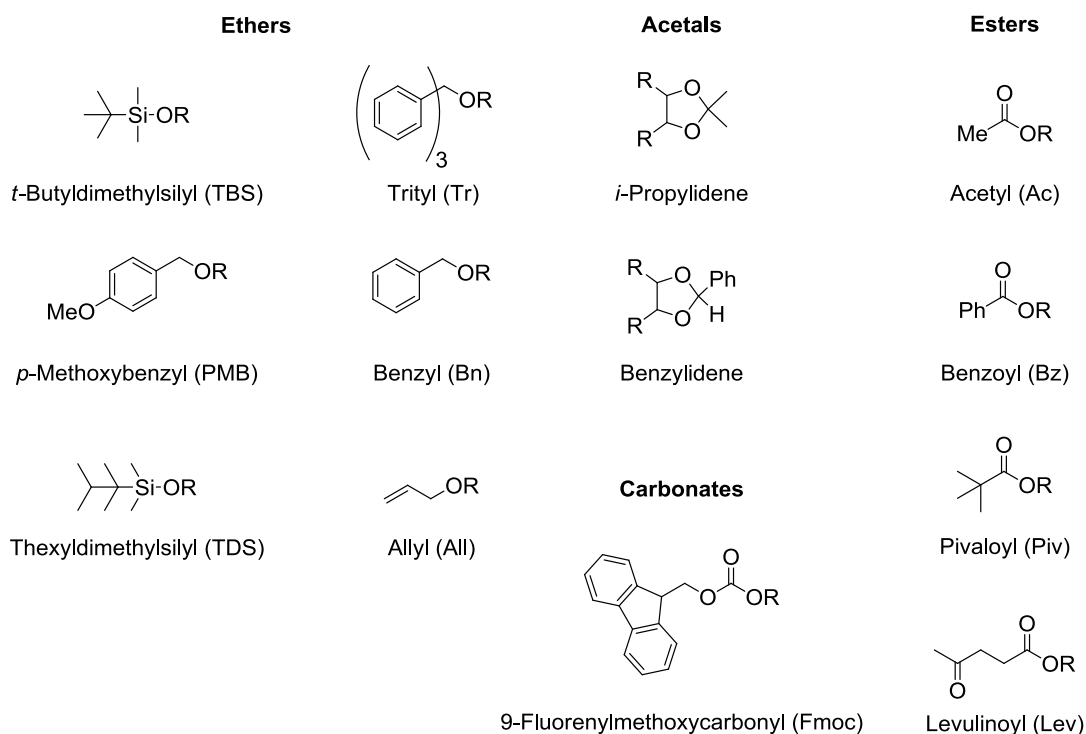
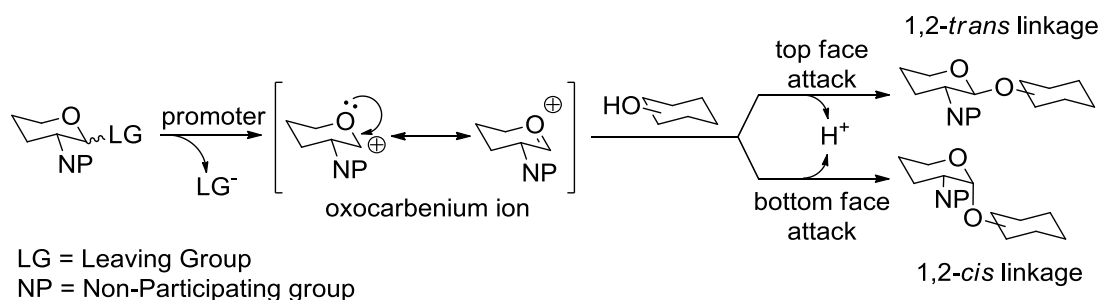


Figure 22: Some of the major protecting groups used for Hp/HS oligosaccharide synthesis. R = carbohydrate.

The glycosylation reaction has been thoroughly studied since it was first reported by different groups (Fischer 1893, 1895, Koenigs and Knorr 1901). It has since been extensively modified, essentially introducing new types of promoters, mainly mercury and silver salts (Boullanger *et al.* 1987, Fürstner *et al.* 2000, Mastelić *et al.* 2004). The impact of the type and polarity of the solvent has been investigated as well (Bills and Green 1967). All the efforts involved in improving the Koenigs-Knorr and Fisher methods paved the way for the development of new methods to form glycosidic bonds (Nicolaou and Mitchell 2001, Zhu and Schmidt 2009).

A chemical glycosylation commonly requires three main components to be performed: a glycosyl donor, a glycosyl acceptor and a promoter. The glycosyl donor is the sugar residue bearing the leaving group (LG) at its anomeric centre (electrophilic entity) and the glycosyl acceptor is the residue presenting a free hydroxyl group (nucleophilic entity). The first step consists of the activation of the glycosyl donor by the activator. This first step results in the departure of the leaving group and the creation of a glycosyl cation intermediate, called an oxocarbenium ion

(Scheme 1). This transient entity can hence be attacked by the free hydroxyl group of the glycosyl acceptor from either the top face or the bottom face of the ring plane, which will finally result in the formation of the new glycosidic bond, with one or the other configuration at C1.

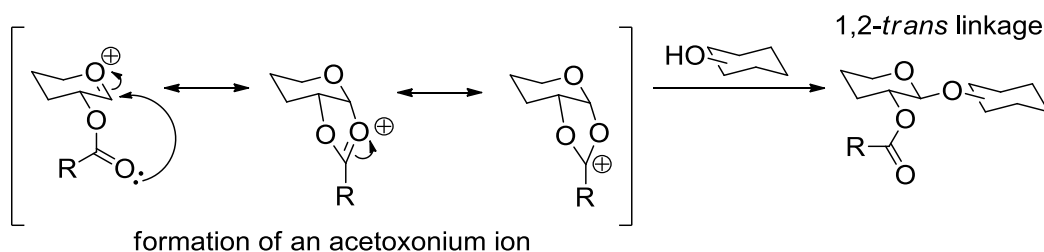


Scheme 1: General mechanism of the chemical *O*-glycosylation.

Several parameters must be taken into account and controlled to perform a high-yield chemical glycosylation that will ultimately afford the desired glycoside. First of all, completely anhydrous conditions must be maintained to avoid the hydrolysis of the activated glycosyl donor that can occur in some cases. The participation of water as a competitive nucleophile can be circumvented by scavenging the water molecules with the addition of molecular sieves to the reaction mixture. However, due to the alkaline nature of the molecular sieves, higher amounts of activator may be necessary to achieve full activation of the donor. This may compromise the stability of the PGs of the building blocks and lead to other side reactions. Secondly, secondary hydroxyl groups are less reactive nucleophiles, leading to lower glycosylation yields. Finally, measures have to be taken to ensure the stereoselectivity of the glycosylation reaction as two different isomers may be formed during the reaction depending on the conformation of the new glycosidic linkage formed: either *1,2-cis* or *1,2-trans* linkage.

In theory, a glycosylation reaction could lead to the formation of both *1,2-cis* and *1,2-trans* glycosides. The resulting stereoselectivity of a glycosylation reaction is governed by many parameters including the stereochemistry of the donor, the reaction temperature, the solvent/anomeric/remote PG effects, the monosaccharide type, the promoter used, the steric hindrance/accessibility and nucleophilicity of the

acceptor. The exclusive formation of one type of glycosidic linkage can be achieved by controlling some of these parameters. The formation of 1,2-*trans* glycosidic linkages can easily be performed using the participating effect of an acyl group installed at position 2 of the glycosylating donor (Scheme 2). The presence of this electron donating moiety stabilises the oxocarbenium cation and leads to the formation of an acetoxonium ion (also called acyloxonium ion). Since one of the faces of the ring plane is blocked, the nucleophilic attack will only be performed from the other side of the plane. Ultimately, this generally leads to the exclusive formation of the 1,2-*trans* glycoside, even though some traces of the 1,2-*cis* glycoside may be detected.



Scheme 2: Synthesis of 1,2-*trans* glycoside via neighbouring group participation.

The formation of 1,2-*cis* glycosidic linkages is much more challenging. Even though the absence of a participating neighbouring group and the anomeric effect (Nishimura *et al.* 1972, Cumpstey 2012) should guarantee the exclusive formation of the 1,2-*cis*-linked glycoside, the stereoselectivity of the glycosylation may be poor. The impact of several parameters on the glycosylation outcome, such as the type of solvent or the structural characteristics of the glycosyl agents, has hence been examined. For instance, the polarity of the solvent has a direct impact on the conformation of the newly formed glycosidic bond. A non-polar solvent such as diethyl ether tends to favour the 1,2-*cis* linkage formation when a polar solvent, such as acetonitrile which stabilises the oxocarbenium ion, favours the formation of the 1,2-*trans* glycoside (Nishimura *et al.* 1972, Fraser-Reid *et al.* 1988). In the case of the synthesis of β -D-mannopyranosides, a very interesting example, it has also been discovered that the challenging β -D-mannosylation reaction could be directly performed using a 4,6-*O*-benzylidene-protected mannosyl sulphoxide (Crich and Sun

1996). In this case, the presence of the acetal leads to the formation of the β -D-mannoside with high yield and selectivity. Before finding this specificity, the synthesis of this type of glycoside could only be obtained through indirect methods, such as the synthesis of β -D-mannoside from β -D-glucoside by intramolecular nucleophilic substitution followed by inversion of configuration. (Kunz and Günther 1988) or the intramolecular aglycon delivery method, which gives access to the desired β -glycoside from the α -glycoside using *N*-iodosuccinimide (Barresi and Hindsgaul 1991). As for the β -D-mannosides, many important direct and indirect methods have been developed in recent years to overcome all the technical limitations to the synthesis of 1,2-*cis* glycosides. For example, Lemieux *et al.* (1975) successfully prepared α -linked disaccharide in a highly stereoselective manner by coupling per-*O*-benzylated α -glycosyl bromide with suitably protected glycosides. Tokimoto *et al.* (2005) demonstrated that the formation of 1,2-*cis* glycosidic linkages can be performed using the long-range effect of bulky 6-*O*-protecting groups. Using suitably protected and activated glycosyl acceptor can also lead to highly stereoselective glycosylations, as shown by Nakagawa *et al.* (2015) who used glycosyl acceptor-derived boronic ester catalyst.

Moreover, even though it is widely agreed that the general mechanism of a chemical glycosylation can be described as depicted in Scheme 1, the exact mechanism is still not fully understood. Several studies have been carried out and several methods, (including the use of the primary ^{13}C kinetic isotope effect (Huang *et al.* 2012), using the low-temperature NMR technique (Frihed *et al.* 2015) or the isolation and study of the glycosyl cation by NMR (Martin *et al.* 2015)) have been used recently to have a better overview of its characteristics. A better understanding of the reaction mechanism, as well as having a better overview of the impact of all the parameters/components on its outcome, will help in finding appropriate solutions to overcome the difficulties still encountered for the synthesis of problematic sugars.

4.1.1.3. Glycosyl donors

One of the most important aspects to take into account for oligosaccharide assembly is the choice of the anomeric leaving group of the glycosyl donor. Ideally, the leaving group should be easily installed, but should also be cleaved in preferably

mild conditions, that will not affect any of the other PGs. It should remain stable for the time between its preparation and use, but also during the glycosylation reaction itself. Many glycosylating agents (Figure 23) have been designed such as glycosyl halides (Lemieux *et al.* 1975, Mukaiyama *et al.* 1981, Toshima 2008), glycosyl trichloroacetimidates (Schmidt and Michel 1980), glycosyl *N*-phenyltrifluoroacetimidates (Yu and Tao 2001), glycosyl sulfoxides (Kahne *et al.* 1989), glycosyl phosphates (Palmacci *et al.* 2002), thioglycosides (Ferrier *et al.* 1973), *n*-pentenyl glycosides (Fraser-Reid *et al.* 1992) or even glycals (Thiem *et al.* 1978). However, despite the wealth of glycosyl donors, there is a need to develop new donors to overcome the issues encountered with the available ones, such as a lack of stability at room temperature, a lack of reactivity during the glycosylation reactions or even difficult and lengthy syntheses.

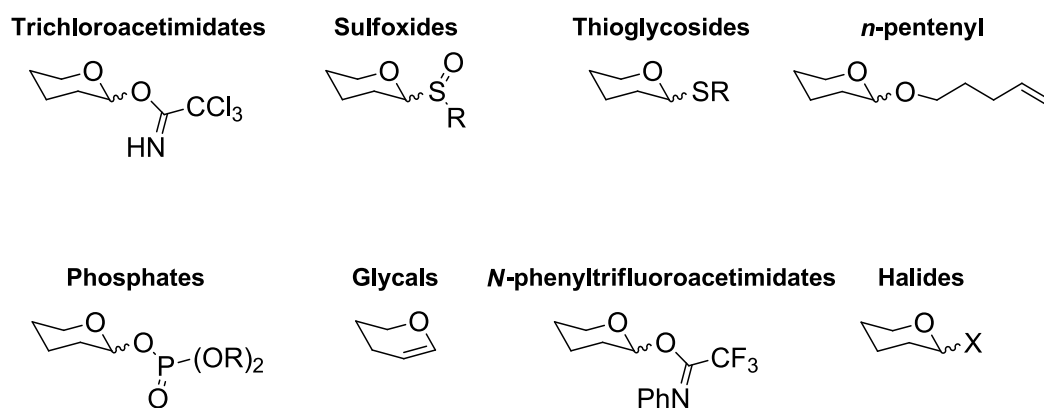
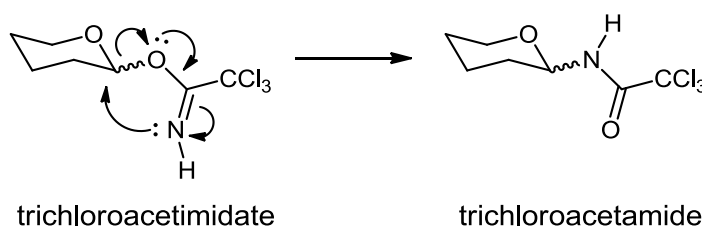


Figure 23: The major types of glycosyl donors.

Amongst all the glycosyl donors listed above, trichloroacetimidates are the most widely used. This can be explained for several reasons. First of all, the methods to prepare these are relatively easy and fast to perform. In addition, they can be stored at low temperatures. They are freshly prepared just before being used in glycosylation reactions and turn out to be very reactive. Moreover, they are rapidly activated with only a catalytic amount of a Lewis acid such as trimethylsilyl trifluoromethanesulphonate (TMSOTf), which does not compromise the stability of the other PGs during glycosylations. However, obtaining this kind of compound usually requires lengthy synthetic routes, with considerable amounts of PG manipulation. Owing to the instability of these types of glycosides in acidic

conditions, their purification with routine silica-based flash chromatography turns out to be rather delicate. The use of only a short pad of silica is hence required, as well as the use of a base such as triethylamine (Et_3N) or pyridine to counter the acidity of the silica. This base must be fully eliminated during the drying process, under high vacuum, prior to glycosylation in order to avoid quenching the Lewis acid used to initiate the reaction. In addition, the high reactivity of these compounds may become a major drawback as well, as they may undergo hydrolysis or rearrangement into trichloroacetamides in acidic conditions (Scheme 3). It should be noted that the Overman rearrangement has been used in certain cases as a powerful tool for the synthesis of nitrogen-containing residues (Overman 1974, Nishikawa *et al.* 1998, Larsen *et al.* 2008). Thus, glycosylation reactions performed with trichloroacetimidate glycosides as glycoside donors must be performed in perfectly anhydrous conditions to avoid these undesirable reactions that will have a considerable impact on the reaction yield.



Scheme 3: Trichloroacetimidate glycoside rearrangement, also known as Overman rearrangement.

4.1.2. In solution synthesis of Hp/HS oligosaccharides: a brief historical review and remaining issues

Even though the role of Hp/HS in disease mechanisms is still not fully understood, they remain potential carbohydrate-based drugs. Some groups have evaluated their potential as therapeutics (Petitou *et al.* 1989, Schwörer *et al.* 2013), emphasising the necessity to develop methodologies to prepare these carbohydrates. In the early 1980s, motivated by the rigorous structural elucidation of the minimal heparin structure required to bind and activate AT-III (Lindahl *et al.* 1984, Atha *et al.* 1985), Petitou, Jacquinet and colleagues carried out the first reported syntheses of fragments of this pentasaccharide (Jacquinet *et al.* 1984, Sinaÿ *et al.* 1984, Petitou *et al.* 1986).

Other crucial work was later published, describing the preparation of AT-binding site analogues to establish if the entire pentasaccharide sequence is required to observe high affinity binding, but also to overcome the complications inherent to the synthesis of its exact structure (Beetz and Van Boeckel 1986, Petitou *et al.* 1987, 1999, Walenga *et al.* 1988).

These pioneering studies have paved the way for the development of the chemical synthesis of a wider range of these types of GAGs and their mimetics. Over the last three decades, three major strategies have emerged. On the one hand, the convergent modular synthesis is based on the sequential assembly of fully differentiated building blocks, until the desired length is reached. This final precursor is then intensively modified to attain the desired functionalised oligosaccharide. Convergent modular synthesis of Hp/HS is nevertheless known for requiring extensive and lengthy synthetic pathways and is more suitable for the preparation of structurally homogenous types of oligosaccharides (de Paz *et al.* 2001, Haller and Boons 2001, Ojeda *et al.* 2002, Lucas *et al.* 2003, Orgueira *et al.* 2003, Arungundram *et al.* 2009, Cole *et al.* 2010, Hu *et al.* 2011, Zong *et al.* 2013, Miller *et al.* 2013, Baráth *et al.* 2015). On the other hand, the divergent synthesis requires the synthesis of one or several common precursors which will undergo structural modifications of their backbone prior to further elongation until the desired size is obtained (Tiruchinapally *et al.* 2011, Schwörer *et al.* 2013, Dulaney *et al.* 2015). The divergent type of synthesis allows easier preparation of a wider range of structures, unlike the convergent modular one. Finally, over the last decade, for the sake of developing concise and more efficient synthetic pathways, much effort has been put into the development of versatile syntheses, which can be defined as an astute combination of both divergent and modular syntheses (Poletti *et al.* 2001, Lubineau *et al.* 2004, Zulueta *et al.* 2012). Despite the differences that can be listed between those synthetic strategies, they all rely on diverse glycosylating agents, which thus appear to be one of the keystones of carbohydrate chemical synthesis.

In general, the synthetic approaches reported in the literature mainly differ in the degree of modulation: monomeric (Codée *et al.* 2005), dimeric (De Paz *et al.* 2003, Arungundram *et al.* 2009), trimeric (Orgueira *et al.* 2003) or even tetrameric (Hansen *et al.* 2015) residues have been used as elongation blocks in modular glycosylation

strategies. They also differ in the type of building blocks used, in the timing of the oxidation of the hydroxyl group at position 6 to obtain the uronic acid and finally in the glycosylation procedures. In the case of Hp/HS, a dimeric glycosylation strategy is often preferred for practical reasons (good to very good coupling reaction yields, greater freedom of modulation, etc.). On this basis, 48 different disaccharide units can theoretically be found in native Hp/HS. These calculations take into account the potential presence of unusual residues bearing uncommon sulphation pattern as well as the presence of both L-iduronic acid and D-glucuronic acid residues. However, only 23 different disaccharides have yet been found to occur in nature (Esko and Selleck 2002). Synthetic routes to attain these 48 disaccharides have been reported in the literature. Lu *et al.* (2006) were the first to report the full synthesis of the first set of 48 fully and orthogonally protected disaccharide precursors that can be used as building blocks for the modular synthesis of Hp/HS oligosaccharides. Later on, Hu *et al.* (2012) also prepared these building blocks in order to investigate the interactions between the sugars and FGF1. A multitude of different size building block precursors have been designed throughout the years (Haller and Boons 2002, Saito *et al.* 2010). The differences between the blocks are essentially based on the type of PGs used, but also on the structural configurations of the building blocks to constrain the exclusive formation of the *1,2-cis*-linked products (Orgueira *et al.* 2002), or even the use of either a glucosamine or a uronic acid monomeric building blocks as glycosyl donor (Tabeur *et al.* 1996). Using uronic acid residues as glycosyl donors could help prevent the formation of a mixture of anomers during the formation of the glycosidic bond thanks to the neighbouring group participation principle, in contrast to the glucosamine residue. Recently, Dhamale *et al.* (2014) reported the synthesis of modular disaccharide building blocks containing glucuronic acid residues. They demonstrated that astutely protected glucuronic acids may be used as glycosyl donors to prepare dimeric precursors with high yields, avoiding the late-stage oxidation step at the very end of the synthetic process.

All the efforts put into the development of new synthetic routes have made possible the preparation of well-defined oligosaccharides of different sizes, first on a milligram-scale, then, more recently, on a gram-scale (Hansen *et al.* 2012). Recently, the total synthesis of a 40-mer heparin-related polysaccharide has also been

performed by Hansen *et al.* (2015), hence proving the feasibility of the synthesis of such lengthy polysaccharides.

Theoretically, carbohydrate chemistry allows the preparation of all sorts of Hp/HS structures, presenting specific sulphation/acetylation patterns and conformational characteristics. However, many limitations remain to be overcome. More specifically, the poor reliability of the glycosylation reactions remains a major issue. As previously mentioned, the exclusive stereoselective formation of α -glycosidic linkages in the absence of a participating neighbouring group is nearly impossible. In addition, uronic acids are known for being poor glycosylating agents and for their poor coupling efficacy due to their lack of reactivity. This is due to the electron withdrawing effect of the carboxyl group at position 5 of the residue which dramatically decreases the nucleophilicity of the neighbouring hydroxyl groups. Work recently published by Hansen *et al.* (2012) yet showed that uronic acids can lead to high yield reactions in some conditions. Idoside and glucoside residues have hence been extensively used as glycosylating agents (Haller and Boons 2001). Performing the selective late-stage oxidations of the hydroxyl groups at position 6 of the idoside and glucoside residues thus affords the desired corresponding uronic acid counterparts as well as helping to circumvent the problematic step of epimerisation of the uronic acid residues at the end of the process. However, high-yielded oxidations become more difficult to achieve as the size of the oligosaccharide increases (Huang and Huang 2007). As an alternative, oxidations are often realised at the mono-, di- or even tri-saccharide stage, thus avoiding the late-stage oxidation of larger and more valuable oligosaccharides. Moreover, due to the major difficulties encountered during both the synthesis of the building blocks and their assemblies, fewer efforts have been put in the study of the deprotection and sulphation of the synthesised oligosaccharide precursors. Thus, the effective compatibility/orthogonality of the PGs remains to be assessed, as well as the general stability of the partially deprotected compounds. Finally, despite the wealth of glycosylating agents and procedures at disposal of chemists, no general and systematic procedure that could accommodate all the characteristics of Hp/HS saccharides has yet been generated.

4.2. Objectives and design of general synthetic strategy

4.2.1. Objectives

The correlation between monosaccharide sequence sulphation pattern of Hp/HS and the biological activities of these GAGs is still under intense investigation. Deciphering the interactions between Hp/HS and FGF-FGFR complexes requires access to well-defined oligosaccharides. Despite some remarkable works reported in the literature (Ornitz *et al.* 1995, Tabeur *et al.* 1999, de Paz *et al.* 2001, Poletti *et al.* 2001, De Paz *et al.* 2006, Noti *et al.* 2006, de Paz *et al.* 2007, Cole *et al.* 2010, Sterner *et al.* 2014) which relate to the preparation of structurally well-defined Hp/HS structures or analogues on different supports and dedicated to the study of these interactions, room for improvements in this domain still exists. As previously mentioned in Section 1.8.1, the isolation of structures presenting specific structural characteristics from natural sources is remarkably difficult, making it an unattractive method. For these reasons, it was decided to resort to chemical synthesis to attempt the synthesis of target molecules. In doing so, setting up a new convenient and short synthetic route, as well as setting up a library of new glycosylating agents, one of the main objectives of this project, was attempted. These new building blocks were evaluated as glycosyl donors and acceptors in glycosylation reactions.

It is generally understood and accepted that the automated synthesis of oligosaccharides will be, in the future, the key to an in-depth study of the SAR of glycans. However, unlike oligonucleotides and oligopeptides (Merrifield 1985) that are generated on a daily basis with the help of solid-phase methods, no general method has yet been set up to generate oligosaccharides. Much progress remains to be made, despite some encouraging results obtained by Seeberger and colleagues in this domain, who successfully prepared both branched and linear oligosaccharides (Plante *et al.* 2001, Eller *et al.* 2013). Studying and setting up new glycosylating agents and glycosylation procedures are keys to improve the automated synthesis of oligosaccharides. Therefore, another objective of this project will be the transfer of the chemistry developed during the in solution-phase synthesis to the solid-phase synthesis. To do so, some parameters required for the solid-phase synthesis such as the type of PGs used or the use of a linker to derivatise the reducing end residue will

have to be taken into account during the multi-step solution synthesis. Guedes and colleagues have recently reported the preparation of similar compounds, derivatised with a carbamate-type linker, proving that such a transfer of chemistry between the two methods is feasible (Czechura *et al.* 2011, Guedes *et al.* 2013). The work reported here was motivated by these promising results and will hopefully contribute to a better understanding of the close relationship between sequence specificities and biological activities of these types of compounds.

4.2.2. General strategy

The strategy that has been adopted for this project is based on the assembly of advanced disaccharide building blocks, yet the assembly of monosaccharide building blocks is also another alternative (Codée *et al.* 2005, Tatai and Fügedi 2008). Even though a monomeric residue iteration-based strategy would have afforded a greater degree of flexibility, the assembly of dimeric building blocks has been preferred over the assembly of monomeric building blocks for several reasons. First of all, the elongation process of the oligosaccharide backbone is undoubtedly considerably shortened. In the case of Hp/HS oligosaccharides synthesis, this quickly appears to be a major advantage, as no less than $8^3=512$ possible hexasaccharide structures can theoretically be synthesised, $8^4=4,096$ and $8^5=32,768$ structures for octasaccharides and decasaccharides respectively (8 structurally different disaccharide units may constitute the oligosaccharides, see Figure 24). However, these calculations are rather simplified, as the possible presence of unusual residues (such as D-glucosamine residues presenting a free amine at C-2 or a sulphate group at C-3, or even the presence of D-glucuronic acid residues) is not included. Moreover, the diversification of the building blocks is done at a very early stage of the process, thus providing the synthesis of oligosaccharides with a broad variety of possible structures in a relatively short time. Secondly, using dimeric building blocks will require fewer glycosylations to reach the desired backbone size, which is another appreciable advantage due to the intrinsic unreliability of glycosylation reactions in most cases. Finally, only a limited number of building blocks are required to afford a wide range of structural motifs. Moreover, despite the fact that modifying the building blocks might appear laborious to achieve at first sight, this is not actually the case as the synthetic routes can be redesigned and modulated relatively easily.

This is due to the extensive and diversified library of PGs and to the multitude of methods available to researchers – library and new methods that are constantly being expanded as chemists develop new ones or redesign existing ones (Jarowicki and Kocienski 2001, Prabhu *et al.* 2003, Wuts and Greene 2006, Codee *et al.* 2011). In addition, many synthetic routes and synthons have already been developed and evaluated as building blocks over recent decades, granting researchers many possibilities to redesign the synthetic routes for their projects.

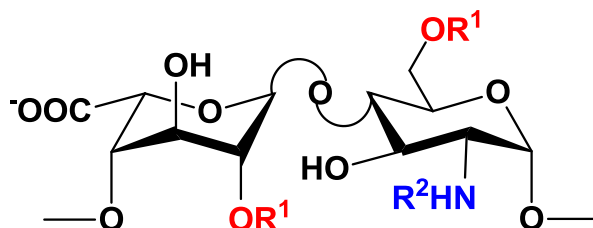
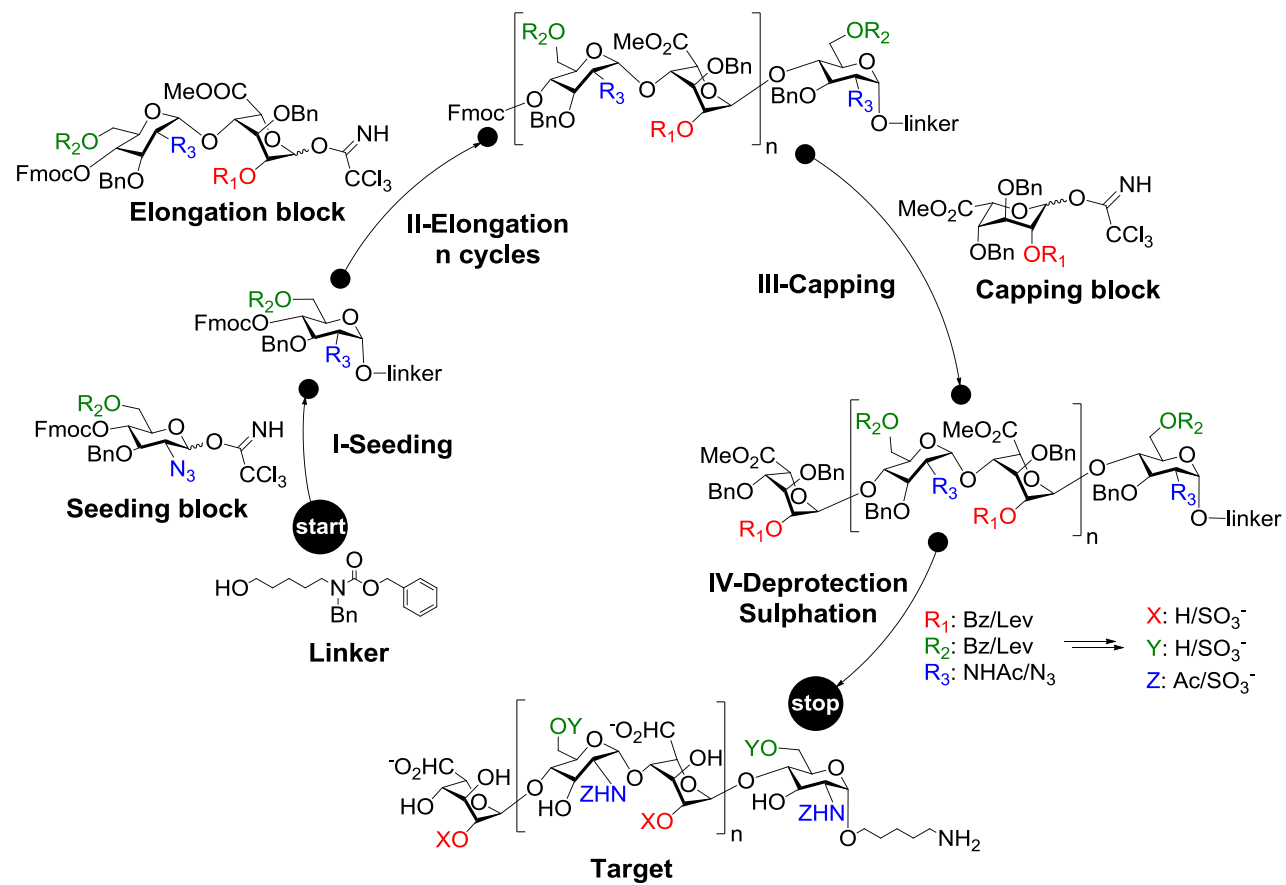


Figure 24: Structures of the disaccharide units constituting Hp/HS oligosaccharides. The basic disaccharide structure can be differentiated at three different positions, labelled R^1 and R^2 . This representation is limited to a single type of uronic acid (L-iduronic acid here) and does not include unusual structural features (3-*O*-sulphate/unsubstituted amino groups) $R^1 = \text{H}$ or SO_3^- ; $R^2 = \text{Ac}$ or SO_3^- .

In the case of the preparation of a library of Hp/HS oligosaccharides, the desired structures will be prepared in four main stages (Scheme 4). The first stage consists of the derivatisation with a linker at the anomeric position of the first glycosyl residue, also called the seeding block. The choice of derivatising the seeding block with this particular linker has been motivated for two reasons. On the one hand, the derivatisation with a linker was favoured over the use of a permanent protective group in order for a potential transfer of the chemistry developed in this case to the solid-phase synthesis of Hp/HS oligosaccharides. On the other hand, as mentioned in Section 4.2.1, this particular linker and similar ones had already been described in the literature and their reactivity assessed. Moreover, two seeding blocks will be used to prepare a total of four different linker-seeding precursors during this first step. This is explained by the use of D-glucosamine residues as seeding blocks.



Scheme 4: General strategy for Hp/HS octasaccharide synthesis.

These residues indeed present two sites at which substitutions can be performed: a hydroxyl or sulphate group can be found at position 6 and an *N*-acetyl or *N*-sulphate group can also be found at position 2.

In the second stage, called the elongation process, disaccharide glycosyl synthons are used to elongate the oligosaccharide backbone through a couple of elongation cycles. The elongation building blocks will be composed of 1-4 linked D-glucosamine and L-iduronic acid residues. In theory, a total of 8 disaccharide building blocks must be synthesised to prepare all possible oligosaccharide structures. However, the backbone can be modified between two elongation cycles, thus allowing a possible reduction of the total number of disaccharide building blocks to be synthesised. The third step consists of terminating the elongation of the backbone with a monosaccharide building block, often termed capping block. Two different capping blocks might be used, thus allowing either a hydroxyl or a sulphate group at position 2 of the L-iduronic acid residue at the non-reducing end of the oligosaccharide.

Finally, the ultimate steps consist of the deprotection and selective sulphation/acetylation of the oligosaccharide precursor, thus affording the targeted oligosaccharide.

All through the process, several parameters will need to be monitored and closely controlled, such as the stability of the PGs, the conformations of the different residues, the nature and conformation of the glycosidic bonds (regio- and stereoselectivity of the glycosidic bond formation). Moreover, in order to make the synthetic route viable and attractive, the best conditions to obtain high-yield glycosylations, deprotection and sulphation reactions will need to be established.

The targeted oligosaccharides will all share the same general structural features. Their sequences - which will essentially consist of 1-4 linked α -L-iduronic acids (IdoA) and α -D-glucosamines – will start with a D-glucosamine residue which is derivatised with a linker at the reducing end and be terminated with an L-iduronic acid residue at the non-reducing end. L-iduronic acid residues represent approximately 30-80% of the total of the uronic acid residues in native Hp/HS oligosaccharides and are required for protein binding (see Section 1.6.2). This

thereby explains why the targeted oligosaccharides will solely contain L-iduronic acid residues.

Ultimately, the only difference between two targets will lie in their sulphation and acetylation patterns. To make the selective modification of the positions of interest possible, all seeding, elongation and capping blocks have been designed in such a way that appropriate PGs will be introduced at specific positions of the residues. These PGs have been chosen according to the type of modifications that will be carried out during subsequent steps of the process. In addition, the building blocks and oligosaccharide precursors must be orthogonally protected, so that all the other PGs will remain stable whilst a group or chemical moiety is being introduced, modified or removed. With all these conditions in mind, three categories of PGs will be used. The first category includes the groups that will not be modified during both the assembly and sulphation of the building blocks and oligosaccharide precursors (the permanent PGs): the benzyl ether (Bn) and benzoate ester (Bz) groups to permanently protect hydroxyl moieties, the acetamido (Ac) group for the amine moieties and the methyl ester (Me) for masking the carboxylic acid moiety of the uronic acid residues. The second category includes the groups that will be used to temporarily protect the sites that will undergo sulphation at a later stage (the temporary PGs): the azido moiety (N_3) to mask the amines and the levulinoyl ester group (Lev) to protect the hydroxyl groups. Finally, the 9-fluorenylmethyloxycarbonyl carbonate (Fmoc) group, which belongs to the third and last category, will be used to protect the acceptor sites of the building blocks and oligosaccharide precursors. The cleavage of the Fmoc group is possible using a hindered base such as triethylamine (Et_3N), which does not affect the other PGs, particularly the Lev ester group.

In addition to all the conditions mentioned above, other requirements have motivated the selection of the protective groups. For instance, on the one hand, the use of a non-participating group such as N_3 at the position 2 of the D-glucosamine residue usually leads to the introduction of 1,2-*cis* glycosidic linkages only. However, under specific conditions, the formation of 1,2-*trans* glycosidic linkages might take place as well, indicating that the non-participatory character of this moiety alone does not guarantee the selectivity of the bond formation (Tsuda *et al.* 2003, Lohman and

Seeberger 2004). Yet, in the case of the synthesis of Hp/HS oligosaccharides, it is now well known that assembling a D-glucosamine derivative bearing a non-participating group at C-2, such as an azido group, and an L-idose/L-iduronic derivative preferably leads to the formation of the α -linked product (Van Boom *et al.* 1996, Kovensky *et al.* 2002, Orgueira *et al.* 2002). On the other hand, as explained in Section 4.1.1.2, the use of an ester group (such as Bz or Lev) at position 2 of the uronic acid residues will exclusively lead to the formation of 1,2-*trans*-directed glycosidic bonds.

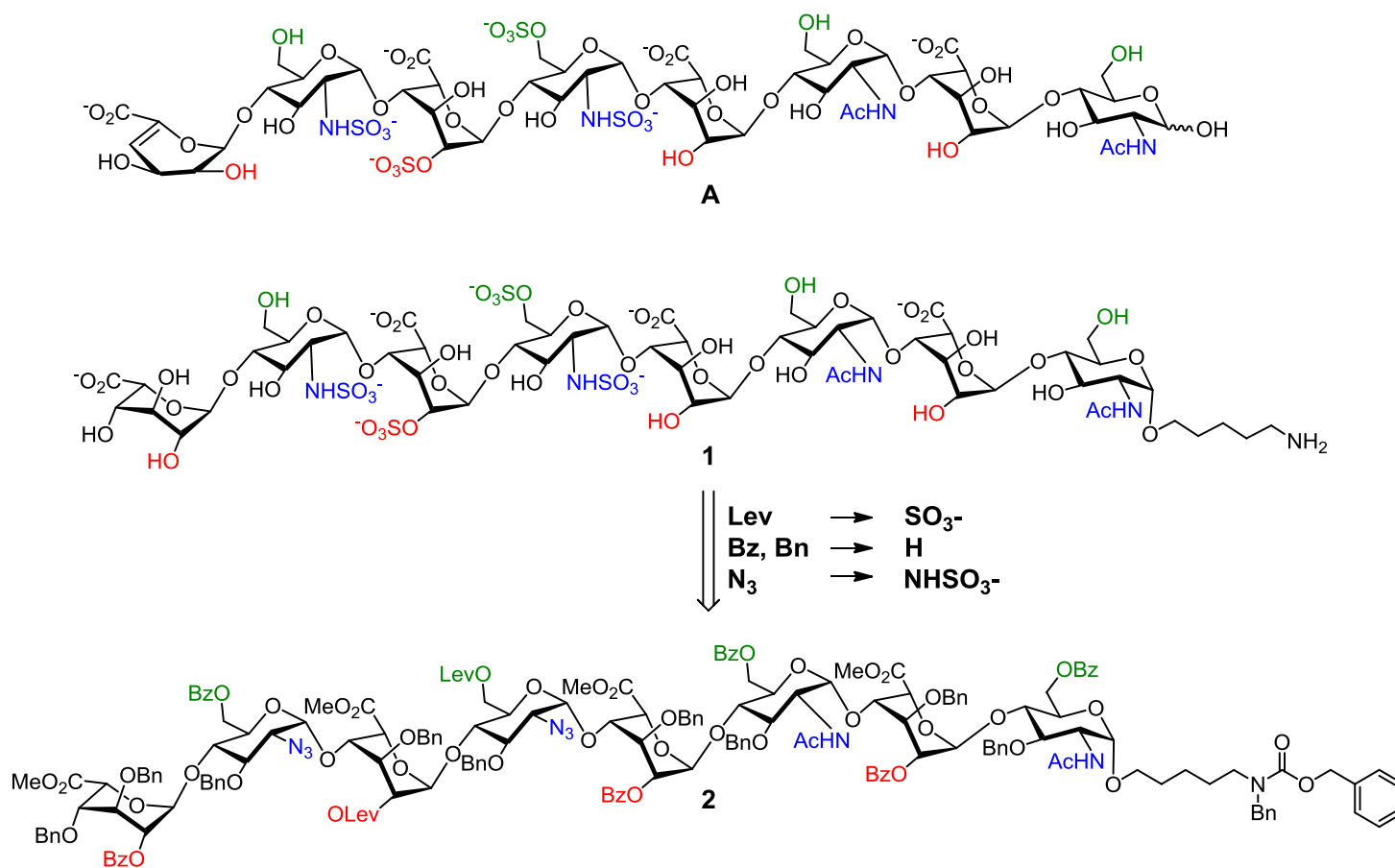
Besides the protective groups described above, the trichloroacetamido (TCA) moiety will also be used, but as a leaving group in glycosylation reactions, for the activation of the glycosyl donors. The activation of O-glycosyl residues presenting Fmoc protected hydroxyl groups with TCA moieties has been made possible thanks to work undertaken by Roussel *et al.* (2000). Fmoc groups are very easily cleaved under basic conditions, which are required for the introduction of a TCA moiety. However, as shown by Roussel and colleagues, using sodium hydride as a catalyst appears to overcome the problem and to grant high yield reactions as well.

4.2.3. First target structure

To test the relevance and feasibility of the synthetic strategy and to evaluate the reactivity of some of the building blocks, the preparation of a first target was planned (Scheme 5). The choice of this particular compound as the first target was motivated by two considerations. First of all, the use of elongation blocks that will afford different sulphation patterns is required, which allows the evaluation of the reactivity of different building blocks for the synthesis of a single compound. Secondly, an analogue **A** of this HS octasaccharide has already been isolated, characterised and screened in bioassays by Ahmed (2010) (Scheme 5). According to the activity assay results that were obtained, this structure appears to facilitate the interactions between FGF2 and the receptor FGFR1c.

Unlike the compound that has been isolated from natural sources, the target molecule that will be synthesised will contain a linker at the reducing end. Thus, the impact of the linker on the ability of this structure to activate FGF-FGFR complexes will be

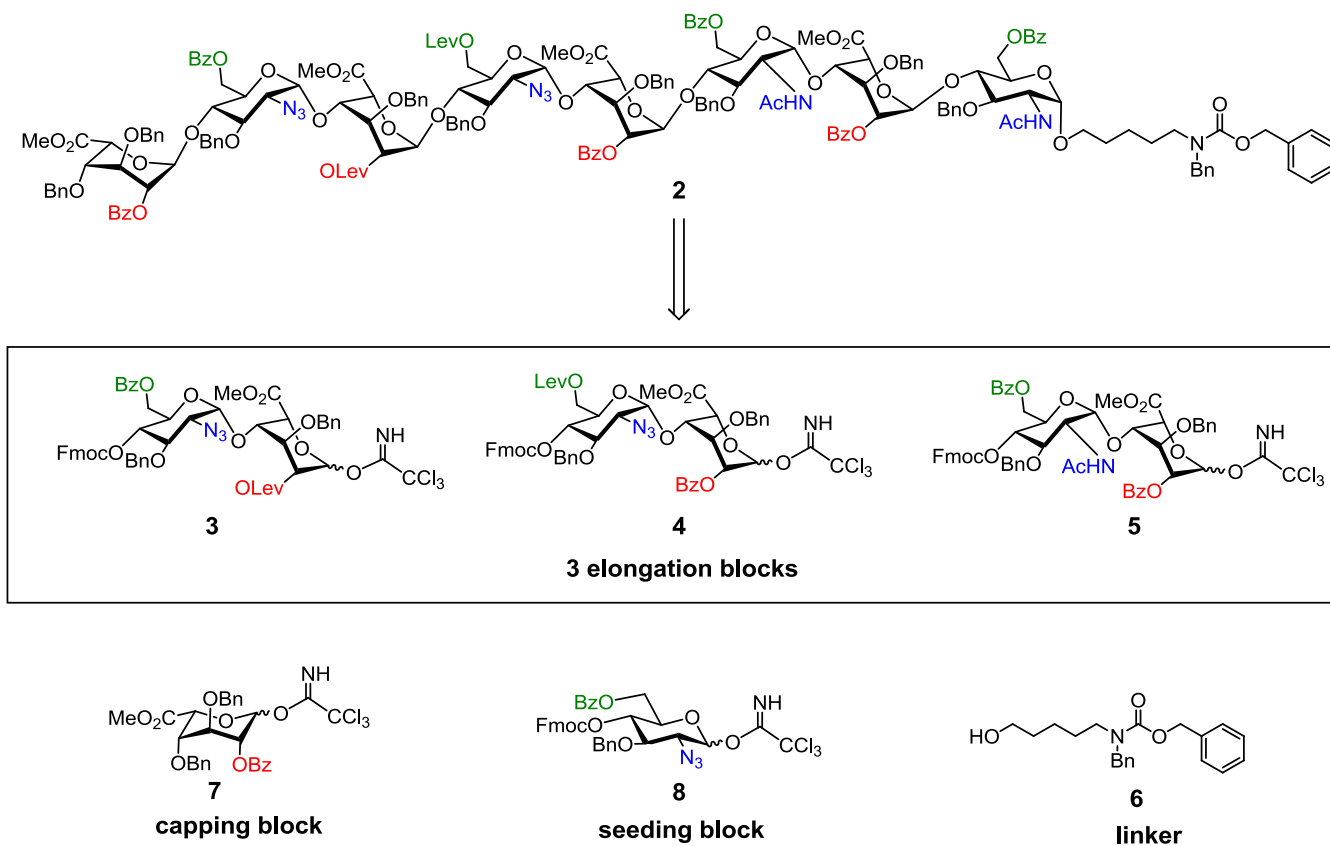
assessed, although no major difference is expected. The sequence of **1** will be as follows, from the non-reducing end to the reducing end (all glycosidic linkages are in α -conformation): IdoA-GlcNS-IdoA(2S)-GlcNS(6S)-IdoA-GlcNAc-IdoA-GlcNAc-linker. As previously mentioned, several chemical moieties will be used to protect/mask the positions of interest. As depicted in Scheme 5, the retrosynthetic analysis of **1** leads to the molecule **2** – the final intermediate which will be obtained at the end of the elongation and capping processes.



Scheme 5: Retrosynthesis of the first target – Structures of the first target and its natural analogue.

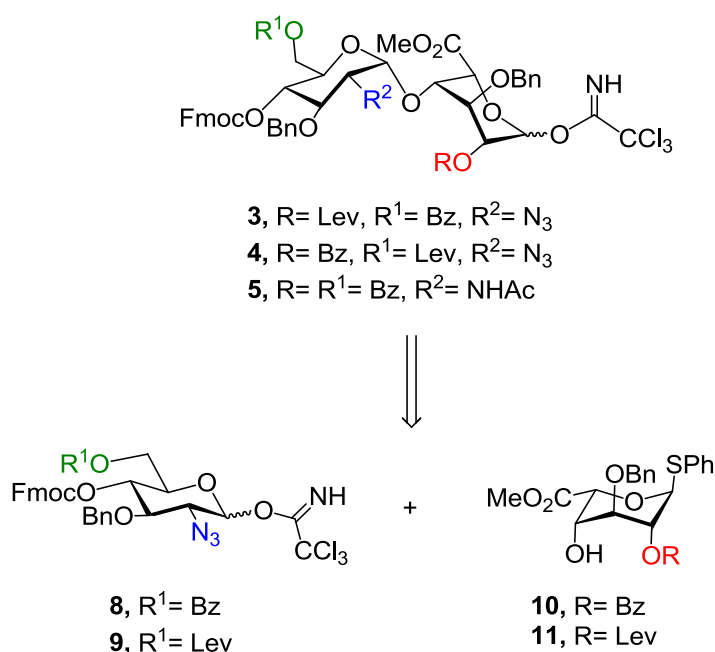
4.3. Initial synthetic approach: synthesis of the elongation blocks

Along with the preparation of the linker **6**, the seeding block **8** and capping block **7**, synthesising the precursor **2** will require the preparation of the three distinct elongation blocks **3-5**, each presenting specific structural characteristics (Scheme 6). Thus, preparing the precursor **2** will provide a global appreciation of the feasibility of the synthesis of the elongation blocks in particular. Moreover, their reactivity in glycosylation reactions will also be assessed, corroborating or disproving the relevance of the modular approach initially drawn up.



Scheme 6: Retrosynthesis of the first target – Building block and linker structures.

As depicted in Scheme 7, preparing the elongation blocks **3-5** will only require the synthesis of two types of glycosyl donors **8** and **9**, as well as two types of glycosyl acceptors **10** and **11**, reducing the total number of glycosylating agents to be prepared to five (**3-5**, **7** and **8**). Thus, it clearly appears that this modular synthetic approach considerably limits the number of manipulations of the backbone between the elongation steps. In addition, most of the building blocks and precursors that will be developed in this case have not been previously described in the literature yet, further expanding the extensive library of glycosyl precursors that has been developed.



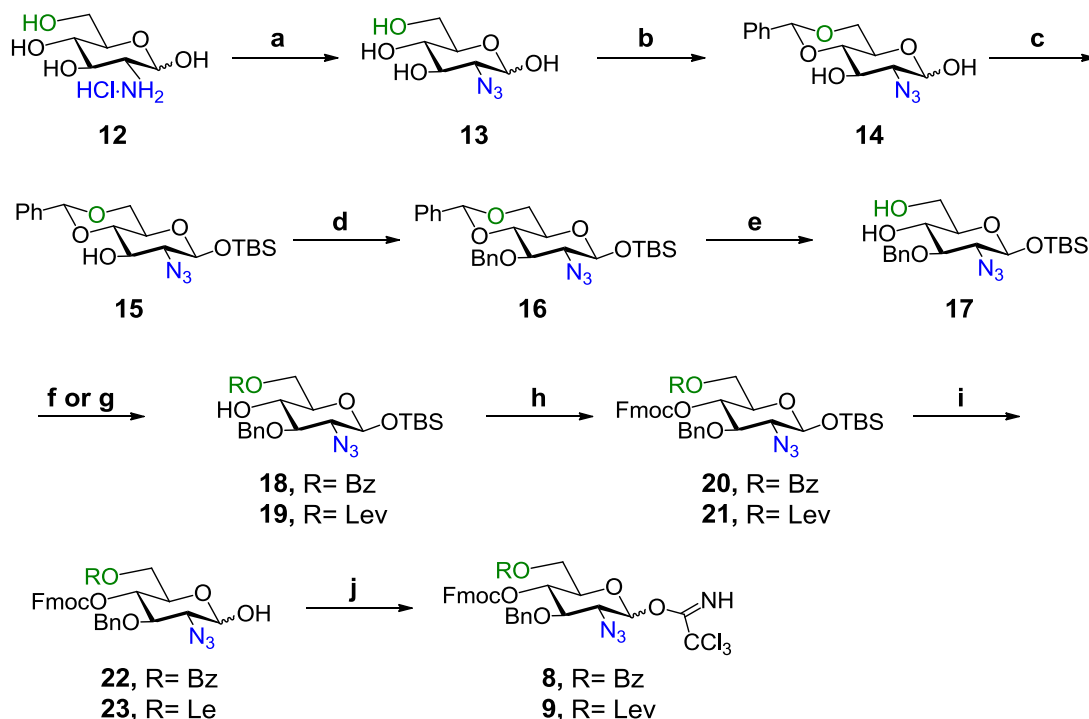
Scheme 7: Retrosynthesis of the elongation blocks – Monomeric building block structures.

In the next sections, the synthesis and evaluation of the seeding and elongation blocks in glycosylation reactions will be discussed as a matter of priority, unlike the capping block and linker that will be discussed later.

4.3.1. Azidoglucose building block synthesis

As explained in the previous section, the modular approach that has been chosen to prepare the intermediate **2** requires the synthesis of only two types of glycosyl donors **8** and **9**. Yet, the chosen approach allows the differentiation of the blocks at a late

stage of the process, as described in Scheme 8. This appears to be a considerable advantage in that it significantly reduces the number of steps and manipulations necessary to produce the desired compounds. Thus, in most cases, a high number of steps induces a low overall yield – a situation that we seek to avoid in the present case.



Scheme 8: Synthesis of the glycosyl donors 8 and 9.

Reagents and conditions: (a) (i) NaN₃, Tf₂O, H₂O, DCM; (ii) NaOMe, DMAP, TfN₃ MeOH; (b) Benzaldehyde dimethyl acetal, *p*-TsOH, ACN (66%, 3 steps); (c) TBSCl, imidazole, DCM (70%); (d) NaH, TBAI, BnBr, DCM (85%); (e) EtSH, *p*-TSOH, DCM (89%); (f) BzCN, Et₃N, ACN (90%); (g) LevOH, CMPI, DABCO, DCM (94%); (h) FmocCl, pyridine, DMAP, DCM (**20**, 96%; **21**, 95%); (i) HF.pyridine, THF (**22**, 81%; **23**, 78%); (j) Cl₃CCN, NaH (**8**, 95%; **9**, 85%).

The production of the imidates **8** and **9**, completed in a nine-step sequence, started with the preparation of **17** from the commercially available 2-amino-2-deoxy-D-glucose hydrochloride **12** (Guedes *et al.* 2013). First of all, 2-amino group of D-glucosamine hydrochloride **12** was converted into the corresponding azide **13** by a diazo transfer reaction from trifluoromethanesulphonyl (triflyl) azide (TfN₃). This direct method was described for the first time by Vasella and colleagues for the preparation of 2-azido-2-deoxy-D-glucose, D-manno, D-galacto and D-allo derivatives (Vasella *et al.* 1991). Although the diazo transfer reaction with TfN₃ is nowadays

widely used, the unpredictability of the reaction (yields may vary, depending on the quality of the reagents used and the preparation of the trifyl azide solution), as well as the inherent explosiveness of TfN_3 when dried, makes it a fairly unreliable reaction. However, the availability of the starting material (SM), its reasonable price, the fact that the reaction can be carried out on a fairly high scale and that the diazo transfer is carried out at a very early stage of the synthetic route makes it convenient to some extent. The resulting intermediate was then treated with benzaldehyde dimethyl acetal in the presence of *p*-toluenesulphonic acid (*p*-TsOH) in acetonitrile to afford the 4,6-*O*-benzylidene derivative **14**. These two reactions may be realised on a relatively large scale (up to 100 g of SM, but usually on a 10-20 g scale for safety reasons) with comfortable yields, making them convenient for Hp/HS oligosaccharides synthesis. The regio- and stereoselective silylation of the anomeric centre was then carried out using *tert*-butyldimethylsilyl chloride (TBSCl) and imidazole, resulting in the exclusive formation of the β -anomer of the product **15**. After protection of the anomeric center, the deprotonation of the hydroxyl group at position 3 of the intermediate was realised with sodium hydride (NaH), followed by its benzylation with benzyl bromide (BnBr) in presence of tetrabutylammonium iodide (TBAI), affording **16**. Treating **16** with ethanethiol (EtSH) in presence of *p*-TSOH resulted in the cleavage of the 4,6-*O*-benzylidene and the formation of the diol **17** (Guedes *et al.* 2013).

Making **17** one of the intermediates of this synthetic route is attractive as it can be synthesised on a large scale. The differentiation of the glycosyl donor residues was then carried out at this stage of the synthesis.

4.3.1.1. Synthesis of the building block 9

The regioselective 6-*O*-levulinoylation of **17** was performed with levulinic acid in dry DCM at -20 °C, in the presence of the activator 2-chloro-1-methyl-1-pyridinium iodide (CMPI) and 1,4-diazabicyclo[2.2.2]octane (DABCO), to afford **19** in a very satisfactory yield of 94% (Koeners *et al.* 1980). The hydroxyl group at position 4, which will be required for the oligosaccharide extension, was protected as Fmoc carbonate using 9-fluorenylmethoxycarbonyl chloride (FmocCl) in presence of the activator 4-dimethylaminopyridine (DMAP) in pyridine to afford the fully protected

compound **21** in a yield of 95%. The cleavage of the *tert*-butyldimethylsilyl ether moiety used to protect the anomeric centre was first attempted under standard conditions (AcOH/TBAF in THF), but the desired compound could not be isolated. The cleavage of the Fmoc group was indeed systematically detected for both SM (**23a**, Figure 25) and product (**23b**, Figure 25). Both **23a** and **23b** were not isolated and were only detected by LC-MS.

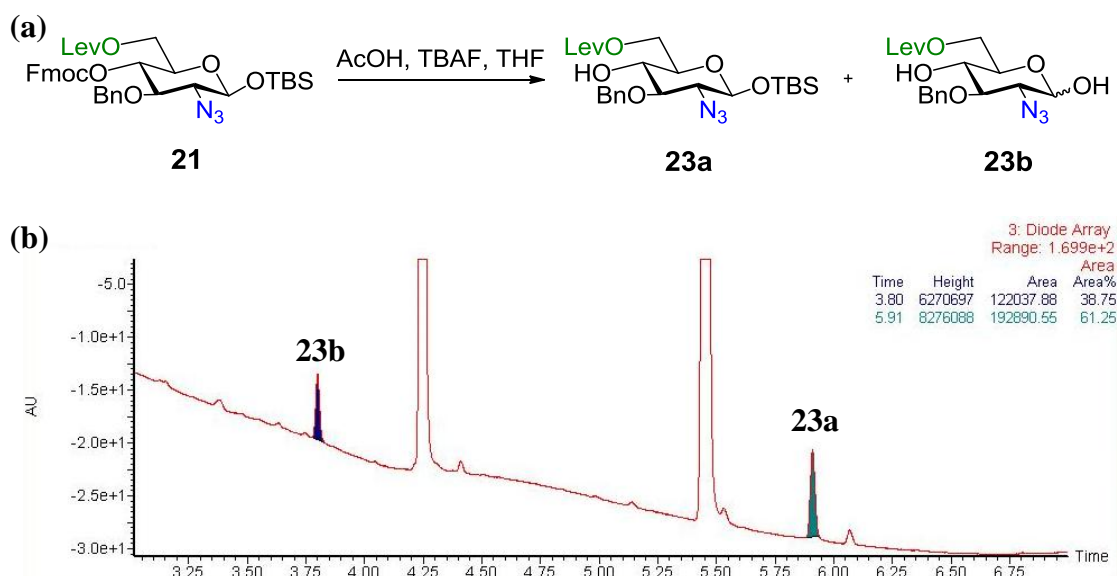


Figure 25: Results for the desilylation of 21 using AcOH and TBAF.

(a) Formation and possible structures of the by-products **23a** and **23b**;
 (b) LC-MS analysis results of the desilylation of the residue **21** using AcOH/TBAF in THF. Retention time: 3.8 min (calcd for $\text{C}_{18}\text{H}_{23}\text{N}_3\text{O}_7$: 393.1 [M], found m/z 411.1 [$\text{M}+\text{NH}_4$] $^+$, 416.1 [$\text{M}+\text{Na}$] $^+$): by-product **23b**; retention time: 5.91 min (calcd. for $\text{C}_{24}\text{H}_{37}\text{N}_3\text{O}_7\text{Si}$: 507.2 [M], found m/z 525.2 [$\text{M}+\text{NH}_4$] $^+$, 530.1 [$\text{M}+\text{Na}$] $^+$): by-product **23a**; Unidentified peaks: retention times 4.25 min and 5.49 min.

This may be explained by the base-labile property of the Fmoc group, which appeared to be unstable in the presence of tetrabutylammonium fluoride (TBAF). The deprotection of the anomeric centre of **21** was next realised with hydrofluoric acid.pyridine (HF.pyridine) in dry THF and afforded **23** as a mixture of anomers (α/β 2/1, determined by ^1H NMR) in 78% yield. No loss of Fmoc group was detected at any stage of the process; making HF.pyridine an attractive alternative despite being a relatively hazardous reagent that should be manipulated with extra care. The activation of **23** was then realised using trichloroacetonitrile and a catalytic amount of NaH, as described by Roussel and colleagues (Roussel *et al.* 2000) and afforded the imidate **9** as an α/β -mixture (α/β 1/4, determined by ^1H NMR) in 85% yield.

4.3.1.2. Synthesis of the building block **8**

The regioselective 6-*O*-benzoylation was realised by treating **17** with benzoyl cyanide (BzCN) and a catalytic amount of triethylamine (Et₃N) in dry acetonitrile to form **18**, as described by Guedes *et al.* (2013). In analogy to the preparation of intermediate **21**, the C-4 hydroxyl group was protected with FmocCl, in the presence of DMAP and affording **20** in 96% yield. The *tert*-butyldimethylsilyl ether moiety used to protect the anomeric center was then easily cleaved with hydrofluoric acid in pyridine in THF and produced **22** as a mixture of anomers (α/β 2/1, determined by ¹H NMR) in 81% yield. The presence of a Bz group instead of a Lev group at position 6 (as for **21**) apparently did not have any effect on the overall reactivity of the D-glucosamine residue. Finally, as for the preparation of **9**, treating the lactol **22** with NaH and trichloroacetonitrile gave the trichloroacetimidate **8** in 95% yield (α/β 1/2, determined by ¹H NMR).

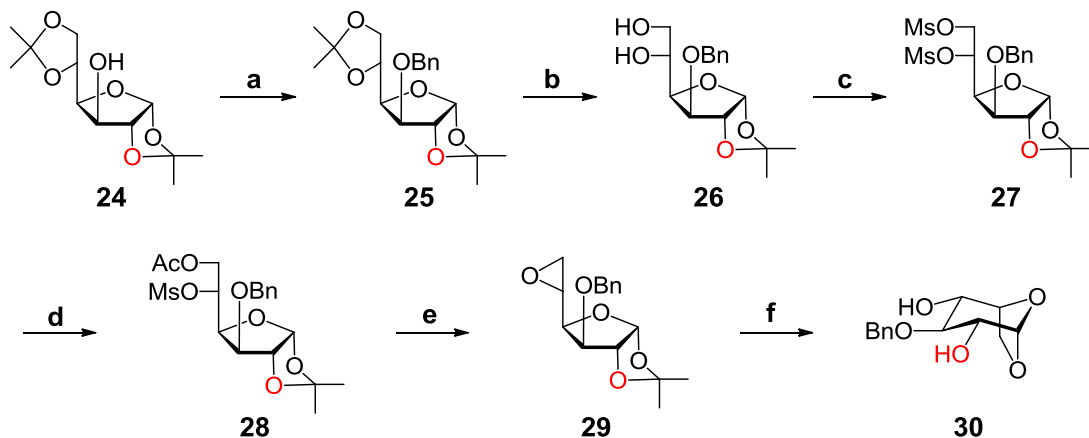
4.3.2. L-iduronic acid building block synthesis

As mentioned in the previous sections, the synthesis of only two types of glycosyl acceptors **10** and **11** is required for the preparation of the fully protected octasaccharide intermediate **2**. As for the glycosyl donor residues, the differentiation of the intermediates that will lead to the two final L-iduronic acid building blocks will be performed at a later stage of the synthetic route.

Both L-iduronic acid and L-idose are commercially available, but very costly, making them not attractive as SM. For this very reason, many synthetic routes for the preparation of L-iduronic acid derivatives have been developed from diverse SMs.

The preparation of the desired compounds **10** and **11** demanded the preparation of the well-known intermediate **30** (Scheme 9), available on a gram scale, obtained from the cheap and easily available D-glucose derivative **24** (diacetone glucose) in a 6 step-sequence (Van Boeckel *et al.* 1985, Lu *et al.* 2006, Hung *et al.* 2012). First, **26** was generated from **24** via the benzylation of the hydroxyl group at position 3 using BnBr, NaH and catalytic TBAI in dimethylformamide (DMF), followed by the selective cleavage of the 5,6-*O*-isopropylidene ring using a 66% solution acetic acid (88% yield, 2 steps). The diol **26** was next mesylated using to afford **27** in 90% yield.

The selective substitution of the primary mesylate group was performed by treating **27** with potassium acetate (KOAc) in the presence of crown-ether to afford **28** in 85% yield. The intermediate **30** was obtained after treatment of **28** with potassium *tert*-butoxide (*t*-BuOK) in *tert*-butanol (*t*-BuOH) and DCM, followed by acidic hydrolysis using 1 M H₂SO₄ in dioxane. At this stage of the synthetic route, the differentiation of the intermediate was undertaken.

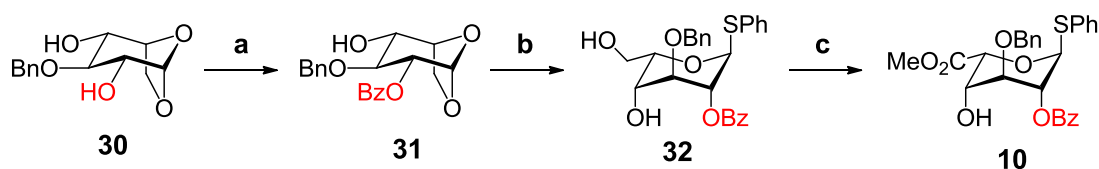


Scheme 9: Synthesis of the intermediate 30.

Reagents and conditions: (a) BnBr, NaH, cat. TBAI, DMF; (b) AcOH (66%), H₂O (88%, 2 steps); (c) MsCl, pyridine, DCM (90%); (d) KOAc, 18-crown-6, ACN (85%); (e) *t*-BuOK, *t*-BuOH, DCM (74%); (f) 1 M H₂SO₄, dioxane, 120 °C, microwave (50%).

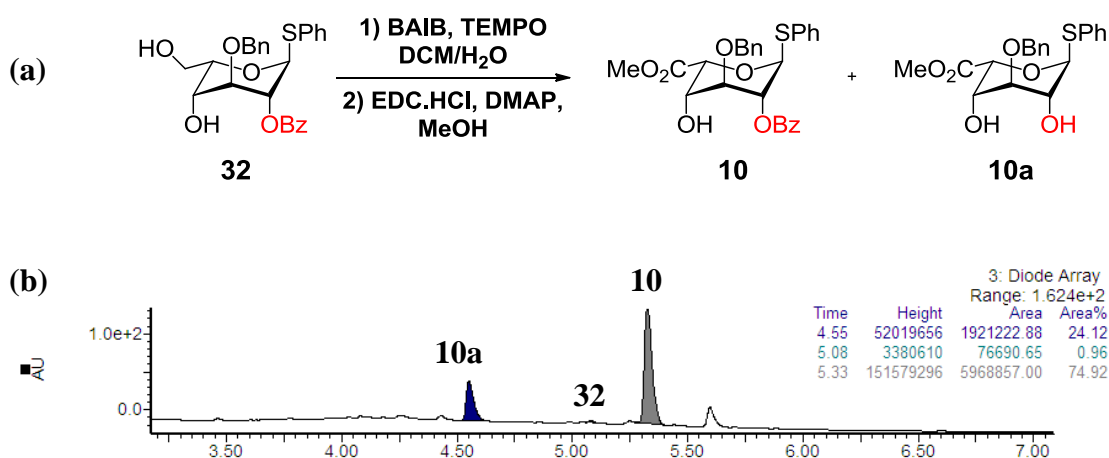
4.3.2.1. Synthesis of the building block 10

The regioselective benzylation of the hydroxyl group at position 2 of **30** was carried out (Lee *et al.* 2004) (Scheme 10). The resulting residue **31** then underwent zinc iodide-assisted thiolysis with trimethyl(phenylthio)silane in dry conditions to give exclusively the α -thioglycoside **32** in 77% yield, as described by Guedes *et al.* (2013). The chemo- and regio-selective oxidation of the primary hydroxyl group at position 6 of **32** into the corresponding carboxylic acid was made possible in aqueous conditions (Siedlecka *et al.* 1990) and was accomplished with the combination of 2,2,6,6-tetramethyl-1-piperidinyloxy (TEMPO) and a catalytic amount of [bis(acetoxy)-iodo]benzene (BAIB) (Epp and Widlanski 1999, Codée *et al.* 2005).

**Scheme 10: Synthesis of the building block 10.**

Reagents and conditions: (a) BzCl, pyridine (85%); (b) Me₃SiSPh, ZnI₂ (77%); (c) (i) TEMPO, BAIB, DCM, H₂O; (ii) MeOH, Amberlite IR-120 (H⁺), 4 Å ms, microwave (82%, 2 steps).

Initially, the conversion of the resulting intermediate into the corresponding methyl ester **10** was attempted via Steglich esterification with *N*-(3-dimethylaminopropyl)-*N'*-ethylcarbodiimide hydrochloride (EDC.HCl) and a catalytic amount of DMAP. However, the results obtained with this method turned out to be unsatisfactory due to long reaction times (the complete consumption of the SM was detected after 48h of reaction) and low yields varying between 30% and 47%. Moreover, significant formation (about 25%) of the debenzoylated by-product **10a** was observed by LC-MS analysis (but not isolated), as depicted in Figure 26.

**Figure 26: Results of the Steglich esterification of 32.**

(a) Formation and structures of the product **10** and by-product **10a**;
 (b) LC-MS analysis results of the Steglich esterification of the building block **32** (48h reaction). Retention time: 4.55 min (calcd for C₂₀H₂₂O₆S: 390.1 [M], found *m/z* 408.1 [M+NH₄]⁺, 413.1 [M+Na]⁺): by-product **10a**; retention time: 5.08 min (calcd. for C₂₆H₂₆O₆S: 466.1 [M], found *m/z* 484.2 [M+NH₄]⁺, 489.1 [M+Na]⁺): starting material **32**; retention time: 5.33 min (calcd for C₂₇H₂₆O₇S: 494.1 [M], found *m/z* 495.2 [M+H]⁺, 512.1 [M+NH₄]⁺, 517.1 [M+Na]⁺): product **10**.

The microwave-assisted Fischer esterification of the intermediate was hence attempted using Amberlite IR-120 (H^+), freshly prepared molecular sieves and dry methanol (MeOH). The impact of several parameters over the reaction outcome was assessed, such as the type of molecular sieve used, the reaction time and the temperature. From the results that were obtained and which are summarised in Figure 27 (b), the type of molecular sieve used (beads over powder, entries 2 and 3) appears to be of critical importance, as well as the reaction temperature. The reaction time was drastically decreased by increasing the temperature (entries 1-3). However, using a mass to mass ratio (SM/Amberlite 1/1) resulted in the formation of the by-product **10b** (observed by LC-MS analysis, by-product not isolated), probably due to the acidity of the solution (entries 3 and 4). Finally, the desired L-iduronic building block **10** was obtained with a yield of 82% over two steps.

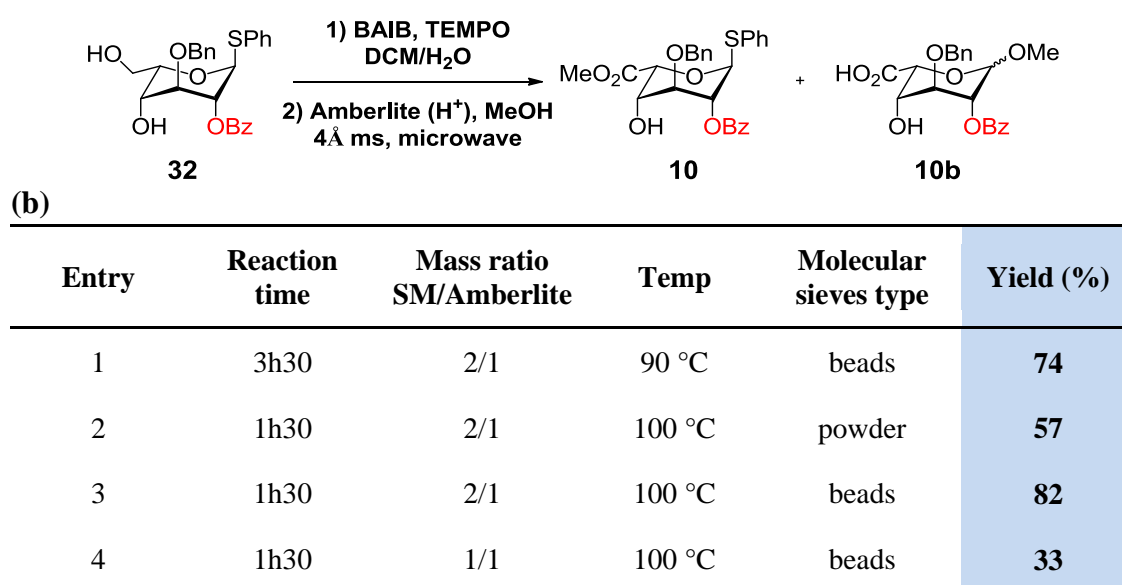


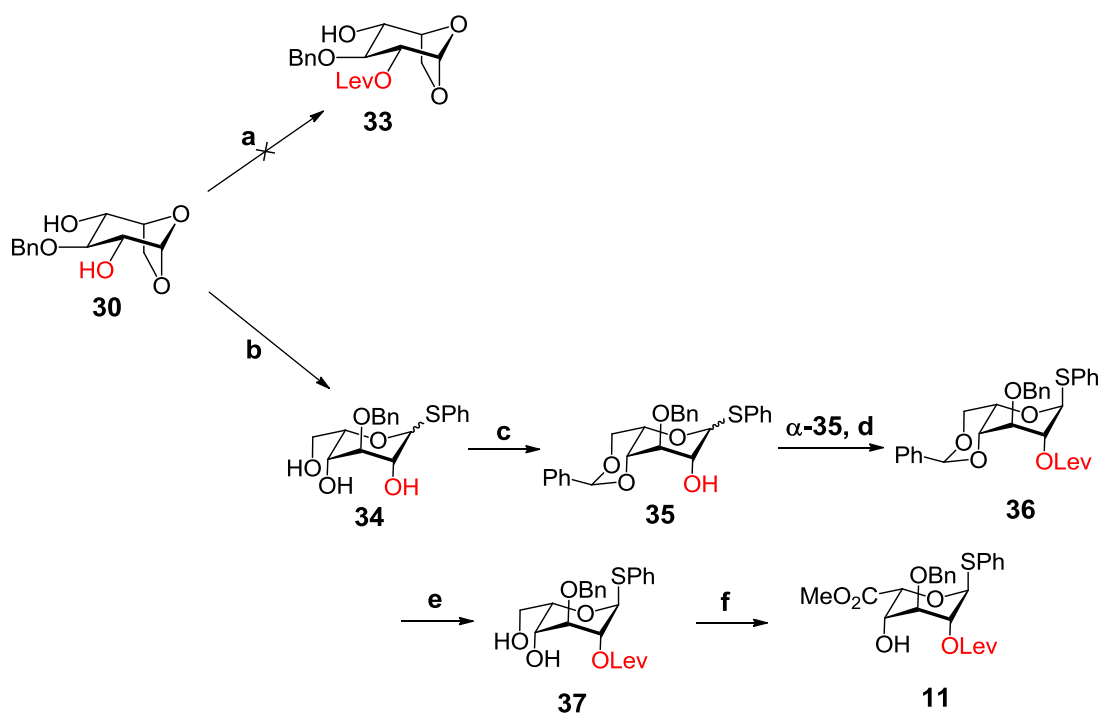
Figure 27: Preparation of building block 10.

(a) Formation and structures of the product **10** and possible by-product **10b**;
 (b) Reaction conditions and results for the esterification of **32**.

4.3.2.2. Synthesis of the intermediate **34**

The preparation of the synthon **11** was also undertaken (Scheme 11). As for the other type of L-iduronic building block **10**, the direct selective levulinoylation of the position 2 of the intermediate **30** was attempted, with the same conditions used for the levulinoylation of **17**. However, as the formation of **33** was not detected (the SM remain unchanged), which was probably due to a lack of reactivity of the SM, this

method was abandoned in favour of a longer, but more reliable synthetic route, as depicted in Scheme 11.

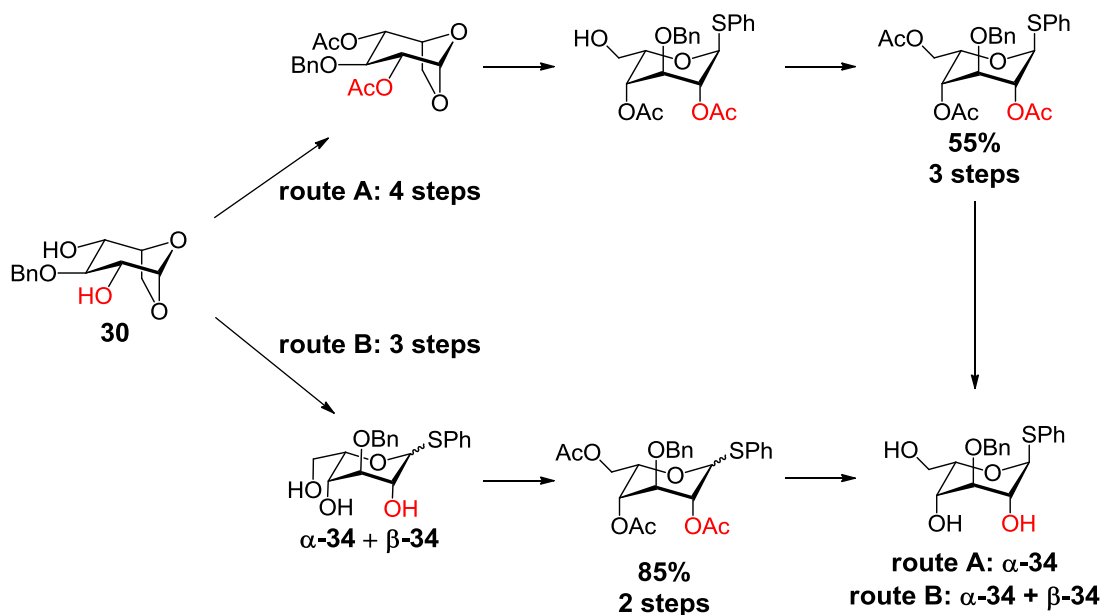


Scheme 11: Synthesis of the building block 11.

Reagents and conditions: (a) LevOH, CMPI, DABCO, DCM; (b) (i) Me_3SiSPh , ZnI_2 , DCM; (ii) Ac_2O , pyridine; NaOMe, MeOH (78%, 3 steps); (c) $\text{PhCH}(\text{OMe})_2$, CSA, ACN (75%); (d) LevOH, EDC.HCl, DMAP, DCM (92%); (e) DCM/TFA/ H_2O (75%); (f) (i) TEMPO, BAIB, DCM, H_2O ; (ii) MeOH, Amberlite IR-120 (H^+), 4 Å ms, microwave (76%, 2 steps).

Despite the fact that the synthesis of the known synthon **34** from the residue **30** in a four-step sequence (route A, Scheme 12) has previously been described by Tatai *et al.* (2008), the unsatisfactory results that were obtained with this method stimulated the investigation of a shorter and more efficient synthetic route (route B, Scheme 12). Unlike the process undertaken by Tatai and colleagues, **30** was directly treated with trimethyl(phenylthio)silane and zinc-iodide to afford the triol **34** as a mixture of anomers which were arduous to purify. In order to simplify the purification and isolation of the compounds, the peracetylation of the triols α -**34** and β -**34** was performed using acetic anhydride (Ac_2O) in dry pyridine. The peracetylated compound was obtained with a yield of 85% (2 steps, route B, anomers mixture) or with a yield of 55% (3 steps, route A, α -anomer only). The resulting peracetylated

anomers were directly deacetylated with sodium methoxide (NaOMe) in dry MeOH to afford **34**, after simple filtration (79% yield over 3 steps for route B). Finally, despite the inevitable and unwanted formation of the β -anomer obtained with route B, it appeared that the formation of the thioglycosyl intermediate through the ring-opening of the 1,6-anhydro compound **30** is more advantageous if the peracetylation is performed after the ring opening.



Scheme 12: Possible synthetic routes to prepare the building block 34.

4.3.2.3. Synthesis of the building block 11

The hydroxyl groups at position 4 and 6 of **34** were then selectively protected with a benzylidene group using benzaldehyde dimethyl acetal and a catalytic amount of (1S)-(+)-10-camphorsulphonic acid (CSA) in acetonitrile to furnish **35** with a yield of 75% as a mixture of anomers (α/β 3/1, determined by ¹H NMR). The anomers could be separated at this stage of the synthesis by flash chromatography. The levulinoylation of the remaining free hydroxyl group at position 2 of α -**35** was then carried out using standard conditions (levulinic acid/DMAP/EDC.HCl in DCM) to afford **36** with a 92% yield.

The cleavage of the benzylidene acetal was then first attempted using EtSH and a catalytic amount of $\text{BF}_3 \cdot \text{O}(\text{Et})_2$. The poor yield (35%) obtained prompted us to explore other approaches for the cleavage of the acetal. A combination of trifluoroacetic acid (TFA/DCM/ H_2O) was then tested at room temperature, increasing the yield of the reaction (51%). Another trial, with the same combination of reagents (TFA/DCM/ H_2O), but performed at 0 °C afforded **37** with a yield of 76%.

The chemo- and regio-selective oxidation of the hydroxyl group at position 6 of **37** into the corresponding carboxylic acid was performed as for the synthesis of **32** into **10**, using a combination of TEMPO/BAIB. The resulting carboxylic acid intermediate was then dried and involved in the esterification step without any further purification. As for the synthesis of the building block **10**, the Steglich esterification method (EDC.HCl/DMAP/dry MeOH) gave unsatisfactory results (35% yield). Based on the promising results obtained for the preparation of **10**, the esterification of the carboxylic acid intermediate was attempted using Amberlite IR-120 (H^+) in combination with freshly activated molecular sieves in the presence of dry MeOH (Table 5). Finally, the microwave-assisted esterification, performed as a single cycle of 1h30 at 95 °C afforded **11** (76% over two steps).

Entry	Reaction time	Mass ratio SM/Amberlite	Temp	Molecular sieves type	Yield (%)
1	1h30	2/1	100 °C	powder	20
2	1h30	2/1	90 °C	beads	60
3	1h30	2/1	95 °C	beads	76

Table 5: Reaction conditions and results for the preparation of the building block 11.

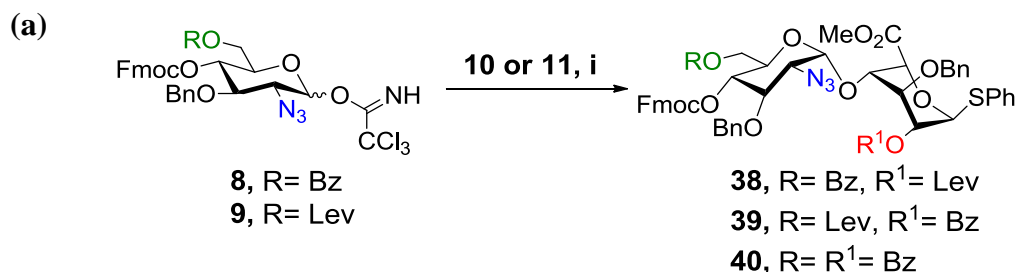
4.3.3. Elongation blocks synthesis: evaluation of the azidoglucose and iduronic acid building blocks in glycosylation reactions

The next step was the evaluation of the two L-iduronic acid building blocks **10** and **11** as glycosyl acceptors and the blocks **8-9** as glycosyl donors in glycosylation reactions to prepare the precursors **38-40**.

As described in Section 4.1.1.3, the reactions were always carried out in very dry conditions, as trichloroacetimidates are rapidly hydrolysed in moist and acidic environments and may even undergo rearrangement. The need to prevent these side reactions from occurring requires some precautions. Prior to use, all reagents and solvents needed to be perfectly dried. Glycosyl donors and acceptors are dried overnight under high vacuum conditions. The solvent is also dried over freshly activated molecular sieves and the reactions are performed in the presence of freshly activated molecular sieve powder. Moreover, the reactions can be performed in two ways: either the conventional (also called normal) procedure or the inverse procedure. The conventional procedure consists of adding the acid to a solution of donor and acceptor to initiate the reaction. The inverse procedure consists of a slow and dropwise addition of the donor to a mixed solution of acceptor and promoter. In difficult glycosylations (e.g. including acceptor of low reactivity), the inverse procedure offers slightly better results as the acceptor is present in large excess compared to the donor, at any given time point. However, the inverse procedure is not always required to carry out a glycosylation, as the side reactions (hydrolysis/rearrangement of the donor) are disadvantaged compared with the glycosylation reaction in most cases. To avoid loss of the base-labile Fmoc group, the reaction was quenched by the addition of water instead of a base such as triethylamine.

To evaluate the impact of different parameters on the reaction results, several tests were realised (replicates were carried out and are not listed here). As depicted in Figure 28 (b), this evaluation was mostly carried out whilst coupling the synthons **9** and **10**, which were the first two to become available. In total, eight sets of parameters were tested for the preparation of **39** (Figure 28 (b), entries 4-11). Thus, the influence of the donor/acceptor/acid ratio over the reaction yields was assessed,

as well as the type of acid used and the concentration at which the reaction was carried out. Moreover, the ideal temperature to perform the reaction is also of great importance and was then investigated, in order to favour glycosylation over the hydrolysis/rearrangement kinetics.



(b)

Entry	Donor	Equiv. of donor	Equiv. of activator	Temp	Solution Conc.	Procedure	Product	Yield (%)
1	8	1.5	0.1 ^b	-20 °C	0.1 M	normal	40	21
2	8	1.5	0.1 ^b	-20 °C	0.1 M	normal	38	32
3	8	1.5	0.1 ^b	-30 °C	0.1 M	normal	38	30
4	9	1.2	0.1 ^b	-20 °C	0.05 M	normal	39	24
5	9	1.5	0.1 ^b	-20 °C	0.05 M	normal	39	51
6	9	1.5	0.2 ^b	-20 °C	0.05 M	normal	39	43
7	9	1.5	0.1 ^b	-30 °C	0.05 M	normal	39	36
8	9	1.5	0.1 ^b	-30 °C	0.2 M	inverse	39	19
9	9	1.5	0.1 ^c	-30 °C	0.2 M	inverse	39	25
10	9	1.5	0.1 ^b	-50 °C	0.1 M	normal	39	32
11	9	1.5	0.1 ^b	-80 °C	0.1 M	normal	39	23

Figure 28: Evaluation of the building blocks 10 and 11 as glycosyl acceptor in glycosylation reactions.

(a) Synthesis of the disaccharide intermediates **38-40**. Reagents and conditions: (i) TMSOTf or TBSOTf, DCM, for yields, see table (b);

(b) Reaction conditions and results for the glycosylations of the glycosyl donors **8** and **9** with the glycosyl acceptors **10** and **11**.

^bTMSOTf; ^cTBSOTf.

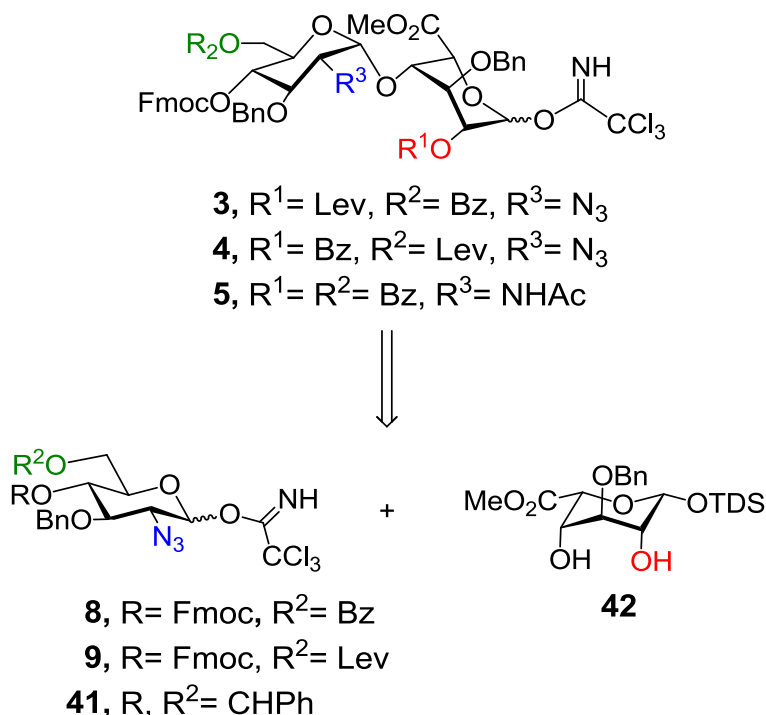
Based on the results that were obtained (Figure 28 (b)), the following conclusions could be drawn. First of all, and as expected, the 1,2-*trans* glycoside was virtually undetected (the nature of the new glycosidic linkage was determined by NMR, the value of the vicinal coupling constant $^3J_{H1,H2}=\pm 4\text{Hz}$ confirmed the formation of the α -anomer). Secondly, monitoring the reaction by UPLC/MS and by TLC also revealed that the glycosylation takes place as the reagents are mixed, as soon as the donor is activated by the acid. Thirdly, it appeared that a concentration of 1.5 equivalents of donor (entries 4 and 5), 0.1 equivalent of TMSOTf (entries 5 and 6), a temperature of -20 °C (entries 5 and 7) and a concentration of 0.05 M constituted the ideal set of parameters and afforded **39** in a yield of 51% (entry 5). The inverse procedure does not seem to afford better yields, even by lowering the temperature down to -50 °C or -80 °C. However, the results obtained with the replicates were not consistent (results not listed here) and the corresponding yields were varying from nearly 20% to around 40%, with a peak at 51%, which is rather low (entry 5). This inconsistency, which could be explained by a lack of control over some of the parameters impacting the glycosylation reaction, was also observed for the synthesis of the disaccharide building blocks **38** and **40**, which were also obtained in low yields (entries 1-3). Yet, these low yields were expected due to the lower reactivity of L-iduronic synthons, as the hydroxyl group at position 4 of the glycosyl acceptor is considerably reduced by the presence of the electron withdrawing carboxylate function at position 5.

Thus, despite the efforts put into finding the best conditions to obtain the elongation blocks **38-40** with satisfactory yields, the variability of the glycosylation reactions and the low reaction yields obtained, which were probably due to a mismatch of reactivity between the acceptor and donor, incited to bring some changes to the initial synthetic approach.

4.3.4. Elongation blocks synthesis: revision of the initial strategy

With the rather unsatisfactory results obtained for the synthesis of **38-40** in hand, some changes needed to be brought to the original synthetic route in order to circumvent the mismatch of reactivity between the glycosylating agents. For this

reason, new monomeric building blocks to synthesise **3-5** needed to be designed (Scheme 13).



Scheme 13: Retrosynthesis of the new elongation blocks – Monomeric building block structures.

The preparation of the known synthons **41** and **42** was hence undertaken. The glycosyl acceptor **42** has already been prepared by Ojeda *et al.* (1999) and **41** had been prepared for the first time by La Ferla *et al.* (1999). The coupling efficacy of these compounds has also been already evaluated by de De Paz *et al.* (2003) and was rather satisfactory (62% yield). They showed that the C-4-directed glycosylation of these two compounds is favoured over the C-2-directed glycosylation, probably due to the high steric hindrance of the C-2 position, caused by the presence of the dimethylthexylsilyl (TDS) installed at the anomeric centre of **42** (desired 4-*O*-glycosylated product: 62%, recovered acceptor: 35%, by-products (including 2-*O*-glycosylated disaccharide): 3%).

The coupling of **42** with **8** and **9** was also evaluated to take advantage of the already existing compounds and to determine whether these could be of any use for the synthesis of the disaccharide building blocks. However, the glycosyl donor **41** was

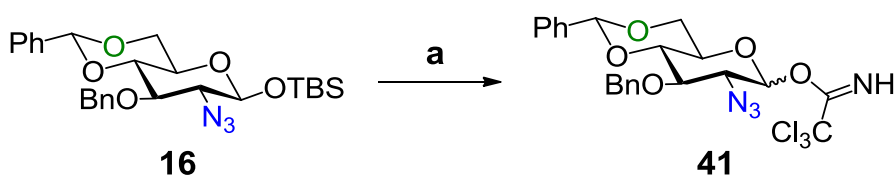
prepared as well, on the assumption that a mismatch of reactivity could be detected whilst using **8** and **9** as glycosyl donors.

At this stage, it is important to note that the preparation of the known building blocks **41** and **42** would not offer the possibility of developing a new synthetic methodology for the synthesis of HS and heparin oligosaccharides. Nevertheless, the relatively short synthetic routes to prepare these compounds are already known and tested, allowing for a significant gain of time.

4.3.5. New azidoglucose building block synthesis

The choice of using **41** as the new glycosyl donor for the synthesis of the disaccharide building blocks was motivated by the fact that this new compound shares a couple of intermediates with the ones that were previously prepared (**8** and **9**), which is undoubtedly a considerable advantage.

Like the donors **8** and **9**, the synthesis of **41** started with the preparation of **16** from the commercially available 2-amino-2-deoxy-D-glucose hydrochloride **12** as described in detail in Section 4.3.1. The final compound **41** was obtained in a two-step sequence from **16** by conventional desilylation followed by the anomeric activation of the resulting intermediate using trichloroacetonitrile in the presence of 1,8-Diazabicyclo[5.4.0]undec-7-ene (DBU) as described by De Paz *et al.* (2003) (Scheme 14).

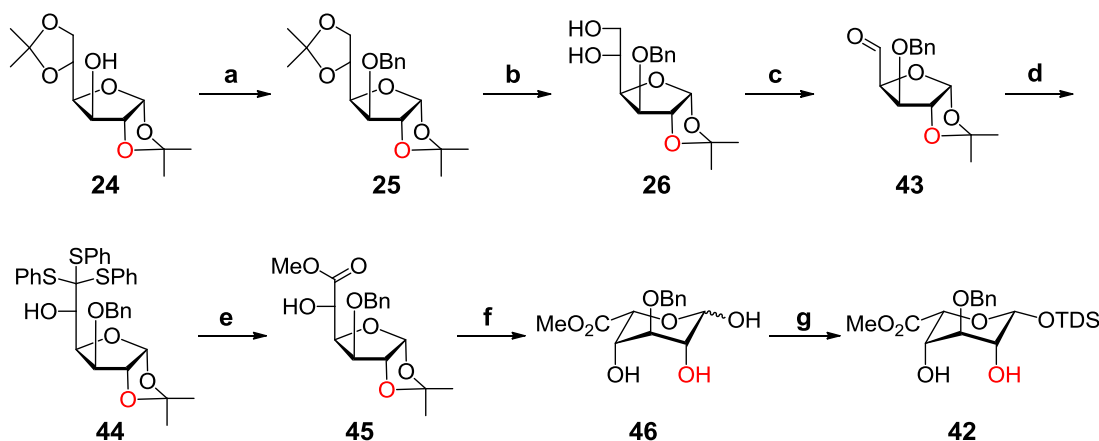


Scheme 14: Preparation of the new glycosyl donor 41.

Reagents and conditions: (a) (i) TBAF, AcOH, THF; (ii) Cl_3CCN , DBU, DCM (85%, 2 steps).

4.3.6. New L-iduronic acid building block synthesis

The synthesis of the new glycosyl acceptor **42** was performed as described by Lohman *et al.* (2003) and Ojeda *et al.* (1999) and was obtained in a seven-steps sequence from commercially available diacetone-D-glucose **24** (Scheme 15).



Scheme 15: Preparation of the new glycosyl acceptor 42.

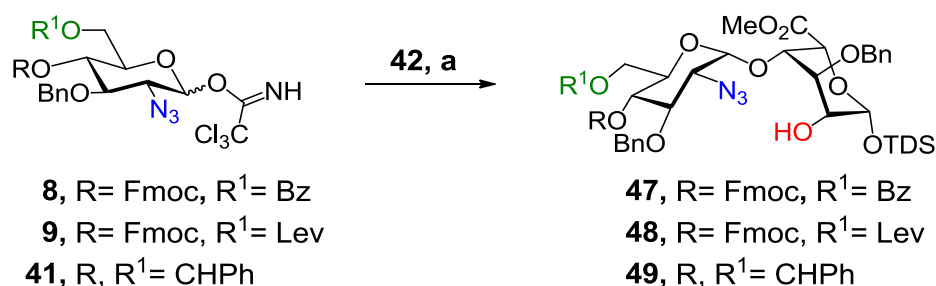
Reagents and conditions: (a) BnBr, NaH, cat. TBAI, DMF; (b) AcOH (66%), H₂O (90%, 2 steps); (c) NaIO₄, silica gel, H₂O, DCM; (d) (PhS)₃CLi, THF; (e) (i) CuCl₂, CuO, MeOH, H₂O, DCM; (ii) K₂CO₃, MeOH (83%, 4 steps); (f) TFA (90%), H₂O (72%); (g) TDSCl, imidazole, DCM (65%).

As for the synthesis of **10** and **11**, the first step consists in the benzylation of the only free hydroxyl group of **24**. Selective acetal cleavage afforded the diol intermediate **26** that was then subsequently treated with an aqueous solution of sodium periodate adsorbed onto silica to afford the corresponding aldehyde **43** (Lohman *et al.* 2003). The latter was then treated with trithiophenylmethyl lithium and exclusively afforded the L-idose-configured thioortho ester intermediate **44** (no D-glucose product was detected unlike with other methods involving the use of organometallic reagents (Lubineau *et al.* 2000)). The freshly obtained thioortho ester was then directly treated with CuCl₂/CuO to obtain the desired furano methyl ester derivative **45** along with a relatively small amount of the phenylthioester by-product that was converted into the desired intermediate by treatment with K₂CO₃ in methanol. The cleavage of the isopropylidene acetal was achieved using a 90% TFA solution (v/v) and led to the 3-*O*-benzyl L-iduronic methyl ester residue **46** in its pyranose form (the ¹C₄ conformation was confirmed by [NMR](#)). Regio- and stereo- selective silylation of the

anomeric position with dimethylthexylsilyl chloride was carried out in order to exclusively obtain the final compound **42**.

4.3.7. Elongation blocks synthesis: evaluation of the new azidoglucose and L-iduronic acid building blocks

With all the glycosyl donors (**8**, **9** and **41**) and acceptor (**42**) in hand, the preparation of the dimeric building blocks **47-49** was undertaken (Scheme 16).



Scheme 16: Assembly of the disaccharides 47-49.

Reagents and conditions: (a) TMSOTf or TBSOTf, DCM, for yields see Table 6.

A significant number of trials were carried out in this case, in order to determine the best conditions to perform the glycosylation reactions. Trials involving the donor **41** to form the disaccharide **49** gave similar results to the ones obtained by De Paz *et al.* (2003) (Table 6, entries 6-9). As described in their work, the formation of the 2-*O*-glycosylated disaccharide was also observed, as well as the formation of the trisaccharide, but with moderate ratios (determined by LC-MS analysis, results not shown here). Further trials were carried out with the glycosyl donors **8** (affording **47**) and **9** (affording **48**) in order to compare the reactivity of the three donors.

Based on the results obtained (Table 6), a number of conclusions could be drawn. As expected, the dropwise addition of the donor to a solution of acceptor and acid afforded higher yields. Secondly, it appears that the coupling efficacy of **42** is undoubtedly higher than those of **10** and **11**, as the yields obtained when using **42** as the glycosyl acceptor are relatively higher, with a peak at 65% (entry 3). Thirdly, two different catalysts were tested (TMSOTf and TBSOTf) at different concentrations, as well as different reaction temperatures. From the yields obtained, it appears that the

conditions determined by De Paz and colleagues were the most appropriate ones for the glycosyl donors **9** and **41**. However, using TBSOTf as an activator significantly increased the yield of the assembly of the donor **8** and the acceptor **42** (entry 3). As already described by De Paz and hence, as expected, the formation of the 2-*O*-glycosylated disaccharide and the trisaccharide were also observed (LC-MS analysis, not shown here). However, they were not isolated as their ratios were mainly negligible compared to the conversion rate of the desired product. The most appreciated aspect of using **42** over **10** and **11** is the constancy and the reproducibility of the results (replicates not listed here).

Entry	Donor	Equiv. of donor	Equiv. of activator	Temp	Solution Conc.	Procedure	Product	Yield (%)
1	8	0.6	0.2 ^a	0 °C	0.03 M	inverse	47	15 ^c
2	8	0.6	0.2 ^a	-20 °C	0.03 M	inverse	47	40 ^c
3	8	0.6	0.2 ^b	0 °C	0.03 M	inverse	47	65 ^c
4	9	0.6	0.1 ^a	0 °C	0.03 M	normal	48	39
5	9	0.6	0.2 ^a	0 °C	0.03 M	inverse	48	45
6	41	0.6	0.2 ^a	0 °C	0.03 M	inverse	49	59
7	41	0.6	0.1 ^b	0 °C	0.03 M	inverse	49	47
8	41	0.6	0.1 ^a	-10 °C	0.03 M	inverse	49	36
9	41	0.6	0.2 ^a	-10 °C	0.03 M	normal	49	32

Table 6: Reaction conditions and results for the assemblies of the glycosyl donors **8, **9** and **41** with the glycosyl donor **42**.**

^aTMSOTf; ^bTBSOTf; ^cconversion determined by LC-MS data analysis.

Finally, choosing the new disaccharide **49** over the disaccharides **47** and **48** as the precursor for the synthesis of the elongation blocks appeared to be more judicious for many reasons. Using an excess of glycosyl acceptor instead of glycosyl donor is quite advantageous and valuable. The acceptor may indeed be recovered and used directly after purification, unlike the donor which will need to be reactivated in case of hydrolysis. It might also have undergone rearrangement which makes it unsuitable

for another glycosylation reaction. In addition, despite the promising results obtained during the coupling of **8** and **42** (65% yield), such good results could not be produced by coupling of **9** and **42** (45% yield). Coupling **8** and **9** with **42** also implied the post-glycosylation installation of a levulinoyl/benzoyl group at position 2 of **47** and **48**. Owing to the presence of the Fmoc group, these esterification reactions might be quite problematic, or even impossible, to perform, as they require the use of strong base.

4.3.8. Conclusions

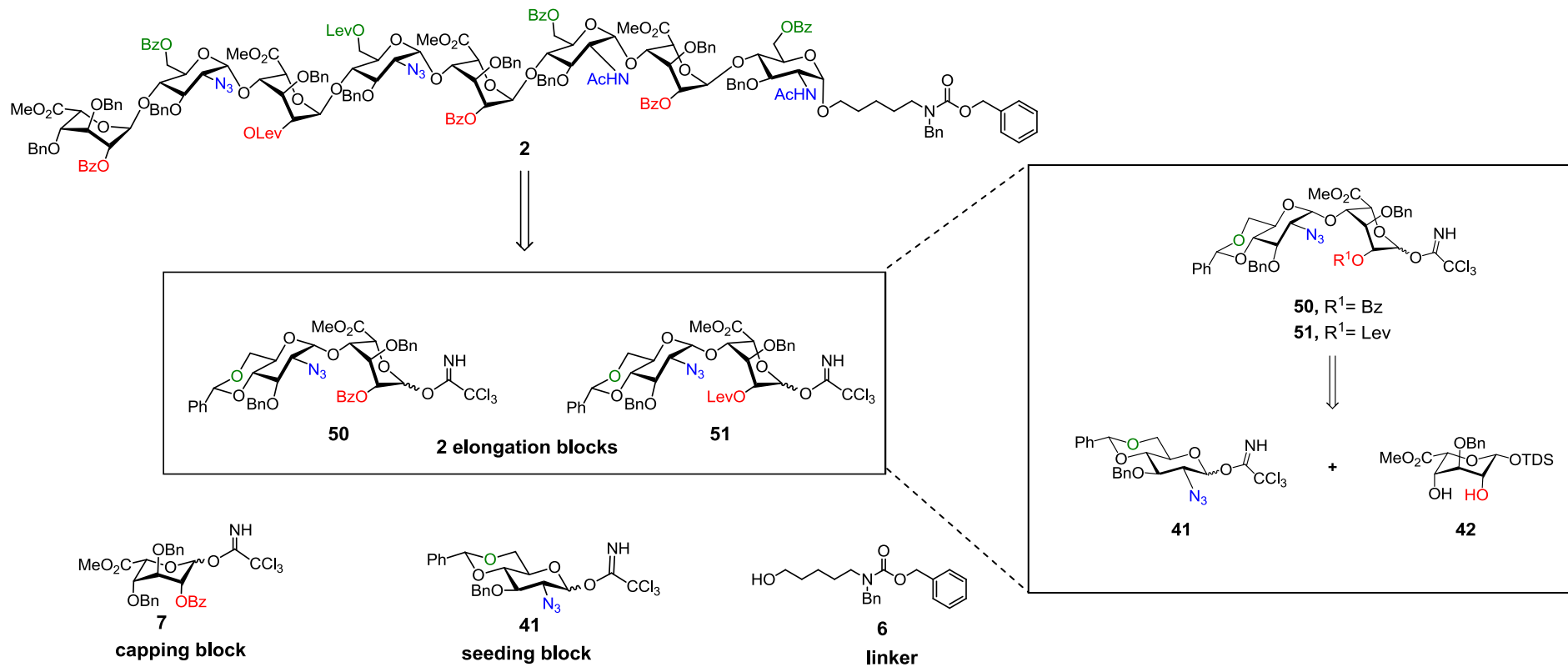
One of the main objectives of the present project was the development of a new synthetic route and the synthesis of new glycosyl synthons which would ultimately help to generate Hp/HS oligosaccharide libraries quickly. The syntheses of the new monomeric building blocks (**8-11**) were successfully carried out with satisfactory yields for every PG manipulation step. Their respective coupling efficacies were next evaluated in glycosylation reactions. As expected, the trichloroacetimidate synthons **8** and **9** proved to be very reactive and good glycosyl donors. Even though they underwent rearrangement (to afford the corresponding trichloroacetamide residues) or were hydrolysed, the detected by-products/product ratios were satisfactory and similar to the ones already reported in the literature. However, the L-iduronic acid synthons **10** and **11** turned out to be poor glycosyl acceptors, resulting in non-reproducible and low- to moderate-yield glycosylation reactions, which was also expected. The mismatch of reactivity between the glycosylating agents compelled us to modify the original strategy. Two reported monomeric glycosyl donor and acceptor (respectively **41** (De Paz *et al.* 2003) and **42** (Ojeda *et al.* 1999)) were prepared and the assemblies of **8** and **9** with **42** were also evaluated. The glycosylation results obtained and the post-glycosylation transformations that would have been required if working with **8** and **9** invited a review of the whole synthetic strategy. It was hence decided to exclusively assemble **41** and **42** to form the precursors of the desired disaccharide elongation blocks.

4.4. New synthetic approach: synthesis of the new elongation blocks

The decision to use different monosaccharide building blocks than the ones initially designed to prepare the elongation blocks naturally led us to rethink the scaffolds of the majority of the building blocks. As depicted in Scheme 17, the new retrosynthetic analysis of **2** provided a total of five building blocks that would be needed to complete the synthesis of the oligosaccharide target. Interestingly, the linker and capping blocks remained unchanged. Moreover, the preparation of only two new elongation blocks **50** and **51** was required – elongation blocks that would necessitate the synthesis of the two known monomeric building blocks **41** and **42**. Finally, the new seeding block and the glycosyl donor **41** appeared to be the same molecule, thereby decreasing the number of distinct compounds required. In total, a limited number of seven glycosylating agents would be necessary to bring the synthesis of the target to completion.

Unlike the previous approach, the backbone of the oligosaccharide target would need to undergo many modifications between two elongation steps: if required, the reduction of the azido groups and the acetylation of the amines newly formed; the cleavage of the benzylidene acetal moiety and the installation of the appropriate PG at the position 6 of the glucosamine/azidoglucose moiety at the non-reducing end.

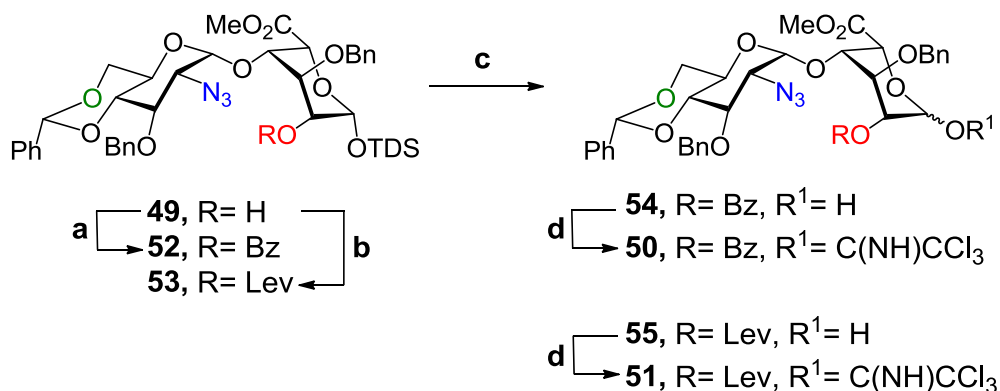
With the design of the new building blocks in hand, their syntheses were undertaken.



Scheme 17: Retrosynthetic analysis of the new building blocks.

4.5. New elongation blocks synthesis

The preparation of the new elongation blocks started with the preparation of the precursor **49**, as described in Section 4.3.7. The intermediate **49** was then differentiated at this stage of the synthesis (Scheme 18).



Scheme 18: Synthesis of the elongation blocks 50 and 51.

Reagents and conditions: (a) BzCl, pyridine (95%); (b) LevOH, EDC.HCl, cat. DMAP, DCM (83%); (c) HF.pyr, THF (80%); (d) Cl₃CCN, K₂CO₃, DCM (75%).

The disaccharide **49** was converted into **50** in a three-step sequence as described by Lucas *et al.* (2003). The installation of the benzoyl group at position 2 of the L-iduronic residue with benzoyl chloride (BzCl) in pyridine (affording **52**) was followed by the desilylation of the anomeric centre with an excess of HF.pyridine in THF (affording **54**). Finally, the activation of the anomeric centre was performed with trichloroacetonitrile and activated K₂CO₃ to afford **50**.

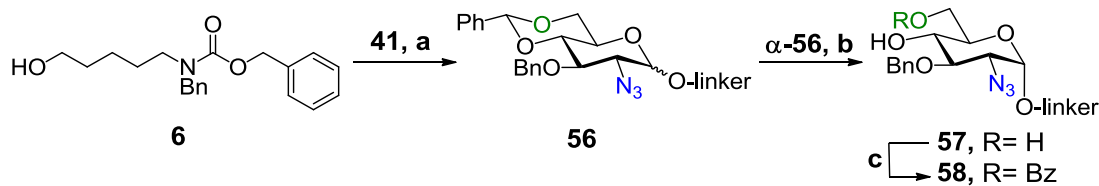
The disaccharide **49** was also converted into **51** in a three-step sequence as described by De Paz and Martín-Lomas (2005). The conventional 2-*O*-levulinoylation was first performed (affording **53**), followed by the cleavage of the silyl group at the anomeric position with HF.pyridine (affording **55**) and the anomeric activation with trichloroacetonitrile and K₂CO₃ to afford **51**.

4.6. Towards the synthesis of the first target

With the elongation and seeding blocks **41**, **50** and **51** in hand, the synthesis of the target **2** was then initiated. The first step consisted of the derivatisation of the seeding block **41** with the linker **6**, followed by the elongation of the backbone to form the corresponding oligosaccharide intermediates (trisaccharide, pentasaccharide and so on).

4.6.1. Seeding block synthesis

The linker *N*-(benzyl)-benzyloxycarbonyl-5-aminopentan-1-ol **6** was prepared from commercially available 5-amino-pentan-1-ol (Delcros *et al.* 2002, Noti *et al.* 2006). The preparation of the final seeding block **58** was performed in a three-step sequence (Scheme 19). The intermediates **56** and **57** had been previously reported by Arungundram *et al.* (2009), but here an alternative route to obtain these compounds is reported.



Scheme 19: Synthesis of seeding block 58.

Reagents and conditions: (a) TMSOTf, Et_2O (72%); (b) EtSH, $\text{BF}_3 \cdot \text{O}(\text{Et})_2$, DCM (92%); (c) BzCN, Et_3N , ACN (89%). Linker = $(\text{CH}_2)_5\text{N}(\text{Bn})\text{CBz}$.

The derivatisation of **41** was first realised with **6** in a glycosylation reaction with a catalytic amount of TMSOTf in dry diethyl ether Et_2O and afforded **56** as a mixture of anomers (α/β 2/1, determined by $^1\text{H NMR}$) in 72% yield. Both anomers α -**56** and β -**56** were obtained despite the non-participating effect of the azido group at position 2 of **41** - which should have favoured the formation of the α -directed compound only, as explained in Section 4.2.2. However, both compounds can be separated by flash chromatography. Moreover, the choice of the solvent appeared to be of great importance. On the one hand, performing such glycosylation reactions with similar glycosyl donors (not listed here) in DCM indeed leads to more substantial formation of the β -anomer (nearly α/β 1/2 in some cases). On the other hand, performing the

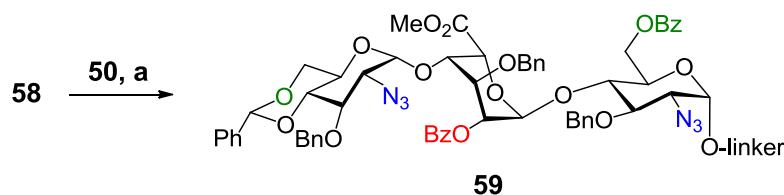
reaction in Et₂O afforded **56** as a mixture of anomers, with a ratio of α/β 2/1. This is explained by the fact that non-polar ethereal solvents, such as Et₂O, participate in the reaction, preferably form the equatorial intermediate (Nigudkar and Demchenko 2015) and, therefore, promote the formation of α -linkages, as explained in Section 4.1.1.2.

The cleavage of the benzylidene acetal of α -**56** was then carried out with EtSH in presence of BF₃.O(Et)₂ and gave **57** with a yield of 92%. The resulting diol finally underwent regioselective benzylation using BzCN and a catalytic amount of triethylamine in dry acetonitrile to afford the final compound **58** in 89% yield.

4.6.2. Trisaccharide precursor synthesis

With the seeding-linker building block **58** and the elongation blocks **50** and **51** in hand, the next step consisted in a first cycle of elongation of the backbone which afforded the first trisaccharide precursor. The latter was then modified in order to transform it into the glycosyl acceptor for the next elongation step.

The trisaccharide precursor **59** was prepared by coupling the linker-derivatised seeding block **58** and the 2-*O*-benzoylated elongation block **50** in the presence of TMSOTf and molecular sieves in dry DCM (Scheme 20) and was obtained with 95% yield. As expected, the formation of the 1,2-*trans* product only was observed (coupling constant: $^1J_{C1,H1}=171\text{Hz}$ (Bock and Pedersen 1974)), due to the neighbouring group participation of the Bz group of the L-iduronic acid residue.



Scheme 20: Synthesis of trisaccharide precursor 59.

Reagents and conditions: (a) TMSOTf, DCM (95%).

Linker = (CH₂)₅N(Bn)CBz.

Prior to the benzylidene acetal cleavage that will make the desired hydroxyl group at position 4 accessible for further glycosylation, the transformation of the azido groups into the corresponding acetamido groups was performed. The transformation had to be performed at such an early stage of the process to permit the simultaneous presence of differently protected amino moieties on the target molecule **2**.

4.6.2.1. Synthesis of the intermediate 60: preliminary results

The direct transformation of the two azido groups of the azidoglucose residues into acetamido groups was attempted, using thioacetic acid AcSH, as first reported by Rosen *et al.* (1988). Several trials were carried out to determine the best conditions to perform the transformation of the diazido trisaccharide **59** into the diacetamido intermediate **60**.

For the first trial, thioacetic acid (100 equivalents) was added to a solution of **59** in dry pyridine under argon (Kuduk *et al.* 1998). After 24 hours of stirring at room temperature, LC-MS analysis of an aliquot of the reaction indicated that the reaction was taking place, but was sluggish and showed low conversion. Significant amounts of starting material **59** (around 70%) and intermediate compounds **60a** (around 25%) were still detected (the intermediates were not isolated). Even after running the reaction for another 48 hours at 50 °C, only around 50% of the SM was converted. Both mono-acetylated intermediates accounted, for their part, for around 40% of the total of the carbohydrate mass. The addition of another 100 equivalents of thioacetic acid and stirring the reaction for 3 hours at 80 °C remarkably shifted the ratio between compounds (SM: around 20%, intermediates: around 50%, product: around 30%), but completion of the reaction could still not be attained (Figure 29). It was then decided to perform another trial directly using thioacetic acid as both solvent and reagent.

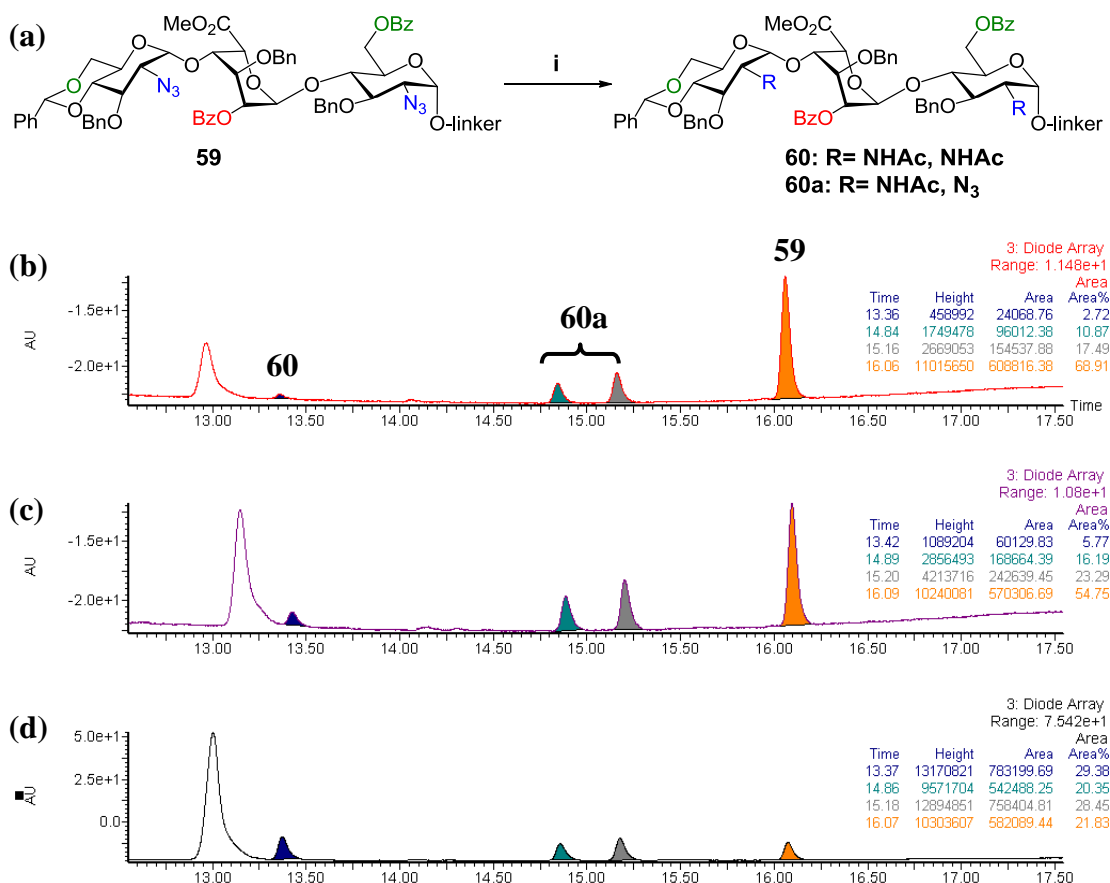


Figure 29: Analysis of the evolution of the direct transformation of the azido groups of **59 into acetamido groups using thioacetic acid in pyridine.**

(a) Direct synthesis of trisaccharide precursor **60** using thioacetic acid in pyridine and possible structures of the mono-acetylated intermediates **60a**. Reagents and conditions: (i) AcSH, pyridine.

Linker = (CH₂)₅N(Bn)CBz;

(b) LC-MS data for the conversion of **59** into **60** after 24 hours stirring at R.T. Retention time: 13.4 min (calcd for C₈₅H₉₁N₃O₂₁: 1489.6 [M], found *m/z* 1490.3 [M+H]⁺, 1512.3 [M+Na]⁺): product **60**; retention times: 14.8 min and 15.2 min (calcd for C₈₃H₈₇N₅O₂₀: 1473.6 [M], found *m/z* 1474.3 [M+H]⁺, 1496.3 [M+Na]⁺: intermediates **60a**; retention time: 16.1 min (calcd for C₈₁H₈₃N₇O₁₉: 1457.6 [M], found *m/z* 1475.3 [M+NH₄]⁺, 1480.3 [M+Na]⁺: starting material **59**;

(c) LC-MS data for the conversion of **59** into **60** after 48 hours stirring at 50 °C;

(d) LC-MS data for the conversion of **59** into **60** after 3 hours stirring at 80 °C.

For the second trial, the starting material **59** was dissolved in pure thioacetic acid and the solution was stirred at room temperature under argon (Schwarz *et al.* 1999). After 72 hours, TLC and LC-MS analyses revealed that the SM had been completely consumed. However, an important formation (around 30%) of the undesired by-products **60b** was then detected as well (Figure 30, (b)) (the by-products were not

isolated). No loss of the benzylidene acetal group was detected, despite the acidity of the reaction mixture.

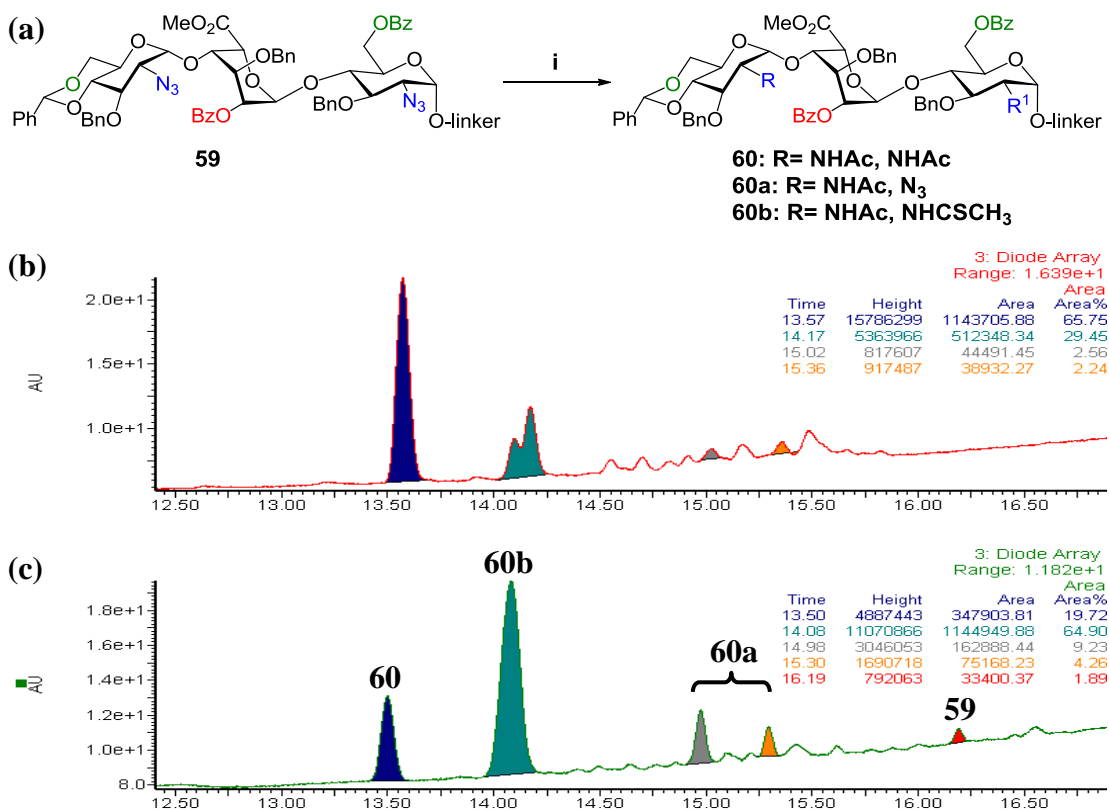


Figure 30: Analysis of the evolution of the direct transformation of the azido groups of **59 into acetamido groups using pure thioacetic acid.**

(a) Direct synthesis of trisaccharide precursor **60** using pure thioacetic acid and possible structures of the intermediates/by-products **60a**/**60b**. Reagents and conditions: (i) AcSH.

Linker = $(CH_2)_5N(Bn)CBz$;

(b) LC-MS data for the conversion of **59** into **60** after 72 hours stirring at R.T. Retention time: 13.5 min (calcd for $C_{85}H_{91}N_3O_{21}$: 1489.6 [M], found m/z 745.6 $[M+2H]^{2+}$, 756.6 $[M+H+Na]^{2+}$, 767.6 $[M+2Na]^{2+}$): product **60**; retention time: 14.1 min (calcd for : 1505.6 [M], found m/z 753.6 $[M+2H]^{2+}$, 764.6 $[M+H+Na]^{2+}$, 775.6 $[M+2Na]^{2+}$): by-products **60b**; retention times: 15.0 min and 15.3 min (calcd for $C_{83}H_{87}N_5O_{20}$: 1473.6 [M], found m/z 737.6 $[M+2H]^{2+}$, 748.6 $[M+H+Na]^{2+}$, 759.6 $[M+2Na]^{2+}$): intermediates **60a**; retention time: 16.2 min (calcd for $C_{81}H_{83}N_7O_{19}$: 1457.6 [M], found m/z 729.6 $[M+2H]^{2+}$, 740.6 $[M+H+Na]^{2+}$, 751.6 $[M+2Na]^{2+}$): starting material **59**;

(c) LC-MS data for the conversion of **59** into **60** after 30 min irradiation in a microwave oven at 90 °C.

Linker = $(CH_2)_5N(Bn)CBz$.

The irradiation of a solution of **59** in pure thioacetic acid for 30 min at 90 °C under inert atmosphere with microwave oven also led to the significant formation of these by-products (Figure 30 (c)) as they represented about 65% of the total of the

carbohydrates. Thus, using pure thioacetic acid appears to promote the transformation of the azido moieties, yet the absence of a base appears to lead to the formation of the thioamide by-products. Mühlberg *et al.* (2014) proposed that, in the absence of a base (low pH), the C=O tautomer of the thioacetic acid would be favoured over the C=S tautomer. The concerted cyclisation would therefore lead to the formation of the oxatriazolidine intermediate, which would ultimately deliver the corresponding thioamide.

A last test was performed, using the conditions described by Williams and colleagues (Shangguan *et al.* 2003). In this case, the base 2,6-lutidine was added to a solution of starting material **59** in chloroform in order to prevent the formation of the by-products (with a equivalent/equivalent ratio AcSH/2,6-lutidine of 1/1). The solution was irradiated in a microwave oven for 8 cycles of 1 hour, at 60 °C and under inert atmosphere. However, TLC monitoring of the reaction progress showed that the SM had not been completely consumed after 8 hours of irradiation.

Entry	Total reaction time	Conditions	Temp	Compound distribution ^b			
				SM 59 (%)	Int 60a (%)	P 60 (%)	BPs 60b (%)
1	73 h	AcSH/pyridine	R.T.to 80 °C	20	50	30	0
2	72 h	AcSH	R.T.	0	5	65	30
3	30 min	AcSH ^a	90 °C	2	13	20	65
4	8 h	AcSH/2,6-lutidine CH ₃ Cl ^a	60 °C	N.D.	N.D.	N.D.	N.D.

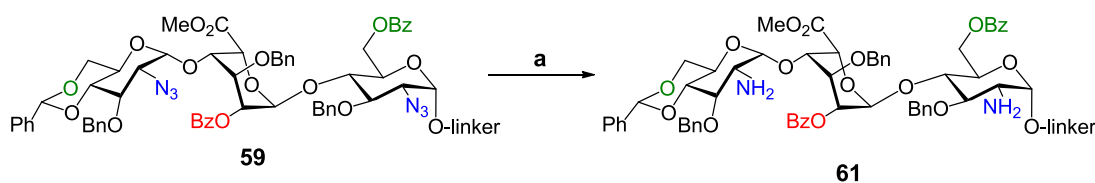
Table 7: Reagents, conditions and results for the direct synthesis of **60 using thioacetic acid.**

^amicrowave-assisted synthesis; ^bdetermined by LC-MS data analysis; SM: starting material; Int: intermediates; P: product; BPs: by-products; N.D.: no data.

The poor results obtained with this direct method (Table 7) motivated the evaluation of other methods for the transformation of the azido groups. Other methods are used widely, but require the reduction of the azides, followed by acetylation of the resulting primary amines.

4.6.2.2. Synthesis of the intermediate **61**

As no direct synthesis of the diacetylated intermediate **60** could be performed, the reduction of the azido groups into primary amines and which would lead to the formation of the diamino intermediate **61** was hence attempted (Scheme 21). The common method for the reduction of such moieties implies the use of trisubstituted phosphines, such as triphenylphosphine PPh_3 or even trimethylphosphine PMe_3 (Staudinger reaction) (Wuts and Greene 2006).



Scheme 21: Synthesis of trisaccharide **61**.

Reagents and conditions: (a) PMe_3 , NaOH , THF, H_2O (quant.).

Linker = $(\text{CH}_2)_5\text{N}(\text{Bn})\text{CBz}$.

The reduction of the azido moieties was first attempted with an excess of triphenylphosphine PPh_3 (3 equivalents per azido group) in a mixture of THF/ H_2O . The reaction was stirred at room temperature for 12 hours. Small aliquots were taken at regular intervals and analysed by MALDI-TOF mass spectrometry to monitor the progress of the reaction. The analyses revealed that the SM was completely consumed after 1 hour of stirring (Figure 31), but no product could be detected at any time point. As expected, the formation of the ions, resulting from the expulsion of N_2 due to the fragmentation of the azido moieties, was detected (Li *et al.* 2010). The MALDI-TOF mass spectra showed the formation of the very stable transient entities iminophosphoranes **61a** and **61b** (Figure 31 (c)). The loss of a benzoyl group was systematically detected for every iminophosphorane intermediate as well (by-products **61c** and **61d**), due to the basicity of the reaction (Figure 31 (c)). Neither the transient entities nor the by-products were isolated.

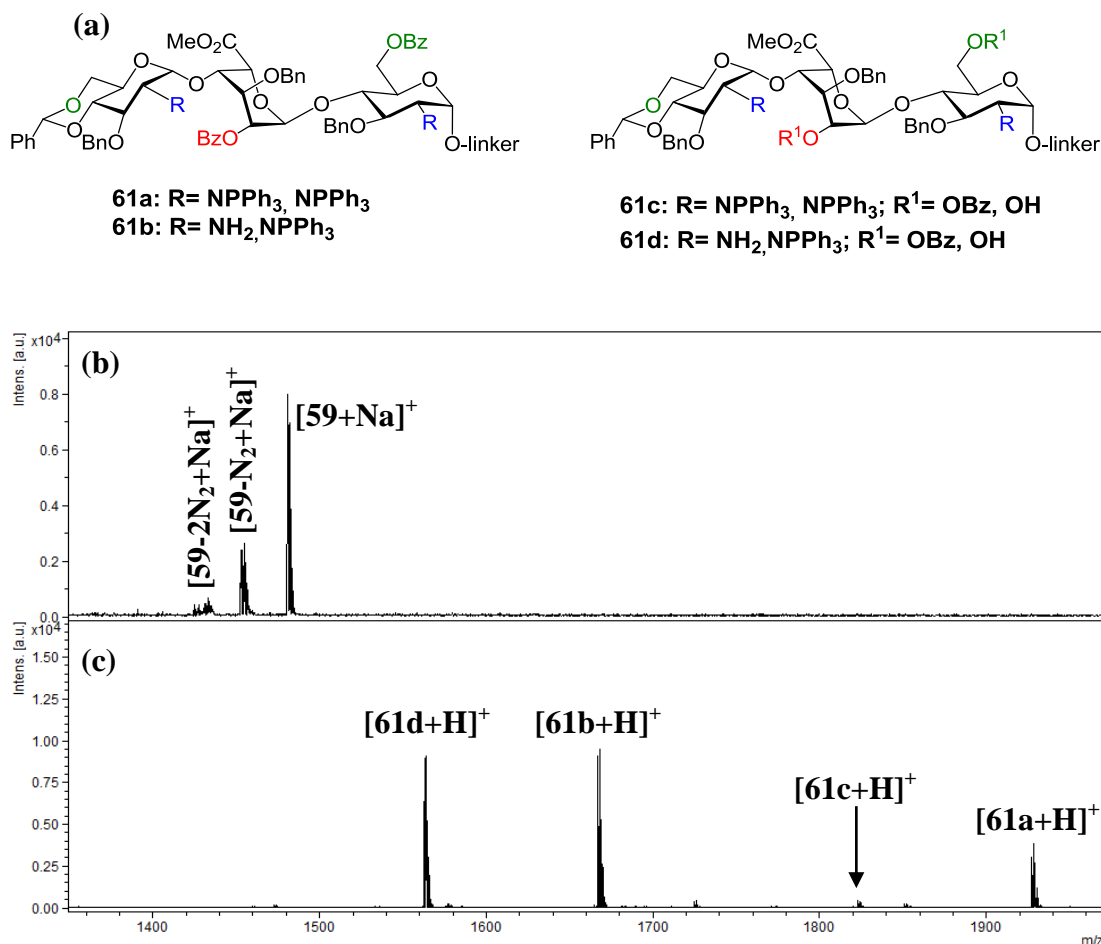


Figure 31: Analysis of the reduction of the azido groups using PPh_3 .

(a) Possible structures of the main transient entities **61a** and **61b** and of the by-products **61c** and **61d** detected by MALDI-TOF analysis.

Linker = $(\text{CH}_2)_5\text{N}(\text{Bn})\text{CBz}$;

(b) MALDI-TOF mass spectrum of the starting material **59**. Calcd for $\text{C}_{81}\text{H}_{83}\text{N}_7\text{O}_{19}$: 1458.6 [M], found m/z 1481.0 $[\text{M} + \text{Na}]^+$, 1453.0 $[\text{M} - \text{N}_2 + \text{Na}]^+$, 1425.0 $[\text{M} - 2\text{N}_2 + \text{Na}]^+$;

(c) MALDI-TOF mass spectrum of the reaction crude after 12 hours stirring at R.T. Calcd for $\text{C}_{117}\text{H}_{113}\text{N}_3\text{O}_{19}\text{P}_2$: 1925.7 [M], found m/z 1927.2 $[\text{M} + \text{H}]^+$: intermediate **61a**; calcd for $\text{C}_{110}\text{H}_{109}\text{N}_3\text{O}_{18}\text{P}_2$: 1821.7 [M], found 1823.2 $[\text{M} + \text{H}]^+$: by-product **61c**; calcd for $\text{C}_{99}\text{H}_{100}\text{N}_3\text{O}_{19}\text{P}$: 1665.7 [M], found m/z 1667.1 $[\text{M} + \text{H}]^+$: intermediate **61b**; calcd for $\text{C}_{92}\text{H}_{96}\text{N}_3\text{O}_{18}\text{P}$: 1561.6 [M], found m/z 1563.0 $[\text{M} + \text{H}]^+$: by-product **61d**.

To circumvent the loss of any benzoyl group, the reduction of the azido groups was then attempted using resin-bound phosphine. Using such resin-bound reagents appears to be quite advantageous, because the purification of the product will be facilitated. A simple wash of the resin and filtration work-up should then be enough to isolate the product.

A first trial was realised in a mixture of THF/H₂O using 1.1 equivalents of a resin of polystyrene-triphenylphosphine (PS-PPh₃, 2.14 mmol/g) per azido group. The solution was stirred at room temperature for 6 hours and monitored by TLC and MALDI-TOF analysis. Aliquots were analysed every hour to control the adsorption of the SM onto the resin. However, no clear evolution was detected over the 6 hours of stirring as TLC and MALDI-TOF qualitative analyses both clearly showed the substantial presence of the SM in the supernatant at every time point. In addition, the product was virtually undetectable.

A second test was performed using 5 equivalents PS-PPh₃ (2.14 mmol/g) per azido group at room temperature. Unlike for the first trial, both the consumption of the SM and the formation of the product were detected. However, after 6 hours of stirring at normal temperature and pressure conditions, the SM had not been fully adsorbed onto the resin. To determine whether increasing the temperature of the reaction would influence the kinetics of the reaction, the reaction mixture was transferred into a microwave vial and irradiated at 40 °C for 30 min. Qualitative analysis of the supernatant by MALDI-TOF mass spectrometry hence clearly showed the complete adsorption of the SM onto the resin after irradiation. The product was isolated after filtration with a yield of 30%. The results obtained (poor yield and no detection of **59** in the supernatant) clearly indicated that the SM was indeed adsorbed on the resin to form the stable resin-bound iminophosphorane transient entities, but the latter were not cleaved off the resin.

Microwave-assisted synthesis of the diamino intermediate **61** was then attempted, using 5 equivalents of PS-PPh₃ (2.14 mmol/g) per azido group. A solution of **59** and PS-PPh₃ in THF/H₂O in a microwave vial equipped with a stirring bar was irradiated in a microwave oven for cycles of 1 hour at 50 °C. After a total of 3 cycles, MALDI-TOF analysis showed the complete consumption of the SM. However, the product was virtually undetected by LC-MS analysis (Figure 32, (a)). The solution mixture was then irradiated for another cycle of 30 min at 100 °C and analysed by LC-MS. As depicted in Figure 32 (b), the cleavage of the sugar from the resin was performed. The product was isolated and analysed by ¹H NMR, which revealed an important contamination of the sugar sample by aliphatic residues (results not shown here).

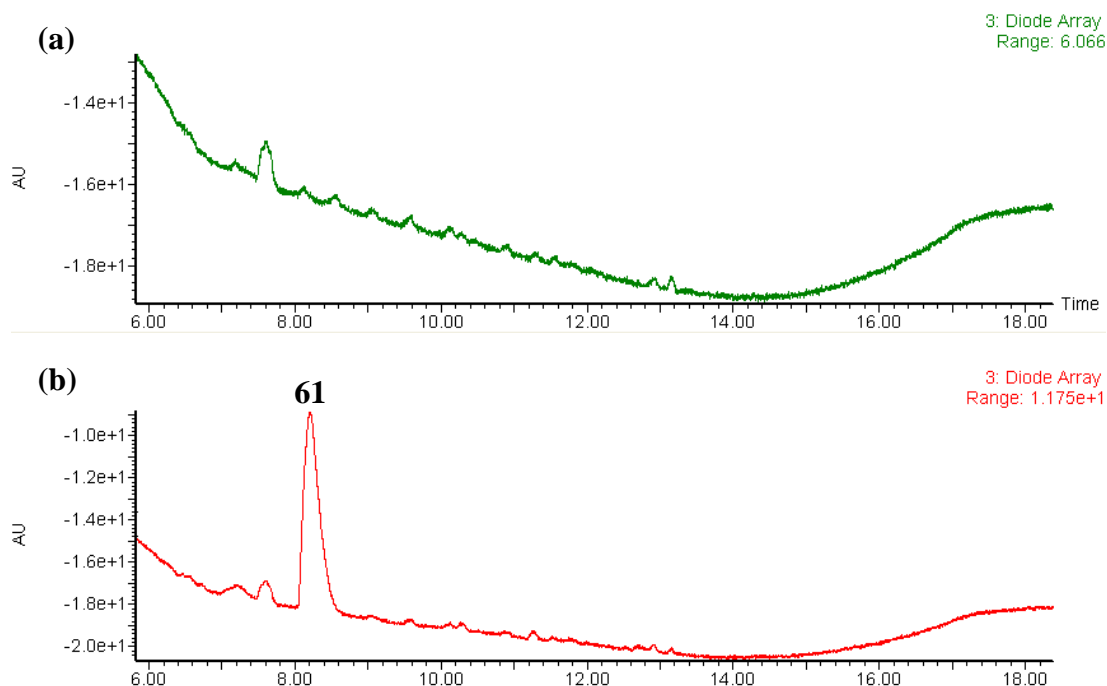


Figure 32: LC-MS data for the microwave-assisted conversion of **59 using PS-PPh₃.**

(a) LC-MS analysis data of the reaction after 3 hours of irradiation (3 cycles of 1 hour at 50 °C). Both starting material **59** and product **61** could not be detected.

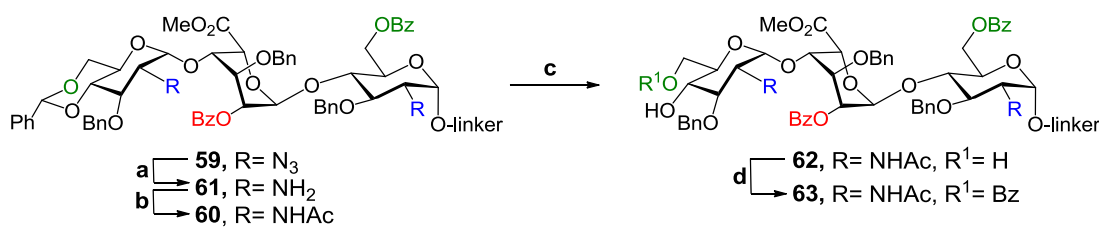
(b) LC-MS analysis data of the reaction after 3.5 hours of irradiation (3 cycles of 1 hour at 50 °C followed by a 1 cycle of 30 min at 100 °C). Retention time: 8.2 min (calcd for C₈₁H₈₇N₃O₁₉: 1405.6 [M], found m/z 1406.3 [M+H]⁺, 1423.5 [M+NH₄]⁺, 1428.5 [M+Na]⁺): product **61**.

Finally, PMe₃ was evaluated as the reductive agent. The trisaccharide **59** in a mixture of THF/H₂O (4/1 v/v) was then treated with a 1 M PMe₃ solution in presence of NaOH at room temperature for 5 hours. The complete conversion of the SM was monitored by MALDI-TOF analysis and no by-product formation was detected. The NaOH solution was quenched by addition of a 1 M HCl aqueous solution to avoid any cleavage of benzoyl groups. However, due to the significant increase of polarity of the compounds caused by the presence of the amine moieties, the different attempts to isolate **61** remained unsuccessful. Routine flash chromatography resulted in very poor yield as elution of the compound could not be properly performed using the routine combinations of solvents (in this case, mainly methanol and dichloromethane). The use of a base such as Et₃N did not improve the method. Purification using Sephadex LH-20 columns was also attempted, but several cycles of purification were necessary to obtain perfect separation of the salts and the

product. This resulted in a consequent loss of the product mass. In order to avoid the loss of such valuable compounds, it was decided to only dry the crude residue of the reduction reaction under high vacuum and carry it through to the next reaction.

4.6.2.3. Synthesis of the intermediate 63

The synthesis of the glycosyl acceptor **63** from the trisaccharide **59** was then performed in a four-step sequence (Scheme 22). As described in the previous sections, the azido moieties of **59** were first reduced using PMe_3 in $\text{THF}/\text{H}_2\text{O}$ in presence of NaOH . The resulting residue was then thoroughly dried under high vacuum and directly acetylated using acetic anhydride in dry Et_3N at $0\text{ }^\circ\text{C}$. The purification of the resulting crude was performed with a Sephadex LH-20 column and afforded [the desired diacetylated trisaccharide 60](#) (69 %, 2 steps).



Scheme 22: Synthesis of the glycosyl acceptor 63.

Reagents and conditions: (a) PMe_3 , NaOH , THF , H_2O ; (b) Ac_2O , Et_3N (69%, 2 steps); (c) EtSH , TMSOTf , DCM ; (d) BzCN , Et_3N , ACN (70%, 2 steps).

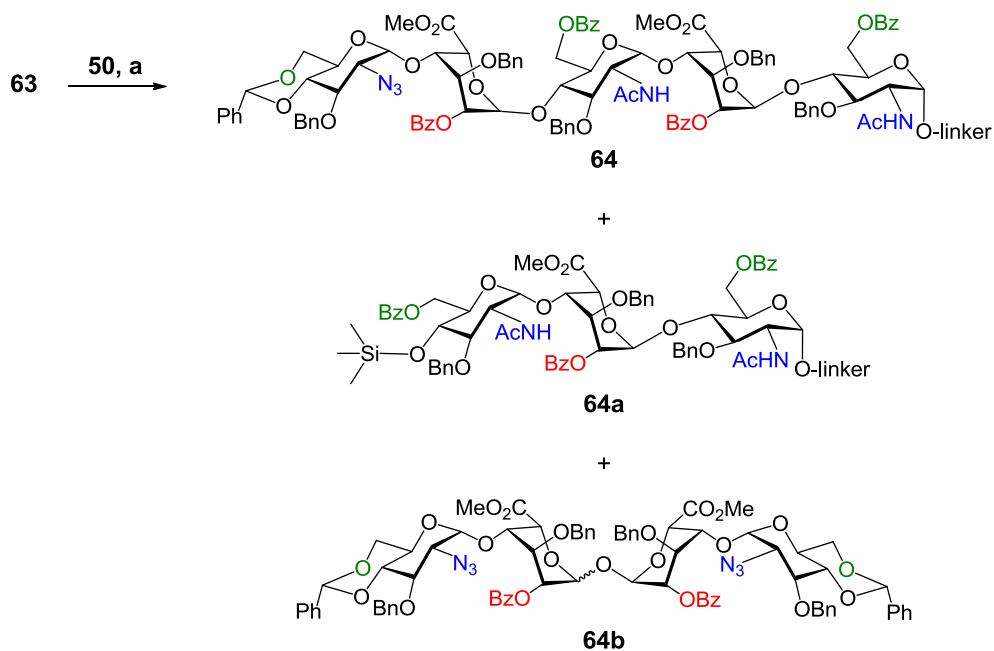
Linker = $(\text{CH}_2)_5\text{N}(\text{Bn})\text{CBz}$.

The benzylidene cleavage was first attempted using EtSH in the presence of $\text{BF}_3 \cdot \text{O}(\text{Et})_2$. As no initiation of the reaction was detected by MALDI-TOF analysis, the acid was then substituted by TMSOTf in another trial and the formation of the desired diol **62** could then be detected. The majority of salts formed during the reaction and excess of the reagents were removed using a Sephadex LH-20 column. The resulting diol residue was dried under high vacuum and directly treated with benzoyl cyanide (BzCN) and a catalytic amount of triethylamine (Et_3N) in dry acetonitrile, as was the seeding block **57**. The desired regioselectively protected trisaccharide **63** was obtained (determined by [MALDI-TOF analysis](#) and [\$^1\text{H}\$ NMR](#)) with a yield of 70% over 2 steps.

4.6.3. Pentasaccharide precursor synthesis: preliminary results

With the glycosyl acceptor **63** and the glycosyl donor **50** in hand, the second step of elongation was carried out to form the pentasaccharide precursor **64** (Scheme 23).

The different tests for the assembly of **50** and **63** were realised using the normal procedure. The qualitative progress of the glycosylation reactions was mainly monitored by TLC and [LC-MS](#), even though for the latter method, the varying number of chromophore groups amongst the compounds of interest did not allow any quantitative interpretation of the results. Analyses of aliquots taken at different time points (5 min, 15 min, 1 hour and 2 hours) suggested that the glycosylation reaction takes place as soon as the acid is added to the glycosyl acceptor/donor mixture as no clear evolution was detected as a function of time. All the LC-MS analyses realised for the different tests were in agreement with this observation (not shown here).



Scheme 23: Test synthesis of the pentasaccharide 64.

Reagents and conditions: (a) TMSOTf or TBSOTf, DCM, for yields, see Table 8.

Linker = (CH₂)₅N(Bn)CBz.

From the results that were obtained (Table 8), several conclusive remarks could be drawn. First of all, the silylation of the glycosyl acceptor (by-product **64a**) and the formation of the tetrasaccharide, resulting from the side glycosylation between the

glycosyl donor and its hydrolysed counterpart (by-product **64b**), were systematically detected when TMSOTf was used as the promoter agent (Figure 33). To prevent the formation of the silylated by-product **64a**, triflic acid (TfOH) was used as the promoter (Table 8, entries 6 and 7). However, the reaction was not initiated as no product could be detected at any point. Interestingly, the tetrasaccharide **64b** was not detected either, suggesting than TfOH was not able to activate the donor **50**. The option of using TfOH was then abandoned.

Entry	Equiv. of donor	Equiv. of activator	Temp	Solution Conc.	Compound distribution ^c		
					Acc 63 (%)	P 64 (%)	BP 64a (%)
1	1.5	0.1 ^a	-20 °C	0.1 M	80	13	7
2	1.5	0.2 ^a	0 °C	0.5 M	57	27	16
3	5	0.2 ^a	-20 °C	0.01 M	62	33	5
4	2.5	0.2 ^a	-40 °C	0.01 M	90	6	4
5	1.5	0.2 ^a	-80 °C	0.01 M	65	15	20
6	1.5	0.2 ^b	-20 °C	0.01 M	100	0	0
7	1.5	0.2 ^b	-80 °C	0.01 M	100	0	0

Table 8: Reaction conditions and results for the assemblies of the glycosyl donor 50 with the glycosyl acceptor 63.

^aTMSOTf; ^bTfOH; ^cdetermined by LC-MS data analysis; Acc: glycosyl acceptor; P: product; BP: by-product.

Secondly, several sets of conditions were tested in order to determine if any parameter would emerge as essential to attain high yield glycosylation (Table 8, entries 1-5). However, the yields remained quite low in every case. The highest conversion was obtained when performing the reaction with the conditions described in entry 3 of Table 8. However, a fairly large excess of donor was required to obtain such a result (5 equivalents), which was not an acceptable solution. In addition, the conversion obtained in this case was low and was not so different from those obtained in the other cases, which suggested investigation of other solutions.

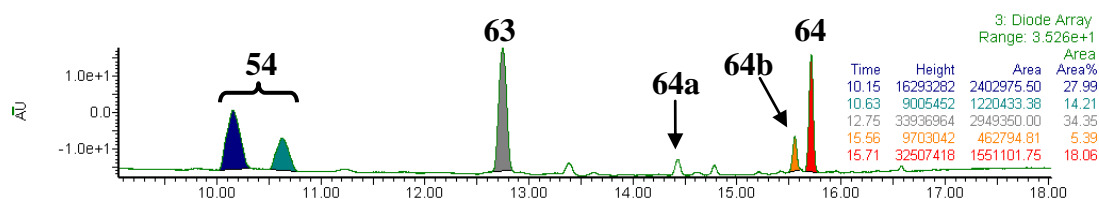


Figure 33: Typical LC-MS spectrum profile obtained for the assembly of **50 with **63**.**

For conditions, see Table 8, entry 3. Retention times: 10.15 min and 10.63 min (calcd for $C_{41}H_{41}N_3O_{12}$: 767.3 [M], found m/z 785.4 $[M+NH_4]^+$, 790.4 $[M+Na]^+$): hydrolysed donor **54**; retention time: 12.75 min (calcd for $C_{85}H_{91}N_3O_{22}$: 1505.6 [M], found m/z 1506.8 $[M+NH_4]^+$, 1528.9 $[M+Na]^+$): acceptor **63**; retention time: 14.43 min (calcd for $C_{88}H_{99}N_3O_{22}Si$: 1578.8 [M], found m/z 1601.8 $[M+Na]^+$): silylated acceptor **64a**; retention time: 15.56 min (calcd for $C_{82}H_{80}N_6O_{23}$: 1516.5 [M], found m/z 1534.8 $[M+NH_4]^+$, 1539.8 $[M+Na]^+$): by-product **64b**; retention time: 15.71 min (calcd for $C_{126}H_{130}N_6O_{33}$: 2254.9, found m/z 1128.7 $[M+2H]^{2+}$, 1140.2 $[M+H+Na]^{2+}$): product **64**.

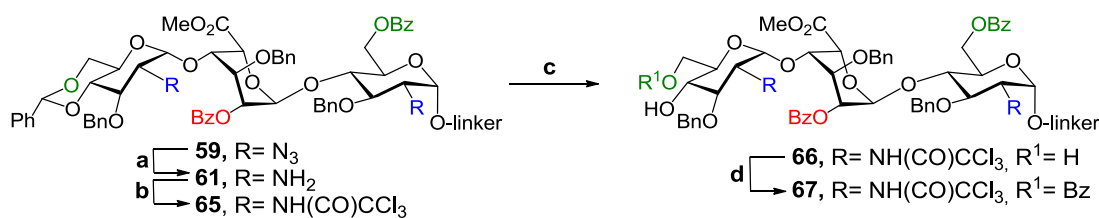
The low coupling efficiency between **50** and **63** that was observed may be explained by a strong mismatch of reactivity between the glycosyl donor and acceptor. While the trichloroacetimidate donor is indeed very reactive, both the presence of an L-iduronic acid residue and the introduction of the acetamido moieties appeared to drastically lower the acceptor reactivity. The latter was still expected to have an impact on the outcome of the assembly reaction, as the hydroxyl group at position 4 of D-glucosamine residues bearing an acetamido moiety has long been known to lack reactivity in glycosylation reactions (Paulsen 1982, Crich and Dudkin 2001). In addition, the unavoidable and important formation of the by-products, as well as the difficulties encountered for the isolation of the product, encouraged the synthesis and evaluation of a new type of acceptor for the formation of the desired pentasaccharide backbone.

4.6.4. Synthesis of the new trisaccharide precursor **67**

Amongst the multitude of groups that are available for masking the amine moieties of the D-glucosamine residues, it was decided to resort to the trichloroacetamide (TCA) protecting group for several reasons. First of all, *N*-trichloroacetyl groups are more stable and less prone to migration than *N*-acetyl groups. In addition, the installation of the TCA protecting group is rather easily done, in mild conditions, which should not compromise the stability of the other PGs. Moreover, unlike with other PGs, TCA groups can be directly transformed into acetamido groups by radical

reduction using azobisisobutyronitrile (AIBN) and an organotin compound such as tributyltin hydride ((Bu)₃SnH) as a source of hydrogen atom (Blatter *et al.* 1994). Despite being a robust method used for routine radical dehalogenation, the latter required slight modifications to be performed in some cases, as for the synthesis of chondroitin sulphate precursors by Hsieh-Wilson and co-workers, dimethylacetamide has been used as a co-solvent with benzene (Tully *et al.* 2004). In another case described by Bräse and coworkers, this method proved itself to be unsuitable, since it led to the decomposition of the SM and more specifically to the cleavage of the β -1,4-glycosidic bond of the hyaluronic acid tetrasaccharide (Virlouvet *et al.* 2010). Moreover, the well-known high toxicity of stannane compounds and benzene remain major drawbacks which have motivated researchers to investigate new methods of dehalogenation. In the study published in 2010, Virlouvet and colleagues also attempted the dehalogenation of the hyaluronic acid precursors using a combination of zinc and acetic acid (Zn/AcOH) in 1,4-dioxane, another common way of reducing trichloroacetamides. In this case however, the formation of the desired product was detected in low yield (around 20%) and this method also led to the decomposition of the material. Finally, the reduction of trichloroacetamides can be performed under catalytic hydrogenation conditions (Kandasamy *et al.* 2014). In addition, the last two methods also allow the reduction of the azido groups, which make them very interesting and convenient for the synthesis of some specific octasaccharide targets.

As for the preparation of the trisaccharide precursor **63**, the four-step sequence synthesis of the desired glycosyl acceptor **67** started with the reduction of the azido groups using PMe₃ in THF/H₂O in the presence of NaOH (Scheme 24). The resulting residue was then dried under high vacuum for a minimum of 12 hours and the installation of the trichloroacetamide moieties was directly performed using trichloroacetyl chloride under basic conditions to quench the HCl formed during the reaction. The purification of the resulting crude was performed with a Sephadex LH-20 column and afforded the desired trisaccharide **65** (55 %, 2 steps).



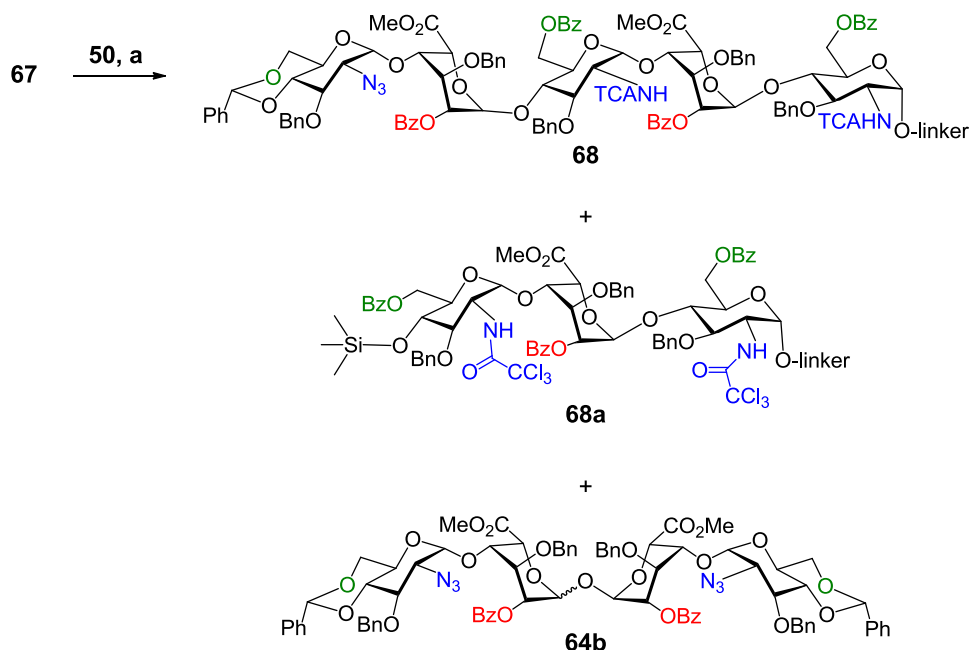
Scheme 24: Synthesis of the glycosyl acceptor 67.

Reagents and conditions: (a) PMe₃, NaOH, THF, H₂O; (b) Cl₃CCOCl, Et₃N (55%, 2 steps); (c) EtSH, TMSOTf, DCM; (d) BzCN, Et₃N, ACN (51%, 2 steps). Linker = (CH₂)₅N(Bn)CBz.

The benzylidene cleavage was performed using EtSH in presence of TMSOTf and the progress of the reaction was monitored by MALDI-TOF mass analyses (not shown here). As for the synthesis of the trisaccharide precursor **62**, the majority of salts formed during the reaction and excess of the reagents were removed using a Sephadex LH-20 column. The resulting crude was dried under high vacuum and directly treated with benzoyl cyanide (BzCN) and a catalytic amount of triethylamine (Et₃N). The desired regioselectively protected trisaccharide **67** was obtained (determined by ¹H NMR) with a yield of 51% over 2 steps.

4.6.5. New pentasaccharide precursor synthesis: evaluation of the new trisaccharide building block 67

The newly synthesised trisaccharide building block **67** was then evaluated as potential glycosyl acceptor for the preparation of the pentasaccharide target (Scheme 25). Two tests for the assembly of **50** and **67** were realised using the normal procedure. As for the preparation of the pentasaccharide **64**, the qualitative progress of the glycosylation reactions was mainly monitored by TLC and LC-MS. Similarly, analyses of aliquots taken at different time points (5 min, 15 min, 1 hour and 2 hours) suggested that the glycosylation reaction takes place as soon as the Lewis acid is added to the glycosyl acceptor/donor mixture.



Scheme 25: Test synthesis of the pentasaccharide 68.

Reagents and conditions: (a) TMSOTf, DCM, for yields, see Figure 34. Linker = $(\text{CH}_2)_5\text{N}(\text{Bn})\text{CBz}$.

TMSOTf was used as the promoter agent for both tests. As expected, the formation of the silylated glycosyl acceptor analogous **68a** was observed by LC-MS analyses (Figure 34 (a)). Similarly, and as for the preparation of the pentasaccharide **64**, the presence of the tetrasaccharide **64b** was also detected (Figure 34, (a)).

The results obtained with the first test suggested that the formation of the product was more important with the new glycosyl acceptor (Figure 34 (b), entry 1) and were very encouraging (52% compound distribution). In addition, a replicate of the reaction was carried out but gave an unexpectedly very low conversion. The coupling reaction between **50** and **67** hence showed signs of poor reproducibility. However, these observations were drawn from the results obtained with only two reaction tests. Other conditions must be assessed to determine their impact on the reaction outcome.

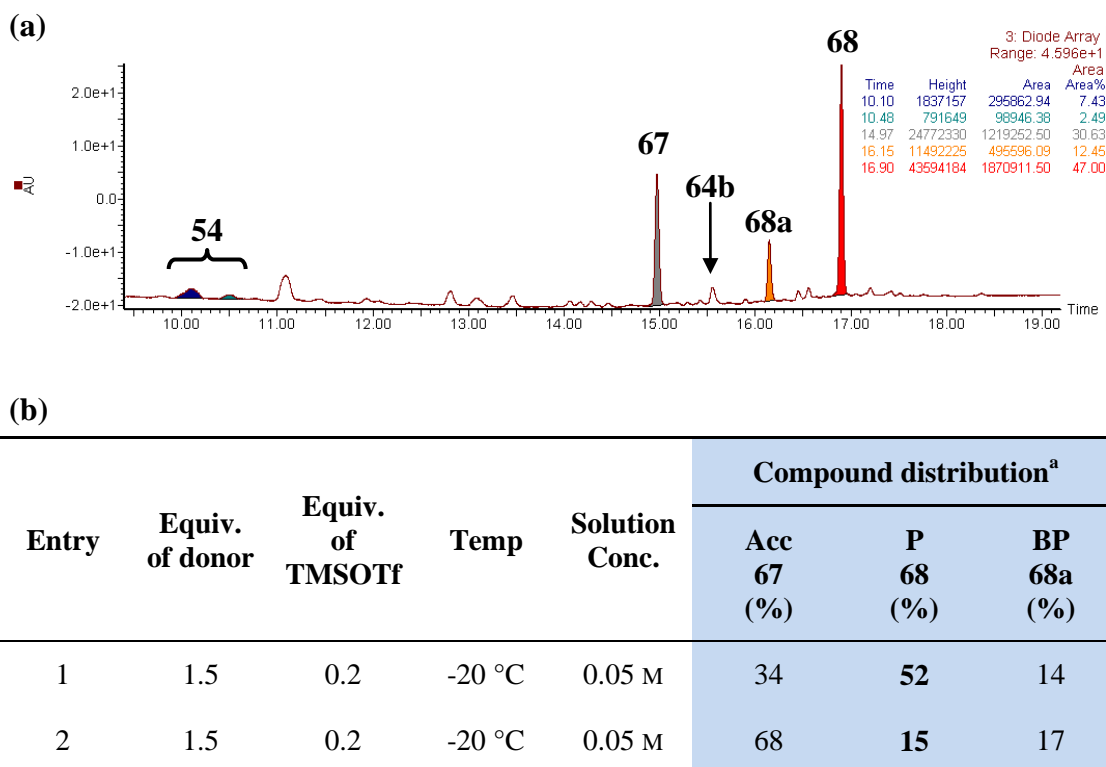


Figure 34: Analysis of the assembly of **50 with **67**.**

(a) Typical LC-MS spectrum profile obtained for the assembly of **50** with **67** (for conditions, see table (b), entry 1). Retention times: 10.10 min and 10.48 min (calcd for $C_{41}H_{41}N_3O_{12}$: 767.3 [M], found m/z 785.4 [M+NH₄]⁺, 790.4 [M+Na]⁺): hydrolysed donor **54**; retention time: 14.97 min (calcd for $C_{85}H_{85}Cl_6N_3O_{22}$: 1713.3 [M], found m/z 1714.4 [M+H]⁺, 1731.4 [M+NH₄]⁺, 1736.3 [M+Na]⁺): acceptor **67**; retention time: 15.56 min (calcd for $C_{82}H_{80}N_6O_{23}$: 1516.5 [M], found m/z 1534.8 [M+NH₄]⁺, 1539.8 [M+Na]⁺): by-product **64b**; retention time: 16.15 min (calcd for $C_{88}H_{93}Cl_6N_3O_{22}Si$: 1785.5 [M], found m/z 1786.5 [M+NH₄]⁺, 1803.5 [M+H]⁺, 1809.5 [M+Na]⁺): by-product **68a**; retention time: 16.90 min (calcd for $C_{126}H_{124}Cl_6N_6O_{33}$: 2463.1, found m/z 1254.4 [M+2Na]²⁺): product **68**.

(b) Reaction conditions and results for the assemblies of the glycosyl donor **50** with the glycosyl acceptor **67**.

^adetermined by LC-MS data analysis; Acc: glycosyl acceptor; P: product; BP: by-product.

4.6.6. Conclusions

Following the unsuccessful development of a new synthetic route in the first part of this Chapter 4, the original plan was modified. Owing to time constraints, it was decided to resort to dimeric building blocks (**50** and **51**) that have already been described in the literature (Lucas *et al.* 2003, De Paz and Martín-Lomas 2005) and to include them in the current project. With the new dimeric building blocks in hand, the synthesis of the oligosaccharide target was initiated. The preparation of both the

seeding block **58** and the first trisaccharide precursor **59** was successfully achieved. The direct transformation of the azido groups of **59** into acetamido groups was first attempted using thioacetic acid but led to the large formation of the reaction intermediates and could not be brought to completion. Other methods were explored, requiring the reduction of the azido groups into primary amino groups (to afford **61**). This, however, led to drastic changes in reactivity in routine chemical reactions and workup/purification steps. This seriously hampered the successful synthesis of the other trisaccharide glycosyl acceptors **63** and **67**. The preparation of the pentasaccharide precursors **64** and **68** were attempted but gave unsatisfactory results, probably owing to the gap of reactivity between the donors and the acceptors.

4.7. General conclusions

For the sake of simplicity and with a view to saving time and resources, chemists often aim for the preparation of rather short and homogenous structures. However, the latter do not reflect the complete range of intrinsic heterogeneity of these carbohydrates. With the perspective of developing a new modular synthetic strategy that would allow an easy and rapid preparation of structurally heterogeneous structures, the synthesis of the natural octasaccharide **A** (Scheme 5) isolated by Prof. Turnbull's team (Ahmed 2010) was attempted. The new route was designed in such a way that the chemistry would ultimately be transferred to solid-phase synthesis. A number of novel advances were made. Firstly, convenient methods for the preparation of new monomeric and dimeric building blocks were successfully developed and oligosaccharide structures, up to pentasaccharide precursors, were successfully prepared. Secondly, the possibility of using resin-bound triphenylphosphine to achieve the reduction of azido moieties was also successfully demonstrated. Developing the use of such solid phase-based methods as well as the microwave-assisted synthesis in carbohydrate chemistry may be of upmost importance in the development of cheap, fast and hassle-free synthetic pathways.

As anticipated, a number of issues arose during the syntheses of longer saccharides, including poor coupling efficacies and changes of reactivity. Owing to some of these issues, major modifications were brought to the initial plan and the modular strategy was eventually abandoned in favour of the development of a more versatile synthetic

route. During both phases, the poor coupling character of the L-iduronic acid residues turned out to be an obstacle to attainment of high-yield coupling reactions. With the reduction of the azido groups also arose other issues, such as difficult work-up and purification steps, as well as consequent changes in reactivity in routine chemical reactions.

Therefore, some aspects arising from the work here require further investigation in the future. The poor coupling efficacies observed remain the major obstacle to overcome. Using more electron donating PGs to reduce the gap between the reactivity properties of both the glycosyl donor and acceptor may be a first plausible option. Using idose residues as glycosyl acceptors may represent another possibility, as they are well-known for being more reactive than their L-iduronic acid analogues. This option will require the late-stage C-6 oxidation into the uronic acid residues, which may become more problematic as the oligosaccharide size is extended. Another issue that would require attention is the impact of acetamido and trichloroacetamido moieties as PGs as they drastically affect the behaviour of the compounds, due to their electron withdrawing effect. Using different PGs such as *N*-phthalimides may help prevent such an undesired effect. Additional trials of the synthesis of the pentasaccharide bearing trichloroacetamide moieties must be carried out in order to evaluate the reproducibility of this glycosylation reaction. Finally, with a pentasaccharide precursor in hand, it would be interesting to undertake the deprotection and sulphation steps in order to investigate their feasibility on such structurally disparate structures.

**5. Chapter 5 – Evaluation of Hp/HS oligosaccharide
specificity/selectivity in FGF signalling**

5.1. Introduction

Fibroblast Growth Factors (FGFs) and their receptors (FGFRs) are involved in many biological processes such as cellular proliferation and migration, survival and differentiation, but also wound healing and angiogenesis, to name but a few (Beenken and Mohammadi 2009, Ornitz and Itoh 2015). Aberrant FGF signalling has been linked to many disorders and diseases such as metabolic and cardiovascular disorders (Li, Wang, *et al.* 2016) and cancers (Jorgen *et al.* 2011).

Several studies showed that FGF signalling depends on the formation of FGF-FGFR-HS complex to be effective (Flaumenhaft *et al.* 1990, Klagsbrun and Baird 1991, Rapraeger *et al.* 1991, Yayon *et al.* 1991). Deciphering the structure activity relationship (SAR) of HS in FGF signalling is hence of crucial importance for understanding the functional role of HS and potentially for the development of novel glycan therapeutics (Yip *et al.* 2006).

Some major findings on HS SAR have been achieved over recent decades, such as determining the minimum size needed for HS-protein interactions (heparin octasaccharides were shown to be efficient to support FGF2 activity Ornitz *et al.* (1992)) and the fact that distinct structural determinants are required for different FGF-FGFR complexes (Guimond and Turnbull 1999, Pye *et al.* 2000, Ostrovsky *et al.* 2002). As developed in more detail in chapter 1, the regulation of FGF signalling has been shown to depend on many factors including the HS saccharides sulphation patterns (e.g. Guimond and Turnbull (1999); Pye *et al.* (2000)), the nature of the solvent/coordinated ions (Rudd *et al.* 2007, Guimond *et al.* 2009) and the plasticity of both the L-iduronic acid residues and the saccharide chains (Raman *et al.* 2003, Rudd and Yates 2010). Despite the intensive investigation that has been carried out to elucidate the molecular mechanisms of FGF signalling (see Section 1.7), the interactions between HS, FGF and FGFR which lead to functional activity still remain elusive. In particular, the concept of specificity/selectivity in these interactions is still extensively debated, as mentioned in 1.7.4, and clearly needs to be addressed.

Owing to the lack of efficient and appropriate methods to both prepare and sequence HS oligosaccharides (see Section 1.8), most of the studies assessing HS-FGF-FGFR interactions to date have been conducted using either oligosaccharide mixtures (e.g., Guimond and Turnbull (1999); Zhang, Zhang, *et al.* (2009)) or saccharides which were not fully structurally determined (for example, the nature of the exact sulphation pattern or the uronic acid residue was often unknown) (e.g. Guimond and Turnbull (1999); Ashikari-Hada *et al.* (2004)). In addition, the function of specific and unusual structural features - namely the 3-*O*-sulphate groups (Thacker *et al.* 2014) and also unsubstituted glucosamine residues - could not be properly assessed. In several studies where the isolation of the saccharides was achieved, the structural differences between the compounds were however too diverse to determine the effects of small structural changes (Belford *et al.* 1992, Wu *et al.* 2003).

Further advances in the meticulous study of HS SAR in FGF signalling now requires the use of pure and well-defined HS saccharides. Such compounds would allow the study of the impact of a variety of structural modifications on FGF activity. Ultimately, this would also provide the key to a better understanding of the specificity/selectivity of HS-FGF-FGFR interactions.

5.1.1. Aim

The work presented in this chapter aimed to evaluate the impact of several types and degrees of structural differences on the ability of HS saccharides to stimulate FGF signalling, using precise ligand-receptor activity assays with the help of structurally defined HS oligosaccharides of various sizes. More specifically, the impact of both general versus subtle modifications of the sulphation pattern, high versus low levels of sulphation, changes of uronic acid residues and size changes were all examined.

5.1.2. Strategy and method

Most of the structural and biochemical work published in the literature is based on the examination of FGF1-FGFR2 and FGF2-FGFR1 complexes only and other complexes have generally not been considered. This chapter focuses on a total of 4 complexes: FGF2-FGFR1c, FGF1-FGFR1c, FGF1-FGFR2b and FGF7-FGFR2b. These complexes were chosen for several reasons. First of all, FGF1 is known to

signal through all types of receptors and is often termed the universal FGFR ligand (the complexes FGF1-FGFR1c and FGF1-FGFR2b would hence be used as positive controls). In contrast, FGF7 is known to signal exclusively through FGFR2b (Ornitz *et al.* 1996, Zhang *et al.* 2006). In addition, FGF2 and FGF1 both signal through receptor FGFR1c in a similar fashion (Guimond and Turnbull 1999). By comparing the results obtained with these different FGF-FGFR complexes, it may be possible to have some insights into the structural determinants that are optimal for each signalling protein and receptor combination.

To assess the signalling activities, a total of 19 Hp/HS oligosaccharides, which are described in more detail in Section 5.2, were screened in these bioassays (BaF3 assays are described in the following Section 5.1.2.1).

5.1.2.1. BaF3 bioassays

BaF3, the murine Interleukin-3 (IL-3) dependent pro-B cell line that does not naturally express either endogenous HS or FGFR was used in bioassays to investigate FGF signalling. Upon removal of IL-3, BaF3 cells undergo apoptosis (programmed cell death). Alternatively, the cells can be transfected with individual FGFRs and the survival, growth and proliferation of the cells are assured if they are incubated with the appropriate FGF and suitable Hp/HS saccharides to generate productive signalling (Ornitz *et al.* 1996). The cells used for this project were transfected with either FGFR1c or FGFR2b (Ornitz *et al.* 1996). They were previously used as an HS-dependent assay for FGF signalling responses (Guimond and Turnbull 1999). The transfected cells were incubated in the presence of either FGF1/FGF2/FGF7 and with Hp/HS oligosaccharides (for details about the saccharides, see Section 5.2). Upon activation of the FGF-FGFR complex by Hp/HS, the cells proliferate and their mitogenic activity is measured using the tetrazolium dye MTT (3-[4,5-dimethylthiazol-2-yl]-2,5-diphenyltetrazolium bromide). The mitochondrial reductase enzymes of viable cells reduce MTT to purple formazan which can be read at $\lambda = 570$ nm. The absorbance is proportional to live cells and cell proliferation, and therefore to FGF signalling (Guimond and Turnbull 1999). For more details about the conditions for bioassays, see Section 2.2.

Prior to any bioassay, the activity of the saccharides alone (cells in growth medium and in the presence of the oligosaccharides) was assessed. Responses to Hp/HS saccharides alone (cells in growth medium and in the presence of the oligosaccharides) were identical to the background controls (cells in BaF3 growth medium) (see Section 5.3). The saccharides were next screened in primary bioassays (at a concentration of 3 µg/mL, previously determined as optimal for heparin and heparin saccharides), as described in Section 2.2. FGFs were used at different concentrations (0.1 nM FGF2, 1 nM FGF1 and 3 nM FGF7) to obtain comparable assay response levels. Briefly, for each FGF-FGFR pair, three replicates of the bioassays were carried out, and triplicates were carried out in each bioassay plate (for a total of 9 absorbance values per oligosaccharide-FGF-FGFR combination). For dose response curves, the assays were carried out once (triplicates on each assay plate). For all types of assays, the values of the background controls (cells in culture medium and treated with FGF alone) were subtracted from the values of interest (cells in culture medium and in the presence of full-length Hp/HS oligosaccharide of interest).

For primary bioassays, the data were normalised to that of full-length Hp (optimal 3 µg/mL) in order to correct the variability caused by slightly different experimental conditions between plates (e.g., number and response levels of the cells). Normalised data also allowed assessment of the relative mitogenic activity of the compounds for each FGF-FGFR pair and to make comparisons between different FGFs or different FGFRs. The compounds were tested using a one-sample t-test (one tailed) to determine whether their relative activities were significantly higher than the different reference values or not (reference values: 5%, 50% and 100% activity, relative to full-length Hp). 5% was designated as the threshold value for minimum activity. Selected compounds were also tested using a two-sided t-test. Data analyses were performed with R statistical software v.3.3.0.

5.2. Libraries of well-defined Hp/HS oligosaccharides

[This work was carried out in collaboration with Prof. J. Liu (The University of North Carolina, Chapel Hill, NC, USA) and Prof. P. Tyler (Victoria University of Wellington, New Zealand), who provided the defined HS saccharides].

5.2.1. From chemical sources

Schwörer *et al.* (2013) successfully developed the chemical synthesis of a set of structurally varied HS oligosaccharides, ranging from hexa- to dodeca-saccharides. The oligosaccharides were targeted for inhibition of the BACE-1 protease, and were rather low sulphated (fully *N*-Acetylated and 6-*O*-sulphated oligosaccharides) and most displayed exclusively either L-iduronic acid or D-glucuronic acid residues. As part of the collaboration between our two teams, a total of 10 compounds (4 octasaccharides, 4 decasaccharides and 2 dodecasaccharides) were generously provided by Prof. P Tyler's team to be screened in BaF3 bioassays. These structures are illustrated in Table 9. The structural homogeneity of these structures repeat disaccharide units allowed mainly the investigation of the impact of the size, the nature of the uronic acids, 2-*O*-sulphation and the lack of *N*-sulphate groups on the functional activity of HS saccharides.

5.2.2. From chemoenzymatic sources

Since 2000, Prof. J. Liu's team have been developing alternative, robust and fast synthetic and enzymatic strategies to prepare Hp/HS oligosaccharides (Liu *et al.* 2010, Moon *et al.* 2012, Xu, Pempe, *et al.* 2012, Hsieh *et al.* 2014). Notably, Xu *et al.* (2014) successfully developed a chemoenzymatic method to prepare Low Molecular Weight Hp (LMWHp) structures. This method allowed the synthesis of saccharides ranging from hexa- to dodeca-saccharides, with some displaying the unusual structural feature 3-*O*-sulphate group towards the non-reducing end. Compared to the saccharides prepared by Prof. Tyler's team, which were rather structurally homogeneous, Xu *et al.* (2014) successfully prepared structures containing both types of uronic acid residues. As part of collaboration between our two teams, Prof. Liu's team generously provided a total of 9 compounds (3 octasaccharides, 3 decasaccharides and 3 dodecasaccharides) for bioassay screening. These structures are illustrated in Table 10. The structural features of these compounds allowed assessment of the impact of the size, 6-*O*-sulphate and 3-*O*-sulphate groups on the functional activity of HS saccharides.

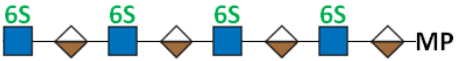

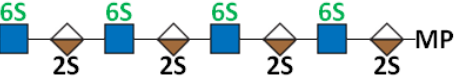
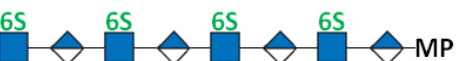


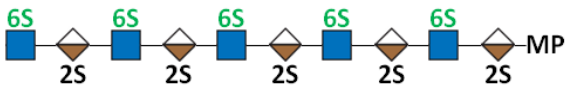

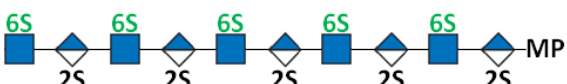


Name	Structure	Legend
Oct6SIdo		 GlcNAc IdoA GlcA
Oct6SIdo2S		
Oct6SGlc		
Oct6SGlc2S		
Dec6SIdo		
Dec6SIdo2S		
Dec6SGlc		
Dec6SGlc2S		
Dod6SIdo		
Dod6SIdo2S		

Table 9: Schematic representation of the structures of the HS oligosaccharides prepared by chemical synthesis (Schwörer *et al.* 2013). 2S: 2-*O*-sulphate; 6S: 6-*O*-sulphate; GlcA: β -D-glucuronic acid; GlcNAc: *N*-acetyl- α -D-glucosamine; IdoA: α -L-iduronic acid; MP: methoxyphenyl.






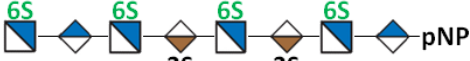

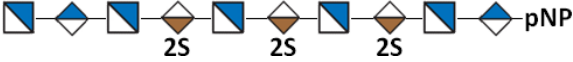





Name	Structure	Legend
Oct2S		 GlcNAc  GlcNS  IdoA  GlcA
Oct2,6S		
Oct2,6+3S		
Dec2S		
Dec2,6S		
Dec2,6+3S		
Dod2S		
Dod2,6S		
Dod2,6+3S		

Table 10: Schematic representation of the structures of the HS oligosaccharides prepared by chemoenzymatic synthesis (Xu *et al.* 2014). 2S: 2-*O*-sulphate; 3S: 3-*O*-sulphate; 6S: 6-*O*-sulphate; GlcA: β -D-glucuronic acid; GlcNAc: *N*-acetyl- α -D-glucosamine; IdoA: α -L-iduronic acid; pNP: *para*-nitrophenyl.

Overall, two sets of libraries were collected, for a total of 7 octasaccharides, 7 decasaccharides and 5 dodecasaccharides. These 19 fully defined structures displayed interesting structural differences that allowed initial studies of the role of 2-*O*-, 6-*O*- and 3-*O*-sulphation and the size of saccharides on FGF signalling.

5.3. Results

5.3.1. Assessing the ability of Hp/HS oligosaccharides to induce FGF2 and FGF1 signalling through FGFR1c

Prior to any activity screening of the 19 compounds, the response of the cells expressing FGFR1c in the presence of FGF2/FGF1 and of different concentrations of full-length Hp was assessed (Figure 35). The curves obtained here were in agreement with previously published values (Ornitz *et al.* 1996, Guimond and Turnbull 1999).

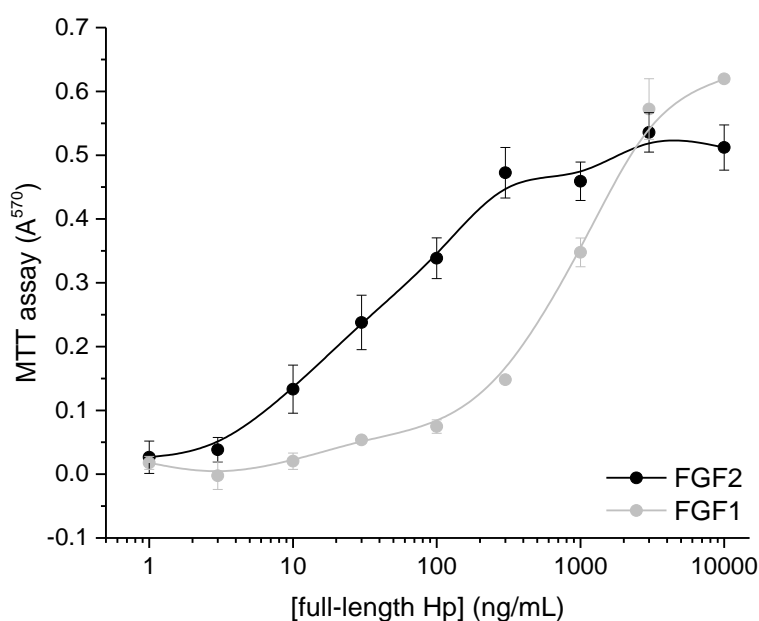


Figure 35: Dose response curves (mean \pm S.D.) for full-length Hp activation of FGF2 (0.1 nM) and FGF1 (1 nM) signalling through FGFR1c. Values are the mean of triplicate samples.

The activity of the saccharides alone (cells in growth medium and in the presence of the oligosaccharides) was also assessed. Responses to Hp/HS saccharides alone (cells in growth medium and in the presence of the oligosaccharides) were identical to the background controls (cells in BaF3 growth medium) (Figure 36).

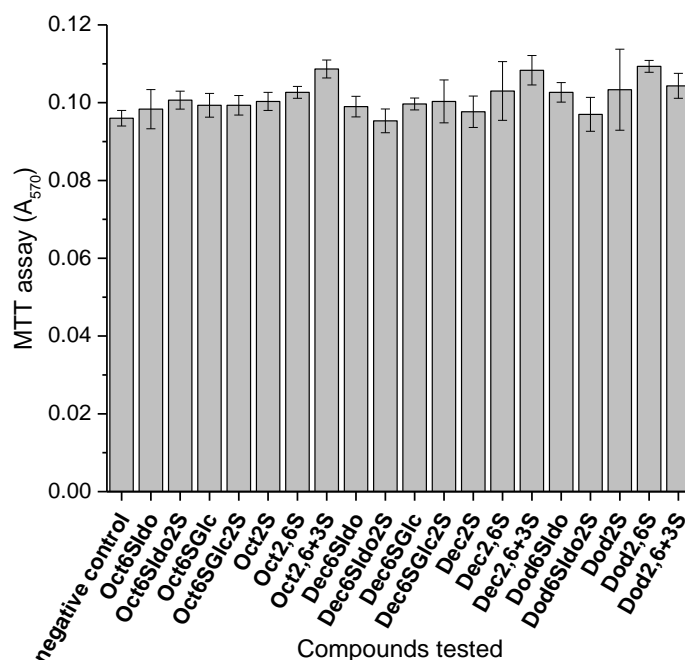


Figure 36: Evaluating the bioactivity of the compounds alone at 3 µg/mL in bioassays with cells expressing FGFR1c. The negative control refers to the cells in BaF3 medium only (background). The values are the mean of triplicate samples and the error bars represent the standard deviation (S.D.).

The capability of the oligosaccharides to stimulate the mitogenic activity through the ligand-receptor pairings of FGF2-FGFR1c and FGF1-FGFR1c was next assessed (Figure 37). To determine whether the relative activities of the compounds were higher than 5%, 50% or 100% activity (relative to full-length Hp), statistical tests were performed (one-sample t-tests (one tailed) - the results are listed in Table 11). Selected compounds were also compared using a two-sided t-test.

For these two complexes, the oligosaccharides displayed various degrees of activation, independently of the FGF-FGFR complex. At the fixed concentration of 3 µg/mL, some oligosaccharides were observed to be very potent activators (relative

activity higher than 100%, relative to full-length Hp – e.g., Dec2,6+3S and Dod2,6S) whereas some displayed very low to high levels of activation (relative activities ranging from 5% to 100%, relative to full-length Hp – e.g., Oct2,6S, Oct2,6+3S, Dec2,6S and Dod2,6+3S). Some Hp/HS saccharides also showed no activation at all (relative activities lower than 5%, relative to full-length Hp – e.g., all the chemically prepared compounds) or even displayed possibly negative activities (e.g, Oct2S and Oct2,6S), though the latter were not statistically significant.

More specifically, in the case of FGF2-FGFR1c, the 4 compounds Dec2,6S, Dec2,6+3S, Dod2,6S and Dod2,6+3S were the only oligosaccharides capable of stimulating mitogenic activity (Figure 37 (a)). They displayed rather similar and high levels of activity (around 90%) and no significant difference was tested between the two decasaccharides and between the two dodecasaccharides. However, none of these compounds were more active than Hp (on a weight basis).

In contrast, in the case of FGF1-FGFR1c, a total of 6 compounds (Oct2,6S, Oct2,6+3S, Dec2,6S, Dec2,6+3S, Dod2,6S and Dod2,6+3S) were capable of supporting FGF1 signalling, with the remaining 13 other compounds being inactive (Figure 37 (b)). Out of the 6 active compounds, 5 were shown to display an activity level significantly higher than 50%, whereas Oct2,6S showed a rather low level of activity – about 20%. Importantly, octasaccharides were also able to stimulate FGFR1c when FGF1 was the ligand. Two-sided t-tests showed that a significant difference could be observed between Oct2,6S and Oct2,6+3S ($t_{2,698} = -8.568$, $p = 0.005$), Dec2,6S and Dec2,6+3S ($t_{2,146} = -5.731$, $p = 0.025$) but not between Dod2,6S and Dod2,6+3S. Also, unlike for FGF2, 2 compounds (Dec2,6+3S and Dod2,6S) were significantly stronger activators compared to Hp (on a weight basis, at the fixed concentration of 3 $\mu\text{g/mL}$). It was hence decided to study the ability of these two saccharides to stimulate mitogenic activity in more detail.

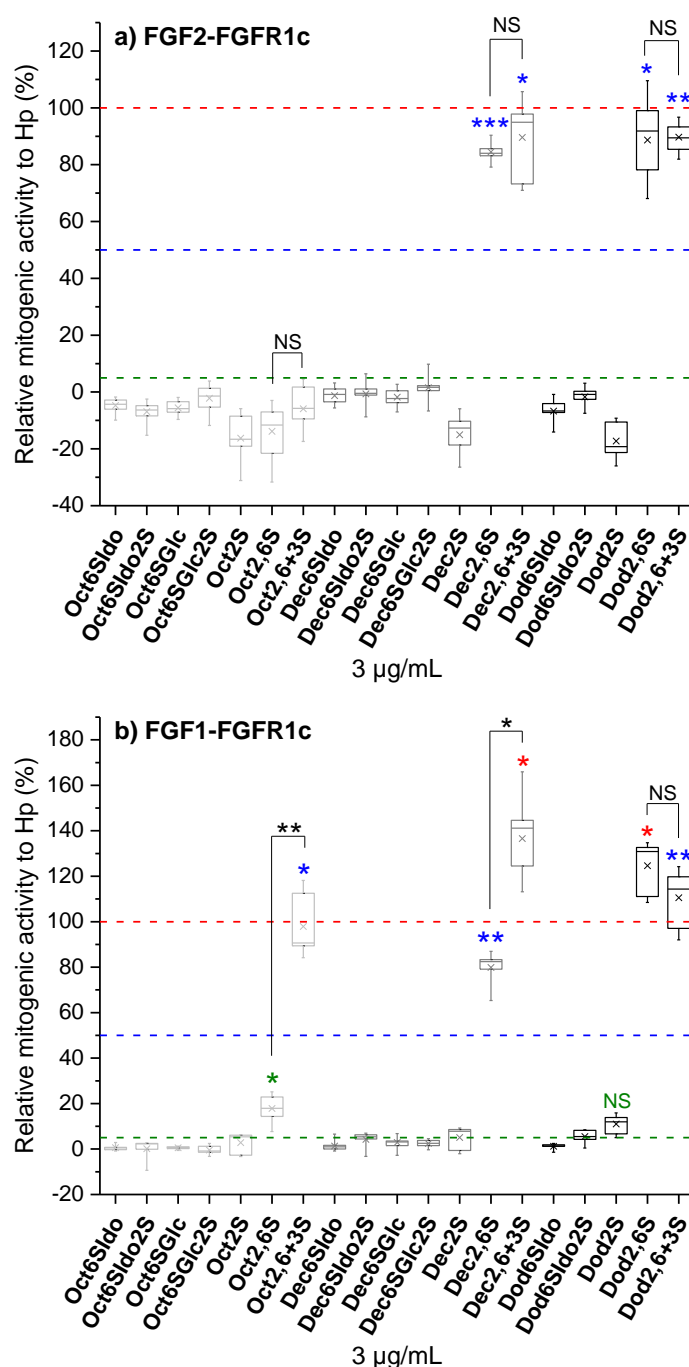


Figure 37: Assessing the capability of fully defined Hp/HS oligosaccharides (at 3 µg/mL) to regulate (a) FGF2 (0.1 nM) and (b) FGF1 (1 nM) signalling through FGFR1c. The relative mitogenic activities (N=9) were expressed as a percentage of the Hp control and plotted as box plots. Box plots show median (horizontal line), 25th and 75th percentiles (edges of the box), minimum and maximum values (whiskers) and mean (cross). The activities were tested using a one-sample t-test (N=3) to determine if their relative activities were significantly higher than the reference values: 5% (**green**), 50% (**blue**) and 100% (**red**) (all reference values are relative to full-length Hp); Selected compounds were also tested using two-sided t-test (N=3) (**black**); *p<0.05; **p<0.01; ***p<0.001; NS: non-significant (p≥0.05). Oligosaccharides are categorised as follows: octa- (light grey boxes), deca- (grey boxes), dodeca-saccharides (black boxes).

Oligosaccharide	FGF2-FGFR1c					FGF1-FGFR1c				
	Relative mitogenic activity (% mean±S.D.)	Reference value (% activity)	t	Degree of freedom	p value	Relative mitogenic activity (% mean±S.D.)	Reference value (% activity)	t	Degree of freedom	p value
Oct2,6S	-	-	-	-	-	17.9 ±6.3	5	3.53	2	0.036*
Oct2,6+3S	-	-	-	-	-	97.9 ±14.9	50	5.57	2	0.015*
Dec2,6S	84.5 ±2.4	50	25.24	2	0.001***	79.9 ±3.2	50	16.08	2	0.002**
Dec2,6+3S	89.6 ±15.6	50	4.40	2	0.024*	136.6 ±16.8	100	3.76	2	0.032*
Dod2,6S	88.7 ±16.1	50	4.16	2	0.027*	124.6 ±12.8	100	3.34	2	0.039*
Dod2,6+3S	89.7 ±5.2	50	13.18	2	0.003**	110.6 ±14.5	50	7.26	2	0.009**

Table 11: Results of one-sample t-tests (one-tailed, N=3) for FGF2-FGFR1c and FGF1-FGFR1c. Compounds were tested using one-sample t-tests to determine if their relative activities were higher than the reference values 5% (**green**), 50% (**blue**) and 100% (**red**) relative activity (relative to Hp) .Compounds that are not shown were not significantly higher than the 5% reference value (threshold for minimum activity). *p<0.05; **p<0.01; ***p<0.001.

The dose response curves for these two compounds were generated and are shown in Figure 38. Both Dec2,6+3S and Dod2,6S showed some activation at very low concentrations and reached plateau at 3,000 ng/mL. These titration curves clearly demonstrate that both Dec2,6+3S and Dod2,6S are better activators than Hp, across concentrations ranging from 30 ng/mL to 3,000 ng/mL. This observation is particularly notable for Dec2,6+3S. It should be noted that these observations were made on a weight basis. The EC₅₀ values (given in Figure 38), however, interestingly confirmed that Dec2,6+3S was effectively more potent than Hp for low concentrations (average of 10,000 Da for Hp versus 3,000-3,500 Da for the oligosaccharides). Above 8,000 ng/mL, the activation levels of the three species are relatively similar.

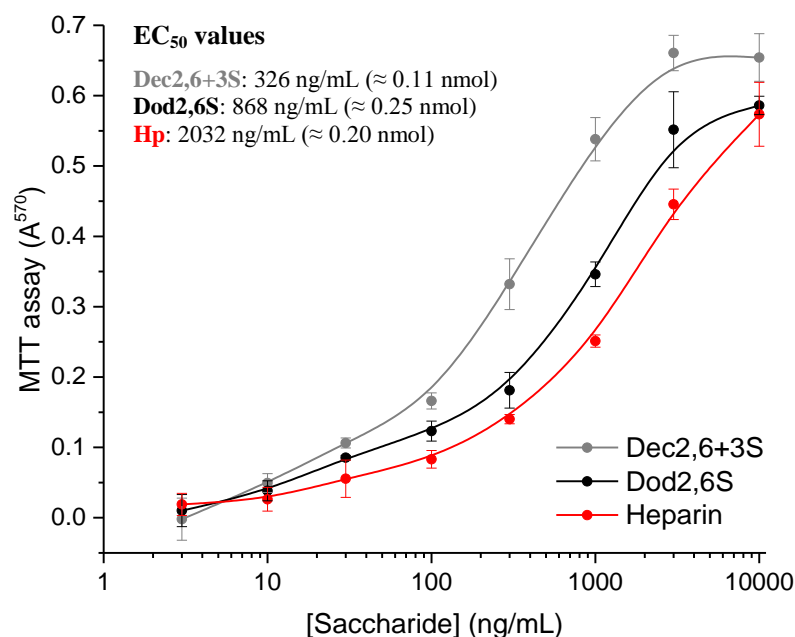


Figure 38: Dose response curves (mean \pm S.D.) for Dec2,6+3S and Dod2,6S activation of FGF1 signalling through FGFR1c. FGFR1c cells were treated with 1 nM FGF1 and were grown in the presence of full-length Hp (●), Dec2,6+3S (●) or Dod2,6S (●). Values are the mean of triplicate samples. The EC₅₀ values are also given.

5.3.2. Assessing the ability of Hp/HS oligosaccharides to induce FGF7 and FGF1 signalling through FGFR2b

The 19 compounds were next screened in bioassays involving FGF7-FGFR2b and FGF1-FGFR2b pairings. As for tests with FGF1/FGF2-FGFR1c, and prior to any activity screening, the response of the cells expressing FGFR2b in the presence of FGF7/FGF1 and of different concentrations of full-length Hp was assessed (Figure 39). The curves obtained were in agreement with previously published values (Ornitz *et al.* 1996).

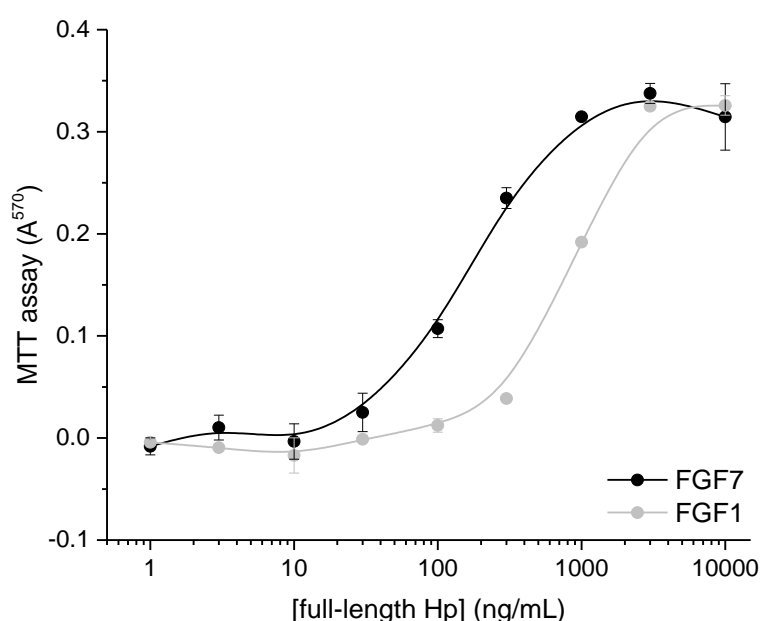


Figure 39: Dose response curves (mean \pm S.D.) for full-length Hp activation of FGF7 (3 nM) and FGF1 (1 nM) signalling through FGFR2b. Values are the mean of triplicate samples.

The activity of the saccharides alone (cells in growth medium and in the presence of the oligosaccharides) was also assessed. Responses to Hp/HS saccharides alone (cells in growth medium and in the presence of the oligosaccharides) were identical to the background controls (cells in BaF3 growth medium) (Figure 40).

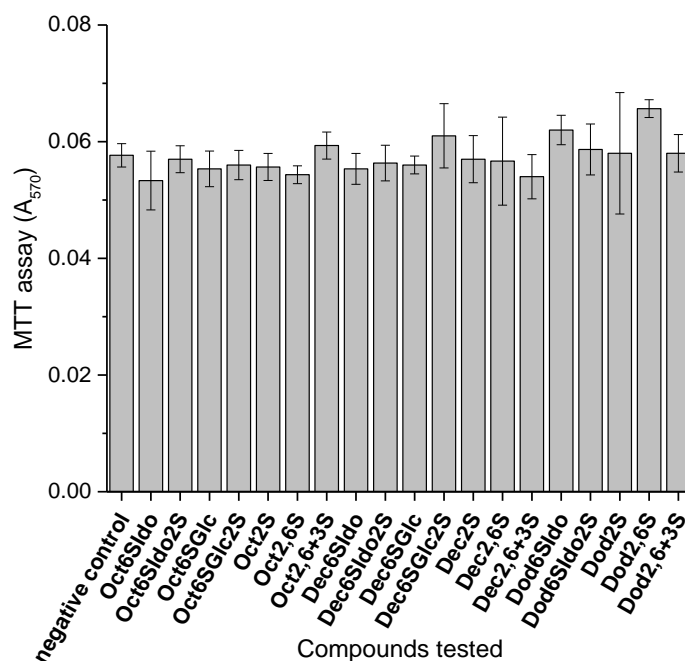


Figure 40: Evaluating the bioactivity of the compounds alone at 3 µg/mL in bioassays with cells expressing FGFR2b. The negative control refers to the cells in BaF3 medium only (background). The values are the mean of triplicate samples and the error bars represent the standard deviation (S.D.).

Statistical tests were also performed with these FGF-FGFR combinations (one-sample t-tests (one tailed)) to determine whether the relative activities of the compounds were higher than 5%, 50% or 100% activity (relative to full-length Hp). The results are listed in Table 12. Selected compounds were also compared using a two-sided t-test.

As previously observed for FGF2-FGFR1c and FGF1-FGFR1c, at the fixed concentration of 3 µg/mL, the oligosaccharides displayed various levels of activation, ranging from no activation (less than 5%, relative to full-length Hp - e.g. Dec2S and Dod2S) to high level of activation (higher than 50% but lower than 100%, relative to full-length Hp - e.g., Oct2,6+3S, Dec2,6+3S and Dod2,6+3S) (Figure 41).

In the case of FGF7-FGFR2b (Figure 41 (a)), it clearly appeared that none of the 19 compounds were able to stimulate the mitogenic activity as efficiently as full-length Hp. Only a total of 4 oligosaccharides (Dec2,6S, Dec2,6+3S, Dod2,6S and Dod2,6+3S) were able to support FGF7 signalling. The 3 most active structures (Dec2,6+3S, Dod2,6S and Dod2,6+3S) displayed activation levels significantly higher than the 5% threshold only. Comparatively, the activity levels of the compounds which were the most active for FGF1-FGFR2b (Figure 41 (b)) were significantly higher (relative to 50% level). Two-sided t-tests showed that a significant difference could be observed between Dec2,6S and Dec2,6+3S ($t_{2,298} = -5.839$, $p = 0.020$) and between Dod2,6S and Dod2,6+3S ($t_{3,774} = -8.532$, $p = 0.001$). However, no significant difference was observed between Oct2,6S and Oct2,6+3S.

In the case of the FGF1-FGFR2b pairing, Oct2,6S, Oct2,6+3S, Dec2,6S, Dec2,6+3S, Dod2,6S and Dod2,6+3S were capable of supporting FGF1 signalling through FGFR2b. Amongst those active oligosaccharides, Oct2,6S was the only one displaying a rather low level of activation (about 20%). Two-sided t-tests showed that a significant difference could be observed between Oct2,6S and Oct2,6+3S ($t_{2,995} = -10.682$, $p = 0.002$) only. No significant difference was observed between Dec2,6S and Dec2,6+3S and between Dod2,6S and Dod2,6+3S. For the FGF7-FGFR2b pairing, no oligosaccharide was as active as Hp, whereas for FGF1-FGFR2b, the 4 most potent saccharides displayed the same activity as Hp.

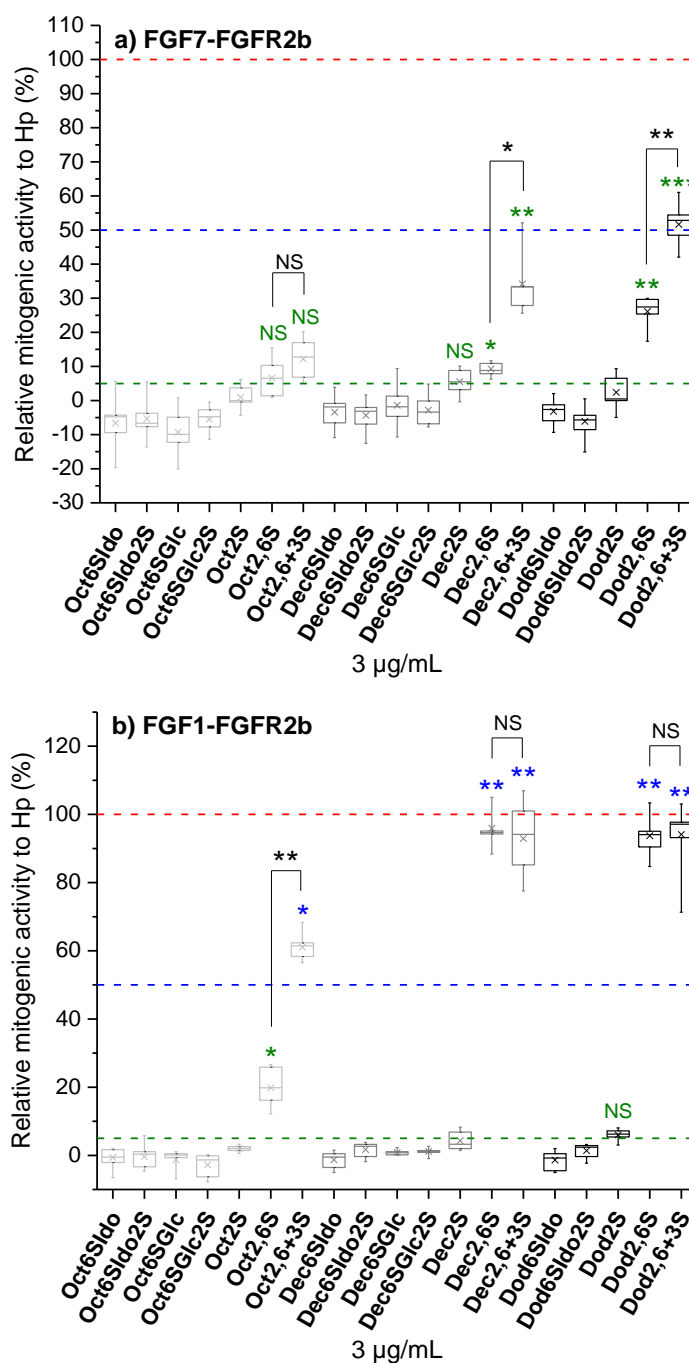


Figure 41: Assessing the capability of Hp/HS oligosaccharides (at 3 µg/mL) to regulate (a) FGF7 (3 nM) and (b) FGF1 (1 nM) signalling through FGFR2b. The relative mitogenic activities (N=9) were expressed as a percentage of the Hp control and plotted as box plots. Box plots show median (horizontal line), 25th and 75th percentiles (edges of the box), minimum and maximum values (whiskers) and mean (cross). The activities were tested using a one-sample t-test (N=3) to determine if their relative activities were significantly higher than the reference values: 5% (**green**), 50% (**blue**) and 100% (**red**) (all reference values are relative to full-length Hp); Selected compounds were also tested using two-sided t-test (N=3) (**black**); *p<0.05; **p<0.01; ***p<0.001; NS: non-significant (p≥0.05). Oligosaccharides are categorised as follows: octa- (light grey boxes), deca- (grey boxes), dodeca-saccharides (black boxes).

Oligosaccharide	FGF7-FGFR2b					FGF1-FGFR2b				
	Relative mitogenic activity (%, mean±S.D.)	Reference value (% activity)	t	Degree of freedom	p value	Relative mitogenic activity (%, mean±S.D.)	Reference value (% activity)	t	Degree of freedom	p value
Oct2,6S	-	-	-	-	-	19.8 ±5.9	5	4.31	2	0.025*
Oct2,6+3S	-	-	-	-	-	61.1 ±3.1	50	6.25	2	0.012*
Dec2,6S	9.3 ±1.9	5	3.81	2	0.031*	95.9 ±4.1	50	19.62	2	0.001**
Dec2,6+3S	34.2 ±7.1	5	7.10	2	0.009**	92.9 ±10.6	50	7.03	2	0.009**
Dod2,6S	26.1 ±4.1	5	8.93	2	0.006**	93.7 ±5.4	50	14.09	2	0.003**
Dod2,6+3S	51.6 ±3.2	5	25.35	2	0.001***	94.1 ±6.6	50	11.51	2	0.004**

Table 12: Results of one-sample t-tests (one-tailed, N=3) for FGF7-FGFR2b and FGF1-FGFR2b. Compounds were tested using one-sample t-tests to determine if their relative activities were higher than the reference values 5% (**green**), 50% (**blue**) and 100% (**red**) relative activity (relative to Hp) .Compounds that are not shown were not significantly higher than the 5% reference value (threshold for minimum activity). *p<0.05; **p<0.01; ***p<0.001.

5.4. Discussion

The work presented here was aimed at providing insights into the interactions between HS, FGF and FGFR. To do so, the impact of several degrees of structural changes on the ability of HS saccharides to activate specific FGF-FGFR complexes was evaluated. Deciphering the molecular mechanisms that regulate these interactions will help understand the role of HS in biological processes in which FGF and FGFR are involved (reviewed in Ornitz and Itoh (2015)).

To study HS structure-activity relationships (SAR), 19 chemically and chemoenzymatically prepared oligosaccharides of different sizes (ranging from octa- to dodeca-saccharides) and displaying various structural features were tested in BaF3 assays. Several conclusions could be drawn from the activity screenings of these compounds (the results are summarised in Table 13).

First of all, only a certain number of structures were shown to be activators whereas the majority did not show any ability to support activation at signalling. Interestingly, all the saccharides composed of *N*-acetylated glucosamine and unsulphated uronic acid residues only were unable to support FGF signalling (these compounds are coloured in grey in Table 13). This might be explained by the fact that these oligosaccharides lack two important structural features, which are thought to be crucial for both HS-FGF and HS-FGFR interactions: the *N*-sulphate groups and the 2-*O*-sulphated iduronic acid residues (Turnbull *et al.* 1992, Guimond *et al.* 1993, Maccarana *et al.* 1993, Walker *et al.* 1994, Pye *et al.* 2000). Hence, the data here with fully defined saccharides confirm these basic structural requirements.

Secondly, the active compounds were clearly shown to be active in an FGF-FGFR complex-specific manner (e.g., Oct2,6+3S activates FGF1-FGFR1c and FGF1-FGFR2b complexes but does not activate FGF2-FGFR1c and FGF7-FGFR2b complexes, as shown in Table 13). This is in agreement with a number of studies published using complex Hp and HS mixtures or partially purified saccharides which demonstrated that each FGF-FGFR system may differ in their specific HS structural determinants to be activated (Guimond *et al.* 1993, Guimond and Turnbull 1999, Pye *et al.* 2000, Ye *et al.* 2001, Ostrovsky *et al.* 2002, Powell *et al.* 2002).

		FGF-FGFR complex				Legend
		FGF2 FGFR1c (±S.D.)	FGF1 FGFR1c (±S.D.)	FGF1 FGFR2b (±S.D.)	FGF7 FGFR2b (±S.D.)	
S A C C H A R I D E S	Oct6SIdo	-4.76 ±1.1	0.61 ±1.1	-0.62 ±2.8	-6.62 ±2.2	
	Oct6SIdo2S	-6.89 ±2.6	0.12 ±3.7	-0.43 ±3.2	-5.32 ±2.4	131-140%
	Oct6SGlc	-5.56 ±2.8	0.56 ±0.5	-1.28 ±2.9	-9.29 ±5.5	121-130%
	Oct6SGlc2S	-2.21 ±3.1	-0.43 ±2.0	-2.75 ±3.8	-5.52 ±3.0	111-120%
	Oct2S	-16.23 ±8.6	2.79 ±5.1	2.00 ±0.4	0.90 ±2.2	101-110%
	Oct2,6S	-13.85 ±10.3	17.87 ±6.3	19.81 ±5.9	6.60 ±4.3	91-100%
	Oct2,6+3S	-5.91 ±7.6	97.89 ±14.9	61.08 ±3.1	12.17 ±5.5	81-90%
	Dec6SIdo	-1.29 ±1.8	1.35 ±1.0	-1.27 ±2.6	-3.43 ±4.9	71-80%
	Dec6SIdo2S	-0.67 ±0.6	4.24 ±2.9	1.71 ±2.4	-4.35 ±3.4	61-70%
	Dec6SGlc	-1.82 ±1.8	2.87 ±0.7	0.84 ±0.4	-1.36 ±4.4	51-60%
	Dec6SGlc2S	1.52 ±2.5	2.44 ±1.1	1.16 ±0.7	-2.82 ±1.8	41-50%
	Dec2S	-15.04 ±6.4	5.07 ±5.7	4.29 ±2.8	5.54 ±2.6	31-40%
	Dec2,6S	84.48 ±2.4	79.88 ±3.2	95.92 ±4.1	9.29 ±2.0	21-30%
	Dec2,6+3S	89.61 ±15.6	136.56 ±16.8	92.93 ±10.6	34.20 ±7.1	11-20%
	Dod6SIdo	-6.73 ±2.2	1.21 ±1.0	-1.36 ±2.9	-3.17 ±2.4	5-10%
	Dod6SIdo2S	-1.72 ±2.5	5.46 ±2.8	1.40 ±2.3	-6.09 ±0.7	-20-4%
	Dod2S	-17.25 ±6.5	10.99 ±4.7	6.01 ±1.5	2.40 ±5.3	
	Dod2,6S	88.66 ±16.1	124.64 ±12.8	93.76 ±5.4	26.09 ±4.1	
	Dod2,6+3S	89.67 ±5.2	110.56 ±14.5	94.10 ±6.6	51.63 ±3.2	

Table 13: Summary of the ability of the Hp/HS oligosaccharides to activate FGF-FGFR complexes. The relative activities are given as a percentage (mean ± S.D.) of the Hp control. The saccharides are categorised as follow: chemically synthesised (grey) and chemoenzymatically synthesised (green).

The observed differences in levels of activation can be explained by two main factors: the size of the oligosaccharides and their sulphation/acetylation patterns. It is clear from the data that FGF1, independently of the receptor type, does not require long saccharides to signal, in contrast with FGF2 and FGF7. This is illustrated by the fact that FGF1-FGFR1c and FGF1-FGFR2b complexes were shown to be activated by oligosaccharides as small as octasaccharides (Oct2,6+3S) whereas FGF2-FGFR1c and FGF7-FGFR2b required longer saccharides (e.g., Dec2,6S) to achieve significant levels of activation (e.g., decasaccharides Dec2,6S for FGF2 and dodecasaccharide Dod2,6+3S for FGF7). The results obtained are in partial agreement with some published studies: Ostrovsky *et al.* (2002) suggested that both FGF7-FGFR2b and FGF1-FGFR1c might require long saccharides to be stimulated whereas Ornitz *et al.* (1995) showed that both FGF1 and FGF2 signalling through FGFR1c can be stimulated by saccharides as small as di- and tri-saccharides. The latter study has always been controversial and has never been repeated (Delehedde *et al.* (2002), Wu *et al.* (2003), J. Turnbull, personal communication). In contrast with Ornitz's findings, FGF2-FGFR1c stimulation could not be achieved by saccharides smaller than decasaccharides in this study. In some studies, fully sulphated Hp hexasaccharides have been shown to activate FGF signalling, but only at high doses compared to those required for more optimal structures such as full-length Hp (Delehedde *et al.* 2002, Ostrovsky *et al.* 2002). Thus, it may be possible for some activity to occur with sub-optimal saccharides at high concentrations.

In addition to the lengths of the saccharides, the ionic charges also play an important role in the activation of the complex (Ori *et al.* 2008). The importance of the 6-*O*-sulphate groups for FGF signalling, which has already been reported for FGF1 and FGF2 and FGFR using modified Hp and HS saccharide mixtures (Guimond *et al.* 1993, Pye *et al.* 1998, 2000, Powell *et al.* 2002), was clearly confirmed here using fully defined Hp/HS saccharides. Drastic changes in terms of activation were observed between 6-*O*-unsulphated oligosaccharides and fully 6-*O*-sulphated oligosaccharides (e.g. Oct2S, Dec2S and Dod2S were completely inactive whereas Oct2,6S, Dec2,6S and Dod2,6S were generally active at varying degrees).

Importantly, the role of 3-*O*-sulphation was also assessed here with defined saccharides for the first time. Interestingly, the addition of a single 3-*O*-sulphate group towards the non-reducing end of the saccharides appeared to have important consequences in terms of activation in some specific cases, resulting in very significant enhancement in activity. More specifically, this effect was observed for Oct2,6+3S for FGF1 signalling through both FGFR1c and FGFR2b, Dec2,6+3S for FGF1-FGFR1c and FGF7-FGFR2b and finally for Dod2,6+3S for FGF7-FGFR2b. This activity enhancement was clearly dependent on context, such as saccharide size. For example, for FGF1-FGFR2b, the addition of a 3-*O*-sulphate onto the *N*-, 2-*O*- and 6-*O*-sulphated backbone of the octasaccharide boosted activity, whereas for the equivalent deca- and dodeca-saccharides, it resulted in no additional activity. The role of 3-*O*-sulphation has long been discussed, but has been under evaluated. This has, however, changed since the publication of studies assessing its role for antithrombic activity (Walenga *et al.* 1988, Guerrini *et al.* 2013) and for herpes simplex virus 1 entry (Shukla *et al.* 1999, O'Donnell *et al.* 2006, Hu *et al.* 2011), to name a few. To the author's knowledge, the role of 3-*O*-sulphation for FGF-FGFR binding/signalling has previously been suggested only through indirect evidence. McKeehan *et al.* (1999) and Ye *et al.* (2001) showed that only Hp fractions having high affinity for antithrombin III (by implication containing 3-*O*-sulphated residues) were able to bind FGFR1c, were able to support FGF1 and FGF2 activity or even FGF1-induced DNA synthesis. Luo *et al.* (2006a, 2006b) suggested that saccharides bearing 3-*O*-sulphate groups may protect FGF7 from proteolysis and also induce FGF7 binding/signalling. On the other hand, Wu *et al.* (2003) reported in their study that oligosaccharides/full-length Hp bearing 3-*O*-sulphate groups may help in the formation of FGF1-FGFR1c-HS ternary complexes, and therefore may help in stimulating FGF1 signalling. Recent biological studies have implicated 3-*O*-sulphation as important for regulating FGF10-FGFR2b signalling in salivary gland development (Patel *et al.* 2014). However, for all the studies cited above, the exact structures of the oligosaccharides were unknown and the authors solely suggested that the 3-*O*-sulphate groups may have a significant impact on Hp/HS activities. Here, the role of those rare 3-*O*-sulphate groups has been clearly demonstrated and linked to high levels of FGF signalling through FGFR1c and FGFR2b for FGF1 and through FGFR2b for FGF7, but not for FGF2 through FGFR1c.

The abilities of the oligosaccharides to stimulate FGF signalling were assessed using BaF3 assays. In such bioassay, the mitogenic activity is proportional to the activity of the FGF-FGFR complex and, therefore, to the ability of the oligosaccharide to stimulate FGF signalling (Ornitz *et al.* 1992). It also permits the comparison of the mitogenic activities of different FGF-FGFR complexes. The BaF3 assay has been used in many studies and is well known and appreciated for allowing the screening of multiple compounds at once, requiring relatively small amounts of material (about 5 µg of compounds are enough to carry out the assays in triplicates), for being cheap, fairly fast and reliable (Ornitz *et al.* 1996, Guimond and Turnbull 1999, Zhang *et al.* 2006). However, it does not allow truly high throughput screening of oligosaccharides, which considerably hampers the fast and meticulous study of HS SAR. Sterner *et al.* (2013) recently developed a BaF3 cell-based microarray platform which could grant the high throughput screening of all types of FGF-FGFR systems (Sterner *et al.* 2014). This might be useful in future studies as larger libraries of defined HS saccharides become available.

The oligosaccharides, which were screened in this study, were selected for specific reasons. Using such compounds indeed offered two major advantages, compared to extracted and partially purified HS saccharides. First, a rather large quantity of material was readily available (about 100 µg was used here). This allowed the replication of the bioassays during this study (compared to, e.g., the amounts collected by enzymatic digestion of PMHS, as described in Chapter 3). Secondly, such compounds are, by definition, structurally fully defined. The position and nature of each residue and chemical moiety is known with precision. Therefore, this provided the possibility to begin to assess the effect of different parameters such as the oligosaccharide size, the sulphation pattern or the presence of specific residues on FGF signalling. Further studies are however required to have a better overview of the SAR of HS in FGF signalling, including the screening of larger libraries. A broader diversity and less homogeneity of the compounds would also be appreciated. Finally, it was observed in this study that some oligosaccharides (e.g., Oct6SIdo2S, Oct6SGlc, Dec6SIdo and Dod6SIdo2S) were showing negative relative activities. Carrying out well-designed inhibitory assays in the future would also give better insights into FGF-FGFR-HS interactions (Guimond and Turnbull 1999).

Differences in activation were indeed observed and related to the presence or absence of specific structural features, a number of which were consistent with previous studies using heterogeneous Hp and HS saccharides. Perhaps most notably, the presence of a single 3-*O*-sulphate group towards the non-reducing end of the oligosaccharides resulted in a significant increase of activation for FGF1-FGFR1c, FGF1-FGFR2b and FGF7-FGFR2b. Taken, together; the results clearly showed that FGF signalling may be regulated by some level of specificity and this provides a better understanding of the underlying rules governing how HS regulates FGF signalling. Understanding these rules in more detail is essential for the development of targeted HS-based drugs which could be developed for many diseases to which FGF and FGFR have been linked.

6. Chapter 6 – General Discussion and Future Directions

- **Specificity/selectivity of HS in FGF signalling is regulated by both general and subtle structural changes**

Biomolecular interactions are key components of a living organism's integrity and fate as they govern all its biological processes. Understanding how these interactions, driven by molecular recognition, are regulated is crucial to comprehend the functions of the biomolecules involved in the biological processes. Amongst the interacting biomolecules, the paracrine fibroblast growth factors (FGFs), which signal through their receptors (FGFRs) located at the cell membrane, are key players in many biological processes including developmental and physiological processes, as well as organogenesis (Beenken and Mohammadi 2009, Goetz and Mohammadi 2013, Li, Wang, *et al.* 2016). Paracrine FGF signalling is regulated by heparan sulphate (HS), a polysulphated polysaccharide which was found to govern the activity of a substantial number of proteins (Lamanna *et al.* 2007, Ori *et al.* 2008). FGF signalling is thought to depend on the formation of the ternary complex FGF-FGFR-HS (Klagsbrun and Baird 1991, Rapraeger *et al.* 1991, Yayon *et al.* 1991) and any malfunction of FGF or FGFR may lead to serious disorders, such as cancers and skeletal defects (Eswarakumar *et al.* 2005, Beenken and Mohammadi 2009, Jorgen *et al.* 2011, Ornitz and Itoh 2015). One possible route for treating diseases involving aberrant signalling may be HS saccharides, since they regulate FGF-FGFR interactions. In order to be able to develop HS-based drugs, but also to have a better understanding of the general molecular mechanisms underlying HS-protein interactions, it is essential to unravel the structure-activity relationships (SAR) of HS. Over the decades, a lot of attention has been brought to the study of FGF-FGFR-HS interactions (reviewed in Goetz and Mohammadi (2013); Pomin (2016)), yet, they still remain elusive. More specifically, the structural features that are required for optimal binding and functional activity, and how those two are inter-related, remain rather unclear and are at the heart of an ongoing debate. Some suggest that the ability of HS to activate the proteins is due to the fine structures of the saccharides, particularly the discrete and specific distribution of their anionic moieties (Guimond and Turnbull 1999, Pye *et al.* 2000, Nakato and Kimata 2002), whereas others suggest that it is due to the general structural layout of the glycans and not to fine structural differences (Kreuger *et al.* 2005, Jastrebova *et al.* 2006).

In order to gain a better insight into FGF-FGFR-HS interactions, and more particularly, to determine to what extent FGF signalling is governed in a specific/selective manner, HS oligosaccharides of varying sizes and motifs were screened in bioassays. These assays resulted in the identification of multiple parameters that may have a crucial impact on FGF signalling, including the size of the saccharides (as a first approximation, the longer the more potent), the *N*-sulphate groups and the 2-*O*-sulphation of the iduronic acids, as well as the 6-*O*-sulphate groups (as already described in many studies: e.g., (Ornitz *et al.* 1992, Turnbull *et al.* 1992, Wu *et al.* 2003, Zhang, Zhang, *et al.* 2009)). Importantly, the presence of a single 3-*O*-sulphate group towards the non-reducing end of the saccharides was shown to significantly increase the mitogenic activity for specific complexes (namely FGF1-FGFR1C, FGF1-FGFR2b and FGF7-FGFR2b) but not for FGF2-FGFR1c. These findings therefore highlighted the importance of both general and subtle structural changes on the ability of the saccharide to support FGF signalling and also showed that they were dependent on the particular ligand and receptor involved.

- **The generation of HS oligosaccharides remains a challenge**

This study employed two main strategies to prepare the HS oligosaccharides that are required for the reductionist approach, which consists of the use of oligosaccharides rather than full-length polysaccharide chains for biochemical and biophysical experiments. The use of shorter saccharides greatly facilitates the studies of HS-FGF-FGFR interactions by reducing the compound's complexity, as native HS is a highly complex polyfunctional saccharide (Stringer and Gallagher 1997). The two main strategies used here are: the extraction of natural, tissue-derived, HS chains and their modification (upstream approach) and the chemical preparation of HS chains from monosaccharides (downstream approach). The combination of both strategies could, in theory, have resulted in an extensive library of oligosaccharides to be screened in bioassays.

The upstream approach is well known for granting rather quick access to broad oligosaccharide libraries to be screened in bioassays (Powell *et al.* 2010). A major issue however lies in the fact that there is limited control over the structures that can be isolated, dependent on the content and diversity of the source material, and the

method (enzymatic or chemical) used to cleave the HS chains to saccharides. Also, the resulting structures are initially unknown, requiring sequencing of the saccharides to be performed at the end of the purification process. Sequencing is still difficult, even with recent advances in mass spectrometry approaches, and requires pure compounds to be effectively carried out. In addition, the lack of fast and efficient methods for sequencing means that exact structures cannot always be fully established, and often, only disaccharide composition analysis is performed (Ashikari-Hada *et al.* 2004, Zhang, Zhang, *et al.* 2009). Moreover, this approach grants access to very restricted amounts of material (typically of the order of low μg quantities), which can seriously hamper the downstream screening and analysis. Although in general the production of very low amounts of compounds is not a major issue for BaF3 bioassays, since they only require a few μg of compound (Guimond *et al.* 2009), the risk of losing material during purification is high, as shown during the CTA-SAX purification step in this study (Chapter 3), and can result in a lack of sufficient material for analysis and further applications. Ultimately, even though the upstream approach has led to major breakthroughs (Ornitz *et al.* 1992, 1995, Guimond *et al.* 1993, Guimond and Turnbull 1999), the exclusive use of compounds isolated from animal tissues currently limits the meticulous study of HS SAR, which requires broad libraries of structurally well-defined structures. This may be addressed in the future by access to larger amounts of starting material, for example from heparin manufacturing by-products (S. Taylor and J. Turnbull, personal communication), and scaling-up of the generation and purification of HS saccharides.

As an alternative, the chemical synthesis of HS octasaccharides was also attempted here (downstream approach). Chemical synthesis, which theoretically can lead to the preparation of all types of compounds (including non-natural ones), grants control over the structures that are prepared through synthetic strategy design and monitoring throughout the preparation process by means of mass spectrometry and NMR. Rather large quantities of material can be synthesised (up to hundreds of mg), allowing their study in many biochemical and biophysical approaches. However, the synthetic pathways are rather long, owing to the extensive manipulation of protective groups. In addition, efficient coupling reactions are often complicated to achieved, due to the presence of low reactive L-iduronic acid residues (Polat and Wong 2007) or the

impossibility of controlling all the parameters (including temperature, reagent concentrations, similarity of the glycosyl synthon reactivities, etc.).

Owing to the discussed complications of the methods used here (Chapters 3 and 4), the saccharides produced in this study were not suitable for exploring HS SAR in FGF signalling. Therefore, compounds produced by Prof. Liu and Prof. Tyler for other studies (Schwörer *et al.* 2013, Xu *et al.* 2014), by means of chemical and chemoenzymatic syntheses, were explored in further studies here. Like the chemical synthesis, both enzymatic and chemoenzymatic methods are robust solutions (downstream approach) to prepare HS oligosaccharides (Kuberan *et al.* 2003, Liu *et al.* 2010, Liu and Linhardt 2014) and resulted in a library of well-defined oligosaccharides with interesting, and in some cases, systematic variations in structure. Yet, some issues still need to be addressed, such as the high substrate selectivity of the enzymes (which are not yet well characterised) and the limited life-time of the enzymes, amongst others.

It is to be noted that the use of short saccharides is a reductionist approach and may lead to loss of biological information compared to HS saccharides within intact HS chains. This possible loss of information may be due to the fact that many parameters may impact the three-dimensional structure of the saccharides when constrained within a HS chain (e.g., the sulphate groups can alter the glycosidic linkages' variations and the thermodynamics of protein binding (Rudd and Yates 2010)). However, these effects may be rather localised and not spread throughout the glycan chain, limiting the possible loss of information when working with oligosaccharides. Even more, the use of oligosaccharides greatly reduced the number of possible epitopes compared to the diversity found in intact chains. However, oligosaccharides can be fully structurally defined which allows for a better precise assessment of the role of each structural feature onto the activity of the saccharides, in contrast to full-length HS.

- **Bioassays are powerful tools to decipher specificity/selectivity in FGF signalling**

Defined HS saccharide compounds were screened in BaF3 bioassays to assess their ability to stimulate FGF signalling. BaF3 bioassay is a well-known cheap and robust

method, which has been used extensively for studying the interactions of HS with FGF and FGFR by measuring the mitogenic activity (Ornitz *et al.* 1992, Powell *et al.* 2002, Wu *et al.* 2003, Sterner *et al.* 2013). The results which were obtained in this study clearly showed that specificity/selectivity regulates HS-FGF-FGFR interactions at the functional, cellular level and that both general and subtle structural modifications play a role in this phenomenon. In particular, this study highlighted the impact of a single 3-*O*-sulphate group towards the non-reducing end of the saccharides on the mitogenic activity of FGF1 on BaF3 cells expressing FGFR1c and FGFR2b and of FGF7 on cells expressing FGFR2b. However, it should be noted that these observations are based on the screening of a limited number of structures with limited variations, typically being mainly homogeneous repeat sequences. For example, owing to the limitations which hamper the production methods of saccharides (as mentioned earlier), it was not possible to prepare regioisomers of the screened structures to determine whether the position of the 3-*O*-sulphate group was crucial or not. For the same reasons, it was not possible to study whether the introduction of another type of sulphate group would have had the same impact or not (e.g., by performing the substitution of the non-sulphated glucuronic acid at the non-reducing end with a sulphated iduronic acid residue). Therefore, extra caution should be taken to avoid overgeneralisation of the results based on those obtained from activity screenings. To further extend the interesting results obtained here, systematic studies could be conducted on a more comprehensive library. However, owing to the lack of high throughput methods of synthesis, such studies are not yet possible via full chemical synthesis. The chemoenzymatic approach is increasingly generating larger libraries, but with the caveat that diversity that can be incorporated is still limited by the specificity of the enzymes used. Nonetheless, activity screening remains a powerful tool to aid in the accumulation of a significant amount of data on specific questions regarding HS biological functions. For the selected library of compounds studied here, the effects of subtle modifications provide important insights into HS SAR in FGF signalling. The data accumulated from these bioassays could lead ultimately to a better understanding of the interactions of HS with FGF and FGFR.

- **But bioassays only give a truncated picture of FGF-FGFR-HS interactions**

Even though activity assays are powerful tools, they should, however, not be considered as the only source of information to decipher HS SAR in FGF signalling. Other aspects must be taken into consideration. The role of HS saccharide sulphation patterns were first thought to be the key to high level of FGF activity as many studies suggested that 2-*O*-, 6-*O*- and *N*-sulphate groups are essential for effective FGF binding and activity (Turnbull *et al.* 1992, Maccarana *et al.* 1993, Ashikari-Hada *et al.* 2004, Zhang, Zhang, *et al.* 2009). In recent years, many other factors such as the nature of the solvent/counter ions, the plasticity of the iduronic acid residues have also been shown to play a role in the regulation of the interactions of HS with its protein ligands (as previously mentioned), therefore indicating that the sulphation pattern is not solely responsible for high levels of activation. Some factors (e.g. the sulphation pattern and the plasticity of the L-iduronic acid residues (Guglieri *et al.* 2008)) have also been shown to impact one another, resulting in another level of complexity for the study of HS-FGF-FGFR interactions. Alongside bioassays, other types of biochemical and biophysical analyses would therefore be useful to better understand the molecular mechanisms underlying FGF signalling. On the one hand, binding assays are another popular method to study HS-FGF-FGFR interactions (Ornitz *et al.* 1995, Rahmoune *et al.* 1998, Noti *et al.* 2006, Zhang, Zhang, *et al.* 2009). However, assessing the ability of HS saccharides to simply bind FGF, FGFR and FGF-FGFR complexes does not necessarily provide a direct understanding of the structural determinants for activating FGF signalling. The situation is indeed rather complex, with many HS saccharides binding to proteins, but only a subset of these showing functional activity (Guimond and Turnbull (1999); Powell *et al.* (2004); Y. Ahmed and J. Turnbull, personal communication). Hence, the relationship between binding and activity is not simple. Indeed, some saccharides may also negatively regulate FGF signalling, as suggested by some data here, and this aspect requires future investigation.

On the other hand, running molecular dynamics simulations or carrying out NMR analyses, with a selection of the oligosaccharides that were screened in this study, may offer the possibility of obtaining a better insight into the interactions at the

molecular level. In the present study, most of the compounds which were able to stimulate high levels of FGF signalling were slightly more enriched in sulphate groups at the non-reducing end than at the reducing end of the chains. This rather supports the symmetric model rather than the asymmetric model, as it is thought that for the symmetric configuration, the proteins interact with the non-reducing ends of the two saccharide chains (Harmer *et al.* 2004, Ibrahimi *et al.* 2005, Wu and Lech 2005, Naimy *et al.* 2011, Brown *et al.* 2013, Nieto *et al.* 2013, Sterner *et al.* 2014) (see also Section 1.7.3, Figure 7). This could contribute to the decision of which model could be used for molecular dynamics simulations. Beyond the study of HS SAR in FGF signalling, the results of the present study may also provide a better insight into the formation of the functional complex, providing candidate structures for interaction and modelling studies.

• Conclusions

During this study, differences in FGF activation were detected and linked to the presence or absence of specific structural features borne by HS saccharides. More specifically, the presence of a single 3-*O*-sulphate group towards the non-reducing end of the oligosaccharides resulted in a significant increase of activation for FGF1-FGFR1c, FGF1-FGFR2b and FGF7-FGFR2b. This indicated that a certain degree of specificity may regulate FGF signalling.

The notion of specificity/selectivity is still at the heart of an intensive debate, owing to the abundance of contradictory data that has been gathered, and its contradictory interpretation, over the last years. This is also partly dependent on how these terms are defined. To illustrate this debate, both Antithrombin III and thrombin are often referred as the examples that respectively endorse the “high-specificity interactions” or the “non-specific interactions” theories (Mosier *et al.* 2012). However, these two hypotheses rule out the many other examples where a certain degree of redundancy in the HS structures which regulate the proteins’ activities has clearly been observed (Meneghetti *et al.* 2015). This redundancy could be explained by appreciating the three-dimensional aspect of the HS saccharide chains, rather than just their primary and linear structural layout and their substitution patterns only. The observed plasticity of the saccharides, which has been shown to be modelled by different

parameters (sulphate groups, glycosidic bonds, counter ions, etc.), as previously mentioned, may explain why compounds of various sizes and various substitution patterns may serve to stimulate protein activities in a similar fashion. Thus, two structurally different saccharides may stimulate a protein activity in a similar fashion, as the differences of flexibility between the two sequences would lead to a similar projection of the functional moieties of the saccharides towards the amino acids of the protein.

HS, its biosynthesis, distribution within tissues and interactions with its protein ligands have been extensively studied over recent decades. Despite being template-free driven, HS biosynthesis is strongly thought to be regulated (Chapter 1). This is mainly supported by the structural variations of HS chains that have been observed and which depend on the nature, the maturity and the state (healthy/diseased) of the tissues (Maccarana *et al.* 1996, Cheng *et al.* 2001, Netelenbos *et al.* 2001, Allen and Rapraeger 2003, Ledin *et al.* 2004). The structures of the HS extracted from the same tissues have, however, been shown to be consistent amongst individuals (Ledin *et al.* 2004). On the other hand, HS interactions with proteins are thought to be regulated by some degree of specificity/selectivity, mainly through the spatial distribution of the sulphate moieties, as demonstrated in this study. Finally, these two observations support the notion of HS being a dynamically modulated system for controlling protein functions (Figure 42). Therefore, some hierarchy, mainly in terms of sulphation and epimerisation, could also be established. The formation of the *N*-sulphated domains and the epimerisation of the D-glucuronic acid residues would serve as a template for creating core backbone structural patterns, which can then be further tuned via sulphation (2-*O*-, 6-*O*- and 3-*O*-sulphation steps). The extracellular tuning of the sequences would finally be further remodelled by the action of the two 6-*O*-sulphatases. This hypothesis was supported in this study, with the significant increase of activity caused particularly by the addition of 6-*O*- and 3-*O*-sulphate groups for most of the ligand-receptor pairings.

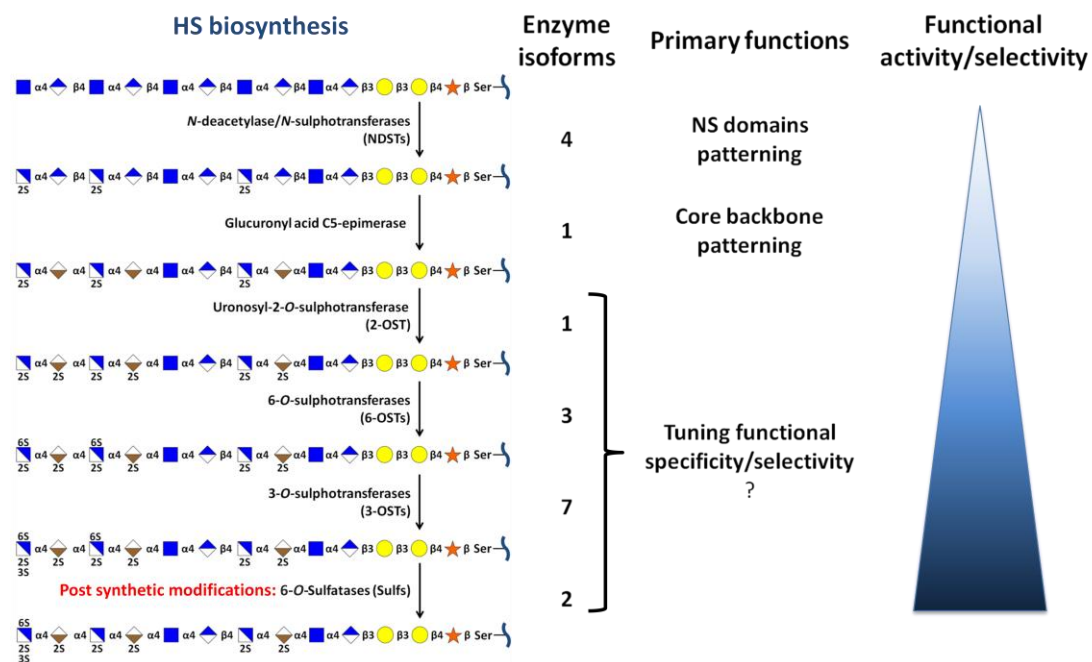


Figure 42: Hierarchical regulatory system – Sulphation and remodelling versus diversity and functional impact.

In addition to the disputed notion of specificity/selectivity, other questions remain to be answered. As a matter of example, differences in levels of interactions are usually observed in binding/activity assays, with compounds that are more active than others, as seen in the present project at the functional level. It has been shown, that HS interacts with its protein ligands mainly through anionic interactions (Rabenstein 2002) and that the different conformations adopted by the L-iduronic acid residues allow the anionic moieties as well as the hydroxyl hydrogens to be presented to the protein's amino acids in different ways, in order to favour stronger electrostatic interactions (Das *et al.* 2001, Raman *et al.* 2003). In addition, HS saccharides are rather flexible glycans and HS-protein interactions may rely on the conformations adopted by the saccharide chains, as mentioned above, rather than the solely spatial distribution of the sulphate groups. Taking these elements into consideration, it could be hypothesised that the biosynthesis of HS could be performed in such a way that a “minimum conformational state” of the chain would be obtained. This minimum conformational state refers to the most basic conformation that is capable of supporting functional activity, in order to assure, in a broader context, the living organism's integrity. In addition, the addition/removal of sulphate groups would

enhance or inhibit the functional activity by locally modifying the conformation of the HS chain. This hypothesis could explain the differences in levels of activation that are observed in binding/activity assays.

Overall, the present study has provided important new insights into HS SAR in FGF signalling by demonstrating that both general and subtle changes may impact greatly the biological activity of these proteins and confirming specificities for different ligand-receptor pairings. Further studies are nonetheless required, due to the complexity that characterises HS-protein interactions, to provide further evidence on the molecular mechanisms underlying a wider range of HS-protein interactions. This is vital not only for fundamental perspectives, but also for the potential development of HS-based drugs.

7. References

- Ahmed, Y. A. M. A., 2010. Heparan sulfate-protein interactions: evidence for sulfate group-dependent selectivity.
- Ai, X., Do, A., Kusche-Gullberg, M., Lindahl, U., Lu, K., and Emerson Jr, C., 2006. Substrate specificity and domain functions of extracellular heparan sulfate 6-O-endosulfatases, QSulf1 and QSulf2. *The Journal of biological chemistry*, 281 (8), 4969.
- Aikawa, J., Grobe, K., Tsujimoto, M., and Esko, J., 2001. Multiple isozymes of heparan sulfate/heparin GlcNAc N-deacetylase/GlcN N-sulfotransferase. Structure and activity of the fourth member, NDST4. *The Journal of biological chemistry*, 276 (8), 5876.
- Allen, B. L. and Rapraeger, A. C., 2003. Spatial and temporal expression of heparan sulfate in mouse development regulates FGF and FGF receptor assembly. *The Journal of cell biology*, 163 (3), 637–648.
- Almond, A. and Sheehan, J., 2003. Predicting the molecular shape of polysaccharides from dynamic interactions with water. *Glycobiology*, 13 (4), 255.
- Arungundram, S., Al-Mafraji, K., Asong, J., Leach III, F. E., Amster, I. J., Venot, A., Turnbull, J. E., and Boons, G.-J., 2009. Modular Synthesis of Heparan Sulfate Oligosaccharides for Structure-Activity Relationship Studies. *Journal of the American Chemical Society*, 131 (47), 17394.
- Asada, M., Shinomiya, M., Suzuki, M., Honda, E., Sugimoto, R., Ikekita, M., and Imamura, T., 2009. Glycosaminoglycan affinity of the complete fibroblast growth factor family. *Biochimica et Biophysica Acta (BBA)-General Subjects*, 1790 (1), 40–48.
- Ashikari-Hada, S., Habuchi, H., Kariya, Y., Itoh, N., Reddi, A. H., and Kimata, K., 2004. Characterization of growth factor-binding structures in heparin/heparan sulfate using an octasaccharide library. *Journal of Biological Chemistry*, 279 (13), 12346–12354.
- Ashikari-Hada, S., Habuchi, H., Sugaya, N., Kobayashi, T., and Kimata, K., 2009. Specific inhibition of FGF-2 signaling with 2-O-sulfated octasaccharides of heparan sulfate. *Glycobiology*, 19 (6), 644–654.
- Atha, D. H., Lormeau, J. C., Petitou, M., Rosenberg, R. D., and Choay, J., 1985. Contribution of monosaccharide residues in heparin binding to antithrombin III. *Biochemistry*, 24 (23), 6723–9.
- Ayotte, L. and Perlin, A. S., 1986. Nmr spectroscopic observations related to the function of sulfate groups in heparin. Calcium binding vs. biological activity. *Carbohydrate research*, 145 (2), 267–277.
- Bäckström, G., Höök, M., Lindahl, U., Feingold, D., Malmström, A., Rodén, n L., and Jacobsson, I., 1979. Biosynthesis of heparin. Assay and properties of the microsomal uronosyl C-5 epimerase. *Journal of Biological Chemistry*, 254 (8),

2975–2982.

- Bai, X. and Esko, J. D., 1996. An animal cell mutant defective in heparan sulfate hexuronic acid 2-O-sulfation. *The Journal of biological chemistry*, 271 (30), 17711–7.
- Bandtlow, C. and Zimmermann, D., 2000. Proteoglycans in the developing brain: new conceptual insights for old proteins. *Physiological reviews*, 80 (4), 1267.
- Baráth, M., Hansen, S. U., Dalton, C. E., Jayson, G. C., Miller, G. J., and Gardiner, J. M., 2015. Modular synthesis of heparin-related tetra-, hexa- and octasaccharides with differential O-6 protections: programming for regiodefined 6-O-modifications. *Molecules*, 20 (4), 6167–6180.
- Barresi, F. and Hindsgaul, O., 1991. Synthesis of β -mannopyranosides by intramolecular aglycon delivery. *Journal of the American Chemical Society*, 113 (24), 9376–9377.
- Bates, C. M., 2007. Role of fibroblast growth factor receptor signaling in kidney development. *Pediatric Nephrology*, 22 (3), 343–349.
- Beenken, A. and Mohammadi, M., 2009. The FGF family: biology, pathophysiology and therapy. *Nature reviews. Drug discovery*, 8 (3), 235.
- Beetz, T. and Van Boeckel, C., 1986. Synthesis of an antithrombin binding heparin-like pentasaccharide lacking 6-O sulphate at its reducing end. *Tetrahedron letters*, 27 (48), 5889–5892.
- Belford, D., Hendry, I., and Parish, C., 1992. Ability of different chemically modified heparins to potentiate the biological activity of heparin-binding growth factor 1: lack of correlation with growth factor binding. *Biochemistry*, 31 (28), 6498.
- Belov, A. A. and Mohammadi, M., 2013. Molecular mechanisms of fibroblast growth factor signaling in physiology and pathology. *Cold Spring Harbor perspectives in biology*, 5 (6), a015958.
- Bills, A. M. and Green, J. W., 1967. The reactivity of the hydroxy-group of methyl β -D-glucopyranoside in the Koenigs-Knorr reaction. *Journal of the Chemical Society B: Physical Organic*, 716–720.
- Bishop, J. R., Schuksz, M., and Esko, J. D., 2007. Heparan sulphate proteoglycans fine-tune mammalian physiology. *Nature*, 446 (7139), 1030–1037.
- Blatter, G., Beau, J.-M., and Jacquinet, J.-C., 1994. The use of 2-deoxy-2-trichloroacetamido-D-glucopyranose derivatives in syntheses of oligosaccharides. *Carbohydrate research*, 260 (2), 189–202.

- Blixt, O. and Razi, N., 2006. Chemoenzymatic synthesis of glycan libraries. *Methods in enzymology*, 415, 137.
- Bock, K. and Pedersen, C., 1974. A study of ^{13}C coupling constants in hexopyranoses. *Journal of the Chemical Society, Perkin Transactions 2*, (3), 293–297.
- Van Boeckel, C., Beetz, T., Vos, J., De Jong, A., Van Aelst, S., Van Den Bosch, R., Mertens, J., and Van Der Vlugt, F., 1985. Synthesis of a pentasaccharide corresponding to the antithrombin III binding fragment of heparin. *Journal of Carbohydrate Chemistry*, 4 (3), 293–321.
- Van Boom, J. H., Sakairi, N., van Der Marel, G. A., Basten, J. E., and Van Boeckel, C. A., 1996. Synthesis of a Conformationally Constrained Heparin-like Pentasaccharide. *Chemistry-A European Journal*, 2 (8), 1007–1013.
- Bouleau, S., Grimal, H., Rincheval, V., Godefroy, N., Mignotte, B., Vayssière, J.-L., and Renaud, F., 2005. FGF1 inhibits p53-dependent apoptosis and cell cycle arrest via an intracrine pathway. *Oncogene*, 24 (53), 7839–7849.
- Boullanger, P., Banoub, J., and Descotes, G., 1987. N-Allyloxycarbonyl derivatives of D-glucosamine as promoters of 1, 2-trans-glucosylation in Koenigs-Knorr reactions and in Lewis acid catalyzed condensations. *Canadian journal of chemistry*, 65 (6), 1343–1348.
- Brown, A., Robinson, C. J., Gallagher, J. T., and Blundell, T. L., 2013. Cooperative heparin-mediated oligomerization of fibroblast growth factor-1 (FGF1) precedes recruitment of FGFR2 to ternary complexes. *Biophysical journal*, 104 (8), 1720–1730.
- Bubb, W. A., 2003. NMR spectroscopy in the study of carbohydrates: Characterizing the structural complexity. *Concepts in Magnetic Resonance Part A*, 19 (1), 1–19.
- Capila, I. and Linhardt, R. J., 2002. Heparin-protein interactions. *Angewandte Chemie International Edition*, 41 (3), 390–412.
- Capila, I., VanderNoot, V., Mealy, T., Seaton, B., and Linhardt, R., 1999. Interaction of heparin with annexin V. *FEBS letters*, 446 (2-3), 327.
- Cardin, A. D. and Weintraub, H., 1989. Molecular modeling of protein-glycosaminoglycan interactions. *Arteriosclerosis, Thrombosis, and Vascular Biology*, 9 (1), 21–32.
- Casu, B., 1979. Structure and biological activity of heparin and other glycosaminoglycans. *Pharmacological research communications*, 11 (1), 1–18.
- Casu, B., Petitou, M., Provasoli, M., and Sinay, P., 1988. Conformational flexibility: a new concept for explaining binding and biological properties of iduronic acid-containing glycosaminoglycans. *Trends in biochemical sciences*, 13 (6), 221–225.

- Chappell, E. P. and Liu, J., 2013. Use of biosynthetic enzymes in heparin and heparan sulfate synthesis. *Bioorganic & medicinal chemistry*, 21 (16), 4786–92.
- Cheng, F., Petersson, P., Arroyo-Yanguas, Y., and Westergren-Thorsson, G., 2001. Differences in the uptake and nuclear localization of anti-proliferative heparan sulfate between human lung fibroblasts and human lung carcinoma cells. *Journal of cellular biochemistry*, 83 (4), 597–606.
- Chi, L., Amster, J., and Linhardt, R. J., 2005. Mass spectrometry for the analysis of highly charged sulfated carbohydrates. *Current Analytical Chemistry*, 1 (3), 223–240.
- Cobucci-Ponzano, B. and Moracci, M., 2012. Glycosynthases as tools for the production of glycan analogs of natural products. *Natural product reports*, 29 (6), 697.
- Cochran, S., Li, C., and Ferro, V., 2009. A surface plasmon resonance-based solution affinity assay for heparan sulfate-binding proteins. *Glycoconjugate journal*, 26 (5), 577.
- Codee, J. D., Ali, A., Overkleeft, H. S., and van der Marel, G. A., 2011. Novel protecting groups in carbohydrate chemistry. *Comptes Rendus Chimie*, 14 (2), 178–193.
- Codée, J., Overkleeft, H., van der Marel, G., and van Boeckel, C., 2004. The synthesis of well-defined heparin and heparan sulfate fragments. *Drug discovery today. Technologies*, 1 (3), 317.
- Codée, J., Stubba, B., Schiattarella, M., Overkleeft, H., van Boeckel, C., van Boom, J., and van der Marel, G., 2005. A modular strategy toward the synthesis of heparin-like oligosaccharides using monomeric building blocks in a sequential glycosylation strategy. *Journal of the American Chemical Society*, 127 (11), 3767.
- Cole, C. L., Hansen, S. U., Barath, M., Rushton, G., Gardiner, J. M., Avizienyte, E., and Jayson, G. C., 2010. Synthetic heparan sulfate oligosaccharides inhibit endothelial cell functions essential for angiogenesis. *PLoS One*, 5 (7), e11644.
- Coombe, D. and Kett, W., 2005. Heparan sulfate-protein interactions: therapeutic potential through structure-function insights. *Cellular and molecular life sciences*, 62 (4), 410–424.
- Copeland, R., Balasubramaniam, A., Tiwari, V., Zhang, F., Bridges, A., Linhardt, R. J., Shukla, D., and Liu, J., 2008. Using a 3-O-Sulfated Heparin Octasaccharide To Inhibit the Entry of Herpes Simplex Virus Type 1†. *Biochemistry*, 47 (21), 5774–5783.
- Coughlin, S. R., Barr, P., Cousens, L., Fretto, L., and Williams, L., 1988. Acidic and basic fibroblast growth factors stimulate tyrosine kinase activity in vivo. *Journal of Biological Chemistry*, 263 (2), 988–993.

- Crich, D. and Dudkin, V., 2001. Why are the hydroxy groups of partially protected N-acetylglucosamine derivatives such poor glycosyl acceptors, and what can be done about it? A comparative study of the reactivity of N-acetyl-, N-phthalimido-, and 2-azido-2-deoxy-glucosamine derivatives in glycosylation. 2-Picolinyl ethers as reactivity-enhancing replacements for benzyl ethers. *Journal of the American Chemical Society*, 123 (28), 6819–6825.
- Crich, D. and Sun, S., 1996. Formation of β -mannopyranosides of primary alcohols using the sulfoxide method. *The Journal of organic chemistry*, 61 (14), 4506–4507.
- Cumpstey, I., 2012. On a so-called“ kinetic anomeric effect” in chemical glycosylation. *Organic & biomolecular chemistry*, 10 (13), 2503.
- Czechura, P., Guedes, N., Kopitzki, S., Vazquez, N., Martin-Lomas, M., and Reichardt, N., 2011. A new linker for solid-phase synthesis of heparan sulfate precursors by sequential assembly of monosaccharide building blocks. *Chemical communications (Cambridge, England)*, 47 (8), 2390.
- Das, S., Mallet, J., Esnault, J., Driguez, P., Duchaussoy, P., Sizun, P., Héroult, J., Herbert, J., Petitou, M., and Sinay, P., 2001. Synthesis of Conformationally Locked Carbohydrates: A Skew-Boat Conformation of L-Iduronic Acid Governs the Antithrombotic Activity of Heparin. *Angewandte Chemie (International ed. in English)*, 40 (9), 1670.
- DeAngelis, P. L., Liu, J., and Linhardt, R. J., 2013. Chemoenzymatic Synthesis of Glycosaminoglycans: Re-creating, Re-modeling, and Re-designing Nature's Longest or Most Complex Carbohydrate Chains. *Glycobiology*.
- Delcros, J.-G., Tomasi, S., Carrington, S., Martin, B., Renault, J., Blagbrough, I. S., and Uriac, P., 2002. Effect of spermine conjugation on the cytotoxicity and cellular transport of acridine. *Journal of medicinal chemistry*, 45 (23), 5098–5111.
- Delehedde, M., Malcolm, L., Gallagher, J. T., Rudland, P. S., and Fernig, D. G., 2002. Fibroblast growth factor-2 binds to small heparin-derived oligosaccharides and stimulates a sustained phosphorylation of p42/44 mitogen-activated protein kinase and proliferation of rat mammary fibroblasts. *Biochemical Journal*, 366 (1), 235–244.
- Van Den Born, J., Gunnarsson, K., Bakker, M. A., Kjellén, L., Kusche-Gullberg, M., Maccarana, M., Berden, J. H., and Lindahl, U., 1995. Presence of N-unsubstituted glucosamine units in native heparan sulfate revealed by a monoclonal antibody. *Journal of Biological Chemistry*, 270 (52), 31303–31309.
- Desai, U., Petitou, M., Björk, I., and Olson, S., 1998. Mechanism of heparin activation of antithrombin. Role of individual residues of the pentasaccharide activating sequence in the recognition of native and activated states of antithrombin. *The Journal of biological chemistry*, 273 (13), 7478.

- Dhamale, O. P., Zong, C., Al-Mafraji, K., and Boons, G.-J., 2014. New Glucuronic Acid Donors for the Modular Synthesis of Heparan Sulfate Oligosaccharides. *Organic & biomolecular chemistry*, 12 (13), 2087.
- Dhoot, G. K., Gustafsson, M. K., Ai, X., Sun, W., Standiford, D. M., and Emerson, C. P., 2001. Regulation of Wnt signaling and embryo patterning by an extracellular sulfatase. *Science*, 293 (5535), 1663–1666.
- DiGabriele, A. D., Lax, I., Chen, D. I., Svahn, C. M., Jaye, M., Schlessinger, J., and Hendrickson, W. A., 1998. Structure of a heparin-linked biologically active dimer of fibroblast growth factor. *Nature*, 393 (6687), 812–817.
- Ding, X., Tiwari, V., Guoqing, X., Clement, C., Shukla, D., and Jian, L., 2005. Characterization of heparan sulphate 3-O-sulphotransferase isoform 6 and its role in assisting the entry of herpes simplex virus type 1. *Biochemical Journal*, 385 (2), 451–459.
- Doneanu, C., Chen, W., and Gebler, J., 2009. Analysis of oligosaccharides derived from heparin by ion-pair reversed-phase chromatography/mass spectrometry. *Analytical chemistry*, 81 (9), 3485.
- Driguez, P.-A., Potier, P., and Trouilleux, P., 2014. Synthetic oligosaccharides as active pharmaceutical ingredients: Lessons learned from the full synthesis of one heparin derivative on a large scale. *Nat. Prod. Rep.*
- Drummond, K., Yates, E., and Turnbull, J., 2001. Electrophoretic sequencing of heparin/heparan sulfate oligosaccharides using a highly sensitive fluorescent end label. *Proteomics*, 1 (2), 304–310.
- Du, J. Y., Chen, L. R., Liu, S., Lin, J. H., Liang, Q. T., Lyon, M., and Wei, Z., 2016. Ion-pairing liquid chromatography with on-line electrospray ion trap mass spectrometry for the structural analysis of N-unsubstituted Heparin/Heparan Sulfate. *Journal of Chromatography B*.
- Duan, D., Werner, S., and Williams, L. T., 1992. A naturally occurring secreted form of fibroblast growth factor (FGF) receptor 1 binds basic FGF in preference over acidic FGF. *Journal of Biological Chemistry*, 267 (23), 16076–16080.
- Duchaussoy, P., Lei, P., Petitou, M., Sinaÿ, P., Lormeau, J., and Choay, J., 1991. The first total synthesis of the antithrombin III binding site of porcine mucosa heparin. *Bioorganic & Medicinal Chemistry Letters*, 1 (2), 99–102.
- Duckworth, C. A., Guimond, S. E., Sindrewicz, P., Hughes, A. J., French, N. S., Lian, L.-Y., Yates, E. A., Pritchard, D. M., Rhodes, J. M., Turnbull, J. E., and others, 2015. Chemically modified, non-anticoagulant heparin derivatives are potent galectin-3 binding inhibitors and inhibit circulating galectin-3-promoted metastasis. *Oncotarget*, 6 (27), 23671.
- Dulaney, S. B. and Huang, X., 2012. Strategies in synthesis of heparin/heparan sulfate oligosaccharides: 2000-present. *Advances in carbohydrate chemistry and*

- biochemistry*, 67, 95.
- Dulaney, S. B., Xu, Y., Wang, P., Tiruchinapally, G., Wang, Z., Kathawa, J., El-Dakdouki, M. H., Yang, B., Liu, J., and Huang, X., 2015. Divergent Synthesis of Heparan Sulfate Oligosaccharides. *The Journal of organic chemistry*.
- Eller, S., Collot, M., Yin, J., Hahm, H., and Seeberger, P., 2013. Automated solid-phase synthesis of chondroitin sulfate glycosaminoglycans. *Angewandte Chemie (International ed. in English)*, 52 (22), 5858.
- Epp, J. B. and Widlanski, T. S., 1999. Facile preparation of nucleoside-5'-carboxylic acids. *The Journal of organic chemistry*, 64 (1), 293–295.
- Esko, J. and Selleck, S., 2002. Order out of chaos: assembly of ligand binding sites in heparan sulfate. *Annual review of biochemistry*, 71, 435.
- Eswarakumar, V., Lax, I., and Schlessinger, J., 2005. Cellular signaling by fibroblast growth factor receptors. *Cytokine & growth factor reviews*, 16 (2), 139.
- Eswarakumar, V. P., Monsonnegro-Ornan, E., Pines, M., Antonopoulou, I., Morriss-Kay, G. M., and Lonai, P., 2002. The IIIc alternative of Fgfr2 is a positive regulator of bone formation. *Development*, 129 (16), 3783–3793.
- Faham, S., Hileman, R., Fromm, J., Linhardt, R., and Rees, D., 1996. Heparin structure and interactions with basic fibroblast growth factor. *Science*, 271 (5252), 1116–1120.
- Faller, B., Mely, Y., Gerard, D., and Bieth, J. G., 1992. Heparin-induced conformational change and activation of mucus proteinase inhibitor. *Biochemistry*, 31 (35), 8285–8290.
- La Ferla, B., Lay, L., Guerrini, M., Poletti, L., Panza, L., and Russo, G., 1999. Synthesis of disaccharidic sub-units of a new series of heparin related oligosaccharides. *Tetrahedron*, 55 (32), 9867–9880.
- Fernig, D. G. and Gallagher, J. T., 1994. Fibroblast growth factors and their receptors: an information network controlling tissue growth, morphogenesis and repair. *Progress in growth factor research*, 5 (4), 353–377.
- Ferrier, R., Hay, R., and Vethaviasar, N., 1973. A potentially versatile synthesis of glycosides. *Carbohydrate Research*, 27 (1), 55–61.
- Ferro, D. R., Provasoli, A., Ragazzi, M., Casu, B., Torri, G., Bossennec, V., Perly, B., Sinaÿ, P., Petitou, M., and Choay, J., 1990. Conformer populations of L-iduronic acid residues in glycosaminoglycan sequences. *Carbohydrate research*, 195 (2), 157–167.
- Feyerabend, T. B., Li, J.-P., Lindahl, U., and Rodewald, H.-R., 2006. Heparan sulfate C5-epimerase is essential for heparin biosynthesis in mast cells. *Nature chemical*

- biology*, 2 (4), 195–196.
- Feyzi, E., Trybala, E., Bergström, T., Lindahl, U., and Spillmann, D., 1997. Structural requirement of heparan sulfate for interaction with herpes simplex virus type 1 virions and isolated glycoprotein C. *Journal of Biological Chemistry*, 272 (40), 24850–24857.
- Fischer, E., 1893. Ueber die glucoside der alkohole. *Berichte der deutschen chemischen Gesellschaft*, 26 (3), 2400–2412.
- Fischer, E., 1895. Ueber die Verbindungen der Zucker mit den Alkoholen und Ketonen. *Berichte der deutschen chemischen Gesellschaft*, 28 (1), 1145–1167.
- Flaumenhaft, R., Moscatelli, D., and Ritkin, D. B., 1990. Heparin and Heparan Sulfate Increase the Radius of Diffusion and Action of Basic Fibroblast Growth Factor. *The Journal of Cell Biology*, 111, 1651–1659.
- Forsberg, E. and Kjellén, L., 2001. Heparan sulfate: lessons from knockout mice. *The Journal of clinical investigation*, 108 (2), 175–180.
- Fransson, L.-A., Silverberg, I., and Carlstedt, I., 1985. Structure of the heparan sulfate-protein linkage region. Demonstration of the sequence galactosyl-galactosyl-xylose-2-phosphate. *Journal of Biological Chemistry*, 260 (27), 14722–14726.
- Fraser-Reid, B., Konradsson, P., Mootoo, D. R., and Udodong, U., 1988. Direct elaboration of pent-4-enyl glycosides into disaccharides. *Journal of the Chemical Society, Chemical Communications*, (12), 823–825.
- Fraser-Reid, B., Udodong, U. E., Wu, Z., Ottosson, H., Merritt, J. R., Rao, C. S., Roberts, C., and Madsen, R., 1992. n-Pentenyl glycosides in organic chemistry: a contemporary example of serendipity. *Synlett*, 1992 (12), 927–942.
- Frihed, T. G., Bols, M., and Pedersen, C. M., 2015. Mechanisms of Glycosylation Reactions Studied by Low-Temperature Nuclear Magnetic Resonance. *Chemical reviews*.
- Fritz, T. A., Gabb, M. M., Wei, G., and Esko, J. D., 1994. Two N-acetylglucosaminyltransferases catalyze the biosynthesis of heparan sulfate. *Journal of Biological Chemistry*, 269 (46), 28809–28814.
- Fromm, J. R., Hileman, R. E., Weiler, J. M., and Linhardt, R. J., 1997. Interaction of fibroblast growth factor-1 and related peptides with heparan sulfate and its oligosaccharides. *Archives of biochemistry and biophysics*, 346 (2), 252–262.
- Fürstner, A., Radkowski, K., Grabowski, J., Wirtz, C., and Mynott, R., 2000. Ring-closing alkyne metathesis. Application to the total synthesis of sophorolipid lactone. *The Journal of organic chemistry*, 65 (25), 8758–8762.

- Gallagher, J. T., 2001. Heparan sulfate: growth control with a restricted sequence menu. *The Journal of Clinical Investigation*, 108 (3), 357–361.
- Gallagher, J. T. and Walker, A., 1985. Molecular distinctions between heparan sulphate and heparin. Analysis of sulphation patterns indicates that heparan sulphate and heparin are separate families of N-sulphated polysaccharides. *Biochemical Journal*, 230 (3), 665.
- Gama, C. I., Tully, S. E., Sotogaku, N., Clark, P. M., Rawat, M., Vaidehi, N., Goddard, W. A., Nishi, A., and Hsieh-Wilson, L. C., 2006. Sulfation patterns of glycosaminoglycans encode molecular recognition and activity. *Nature chemical biology*, 2 (9), 467–473.
- Gambarini, A. G., Miyamoto, C. A., Lima, G. A., Nader, H. B., and Dietrich, C. P., 1993. Mitogenic activity of acidic fibroblast growth factor is enhanced by highly sulfated oligosaccharides derived from heparin and heparan sulfate. *Molecular and cellular biochemistry*, 124 (2), 121–129.
- Gatti, G., Casu, B., Hamer, G., and Perlin, A., 1979. Studies on the conformation of heparin by ¹H and ¹³C NMR spectroscopy. *Macromolecules*, 12 (5), 1001–1007.
- Gerothanassis, I. P., Troganis, A., Exarchou, V., and Barbarossou, K., 2002. Nuclear magnetic resonance (NMR) spectroscopy: basic principles and phenomena, and their applications to chemistry, biology and medicine. *Chemistry Education Research and Practice*, 3 (2), 229–252.
- Goetz, R., Dover, K., Laezza, F., Shtraizent, N., Huang, X., Tchetchik, D., Eliseenkova, A. V., Xu, C.-F., Neubert, T. A., Ornitz, D. M., and others, 2009. Crystal structure of a fibroblast growth factor homologous factor (FHF) defines a conserved surface on FHF for binding and modulation of voltage-gated sodium channels. *Journal of Biological Chemistry*, 284 (26), 17883–17896.
- Goetz, R. and Mohammadi, M., 2013. Exploring mechanisms of FGF signalling through the lens of structural biology. *Nature Reviews Molecular Cell Biology*.
- Goodger, S. J., Robinson, C. J., Murphy, K. J., Gasiunas, N., Harmer, N. J., Blundell, T. L., Pye, D. A., and Gallagher, J. T., 2008. Evidence that heparin saccharides promote FGF2 mitogenesis through two distinct mechanisms. *Journal of Biological Chemistry*, 283 (19), 13001–13008.
- Guedes, N., Czechura, P., Echeverria, B., Ruiz, A., Michelena, O., Martin-Lomas, M., and Reichardt, N., 2013. Toward the solid-phase synthesis of heparan sulfate oligosaccharides: evaluation of iduronic acid and idose building blocks. *The Journal of organic chemistry*, 78 (14), 6911.
- Guedes, N., Kopitzki, S., Echeverria, B., Pazos, R., Elosegui, E., Calvo, J., and Reichardt, N.-C., 2015. Solid-phase assembly of glycosaminoglycan oligosaccharide precursors. *RSC Advances*, 5 (13), 9325–9327.

- Guerrini, M., Agulles, T., Bisio, A., Hricovini, M., Lay, L., Naggi, A., Poletti, L., Sturiale, L., Torri, G., and Casu, B., 2002. Minimal heparin/heparan sulfate sequences for binding to fibroblast growth factor-1. *Biochemical and biophysical research communications*, 292 (1), 222–230.
- Guerrini, M., Beccati, D., Shriver, Z., Naggi, A. M., Bisio, A., Capila, I., Lansing, J., Guglieri, S., Fraser, B., Al-Hakim, A., and others, 2008. Oversulfated Chondroitin Sulfate is a major contaminant in Heparin associated with Adverse Clinical Events. *Nature biotechnology*, 26 (6), 669.
- Guerrini, M., Elli, S., Mourier, P., Rudd, T. R., Gaudesi, D., Casu, B., Boudier, C., Torri, G., and Viskov, C., 2013. An unusual antithrombin-binding heparin octasaccharide with an additional 3-O-sulfated glucosamine in the active pentasaccharide sequence. *Biochemical Journal*, 449 (2), 343–351.
- Guerrini, M., Guglieri, S., Casu, B., Torri, G., Mourier, P., Boudier, C., and Viskov, C., 2008. Antithrombin-binding octasaccharides and role of extensions of the active pentasaccharide sequence in the specificity and strength of interaction. Evidence for very high affinity induced by an unusual glucuronic acid residue. *The Journal of biological chemistry*, 283 (39), 26662.
- Guglieri, S., Hricovini, M., Raman, R., Polito, L., Torri, G., Casu, B., Sasisekharan, R., and Guerrini, M., 2008. Minimum FGF2 Binding Structural Requirements of Heparin and Heparan Sulfate Oligosaccharides As Determined by NMR Spectroscopy†. *Biochemistry*, 47 (52), 13862–13869.
- Guimond, S., Maccarana, M., Olwin, B., Lindahl, U., and Rapraeger, A., 1993. Activating and inhibitory heparin sequences for FGF-2 (basic FGF). Distinct requirements for FGF-1, FGF-2, and FGF-4. *Journal of Biological Chemistry*, 268 (32), 23906–23914.
- Guimond, S., Rudd, T., Skidmore, M., Ori, A., Gaudesi, D., Cosentino, C., Guerrini, M., Edge, R., Collison, D., McInnes, E., and others, 2009. Cations modulate polysaccharide structure to determine FGF-FGFR signaling: a comparison of signaling and inhibitory polysaccharide interactions with FGF-1 in solution. *Biochemistry*, 48 (22), 4772.
- Guimond, S. and Turnbull, J., 1999. Fibroblast growth factor receptor signalling is dictated by specific heparan sulphate saccharides. *Current biology: CB*, 9 (22), 1343.
- Götting, C., Kuhn, J., Zahn, R., Brinkmann, T., and Kleesiek, K., 2000. Molecular cloning and expression of human UDP-d-Xylose: proteoglycan core protein β -d-xylosyltransferase and its first isoform XT-II. *Journal of molecular biology*, 304 (4), 517.
- Habuchi, H., Kobayashi, M., and Kimata, K., 1998. Molecular characterization and expression of heparan-sulfate 6-sulfotransferase. Complete cDNA cloning in human and partial cloning in Chinese hamster ovary cells. *The Journal of*

- biological chemistry*, 273 (15), 9208–13.
- Habuchi, H., Nagai, N., Sugaya, N., Atsumi, F., Stevens, R. L., and Kimata, K., 2007. Mice deficient in heparan sulfate 6-O-sulfotransferase-1 exhibit defective heparan sulfate biosynthesis, abnormal placentation, and late embryonic lethality. *Journal of Biological Chemistry*, 282 (21), 15578–15588.
- Habuchi, H., Tanaka, M., Habuchi, O., Yoshida, K., Suzuki, H., Ban, K., and Kimata, K., 2000. The occurrence of three isoforms of heparan sulfate 6-O-sulfotransferase having different specificities for hexuronic acid adjacent to the targeted N-sulfoglucosamine. *The Journal of biological chemistry*, 275 (4), 2859.
- Hagner-McWhirter, Å., Hannesson, H. H., Campbell, P., Westley, J., Rodén, L., Lindahl, U., and Li, J.-P., 2000. Biosynthesis of heparin/heparan sulfate: kinetic studies of the glucuronyl C5-epimerase with N-sulfated derivatives of the Escherichia coli K5 capsular polysaccharide as substrates. *Glycobiology*, 10 (2), 159–171.
- Haller, M. and Boons, G.-J., 2001. Towards a modular approach for heparin synthesis. *Journal of the Chemical Society, Perkin Transactions 1*, (8), 814–822.
- Haller, M. F. and Boons, G.-J., 2002. Selectively protected disaccharide building blocks for modular synthesis of heparin fragments. *European Journal of Organic Chemistry*, 2002 (13), 2033–2038.
- Hansen, S. U., Miller, G. J., Cliff, M. J., Jayson, G. C., and Gardiner, J. M., 2015. Making the longest sugars: a chemical synthesis of heparin-related [4] n oligosaccharides from 16-mer to 40-mer. *Chemical Science*, 6 (11), 6158–6164.
- Hansen, S. U., Miller, G. J., Jayson, G. C., and Gardiner, J. M., 2012. First Gram-scale synthesis of a heparin-related dodecasaccharide. *Organic letters*, 15 (1), 88–91.
- Harmer, N. J., Ilag, L. L., Mulloy, B., Pellegrini, L., Robinson, C. V., and Blundell, T. L., 2004. Towards a resolution of the stoichiometry of the fibroblast growth factor (FGF)-FGF receptor-heparin complex. *Journal of molecular biology*, 339 (4), 821–834.
- Higashi, K., Hosoyama, S., Ohno, A., Masuko, S., Yang, B., Sterner, E., Wang, Z., Linhardt, R. J., and Toida, T., 2012. Photochemical Preparation of a Novel Low Molecular Weight Heparin. *Carbohydrate polymers*, 67 (2), 1737.
- Hileman, R. E., Fromm, J. R., Weiler, J. M., and Linhardt, R. J., 1998. Glycosaminoglycan-protein interactions: definition of consensus sites in glycosaminoglycan binding proteins. *Bioessays*, 20 (2), 156–167.
- Hileman, R. E., Jennings, R. N., and Linhardt, R. J., 1998. Thermodynamic analysis of the heparin interaction with a basic cyclic peptide using isothermal titration calorimetry. *Biochemistry*, 37 (43), 15231–15237.

- Hook, M., Kjellen, L., Johansson, S., and Robinson, J., 1984. Cell-surface glycosaminoglycans. *Annual review of biochemistry*, 53 (1), 847–869.
- Hricovíni, M., 2011. Effect of solvent and counterions upon structure and NMR spin-spin coupling constants in heparin disaccharide. *The journal of physical chemistry. B*, 115 (6), 1503.
- Hricovíni, M., Guerrini, M., Torri, G., and Casu, B., 1997. Motional properties of E. coli polysaccharide K5 in aqueous solution analyzed by NMR relaxation measurements. *Carbohydrate research*, 300 (1), 69–76.
- Hricovini, M., Guerrini, M., Torri, G., Piani, S., and Ungarelli, F., 1995. Conformational analysis of heparin epoxide in aqueous solution. An NMR relaxation study. *Carbohydrate research*, 277 (1), 11–23.
- Hsieh, P.-H., Thieker, D. F., Guerrini, M., Woods, R. J., and Liu, J., 2016. Uncovering the Relationship between Sulphation Patterns and Conformation of Iduronic Acid in Heparan Sulphate. *Scientific Reports*, 6.
- Hsieh, P.-H., Xu, Y., Keire, D. A., and Liu, J., 2014. Chemoenzymatic synthesis and structural characterization of 2-O-sulfated glucuronic acid-containing heparan sulfate hexasaccharides. *Glycobiology*, 24 (8), 681.
- Hu, Y., Lin, S., Huang, C., Zulueta, M., Liu, J., Chang, W., and Hung, S., 2011. Synthesis of 3-O-sulfonated heparan sulfate octasaccharides that inhibit the herpes simplex virus type 1 host-cell interaction. *Nature chemistry*, 3 (7), 557.
- Hu, Y.-P., Zhong, Y.-Q., Chen, Z.-G., Chen, C.-Y., Shi, Z., Zulueta, M. M. L., Ku, C.-C., Lee, P.-Y., Wang, C.-C., and Hung, S.-C., 2012. Divergent synthesis of 48 heparan sulfate-based disaccharides and probing the specific sugar-fibroblast growth factor-1 interaction. *Journal of the American Chemical Society*, 134 (51), 20722–20727.
- Huang, L. and Huang, X., 2007. Highly efficient syntheses of hyaluronic acid oligosaccharides. *Chemistry-A European Journal*, 13 (2), 529–540.
- Huang, M., Garrett, G. E., Birlirakis, N., Bohé, L., Pratt, D. A., and Crich, D., 2012. Dissecting the mechanisms of a class of chemical glycosylation using primary ¹³C kinetic isotope effects. *Nature chemistry*, 4 (8), 663–667.
- Hung, S., Lu, X., Lee, J., Chang, M., Fang, S., Fan, T., Zulueta, M., and Zhong, Y., 2012. Synthesis of heparin oligosaccharides and their interaction with eosinophil-derived neurotoxin. *Organic & biomolecular chemistry*, 10 (4), 760.
- Ibrahimi, O. A., Yeh, B. K., Eliseenkova, A. V., Zhang, F., Olsen, S. K., Igarashi, M., Aaronson, S. A., Linhardt, R. J., and Mohammadi, M., 2005. Analysis of mutations in fibroblast growth factor (FGF) and a pathogenic mutation in FGF receptor (FGFR) provides direct evidence for the symmetric two-end model for FGFR dimerization. *Science's STKE*, 25 (2), 671.

- Iozzo, R., 1998. Matrix proteoglycans: from molecular design to cellular function. *Annual review of biochemistry*, 67, 609.
- Iozzo, R. V., 2001. Series Introduction: Heparan sulfate proteoglycans: intricate molecules with intriguing functions. *Journal of Clinical Investigation*, 108 (2), 165.
- Ishihara, M., 1994. Structural requirements in heparin for binding and activation of FGF-1 and FGF-4 are different from that for FGF-2. *Glycobiology*, 4 (6), 817–824.
- Itoh, N. and Ornitz, D. M., 2004. Evolution of the Fgf and Fgfr gene families. *TRENDS in Genetics*, 20 (11), 563–569.
- Itoh, N. and Ornitz, D. M., 2011. Fibroblast growth factors: from molecular evolution to roles in development, metabolism and disease. *Journal of biochemistry*, 149 (2), 121–130.
- Jacobsson, I., Lindahl, U., Jensen, J., Rodén, L., Prihar, H., and Feingold, D., 1984. Biosynthesis of heparin. Substrate specificity of heparosan N-sulfate D-glucuronosyl 5-epimerase. *Journal of Biological Chemistry*, 259 (2), 1056–1063.
- Jacquinet, J.-C., Petitou, M., Duchaussoy, P., Lederman, I., Choay, J., Torri, G., and Sinaÿ, P., 1984. Synthesis of heparin fragments. A chemical synthesis of the trisaccharide O-(2-deoxy-2-sulfamido-3, 6-di-O-sulfo- α -D-glucopyranosyl)-(1 \rightarrow 4)-O-(2-O-sulfo- α -L-idopyranosyluronic acid)-(1 \rightarrow 4)-2-deoxy-2-sulfamido-6-O-sulfo-d-glucopyranose heptasodium salt. *Carbohydrate research*, 130, 221–241.
- Jairajpuri, M. A., Lu, A., Desai, U., Olson, S. T., Bjork, I., and Bock, S. C., 2003. Antithrombin III phenylalanines 122 and 121 contribute to its high affinity for heparin and its conformational activation. *Journal of Biological Chemistry*, 278 (18), 15941–15950.
- Jarowicki, K. and Kocienski, P., 2001. Protecting groups. *Journal of the Chemical Society, Perkin Transactions 1*, (18), 2109–2135.
- Jastrebova, N., Vanwildemeersch, M., Rapraeger, A. C., Giménez-Gallego, G., Lindahl, U., and Spillmann, D., 2006. Heparan sulfate-related oligosaccharides in ternary complex formation with fibroblast growth factors 1 and 2 and their receptors. *Journal of Biological Chemistry*, 281 (37), 26884–26892.
- Jemth, P., Kreuger, J., Kusche-Gullberg, M., Sturiale, L., Giménez-Gallego, G., and Lindahl, U., 2002. Biosynthetic oligosaccharide libraries for identification of protein-binding heparan sulfate motifs. Exploring the structural diversity by screening for fibroblast growth factor (FGF) 1 and FGF2 binding. *The Journal of biological chemistry*, 277 (34), 30567.
- Johnson, D. E., Lu, J., Chen, H., Werner, S., and Williams, L. T., 1991. The human fibroblast growth factor receptor genes: a common structural arrangement underlies the mechanisms for generating receptor forms that differ in their third

- immunoglobulin domain. *Molecular and Cellular Biology*, 11 (9), 4627–4634.
- Jones, C., Beni, S., Limtiaco, J., Langeslay, D., and Larive, C., 2011. Heparin characterization: challenges and solutions. *Annual review of analytical chemistry (Palo Alto, Calif.)*, 4, 439.
- Jonker, J. W., Suh, J. M., Atkins, A. R., Ahmadian, M., Li, P., Whyte, J., He, M., Juguilon, H., Yin, Y.-Q., Phillips, C. T., and others, 2012. A PPAR γ -FGF1 axis is required for adaptive adipose remodelling and metabolic homeostasis. *Nature*, 485 (7398), 391.
- Jorgen, W., Kaisa, H., and Ellen, M. H., 2011. Fibroblast growth factors and their receptors in cancer. *Biochemical Journal*, 437 (2), 199–213.
- Kahne, D., Walker, S., Cheng, Y., and Van Engen, D., 1989. Glycosylation of unreactive substrates. *Journal of the American Chemical Society*, 111 (17), 6881–6882.
- Kan, M., Wang, F., Xu, J., Crabb, J., Hou, J., and McKeehan, W., 1993. An essential heparin-binding domain in the fibroblast growth factor receptor kinase. *Science (New York, NY)*, 259 (5103), 1918.
- Kandasamy, J., Schuhmacher, F., Hahm, H. S., Klein, J. C., and Seeberger, P. H., 2014. Modular automated solid phase synthesis of dermatan sulfate oligosaccharides. *Chemical Communications*, 50 (15), 1875–1877.
- Karamanos, N., Vanky, P., Tzanakakis, G., and Hjerpe, A., 1996. High performance capillary electrophoresis method to characterize heparin and heparan sulfate disaccharides. *Electrophoresis*, 17 (2), 391.
- Kariya, Y., Kyogashima, M., Suzuki, K., Isomura, T., Sakamoto, T., Horie, K., Ishihara, M., Takano, R., Kamei, K., and Hara, S., 2000. Preparation of completely 6-O-desulfated heparin and its ability to enhance activity of basic fibroblast growth factor. *The Journal of biological chemistry*, 275 (34), 25949.
- Karlsson, N., Schulz, B., Packer, N., and Whitelock, J., 2005. Use of graphitised carbon negative ion LC-MS to analyse enzymatically digested glycosaminoglycans. *Journal of chromatography. B, Analytical technologies in the biomedical and life sciences*, 824 (1-2), 139.
- Kennett, E. and Davies, M., 2009. Glycosaminoglycans are fragmented by hydroxyl, carbonate, and nitrogen dioxide radicals in a site-selective manner: implications for peroxynitrite-mediated damage at sites of inflammation. *Free radical biology & medicine*, 47 (4), 389.
- Kjellen, L. and Lindahl, U., 1991. Proteoglycans: structures and interactions. *Annual review of biochemistry*, 60 (1), 443–475.

- Klagsbrun, M. and Baird, A., 1991. A dual receptor system is required for basic fibroblast growth factor activity. *Cell*, 67 (2), 229–231.
- Koeners, H., Verhoeven, J., and Van Boom, J., 1980. Synthesis of oligosaccharides by using levulinic ester as an hydroxyl protecting group. *Tetrahedron Letters*, 21 (4), 381–382.
- Koenigs, W. and Knorr, E., 1901. Ueber einige Derivate des Traubenzuckers und der Galactose. *Berichte der deutschen chemischen Gesellschaft*, 34 (1), 957–981.
- Korir, A. and Larive, C., 2009. Advances in the separation, sensitive detection, and characterization of heparin and heparan sulfate. *Analytical and bioanalytical chemistry*, 393 (1), 155.
- Kovensky, J., Duchaussoy, P., Bono, F., Salmivirta, M., Sizun, P., Herbert, J., Petitou, M., and Sinaÿ, P., 1999. A synthetic heparan sulfate pentasaccharide, exclusively containing L-iduronic acid, displays higher affinity for FGF-2 than its D-glucuronic acid-containing isomers. *Bioorganic & medicinal chemistry*, 7 (8), 1567.
- Kovensky, J., Duchaussoy, P., Petitou, M., and Sinaÿ, P., 1996. Binding of heparan sulfate to fibroblast growth factor-2 total synthesis of a putative pentasaccharide binding site. *Tetrahedron: Asymmetry*, 7 (11), 3119–3128.
- Kovensky, J., Mallet, J.-M., Esnault, J., Driguez, P.-A., Sizun, P., Hérault, J.-P., Herbert, J.-M., Petitou, M., and Sinaÿ, P., 2002. Further Evidence for the Critical Role of a Non-Chair Conformation of L-Iduronic Acid in the Activation of Antithrombin. *European Journal of Organic Chemistry*, 2002 (21), 3595–3603.
- Kreuger, J., Jemth, P., Sanders-Lindberg, E., Eliahu, L., Ron, D., Basilico, C., Salmivirta, M., and Lindahl, U., 2005. Fibroblast growth factors share binding sites in heparan sulphate. *Biochemical Journal*, 389 (Pt 1), 145.
- Kreuger, J., Matsumoto, T., Vanwildemeersch, M., Sasaki, T., Timpl, R., Claesson-Welsh, L., Spillmann, D., and Lindahl, U., 2002. Role of heparan sulfate domain organization in endostatin inhibition of endothelial cell function. *The EMBO journal*, 21 (23), 6303–6311.
- Kreuger, J., Prydz, K., Pettersson, R. F., Lindahl, U., and Salmivirta, M., 1999. Characterization of fibroblast growth factor 1 binding heparan sulfate domain. *Glycobiology*, 9 (7), 723–729.
- Kreuger, J., Salmivirta, M., Sturiale, L., Giménez-Gallego, G., and Lindahl, U., 2001. Sequence analysis of heparan sulfate epitopes with graded affinities for fibroblast growth factors 1 and 2. *Journal of Biological Chemistry*, 276 (33), 30744–30752.
- Kuberan, B., Lech, M., Beeler, D., Wu, Z., and Rosenberg, R., 2003. Enzymatic synthesis of antithrombin III-binding heparan sulfate pentasaccharide. *Nature*

- biotechnology*, 21 (11), 1343.
- Kuduk, S. D., Schwarz, J. B., Chen, X.-T., Glunz, P. W., Sames, D., Ragupathi, G., Livingston, P. O., and Danishefsky, S. J., 1998. Synthetic and immunological studies on clustered modes of mucin-related Tn and TF O-linked antigens: The preparation of a glycopeptide-based vaccine for clinical trials against prostate cancer. *Journal of the American Chemical Society*, 120 (48), 12474–12485.
- Kunz, H. and Günther, W., 1988. β -Mannosides from β -Glucosides by Intramolecular Nucleophilic Substitution with Inversion of Configuration. *Angewandte Chemie International Edition in English*, 27 (8), 1086–1087.
- Kuro-o, M., 2012. Klotho in health and disease. *Current opinion in nephrology and hypertension*, 21 (4), 362–368.
- Lamanna, W. C., Baldwin, R. J., Padva, M., Kalus, I., Ten Dam, G., Van Kuppevelt, T. H., Gallagher, J. T., Von Figura, K., Dierks, T., and Merry, C. L., 2006. Heparan sulfate 6-O-endosulfatases: discrete in vivo activities and functional co-operativity. *Biochemical journal*, 400 (1), 63–73.
- Lamanna, W. C., Kalus, I., Padva, M., Baldwin, R. J., Merry, C. L. R., and Dierks, T., 2007. The heparanome—The enigma of encoding and decoding heparan sulfate sulfation. *Journal of biotechnology*, 129 (2), 290–307.
- Larsen, K., Olsen, C. E., and Motawia, M. S., 2008. Acid-catalysed rearrangement of glycosyl trichloroacetimidates: a novel route to glycosylamines. *Carbohydrate research*, 343 (2), 383–387.
- Leary, J., Miller, R., Wei, W., Schwörer, R., Zubkova, O., Tyler, P., and Turnbull, J., 2015. Composition, sequencing and ion mobility mass spectrometry of heparan sulfate-like octasaccharide isomers differing in glucuronic and iduronic acid content. *European journal of mass spectrometry (Chichester, England)*, 21 (3), 245.
- Leavitt, S. and Freire, E., 2001. Direct measurement of protein binding energetics by isothermal titration calorimetry. *Current opinion in structural biology*, 11 (5), 560–566.
- Ledin, J., Staatz, W., Li, J.-P., Götte, M., Selleck, S., Kjellén, L., and Spillmann, D., 2004. Heparan sulfate structure in mice with genetically modified heparan sulfate production. *Journal of Biological Chemistry*, 279 (41), 42732–42741.
- Lee, J.-C., Lu, X.-A., Kulkarni, S. S., Wen, Y.-S., and Hung, S.-C., 2004. Synthesis of heparin oligosaccharides. *Journal of the American Chemical Society*, 126 (2), 476–477.
- Lee, P. L., Johnson, D. E., Cousens, L., Fried, V., and Williams, L., 1989. Purification and complementary DNA cloning of a receptor for basic fibroblast growth factor. *Science*, 245, 57–60.

- Lemieux, R., Hendriks, K., Stick, R., and James, K., 1975. Halide ion catalyzed glycosidation reactions. Syntheses of α -linked disaccharides. *Journal of the American Chemical Society*, 97 (14), 4056–4062.
- Lennarz, W., 2012. *The biochemistry of glycoproteins and proteoglycans*. Springer Science & Business Media.
- Lepenies, B., Yin, J., and Seeberger, P., 2010. Applications of synthetic carbohydrates to chemical biology. *Current opinion in chemical biology*, 14 (3), 404.
- Li, X., Wang, C., Xiao, J., McKeegan, W., and Wang, F., 2016. Fibroblast growth factors, old kids on the new block. In: *Seminars in cell & developmental biology*. 155.
- Li, Y., Hoskins, J. N., Sreerama, S. G., and Grayson, S. M., 2010. MALDI- TOF mass spectral characterization of polymers containing an Azide group: evidence of metastable ions. *Macromolecules*, 43 (14), 6225–6228.
- Li, Y., Sun, C., Yates, E. A., Jiang, C., Wilkinson, M. C., and Fernig, D. G., 2016. Heparin binding preference and structures in the fibroblast growth factor family parallel their evolutionary diversification. *Open biology*, 6 (3), 150275.
- Li, Y.-C., Ho, I.-H., Ku, C.-C., Zhong, Y.-Q., Hu, Y.-P., Chen, Z.-G., Chen, C.-Y., Lin, W.-C., Zulueta, M. M. L., Hung, S.-C., and others, 2014. Interactions that influence the binding of synthetic heparan sulfate based disaccharides to fibroblast growth factor-2. *ACS chemical biology*, 9 (8), 1712–1717.
- Lindahl, U. and Hook, M., 1978. Glycosaminoglycans and their binding to biological macromolecules. *Annual review of biochemistry*, 47 (1), 385–417.
- Lindahl, U., Kusche, M., Lidholt, K., and OSCARSSON, L.-G., 1989. Biosynthesis of Heparin and Heparan Sulfate. *Annals of the New York Academy of Sciences*, 556 (1), 36–50.
- Lindahl, U., Thunberg, L., Bäckström, G., Riesenfeld, J., Nordling, K., and Björk, I., 1984. Extension and structural variability of the antithrombin-binding sequence in heparin. *Journal of Biological Chemistry*, 259 (20), 12368–12376.
- Linhardt, R., Gu, K., Loganathan, D., and Carter, S., 1989. Analysis of glycosaminoglycan-derived oligosaccharides using reversed-phase ion-pairing and ion-exchange chromatography with suppressed conductivity detection. *Analytical biochemistry*, 181 (2), 288.
- Linhardt, R., Turnbull, J. E., Wang, H., Loganathan, D., and Gallagher, J. T., 1990. Examination of the substrate specificity of heparin and heparan sulfate lyases. *Biochemistry*, 29 (10), 2611–2617.

- Liu, J. and Linhardt, R. J., 2014. Chemoenzymatic synthesis of heparan sulfate and heparin. *Natural product reports*, 31 (12), 1676–1685.
- Liu, J. and Pedersen, L. C., 2007. Anticoagulant heparan sulfate: structural specificity and biosynthesis. *Applied microbiology and biotechnology*, 74 (2), 263–272.
- Liu, J., Shriver, Z., Blaiklock, P., Yoshida, K., Sasisekharan, R., and Rosenberg, R., 1999. Heparan sulfate D-glucosaminyl 3-O-sulfotransferase-3A sulfates N-unsubstituted glucosamine residues. *The Journal of biological chemistry*, 274 (53), 38155.
- Liu, J., Shriver, Z., Pope, R. M., Thorp, S. C., Duncan, M. B., Copeland, R. J., Raska, C. S., Yoshida, K., Eisenberg, R. J., Cohen, G., and others, 2002. Characterization of a heparan sulfate octasaccharide that binds to herpes simplex virus type 1 glycoprotein D. *Journal of Biological Chemistry*, 277 (36), 33456–33467.
- Liu, R., Xu, Y., Chen, M., Weiwer, M., Zhou, X., Bridges, A. S., DeAngelis, P. L., Zhang, Q., Linhardt, R. J., and Liu, J., 2010. Chemoenzymatic Design of Heparan Sulfate Oligosaccharides. *The Journal of Biological Chemistry*, 285 (44), 34240.
- Lohman, G., Hunt, D., Högermeier, J., and Seeberger, P., 2003. Synthesis of iduronic acid building blocks for the modular assembly of glycosaminoglycans. *The Journal of organic chemistry*, 68 (19), 7559.
- Lohman, G. J. and Seeberger, P. H., 2004. A stereochemical surprise at the late stage of the synthesis of fully N-differentiated heparin oligosaccharides containing amino, acetamido, and N-sulfonate groups. *The Journal of organic chemistry*, 69 (12), 4081–4093.
- Lortat-Jacob, H., Turnbull, J., and Grimaud, J., 1995. Molecular organization of the interferon gamma-binding domain in heparan sulphate. *Biochemical Journal*, 310 (Pt 2), 497.
- Lu, L.-D., Shie, C.-R., Kulkarni, S. S., Pan, G.-R., Lu, X.-A., and Hung, S.-C., 2006. Synthesis of 48 disaccharide building blocks for the assembly of a heparin and heparan sulfate oligosaccharide library. *Organic letters*, 8 (26), 5995–5998.
- Lubineau, A., Gavard, O., Alais, J., and Bonnaffe, D., 2000. New accesses to-iduronyl synthons. *Tetrahedron Letters*, 41 (3), 307–311.
- Lubineau, A., Lortat-Jacob, H., Gavard, O., Sarrazin, S., and Bonnaffé, D., 2004. Synthesis of tailor-made glycoconjugate mimetics of heparan sulfate that bind IFN-gamma in the nanomolar range. *Chemistry (Weinheim an der Bergstrasse, Germany)*, 10 (17), 4265.
- Lucas, R., Angulo, J., Nieto, P., and Martín-Lomas, M., 2003. Synthesis and structural study of two new heparin-like hexasaccharides. *Organic &*

- biomolecular chemistry*, 1 (13), 2253.
- Luo, Y., Ye, S., Kan, M., and McKeehan, W., 2006a. Control of fibroblast growth factor (FGF) 7- and FGF1-induced mitogenesis and downstream signaling by distinct heparin octasaccharide motifs. *The Journal of biological chemistry*, 281 (30), 21052.
- Luo, Y., Ye, S., Kan, M., and McKeehan, W., 2006b. Structural specificity in a FGF7-affinity purified heparin octasaccharide required for formation of a complex with FGF7 and FGFR2IIIb. *Journal of cellular biochemistry*, 97 (6), 1241.
- Maccarana, M., Casu, B., and Lindahl, U., 1993. Minimal sequence in heparin/heparan sulfate required for binding of basic fibroblast growth factor. *Journal of Biological Chemistry*, 268 (32), 23898–23905.
- Maccarana, M., Sakura, Y., Tawada, A., Yoshida, K., and Lindahl, U., 1996. Domain structure of heparan sulfates from bovine organs. *Journal of Biological Chemistry*, 271 (30), 17804–17810.
- Mach, H., Volkin, D. B., Burke, C. J., Middaugh, C. R., Linhardt, R. J., Fromm, J. R., Loganathan, D., and Mattsson, L., 1993. Nature of the interaction of heparin with acidic fibroblast growth factor. *Biochemistry*, 32 (20), 5480–5489.
- Mackenzie, L. F., Wang, Q., Warren, R. A. J., and Withers, S. G., 1998. Glycosynthases: mutant glycosidases for oligosaccharide synthesis. *Journal of the American Chemical Society*, 120 (22), 5583–5584.
- Martin, A., Arda, A., Désiré, J., Martin-Mingot, A., Probst, N., Sinaÿ, P., Jiménez-Barbero, J., Thibaudeau, S., and Blériot, Y., 2015. Catching elusive glycosylations in a condensed phase with HF/SbF₅ superacid. *Nature Chemistry*.
- Mastelić, J., Jerković, I., Vinković, M., Džolić, Z., and Vikić-Topić, D., 2004. Synthesis of selected naturally occurring glucosides of volatile compounds. Their chromatographic and spectroscopic properties. *Croatica Chemica Acta*, 77 (3), 491–500.
- Masuko, S. and Linhardt, R. J., 2012. Chemoenzymatic synthesis of the next generation of ultralow MW heparin therapeutics. *Future medicinal chemistry*, 4 (3), 289–296.
- McCormick, C., Duncan, G., Goutsos, K. T., and Tufaro, F., 2000. The putative tumor suppressors EXT1 and EXT2 form a stable complex that accumulates in the Golgi apparatus and catalyzes the synthesis of heparan sulfate. *Proceedings of the National Academy of Sciences*, 97 (2), 668–673.
- McCormick, C., Leduc, Y., Martindale, D., Mattison, K., Esford, L., Dyer, A., and Tufaro, F., 1998. The putative tumour suppressor EXT1 alters the expression of cell-surface heparan sulfate. *Nature genetics*, 19 (2), 158–161.

- McKeehan, W. L., Wu, X., and Kan, M., 1999. Requirement for anticoagulant heparan sulfate in the fibroblast growth factor receptor complex. *Journal of Biological Chemistry*, 274 (31), 21511–21514.
- Mellin, T. N., Cashen, D. E., Ronan, J. J., Murphy, B. S., DiSalvo, J., and Thomas, K. A., 1995. Acidic fibroblast growth factor accelerates dermal wound healing in diabetic mice. *Journal of investigative dermatology*, 104 (5), 850–855.
- Mende, M., Bednarek, C., Wawryszyn, M., Sauter, P., Biskup, M. B., Schepers, U., and Bräse, S., 2016. Chemical Synthesis of Glycosaminoglycans. *Chemical Reviews*, 116 (14), 8193–8255.
- Meneghetti, M. C., Hughes, A. J., Rudd, T. R., Nader, H. B., Powell, A. K., Yates, E. A., and Lima, M. A., 2015. Heparan sulfate and heparin interactions with proteins. *Journal of The Royal Society Interface*, 12 (110), 20150589.
- Merrifield, R. B., 1985. Solid phase synthesis (Nobel lecture). *Angewandte Chemie International Edition in English*, 24 (10), 799–810.
- Merry, C. L., Bullock, S. L., Swan, D. C., Backen, A. C., Lyon, M., Beddington, R. S., Wilson, V. A., and Gallagher, J. T., 2001. The Molecular Phenotype of Heparan Sulfate in the Hs2st^{-/-} Mutant Mouse. *Journal of Biological Chemistry*, 276 (38), 35429–35434.
- Merry, C. L., Lyon, M., Deakin, J. A., Hopwood, J. J., and Gallagher, J. T., 1999. Highly sensitive sequencing of the sulfated domains of heparan sulfate. *Journal of Biological Chemistry*, 274 (26), 18455–18462.
- Miller, D. L., Ortega, S., Bashayan, O., Basch, R., and Basilico, C., 2000. Compensation by fibroblast growth factor 1 (FGF1) does not account for the mild phenotypic defects observed in FGF2 null mice. *Molecular and cellular biology*, 20 (6), 2260–2268.
- Miller, G. J., Hansen, S. U., Avizienyte, E., Rushton, G., Cole, C., Jayson, G. C., and Gardiner, J. M., 2013. Efficient chemical synthesis of heparin-like octa-, deca- and dodecasaccharides and inhibition of FGF2- and VEGF 165-mediated endothelial cell functions. *Chemical Science*, 4 (8), 3218–3222.
- Miller, R., 2011. Decoding heparan sulfate structure using glycomics strategies.
- Miller, R., Guimond, S., Shivkumar, M., Blocksidge, J., Austin, J., Leary, J., and Turnbull, J., 2016. Heparin Isomeric Oligosaccharide Separation Using Volatile Salt Strong Anion Exchange Chromatography. *Analytical chemistry*, 88 (23), 11542.
- Mohammadi, M., Olsen, S., and Ibrahimi, O., 2005. Structural basis for fibroblast growth factor receptor activation. *Cytokine & growth factor reviews*, 16 (2), 107.
- Moon, A. F., Xu, Y., Woody, S. M., Krahn, J. M., Linhardt, R. J., Liu, J., and Pedersen, L. C., 2012. Dissecting the substrate recognition of 3-O-sulfotransferase

- for the biosynthesis of anticoagulant heparin. *Proceedings of the National Academy of Sciences of the United States of America*, 109 (14), 5265.
- Morimoto-Tomita, M., Uchimura, K., Werb, Z., Hemmerich, S., and Rosen, S. D., 2002. Cloning and characterization of two extracellular heparin-degrading endosulfatases in mice and humans. *Journal of Biological Chemistry*, 277 (51), 49175–49185.
- Mosier, P. D., Krishnasamy, C., Kellogg, G. E., and Desai, U. R., 2012. On the specificity of heparin/heparan sulfate binding to proteins. Anion-binding sites on antithrombin and thrombin are fundamentally different. *PLoS One*, 7 (11), e48632.
- Mourier, P. A. and Viskov, C., 2004. Chromatographic analysis and sequencing approach of heparin oligosaccharides using cetyltrimethylammonium dynamically coated stationary phases. *Analytical biochemistry*, 332 (2), 299–313.
- Mühlberg, M., Siebertz, K., Schlegel, B., Schmieder, P., and Hackenberger, C., 2014. Controlled thioamide vs. amide formation in the thioacid-azide reaction under acidic aqueous conditions. *Chemical communications (Cambridge, England)*, 50 (35), 4603.
- Mukaiyama, T., Murai, Y., and Shoda, S., 1981. An efficient method for glucosylation of hydroxy compounds using glucopyranosyl fluoride. *Chemistry Letters*, (3), 431–432.
- Mulloy, B. and Forster, M. J., 2000. Conformation and dynamics of heparin and heparan sulfate. *Glycobiology*, 10 (11), 1147–1156.
- Mulloy, B., Forster, M. J., Jones, C., and Davies, D. B., 1993. N.m.r. and molecular-modelling studies of the solution conformation of heparin. *The Biochemical journal*, 293 (Pt 3), 849–58.
- Muñoz-García, J. C., Corzana, F., de Paz, J. L., Angulo, J., and Nieto, P. M., 2013. Conformations of the iduronate ring in short heparin fragments described by time-averaged distance restrained molecular dynamics. *Glycobiology*, 23 (11), 1220–1229.
- Muñoz-García, J. C., López-Prados, J., Angulo, J., Díaz-Contreras, I., Reichardt, N., de Paz, J. L., Martín-Lomas, M., and Nieto, P. M., 2012. Effect of the Substituents of the Neighboring Ring in the Conformational Equilibrium of Iduronate in Heparin-like Trisaccharides. *Chemistry-A European Journal*, 18 (51), 16319–16331.
- Murphy, K. J., Merry, C. L., Lyon, M., Thompson, J. E., Roberts, I. S., and Gallagher, J. T., 2004. A new model for the domain structure of heparan sulfate based on the novel specificity of K5 lyase. *Journal of Biological Chemistry*, 279 (26), 27239–27245.
- Naggar, E., Costello, C., and Zaia, J., 2004. Competing fragmentation processes in tandem mass spectra of heparin-like glycosaminoglycans. *Journal of the American*

- Society for Mass Spectrometry*, 15 (11), 1534.
- Naimy, H., Buczek-Thomas, J. A., Nugent, M. A., Leymarie, N., and Zaia, J., 2011. Highly sulfated nonreducing end-derived heparan sulfate domains bind fibroblast growth factor-2 with high affinity and are enriched in biologically active fractions. *Journal of Biological Chemistry*, 286 (22), 19311–19319.
- Naimy, H., Leymarie, N., Bowman, M. J., Costello, C. E., and Zaia, J., 2008. Amide-HILIC LC/MS for the characterization of Antithrombin III heparin binders. *Biochemistry*, 47 (10), 3155.
- Nakagawa, A., Tanaka, M., Hanamura, S., Takahashi, D., and Toshima, K., 2015. Regioselective and 1, 2-cis- α -Stereoselective Glycosylation Utilizing Glycosyl-Acceptor-Derived Boronic Ester Catalyst. *Angewandte Chemie (International ed. in English)*, 54 (37), 10935.
- Nakato, H. and Kimata, K., 2002. Heparan sulfate fine structure and specificity of proteoglycan functions. *Biochimica Et Biophysica Acta (BBA)-General Subjects*, 1573 (3), 312–318.
- Netelenbos, T., Dräger, A. M., van het Hof, B., Kessler, F. L., Delouis, C., Huijgens, P. C., van den Born, J., and van Dijk, W., 2001. Differences in sulfation patterns of heparan sulfate derived from human bone marrow and umbilical vein endothelial cells. *Experimental hematology*, 29 (7), 884–893.
- Nicolaou, K. and Mitchell, H. J., 2001. Adventures in carbohydrate chemistry: new synthetic technologies, chemical synthesis, molecular design, and chemical biology. *Angewandte Chemie International Edition*, 40 (9), 1576–1624.
- Nieduszynski, I., Gardner, K., and Atkins, E., 1977. X-Ray Diffraction Studies of Heparin Conformation. ACS Publications.
- Nieto, L., Canales, Á., Fernández, I., Santillana, E., González-Corrochano, R., Redondo-Horcajo, M., Cañada, F., Nieto, P., Martín-Lomas, M., Giménez-Gallego, G., and others, 2013. Heparin modulates the mitogenic activity of fibroblast growth factor by inducing dimerization of its receptor. a 3D view by using NMR. *Chembiochem: a European journal of chemical biology*, 14 (14), 1732.
- Nigudkar, S. S. and Demchenko, A. V., 2015. Stereocontrolled 1, 2-cis glycosylation as the driving force of progress in synthetic carbohydrate chemistry. *Chemical Science*, 6 (5), 2687–2704.
- Nishikawa, T., Asai, M., Ohyabu, N., and Isobe, M., 1998. Improved Conditions for Facile Overman Rearrangement¹. *The Journal of organic chemistry*, 63 (1), 188–192.
- Nishimura, D., Hasegawa, A., and Nakajima, M., 1972. Solvent effect and anchimeric assistance on α -glycosylation. *Agricultural and Biological Chemistry*,

- 36 (10), 1767–1772.
- Norgard-Sumnicht, K. and Varki, A., 1995. Endothelial heparan sulfate proteoglycans that bind to L-selectin have glucosamine residues with unsubstituted amino groups. *Journal of Biological Chemistry*, 270 (20), 12012–12024.
- Noti, C., de Paz, J. L., Polito, L., and Seeberger, P. H., 2006. Preparation and use of microarrays containing synthetic heparin oligosaccharides for the rapid analysis of heparin-protein interactions. *Chemistry-A European Journal*, 12 (34), 8664–8686.
- O'Donnell, C. D., Tiwari, V., Oh, M.-J., and Shukla, D., 2006. A role for heparan sulfate 3-O-sulfotransferase isoform 2 in herpes simplex virus type 1 entry and spread. *Virology*, 346 (2), 452–459.
- Oduah, E. I., Linhardt, R. J., and Sharfstein, S. T., 2016. Heparin: Past, Present, and Future. *Pharmaceuticals*, 9 (3), 38.
- Ojeda, R., Angulo, J., Nieto, P. M., and Martín-Lomas, M., 2002. The activation of fibroblast growth factors by heparin: Synthesis and structural study of rationally modified heparin-like oligosaccharides. *Canadian journal of chemistry*, 80 (8), 917–936.
- Ojeda, R., de Paz, J., Martín-Lomas, M., and Lassaletta, J., 1999. A new route to L-iduronate building-blocks for the synthesis of heparin-like oligosaccharides. *Synlett*, 1999 (08), 1316–1318.
- Olsen, S. K., Garbi, M., Zampieri, N., Eliseenkova, A. V., Ornitz, D. M., Goldfarb, M., and Mohammadi, M., 2003. Fibroblast growth factor (FGF) homologous factors share structural but not functional homology with FGFs. *Journal of Biological Chemistry*, 278 (36), 34226–34236.
- Olson, S. T., Halvorson, H., and Björk, I., 1991. Quantitative characterization of the thrombin-heparin interaction. Discrimination between specific and nonspecific binding models. *Journal of Biological Chemistry*, 266 (10), 6342–6352.
- Orellana, A., Hirschberg, C. B., Wei, Z., Swiedler, S. J., and Ishihara, M., 1994. Molecular cloning and expression of a glycosaminoglycan N-acetylglucosaminyl N-deacetylase/N-sulfotransferase from a heparin-producing cell line. *Journal of Biological Chemistry*, 269 (3), 2270–2276.
- Orgueira, H. A., Bartolozzi, A., Schell, P., Litjens, R. E., Palmacci, E. R., and Seeberger, P. H., 2003. Modular synthesis of heparin oligosaccharides. *Chemistry-a European Journal*, 9 (1), 140–169.
- Orgueira, H. A., Bartolozzi, A., Schell, P., and Seeberger, P. H., 2002. Conformational locking of the glycosyl acceptor for stereocontrol in the key step in the synthesis of heparin. *Angewandte Chemie International Edition*, 41 (12), 2128–2131.

- Ori, A., Wilkinson, M., and Fernig, D., 2008. The heparanome and regulation of cell function: structures, functions and challenges. *Frontiers in bioscience: a journal and virtual library*, 13, 4309.
- Ornitz, D., Herr, A., Nilsson, M., Westman, J., Svahn, C., and Waksman, G., 1995. FGF binding and FGF receptor activation by synthetic heparan-derived di- and trisaccharides. *Science (New York, NY)*, 268 (5209), 432.
- Ornitz, D. M., 2000. FGFs, heparan sulfate and FGFRs: complex interactions essential for development. *Bioessays*, 22 (2), 108–112.
- Ornitz, D. M. and Itoh, N., 2001. Fibroblast growth factors. *Genome biology*, 2 (3), 1.
- Ornitz, D. M. and Itoh, N., 2015. The fibroblast growth factor signaling pathway. *Wiley Interdisciplinary Reviews: Developmental Biology*, 4 (3), 215–266.
- Ornitz, D. M., Xu, J., Colvin, J. S., McEwen, D. G., MacArthur, C. A., Coulier, F., Gao, G., and Goldfarb, M., 1996. Receptor specificity of the fibroblast growth factor family. *Journal of Biological Chemistry*, 271 (25), 15292–15297.
- Ornitz, D., Yayon, A., Flanagan, J., Svahn, C., Levi, E., and Leder, P., 1992. Heparin is required for cell-free binding of basic fibroblast growth factor to a soluble receptor and for mitogenesis in whole cells. *Molecular and cellular biology*, 12 (1), 240–247.
- Ostrovsky, O., Berman, B., Gallagher, J., Mulloy, B., Fernig, D. G., Delehedde, M., and Ron, D., 2002. Differential effects of heparin saccharides on the formation of specific fibroblast growth factor (FGF) and FGF receptor complexes. *Journal of Biological Chemistry*, 277 (4), 2444–2453.
- Oulion, S., Bertrand, S., and Escriva, H., 2012. Evolution of the FGF gene family. *International journal of evolutionary biology*, 2012.
- Overman, L. E., 1974. Thermal and mercuric ion catalyzed [3, 3]-sigmatropic rearrangement of allylic trichloroacetimidates. 1, 3 Transposition of alcohol and amine functions. *Journal of the American Chemical Society*, 96 (2), 597–599.
- Palmacci, E. R., Plante, O. J., and Seeberger, P. H., 2002. Oligosaccharide synthesis in solution and on solid support with glycosyl phosphates. *European Journal of Organic Chemistry*, 2002 (4), 595–606.
- Pantoliano, M. W., Horlick, R. A., Springer, B. A., Van Dyk, D. E., Tobery, T., Wetmore, D. R., Lear, J. D., Nahapetian, A. T., Bradley, J. D., and Sisk, W. P., 1994. Multivalent ligand-receptor binding interactions in the fibroblast growth factor system produce a cooperative growth factor and heparin mechanism for receptor dimerization. *Biochemistry*, 33 (34), 10229–10248.
- Park, W. Y., Miranda, B., Lebeche, D., Hashimoto, G., and Cardoso, W. V., 1998. FGF-10 is a chemotactic factor for distal epithelial buds during lung development.

- Developmental biology*, 201 (2), 125–134.
- Partanen, J., Schwartz, L., and Rossant, J., 1998. Opposite phenotypes of hypomorphic and Y766 phosphorylation site mutations reveal a function for Fgfr1 in anteroposterior patterning of mouse embryos. *Genes & Development*, 12 (15), 2332.
- Patel, V. N., Lombaert, I. M., Cowherd, S. N., Shworak, N. W., Xu, Y., Liu, J., and Hoffman, M. P., 2014. Hs3st3-modified heparan sulfate controls KIT⁺ progenitor expansion by regulating 3-O-sulfotransferases. *Developmental cell*, 29 (6), 662.
- Paulsen, H., 1982. Advances in selective chemical syntheses of complex oligosaccharides. *Angewandte Chemie International Edition in English*, 21 (3), 155–173.
- De Paz, J., Angulo, J., Lassaletta, J., Nieto, P., Redondo-Horcajo, M., Lozano, R., Giménez-Gallego, G., and Martín-Lomas, M., 2001. The activation of fibroblast growth factors by heparin: synthesis, structure, and biological activity of heparin-like oligosaccharides. *Chembiochem: a European journal of chemical biology*, 2 (9), 673.
- De Paz, J., Noti, C., Böhm, F., Werner, S., and Seeberger, P., 2007. Potentiation of fibroblast growth factor activity by synthetic heparin oligosaccharide glycodendrimers. *Chemistry & biology*, 14 (8), 879.
- De Paz, J. L. and Martín-Lomas, M., 2005. Synthesis and biological evaluation of a heparin-like hexasaccharide with the structural motifs for binding to FGF and FGFR. *European journal of organic chemistry*, 2005 (9), 1849–1858.
- De Paz, J. L., Noti, C., and Seeberger, P. H., 2006. Microarrays of synthetic heparin oligosaccharides. *Journal of the American Chemical Society*, 128 (9), 2766–2767.
- De Paz, J.-L., Ojeda, R., Reichardt, N., and Martín-Lomas, M., 2003. Some key experimental features of a modular synthesis of heparin-like oligosaccharides. *European Journal of Organic Chemistry*, 2003 (17), 3308–3324.
- Pedersen, C., Olsen, J., Brka, A., and Bols, M., 2011. Quantifying the electronic effects of carbohydrate hydroxy groups by using aminosugar models. *Chemistry (Weinheim an der Bergstrasse, Germany)*, 17 (25), 7080.
- Pellegrini, L., 2001. Role of heparan sulfate in fibroblast growth factor signalling: a structural view. *Current opinion in structural biology*, 11 (5), 629–634.
- Pellegrini, L., Burke, D. F., Von Delft, F., Mulloy, B., and Blundell, T. L., 2000. Crystal structure of fibroblast growth factor receptor ectodomain bound to ligand and heparin. *Nature*, 407 (6807), 1029–1034.
- Petitou, M. and van Boeckel, C., 2004. A synthetic antithrombin III binding pentasaccharide is now a drug! What comes next? *Angewandte Chemie*

- (*International ed. in English*), 43 (24), 3118.
- Petitou, M., Casu, B., and Lindahl, U., 2003. 1976-1983, a critical period in the history of heparin: the discovery of the antithrombin binding site. *Biochimie*, 85 (1-2), 83.
- Petitou, M., Duchaussoy, P., Lederman, I., Choay, J., Jacquinet, J., Sinaÿ, P., and Torri, G., 1987. Synthesis of heparin fragments: a methyl α -pentaoside with high affinity for antithrombin III. *Carbohydrate research*, 167, 67.
- Petitou, M., Duchaussoy, P., Lederman, I., Choay, J., and Sinaÿ, P., 1988. Binding of heparin to antithrombin III: a chemical proof of the critical role played by a 3-sulfated 2-amino-2-deoxy-D-glucose residue. *Carbohydrate research*, 179, 163–172.
- Petitou, M., Duchaussoy, P., Lederman, I., Choay, J., Sinaÿ, P., Jacquinet, J., and Torri, G., 1986. Synthesis of heparin fragments. A chemical synthesis of the pentasaccharide O-(2-deoxy-2-sulfamido-6-O-sulfo- α -D-glucopyranosyl)-(1-4)-O-(β -D-glucopyranosyluronic acid)-(1-4)-O-(2-deoxy-2-sulfamido-3, 6-di-O-sulfo- α -D-glu copyranosyl)-(1-4)-O-(2-O-sulfo- α -L-idopyranosyluronic acid)-(1-4)-2-deoxy-2-sulfamido-6-O-sulfo-D-glucopyranose decasodium salt, a heparin fragment having high affinity for antithrombin III. *Carbohydrate research*, 147 (2), 221.
- Petitou, M., H  rault, J.-P., Bernat, A., Driguez, P.-A., Duchaussoy, P., Lormeau, J.-C., and Herbert, J.-M., 1999. Synthesis of thrombin-inhibiting heparin mimetics without side effects. *Nature*, 398 (6726), 417–422.
- Petitou, M., Jacquinet, J.-C., Sinay, P., Choay, J., Lormeau, J.-C., and Nassr, M., 1989. Process for the organic synthesis of oligosaccharides and derivatives thereof.
- Plante, O. J., Palmacci, E. R., and Seeberger, P. H., 2001. Automated solid-phase synthesis of oligosaccharides. *Science*, 291 (5508), 1523–1527.
- Plotnikov, A. N., Schlessinger, J., Hubbard, S. R., and Mohammadi, M., 1999. Structural basis for FGF receptor dimerization and activation. *Cell*, 98 (5), 641–650.
- Polat, T. and Wong, C.-H., 2007. Anomeric reactivity-based one-pot synthesis of heparin-like oligosaccharides. *Journal of the American Chemical Society*, 129 (42), 12795–12800.
- Poletti, L., Fleischer, M., Vogel, C., Guerrini, M., Torri, G., and Lay, L., 2001. A Rational Approach to Heparin-Related Fragments- Synthesis of Differently Sulfated Tetrasaccharides as Potential Ligands for Fibroblast Growth Factors. *European Journal of Organic Chemistry*, 2001 (14), 2727–2734.
- Poletti, L. and Lay, L., 2003. Chemical contributions to understanding heparin activity: synthesis of related sulfated oligosaccharides. *European Journal of*

- Organic Chemistry*, 2003 (16), 2999–3024.
- Pomin, V. H., 2015. A Dilemma in the Glycosaminoglycan-Based Therapy: Synthetic or Naturally Unique Molecules? *Medicinal research reviews*, 35 (6), 1195–1219.
- Pomin, V. H., 2016. Paradigms in the structural biology of the mitogenic ternary complex FGF: FGFR: heparin. *Biochimie*.
- Ponnusamy, P., 2013. Reverse-phase Ion-Pairing Ultra Performance Liquid Chromatography-Mass Spectrometry In Characterization And Fingerprinting Of Diverse Sulfated Glycosaminoglycan Mimetics.
- Powell, A. K., Ahmed, Y. A., Yates, E. A., and Turnbull, J. E., 2010. Generating heparan sulfate saccharide libraries for glycomics applications. *Nature protocols*, 5 (5), 821–833.
- Powell, A. K., Fernig, D. G., and Turnbull, J. E., 2002. Fibroblast growth factor receptors 1 and 2 interact differently with heparin/heparan sulfate. *Journal of Biological Chemistry*, 277 (32), 28554–28563.
- Powell, A. K., Yates, E. A., Fernig, D. G., and Turnbull, J. E., 2004. Interactions of heparin/heparan sulfate with proteins: appraisal of structural factors and experimental approaches. *Glycobiology*, 14 (4), 17R–30R.
- Powers, C., McLeskey, S., and Wellstein, A., 2000. Fibroblast growth factors, their receptors and signaling. *Endocrine-related cancer*, 7 (3), 165–197.
- Prabhu, A., Venot, A., and Boons, G.-J., 2003. New set of orthogonal protecting groups for the modular synthesis of heparan sulfate fragments. *Organic letters*, 5 (26), 4975–4978.
- Pye, D. A., Vivès, R. R., Hyde, P., and Gallagher, J. T., 2000. Regulation of FGF-1 mitogenic activity by heparan sulfate oligosaccharides is dependent on specific structural features: differential requirements for the modulation of FGF-1 and FGF-2. *Glycobiology*, 10 (11), 1183–1192.
- Pye, D. A., Vives, R. R., Turnbull, J. E., Hyde, P., and Gallagher, J. T., 1998. Heparan sulfate oligosaccharides require 6-O-sulfation for promotion of basic fibroblast growth factor mitogenic activity. *Journal of Biological Chemistry*, 273 (36), 22936–22942.
- Qiao, J., Uzzo, R., Obara-Ishihara, T., Degenstein, L., Fuchs, E., and Herzlinger, D., 1999. FGF-7 modulates ureteric bud growth and nephron number in the developing kidney. *Development*, 126 (3), 547–554.
- Qin, Y., Ke, J., Gu, X., Fang, J., Wang, W., Cong, Q., Li, J., Tan, J., Brunzelle, J. S., Zhang, C., and others, 2015. Structural and functional study of D-glucuronyl C5-epimerase. *Journal of Biological Chemistry*, 290 (8), 4620–4630.

- Rabenstein, D. L., 2002. Heparin and heparan sulfate: structure and function. *Natural product reports*, 19 (3), 312–331.
- Rabenstein, D. L., Robert, J. M., and Peng, J., 1995. Multinuclear magnetic resonance studies of the interaction of inorganic cations with heparin. *Carbohydrate research*, 278 (2), 239–256.
- Rademacher, T., Parekh, R., and Dwek, R., 1988. Glycobiology. *Annual review of biochemistry*, 57 (1), 785–838.
- Rahmoune, H., Chen, H., Gallagher, J., Rudland, P., and Fernig, D., 1998. Interaction of heparan sulfate from mammary cells with acidic fibroblast growth factor (FGF) and basic FGF. Regulation of the activity of basic FGF by high and low affinity binding sites in heparan sulfate. *The Journal of biological chemistry*, 273 (13), 7303.
- Raman, R., Venkataraman, G., Ernst, S., Sasisekharan, V., and Sasisekharan, R., 2003. Structural specificity of heparin binding in the fibroblast growth factor family of proteins. *Proceedings of the National Academy of Sciences of the United States of America*, 100 (5), 2357.
- Rapraeger, A. C., Krufka, A., and Olwin, B. B., 1991. Requirement of heparan sulfate for bFGF-mediated fibroblast growth and myoblast differentiation. *Science*, 252 (5013), 1705–1708.
- Rapraeger, A., Guimond, S., Krufka, A., and Olwin, B., 1994. Regulation by heparan sulfate in fibroblast growth factor signaling. *Methods in enzymology*, 245, 219.
- Rice, K., Kim, Y., Grant, A., Merchant, Z., and Linhardt, R., 1985. High-performance liquid chromatographic separation of heparin-derived oligosaccharides. *Analytical biochemistry*, 150 (2), 325–331.
- Robinson, C., Mulloy, B., Gallagher, J., and Stringer, S., 2006. VEGF165-binding sites within heparan sulfate encompass two highly sulfated domains and can be liberated by K5 lyase. *The Journal of biological chemistry*, 281 (3), 1731.
- Robinson, M. L., 2006. An Essential Role for FGF Receptor Signaling in Lens Development. In: *Seminars in cell & developmental biology*. 726.
- Roghani, M., Mansukhani, A., Dell'Era, P., Bellosta, P., Basilico, C., Rifkin, D. B., and Moscatelli, D., 1994. Heparin increases the affinity of basic fibroblast growth factor for its receptor but is not required for binding. *Journal of Biological Chemistry*, 269 (6), 3976–3984.
- Rong, J., Habuchi, H., Kimata, K., Lindahl, U., and Kusche-Gullberg, M., 2001. Substrate specificity of the heparan sulfate hexuronic acid 2-O-sulfotransferase. *Biochemistry*, 40 (18), 5548–5555.
- Rosen, T., Lico, I. M., and Chu, D. T., 1988. A convenient and highly chemoselective method for the reductive acetylation of azides. *The Journal of*

- Organic Chemistry*, 53 (7), 1580–1582.
- Roussel, F., Knerr, L., Grathwohl, M., and Schmidt, R. R., 2000. O-glycosyl trichloroacetimidates bearing Fmoc as temporary hydroxy protecting group: a new access to solid-phase oligosaccharide synthesis. *Organic letters*, 2 (20), 3043–3046.
- Rudd, T., Guimond, S., Skidmore, M., Duchesne, L., Guerrini, M., Torri, G., Cosentino, C., Brown, A., Clarke, D., Turnbull, J., and others, 2007. Influence of substitution pattern and cation binding on conformation and activity in heparin derivatives. *Glycobiology*, 17 (9), 983.
- Rudd, T. R. and Yates, E. A., 2010. Conformational degeneracy restricts the effective information content of heparan sulfate. *Molecular BioSystems*, 6 (5), 902–908.
- Rudd, T. R. and Yates, E. A., 2012. A highly efficient tree structure for the biosynthesis of heparan sulfate accounts for the commonly observed disaccharides and suggests a mechanism for domain synthesis. *Molecular BioSystems*, 8 (5), 1499–1506.
- Rudd, T., Uniewicz, K., Ori, A., Guimond, S., Skidmore, M., Gaudesi, D., Xu, R., Turnbull, J., Guerrini, M., Torri, G., and others, 2010. Comparable stabilisation, structural changes and activities can be induced in FGF by a variety of HS and non-GAG analogues: implications for sequence-activity relationships. *Organic & biomolecular chemistry*, 8 (23), 5390.
- Rutland, P., Pulleyn, L. J., Reardon, W., Baraitser, M., Hayward, R., Jones, B., Malcolm, S., Winter, R. M., Oldridge, M., and Slaney, S. F., 1995. Identical mutations in the FGFR2 gene cause both Pfeiffer and Crouzon syndrome phenotypes. *Nature genetics*, 9 (2), 173–176.
- Saad, O. and Leary, J., 2003. Compositional analysis and quantification of heparin and heparan sulfate by electrospray ionization ion trap mass spectrometry. *Analytical chemistry*, 75 (13), 2985.
- Saito, A., Wakao, M., Deguchi, H., Mawatari, A., Sobel, M., and Suda, Y., 2010. Toward the assembly of heparin and heparan sulfate oligosaccharide libraries: efficient synthesis of uronic acid and disaccharide building blocks. *Tetrahedron*, 66 (22), 3951–3962.
- Salmivirta, M., Lidholt, K., and Lindahl, U., 1996. Heparan sulfate: a piece of information. *The FASEB journal*, 10 (11), 1270–1279.
- San Antonio, J., Slover, J., Lawler, J., Karnovsky, M., and Lander, A., 1993. Specificity in the interactions of extracellular matrix proteins with subpopulations of the glycosaminoglycan heparin. *Biochemistry*, 32 (18), 4746.
- Sanderson, P. N., Huckerby, T. N., and Nieduszyński, I. A., 1987. Conformational equilibria of alpha-L-iduronate residues in disaccharides derived from heparin.

- Biochem. J.*, 243, 175–181.
- Sarrazin, S., Lamanna, W. C., and Esko, J. D., 2011. Heparan Sulfate Proteoglycans. *Cold Spring Harbor Perspectives in Biology*, 3 (7).
- Schlessinger, J., Plotnikov, A. N., Ibrahimi, O. A., Eliseenkova, A. V., Yeh, B. K., Yayon, A., Linhardt, R. J., and Mohammadi, M., 2000. Crystal structure of a ternary FGF-FGFR-heparin complex reveals a dual role for heparin in FGFR binding and dimerization. *Molecular cell*, 6 (3), 743–750.
- Schmidt, R. R. and Michel, J., 1980. Facile synthesis of α - and β -O-glycosyl imidates; preparation of glycosides and disaccharides. *Angewandte Chemie International Edition in English*, 19 (9), 731–732.
- Schwarz, J. B., Kuduk, S. D., Chen, X.-T., Sames, D., Glunz, P. W., and Danishefsky, S. J., 1999. A broadly applicable method for the efficient synthesis of α -O-linked glycopeptides and clustered sialic acid residues. *Journal of the American Chemical Society*, 121 (12), 2662–2673.
- Schwörer, R., Zubkova, O. V., Turnbull, J. E., and Tyler, P. C., 2013. Synthesis of a Targeted Library of Heparan Sulfate Hexa- to Dodecasaccharides as Inhibitors of β -Secretase: Potential Therapeutics for Alzheimer's Disease. *Chemistry-A European Journal*, 19 (21), 6817–6823.
- Sears, P. and Wong, C.-H., 2001. Toward automated synthesis of oligosaccharides and glycoproteins. *Science*, 291 (5512), 2344–2350.
- Seyrek, E. and Dubin, P., 2010. Glycosaminoglycans as polyelectrolytes. *Advances in colloid and interface science*, 158 (1), 119–129.
- Seyrek, E., Dubin, P. L., and Henriksen, J., 2007. Nonspecific electrostatic binding characteristics of the heparin-antithrombin interaction. *Biopolymers*, 86 (3), 249–259.
- Seyrek, E., Dubin, P. L., Tribet, C., and Gamble, E. A., 2003. Ionic strength dependence of protein-polyelectrolyte interactions. *Biomacromolecules*, 4 (2), 273–282.
- Shangguan, N., Katukojvala, S., Greenberg, R., and Williams, L. J., 2003. The reaction of thio acids with azides: A new mechanism and new synthetic applications. *Journal of the American Chemical Society*, 125 (26), 7754–7755.
- Sheng, J., Liu, R., Xu, Y., and Liu, J., 2011. The dominating role of N-deacetylase/N-sulfotransferase 1 in forming domain structures in heparan sulfate. *Journal of Biological Chemistry*, 286 (22), 19768–19776.
- Shively, J. E. and Conrad, H. E., 1976. Formation of anhydrosugars in the chemical depolymerization of heparin. *Biochemistry*, 15 (18), 3932–3942.

- Shriver, Z., Raman, R., Venkataraman, G., Drummond, K., Turnbull, J., Toida, T., Linhardt, R., Biemann, K., and Sasisekharan, R., 2000. Sequencing of 3-O sulfate containing heparin decasaccharides with a partial antithrombin III binding site. *Proceedings of the National Academy of Sciences*, 97 (19), 10359–10364.
- Shukla, D., Liu, J., Blaiklock, P., Shworak, N., Bai, X., Esko, J., Cohen, G., Eisenberg, R., Rosenberg, R., and Spear, P., 1999. A novel role for 3-O-sulfated heparan sulfate in herpes simplex virus 1 entry. *Cell*, 99 (1), 13.
- Shworak, N. W., Liu, J., Petros, L. M., Zhang, L., Kobayashi, M., Copeland, N. G., Jenkins, N. A., and Rosenberg, R. D., 1999. Multiple Isoforms of Heparan Sulfate D-Glucosaminyl 3-O-Sulfotransferase Isolation, Characterization, and Expression of Human cDNAs and Identification of Distinct Genomic Loci. *Journal of Biological Chemistry*, 274 (8), 5170–5184.
- Siedlecka, R., Skarzewski, J., and Młochowski, J., 1990. Selective oxidation of primary hydroxy groups in primary-secondary diols. *Tetrahedron letters*, 31 (15), 2177–2180.
- Sinaÿ, P., Jacquinet, J.-C., Petitou, M., Duchaussoy, P., Lederman, I., Choay, J., and Torri, G., 1984. Total synthesis of a heparin pentasaccharide fragment having high affinity for antithrombin III. *Carbohydrate Research*, 132 (2), C5–C9.
- Skidmore, M. A., Guimond, S. E., Dumax-Vorzet, A. F., Yates, E. A., and Turnbull, J. E., 2010. Disaccharide compositional analysis of heparan sulfate and heparin polysaccharides using UV or high-sensitivity fluorescence (BODIPY) detection. *Nature protocols*, 5 (12), 1983–1992.
- Skidmore, M., Atrih, A., Yates, E., and Turnbull, J., 2009. Labelling heparan sulphate saccharides with chromophore, fluorescence and mass tags for HPLC and MS separations. *Methods in molecular biology (Clifton, NJ)*, 534, 157.
- Skinner, R., Abrahams, J.-P., Whisstock, J. C., Lesk, A. M., Carrell, R. W., and Wardell, M. R., 1997. The 2.6 Å structure of antithrombin indicates a conformational change at the heparin binding site. *Journal of molecular biology*, 266 (3), 601–609.
- Smeds, E., Habuchi, H., Anh-Tri, D., Hjertson, E., Grundberg, H., Kimata, K., Lindahl, U., and Kusche-Gullberg, M., 2003. Substrate specificities of mouse heparan sulphate glucosaminyl 6-O-sulphotransferases. *Biochemical Journal*, 372 (2), 371–380.
- Sobel, M., Soler, D. F., Kermode, J. C., and Harris, R. B., 1992. Localization and characterization of a heparin binding domain peptide of human von Willebrand factor. *Journal of Biological Chemistry*, 267 (13), 8857–8862.
- Solari, V., Borriello, L., Turcatel, G., Shimada, H., Sposto, R., Fernandez, G. E., Asgharzadeh, S., Yates, E. A., Turnbull, J. E., and DeClerck, Y. A., 2014. MYCN-dependent Expression of Sulfatase-2 Regulates Neuroblastoma Cell

- Survival. *Cancer research*, 74 (21), 5999.
- Solari, V., Rudd, T. R., Guimond, S. E., Powell, A. K., Turnbull, J. E., and Yates, E. A., 2015. Heparan sulfate phage display antibodies recognise epitopes defined by a combination of sugar sequence and cation binding. *Organic & biomolecular chemistry*, 13 (21), 6066–6072.
- Spillmann, D. and Lindahl, U., 1994. Glycosaminoglycan-protein interactions: a question of specificity. *Current Opinion in Structural Biology*, 4 (5), 677–682.
- Spillmann, D., Witt, D., and Lindahl, U., 1998. Defining the interleukin-8-binding domain of heparan sulfate. *Journal of Biological Chemistry*, 273 (25), 15487–15493.
- Spivak-Kroizman, T., Lemmon, M., Dikic, I., Ladbury, J., Pinchasi, D., Huang, J., Jaye, M., Crumley, G., Schlessinger, J., and Lax, I., 1994. Heparin-induced oligomerization of FGF molecules is responsible for FGF receptor dimerization, activation, and cell proliferation. *Cell*, 79 (6), 1015.
- Spivak-Kroizman, T., Mohammadi, M., Hu, P., Jaye, M., Schlessinger, J., and Lax, I., 1994. Point mutation in the fibroblast growth factor receptor eliminates phosphatidylinositol hydrolysis without affecting neuronal differentiation of PC12 cells. *The Journal of biological chemistry*, 269 (20), 14419.
- Springer, B. A., Pantoliano, M. W., Barbera, F. A., Gunyuzlu, P. L., Thompson, L. D., Herblin, W. F., Rosenfeld, S. A., and Book, G. W., 1994. Identification and concerted function of two receptor binding surfaces on basic fibroblast growth factor required for mitogenesis. *Journal of Biological Chemistry*, 269 (43), 26879–26884.
- Sterner, E., Masuko, S., Li, G., Li, L., Green, D. E., Otto, N. J., Xu, Y., DeAngelis, P. L., Liu, J., Dordick, J. S., and others, 2014. Fibroblast Growth Factor-based Signaling through Synthetic Heparan Sulfate Blocks Copolymers Studied Using High Cell Density Three-dimensional Cell Printing. *The Journal of Biological Chemistry*, 289 (14), 9754.
- Sterner, E., Meli, L., Kwon, S.-J., Dordick, J. S., and Linhardt, R. J., 2013. FGF-FGFR Signaling Mediated through Glycosaminoglycans in Microtiter Plate and Cell-Based Microarray Platforms. *Biochemistry*, 52 (50), 9009.
- Stickens, D., Zak, B. M., Rougier, N., Esko, J. D., and Werb, Z., 2005. Mice deficient in Ext2 lack heparan sulfate and develop exostoses. *Development*, 132 (22), 5055–5068.
- Strecker, G., Wieruszeski, J.-M., Martel, C., and Montreuil, J., 1987. Determination of the structure of sulfated tetra- and pentasaccharides obtained by alkaline borohydride degradation of hen ovomucin. A fast atom bombardment-mass spectrometric and ¹H-NMR spectroscopic study. *Glycoconjugate Journal*, 4 (4), 329–337.

- Stringer, S. E. and Gallagher, J. T., 1997. Heparan sulphate. *The international journal of biochemistry & cell biology*, 29 (5), 709–714.
- Sugahara, K. and Kitagawa, H., 2000. Recent advances in the study of the biosynthesis and functions of sulfated glycosaminoglycans. *Current opinion in structural biology*, 10 (5), 518–527.
- Tabeur, C., Machetto, F., Mallet, J. M., Duchaussoy, P., Petitou, M., and Sinaÿ, P., 1996. L-iduronic acid derivatives as glycosyl donors. *Carbohydrate research*, 281 (2), 253–76.
- Tabeur, C., Mallet, J., Bono, F., Herbert, J., Petitou, M., and Sinaÿ, P., 1999. Oligosaccharides corresponding to the regular sequence of heparin: chemical synthesis and interaction with FGF-2. *Bioorganic & medicinal chemistry*, 7 (9), 2003.
- Takada, W., Fukushima, M., Pothacharoen, P., Kongtawelert, P., and Sugahara, K., 2013. A sulfated glycosaminoglycan array for molecular interactions between glycosaminoglycans and growth factors or anti-glycosaminoglycan antibodies. *Analytical biochemistry*, 435 (2), 123–130.
- Tatai, J. and Fügedi, P., 2008. Synthesis of the putative minimal FGF binding motif heparan sulfate trisaccharides by an orthogonal protecting group strategy. *Tetrahedron*, 64 (42), 9865–9873.
- Tatai, J., Osztrovszky, G., Kajtár-Peredy, M., and Fügedi, P., 2008. An efficient synthesis of L-idose and L-iduronic acid thioglycosides and their use for the synthesis of heparin oligosaccharides. *Carbohydrate research*, 343 (4), 596.
- Tekin, M., Hicsmi, B. Ö., Fitoz, S., Özdaug, H., Cengiz, F. B., Sirmaci, A., Aslan, I., Inceoglu, B., Yüksel-Konuk, E. B., Yilmaz, S. T., and others, 2007. Homozygous Mutations in Fibroblast Growth Factor 3 Are Associated with a New Form of Syndromic Deafness Characterized by Inner Ear Agenesis, Microtia, and Microdontia. *American Journal of Human Genetics*, 80 (2), 338.
- Thacker, B. E., Xu, D., Lawrence, R., and Esko, J. D., 2014. Heparan sulfate 3-O-sulfation: A rare modification in search of a function. *Matrix biology: journal of the International Society for Matrix Biology*, 35, 60.
- Thiem, J., Horst, K., and Schwentner, J., 1978. Synthese α -verknüpfter 2'-Deoxy-2'-iododisaccharide. *Synthesis*, 1978 (09), 696–698.
- Thompson, L. D., Pantoliano, M. W., and Springer, B. A., 1994. Energetic characterization of the basic fibroblast growth factor-heparin interaction: identification of the heparin binding domain. *Biochemistry*, 33 (13), 3831–3840.
- Tiruchinapally, G., Yin, Z., El-Dakdouki, M., Wang, Z., and Huang, X., 2011. Divergent heparin oligosaccharide synthesis with preinstalled sulfate esters. *Chemistry-A European Journal*, 17 (36), 10106–10112.

- Tissot, B., Gasiunas, N., Powell, A. K., Ahmed, Y., Zhi, Z., Haslam, S. M., Morris, H. R., Turnbull, J. E., Gallagher, J. T., and Dell, A., 2007. Towards GAG glycomics: analysis of highly sulfated heparins by MALDI-TOF mass spectrometry. *Glycobiology*, 17 (9), 972–982.
- Tiwari, V., O'Donnell, C. D., Oh, M.-J., Valyi-Nagy, T., and Shukla, D., 2005. A role for 3-O-sulfotransferase isoform-4 in assisting HSV-1 entry and spread. *Biochemical and biophysical research communications*, 338 (2), 930–937.
- Tokimoto, H., Fujimoto, Y., Fukase, K., and Kusumoto, S., 2005. Stereoselective glycosylation using the long-range effect of a [2-(4-phenylbenzyl) oxycarbonyl] benzoyl group. *Tetrahedron: Asymmetry*, 16 (2), 441–447.
- Toshima, K., 2008. Glycosyl halides. In: *Glycoscience*. Springer, 429–449.
- Tsuda, T., Nakamura, S., and Hashimoto, S., 2003. A stereocontrolled construction of 2-azido-2-deoxy-1, 2-trans- β -glycosidic linkages utilizing 2-azido-2-deoxyglycopyranosyl diphenyl phosphates. *Tetrahedron letters*, 44 (34), 6453–6457.
- Tully, S. E., Mabon, R., Gama, C. I., Tsai, S. M., Liu, X., and Hsieh-Wilson, L. C., 2004. A chondroitin sulfate small molecule that stimulates neuronal growth. *Journal of the American Chemical Society*, 126 (25), 7736–7737.
- Turnbull, J. E., Fernig, D., Ke, Y., Wilkinson, M. C., and Gallagher, J. T., 1992. Identification of the basic fibroblast growth factor binding sequence in fibroblast heparan sulfate. *Journal of Biological Chemistry*, 267 (15), 10337–10341.
- Turnbull, J. E. and Gallagher, J. T., 1988. Oligosaccharide mapping of heparan sulphate by polyacrylamide-gradient-gel electrophoresis and electrotransfer to nylon membrane. *Biochemical Journal*, 251 (2), 597.
- Turnbull, J. E. and Gallagher, J. T., 1990. Molecular organization of heparan sulphate from human skin fibroblasts. *Biochemical Journal*, 265 (3), 715–724.
- Turnbull, J. E., Hopwood, J. J., and Gallagher, J. T., 1999. A strategy for rapid sequencing of heparan sulfate and heparin saccharides. *Proceedings of the National Academy of Sciences*, 96 (6), 2698.
- Turnbull, J., Powell, A., and Guimond, S., 2001. Heparan sulfate: decoding a dynamic multifunctional cell regulator. *Trends in cell biology*, 11 (2), 75–82.
- Tyrrell, D., Ishihara, M., Rao, N., Horne, A., Kiefer, M., Stauber, G., Lam, L. H., and Stack, R. J., 1993. Structure and biological activities of a heparin-derived hexasaccharide with high affinity for basic fibroblast growth factor. *Journal of Biological Chemistry*, 268 (7), 4684–4689.
- Uniewicz, K., Ori, A., Xu, R., Ahmed, Y., Wilkinson, M., Fernig, D., and Yates, E., 2010. Differential scanning fluorimetry measurement of protein stability changes upon binding to glycosaminoglycans: a screening test for binding specificity.

- Analytical chemistry*, 82 (9), 3796.
- Vanpouille, C., Deligny, A., Delehedde, M., Denys, A., Melchior, A., Liénard, X., Lyon, M., Mazurier, J., Fernig, D. G., and Allain, F., 2007. The heparin/heparan sulfate sequence that interacts with cyclophilin B contains a 3-O-sulfated N-unsubstituted glucosamine residue. *Journal of Biological Chemistry*, 282 (33), 24416–24429.
- Varki, A., 2009. Essentials of Glycobiology; Varki A, Cummings RD, Esko JD, Freeze HH, Stanley P *et al.*, editors.
- Vasella, A., Witzig, C., Chiara, J.-L., and Martin-Lomas, M., 1991. Convenient Synthesis of 2-Azido-2-deoxy-aldoses by Diazo Transfer. *Helvetica chimica acta*, 74 (8), 2073–2077.
- Vicente, C., Lima, M., Yates, E., Nader, H., and Toma, L., 2015. Enhanced tumorigenic potential of colorectal cancer cells by extracellular sulfatases. *Molecular cancer research: MCR*, 13 (3), 510.
- Virlouvet, M., Gartner, M., Koroniak, K., Sleeman, J. P., and Bräse, S., 2010. Multi-Gram Synthesis of a Hyaluronic Acid Subunit and Synthesis of Fully Protected Oligomers. *Advanced Synthesis & Catalysis*, 352 (14-15), 2657–2662.
- Vivès, R. R., Pye, D. A., Salmivirta, M., Hopwood, J. J., Lindahl, U., and Gallagher, J. T., 1999. Sequence analysis of heparan sulphate and heparin oligosaccharides. *Biochemical Journal*, 339 (Pt 3), 767.
- Walenga, J., Petitou, M., Samama, M., Fareed, J., and Choay, J., 1988. Importance of a 3-O-sulfate group in a heparin pentasaccharide for antithrombotic activity. *Thrombosis research*, 52 (6), 553.
- Walker, A., Turnbull, J., and Gallagher, J., 1994. Specific heparan sulfate saccharides mediate the activity of basic fibroblast growth factor. *The Journal of biological chemistry*, 269 (2), 931.
- Wallace, B. and Janes, R., 2010. Synchrotron radiation circular dichroism (SRCD) spectroscopy: an enhanced method for examining protein conformations and protein interactions. *Biochemical Society transactions*, 38 (4), 861.
- Wang, S., Ai, X., Freeman, S. D., Pownall, M. E., Lu, Q., Kessler, D. S., and Emerson, C. P., 2004. QSulf1, a heparan sulfate 6-O-endosulfatase, inhibits fibroblast growth factor signaling in mesoderm induction and angiogenesis. *Proceedings of the National Academy of Sciences of the United States of America*, 101 (14), 4833–4838.
- Wang, Z., Xu, Y., Yang, B., Tiruchinapally, G., Sun, B., Liu, R., Dulaney, S., Liu, J., and Huang, X., 2010. Preactivation-Based, One-Pot Combinatorial Synthesis of Heparin-like Hexasaccharides for the Analysis of Heparin-Protein Interactions. *Chemistry-A European Journal*, 16 (28), 8365–8375.

- Wesley, U. V., McGroarty, M., and Homoyouni, A., 2005. Dipeptidyl peptidase inhibits malignant phenotype of prostate cancer cells by blocking basic fibroblast growth factor signaling pathway. *Cancer research*, 65 (4), 1325–1334.
- White, K. E., Evans, W. E., O’Riordan, J. L., Speer, M. C., Econs, M. J., Lorenz-Depiereux, B., Grabowski, M., Meitinger, T., and Strom, T. M., 2000. Autosomal dominant hypophosphataemic rickets is associated with mutations in FGF23. *Nature genetics*, 26 (3), 345–348.
- Wiedemann, M. and Trueb, B., 2000. Characterization of a novel protein (FGFRL1) from human cartilage related to FGF receptors. *Genomics*, 69 (2), 275–279.
- Wilkie, A., Slaney, S. F., Oldridge, M., Poole, M. D., Ashworth, G. J., Hockley, A. D., Hayward, R. D., David, D. J., Pulleyn, L. J., and Rutland, P., 1995. Apert syndrome results from localized mutations of FGFR2 and is allelic with Crouzon syndrome. *Nature genetics*, 9 (2), 165–172.
- Wong, C.-H., 1995. Enzymatic and chemo-enzymatic synthesis of carbohydrates. *Pure and applied chemistry*, 67 (10), 1609–1616.
- Wu, C.-Y. and Wong, C.-H., 2015. Automated Programmable One-Pot Synthesis of Glycans. *Glycoscience: Biology and Medicine*, 45–52.
- Wu, Z. L. and Lech, M., 2005. Characterizing the non-reducing end structure of heparan sulfate. *Journal of Biological Chemistry*, 280 (40), 33749–33755.
- Wu, Z., Zhang, L., Yabe, T., Kuberan, B., Beeler, D., Love, A., and Rosenberg, R., 2003. The involvement of heparan sulfate (HS) in FGF1/HS/FGFR1 signaling complex. *The Journal of biological chemistry*, 278 (19), 17121.
- Wuts, P. G. and Greene, T. W., 2006. *Greene’s protective groups in organic synthesis*. John Wiley & Sons.
- Xia, G., Chen, J., Tiwari, V., Ju, W., Li, J.-P., Malmström, A., Shukla, D., and Liu, J., 2002. Heparan sulfate 3-O-sulfotransferase isoform 5 generates both an antithrombin-binding site and an entry receptor for herpes simplex virus, type 1. *Journal of Biological Chemistry*, 277 (40), 37912–37919.
- Xu, D. and Esko, J. D., 2014. Demystifying heparan sulfate-protein interactions. *Annual review of biochemistry*, 83, 129–157.
- Xu, R., Ori, A., Rudd, T. R., Uniewicz, K. A., Ahmed, Y. A., Guimond, S. E., Skidmore, M. A., Siligardi, G., Yates, E. A., and Fernig, D. G., 2012. Diversification of the structural determinants of fibroblast growth factor-heparin interactions implications for binding specificity. *Journal of Biological Chemistry*, 287 (47), 40061–40073.
- Xu, X., Weinstein, M., Li, C., Naski, M., Cohen, R. I., Ornitz, D. M., Leder, P., and Deng, C., 1998. Fibroblast growth factor receptor 2 (FGFR2)-mediated reciprocal regulation loop between FGF8 and FGF10 is essential for limb induction.

- Development*, 125 (4), 753–765.
- Xu, Y., Cai, C., Chandarajoti, K., Hsieh, P.-H., Li, L., Pham, T. Q., Sparkenbaugh, E. M., Sheng, J., Key, N. S., Pawlinski, R., and others, 2014. Homogeneous low-molecular-weight heparins with reversible anticoagulant activity. *Nature chemical biology*, 10 (4), 248–250.
- Xu, Y., Masuko, S., Takiuddin, M., Xu, H., Liu, R., Jing, J., Mousa, S. A., Linhardt, R. J., and Liu, J., 2011. Chemoenzymatic synthesis of homogeneous ultralow molecular weight heparins. *Science*, 334 (6055), 498–501.
- Xu, Y., Pempe, E. H., and Liu, J., 2012. Chemoenzymatic Synthesis of Heparin Oligosaccharides with both Anti-factor Xa and Anti-factor IIa Activities. *The Journal of Biological Chemistry*, 287 (34), 29054.
- Xu, Y., Wang, Z., Liu, R., Bridges, A. S., Huang, X., and Liu, J., 2012. Directing the biological activities of heparan sulfate oligosaccharides using a chemoenzymatic approach. *Glycobiology*, 22 (1), 96.
- Yamaguchi, T., Harpal, K., Henkemeyer, M., and Rossant, J., 1994. fgfr-1 is required for embryonic growth and mesodermal patterning during mouse gastrulation. *Genes & development*, 8 (24), 3032.
- Yamashita, T., Konishi, M., Miyake, A., Inui, K., and Itoh, N., 2002. Fibroblast growth factor (FGF)-23 inhibits renal phosphate reabsorption by activation of the mitogen-activated protein kinase pathway. *Journal of Biological Chemistry*, 277 (31), 28265–28270.
- Yang, B., Weyers, A., Baik, J. Y., Sterner, E., Sharfstein, S., Mousa, S. A., Zhang, F., Dordick, J. S., and Linhardt, R. J., 2011. Ultraperformance ion-pairing liquid chromatography with on-line electrospray ion trap mass spectrometry for heparin disaccharide analysis. *Analytical biochemistry*, 415 (1), 59.
- Yates, E. A., Guimond, S. E., and Turnbull, J. E., 2004. Highly diverse heparan sulfate analogue libraries: providing access to expanded areas of sequence space for bioactivity screening. *Journal of medicinal chemistry*, 47 (1), 277–280.
- Yates, E. A., Santini, F., Guerrini, M., Naggi, A., Torri, G., and Casu, B., 1996. ¹H and ¹³C NMR spectral assignments of the major sequences of twelve systematically modified heparin derivatives. *Carbohydrate Research*, 294, 15–27.
- Yayon, A., Klagsbrun, M., Esko, J. D., Leder, P., and Ornitz, D. M., 1991. Cell surface, heparin-like molecules are required for binding of basic fibroblast growth factor to its high affinity receptor. *Cell*, 64 (4), 841–848.
- Ye, S., Luo, Y., Lu, W., Jones, R. B., Linhardt, R. J., Capila, I., Toida, T., Kan, M., Pelletier, H., and McKeehan, W. L., 2001. Structural basis for interaction of FGF-1, FGF-2, and FGF-7 with different heparan sulfate motifs. *Biochemistry*, 40 (48), 14429–14439.

- Yip, G. W., Smollich, M., and Götte, M., 2006. Therapeutic value of glycosaminoglycans in cancer. *Molecular cancer therapeutics*, 5 (9), 2139–2148.
- Yu, B. and Tao, H., 2001. Glycosyl trifluoroacetimidates. Part 1: Preparation and application as new glycosyl donors. *Tetrahedron Letters*, 42 (12), 2405–2407.
- Yu, F., Roy, S., Arevalo, E., Schaeck, J., Wang, J., Holte, K., Duffner, J., Gunay, N. S., Capila, I., and Kaundinya, G. V., 2014. Characterization of heparin-protein interaction by saturation transfer difference (STD) NMR. *Analytical and bioanalytical chemistry*, 406 (13), 3079–3089.
- Yuguchi, Y., Kominato, R., Ban, T., Urakawa, H., Kajiwar, K., Takano, R., Kamei, K., and Hara, S., 2005. Structural observation of complexes of FGF-2 and regioselectively desulfated heparin in aqueous solutions. *International journal of biological macromolecules*, 35 (1), 19–25.
- Zaia, J., 2009. On-line separations combined with MS for analysis of glycosaminoglycans. *Mass spectrometry reviews*, 28 (2), 254.
- Zhang, F., Zhang, Z., Lin, X., Beenken, A., Eliseenkova, A. V., Mohammadi, M., and Linhardt, R. J., 2009. Compositional analysis on heparin/heparan sulfate interacting with FGF• FGFR complexes. *Biochemistry*, 48 (35), 8379.
- Zhang, X., Ibrahimi, O. A., Olsen, S. K., Umemori, H., Mohammadi, M., and Ornitz, D. M., 2006. Receptor specificity of the fibroblast growth factor family The complete mammalian fgf family. *Journal of Biological Chemistry*, 281 (23), 15694–15700.
- Zhang, Z. and Linhardt, R. J., 2009. Sequence analysis of native oligosaccharides using negative ESI tandem MS. *Current analytical chemistry*, 5 (3), 225.
- Zhang, Z., Ollmann, I. R., Ye, X.-S., Wischnat, R., Baasov, T., and Wong, C.-H., 1999. Programmable one-pot oligosaccharide synthesis. *Journal of the American Chemical Society*, 121 (4), 734–753.
- Zhang, Z., Xie, J., Liu, H., Liu, J., and Linhardt, R., 2009. Quantification of heparan sulfate disaccharides using ion-pairing reversed-phase microflow high-performance liquid chromatography with electrospray ionization trap mass spectrometry. *Analytical chemistry*, 81 (11), 4349.
- Zhu, X. and Schmidt, R. R., 2009. New Principles for Glycoside-Bond Formation. *Angewandte Chemie International Edition*, 48 (11), 1900–1934.
- Ziegler, A. and Zaia, J., 2006. Size-exclusion chromatography of heparin oligosaccharides at high and low pressure. *Journal of chromatography. B, Analytical technologies in the biomedical and life sciences*, 837 (1-2), 76.
- Zong, C., Venot, A., Dhamale, O., and Boons, G.-J., 2013. Fluorous supported modular synthesis of heparan sulfate oligosaccharides. *Organic letters*, 15 (2),

342–345.

Zulueta, M., Lin, S., Lin, Y., Huang, C., Wang, C., Ku, C., Shi, Z., Chyan, C., Irene, D., Lim, L., and others, 2012. α -Glycosylation by D-glucosamine-derived donors: synthesis of heparosan and heparin analogues that interact with mycobacterial heparin-binding hemagglutinin. *Journal of the American Chemical Society*, 134 (21), 8988.